June 1-2, 2017

Vienna University of Technology

http://vss.tuwien.ac.at/

Edited by:

Gerald Artner

Antonija Bogadi
Johanna Grames
Irene Hahn
Philipp Hans
Heinz Krebs
Taraneh Rouhi

Cover photo by Matthias Heisler

Published by Book-of-Abstracts.com
Heinz A. Krebs Dipl.-Ing.
Jubiläumsstrasse 17/2
2352 Gumpoldskirchen / Austria

Printed and bound in the Czech Republic

ISBN 978-3-9504017-5-2

Contents:

Welcome from the Organizers

On behalf of the organizing committee it is our great pleasure to welcome you to the 3rd Vienna young Scientists Symposium (VSS). The VSS is a forum for young researchers to exchange information about their research and development in innovative technologies. The symposium focuses on different research areas of the university; it showcases and stimulates interdisciplinary research. The VSS gives early stage researches the opportunity to present their work to a broad academic audience and it supports collaborations among faculties.

The VSS 2017 takes place on 1st and 2nd of June. This year's topics are:

- Civil Engineering
- Chemical Technologies and Bioscience
- Data, Models and Mathematics
- Sustainable Products and Solutions, Architecture and Urban Design

More than 70 abstracts were submitted and after peer-review 66 were accepted for inclusion in the proceedings. All members of TU Wien are invited to participate in the symposium, discuss their scientific work and exchange ideas between disciplines.

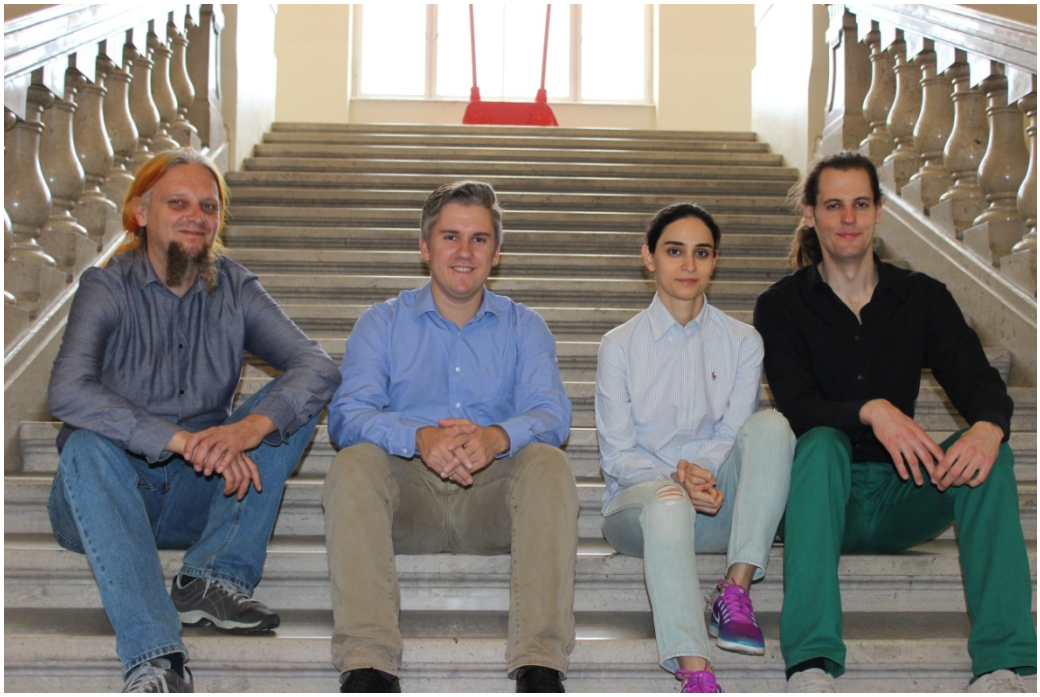

We wish you a cheerful and rewarding Vienna young Scientists Symposium 2017!

Welcome by the Rector
and the Vice Rector for Research and Innovation

The Vienna young Scientists Symposium (VSS) is a platform which aims at bringing highly talented individuals and promising projects together, thus demonstrating our students' enthusiasm both for broadening their own scientific horizons and for thinking outside the box, as well as their internalized interdisciplinary perspective. This initiative serves to enhance scientific research, broadens the findings of research groups and strengthens partnership with industry. The impressive volume of the abstracts compiled here rather eloquently conveys the creativity of our students and young scientists, as does this fantastic event itself.

© Raimund Appel

Scientific work at TU Wien is mainly covered by the five research focal areas of the TUW research matrix, which itself via the embedded research fields is a showcase of TUW scientific expertise.

The VSS 2017 presents research results in the fields of Civil Engineering, Chemical Technologies and Bioscience, Data, Models and Mathematics and Sustainable Products and Solutions, Architecture and Urban Design. All these interdisciplinary topics provide vivid evidence of the existing TUW research network.

© Raimund Appel

We would like to express our gratitude towards the organizers and supporters of VSS, who contributed to realizing an outstanding event. Our young scientific talents play an important role in the research advancement for the "TU Wien of tomorrow".

Sabine Seidler, Rector of TU Wien
Johannes Fröhlich, Vice Rector for Research and Innovation

Guest Lectures

Barbara **Haberl**

Österreichische Akademie der Wissenschaften

STIPENDIEN DER ÖAW FÜR PRAE- UND POST-DOCS

Georg **Kopetz**
TTTech

FORSCHUNGSORIENTIERUNG ALS WETTBEWERBSVORTEIL FÜR TECHNOLOGIE UNTERNEHMEN

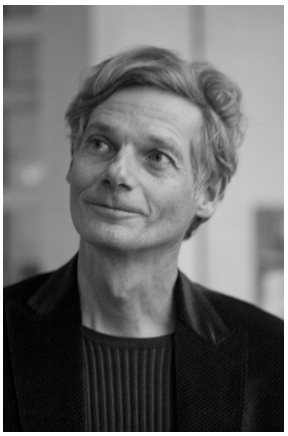

Andreas **Spiegl**
Akademie der bildenden Künste Wien

» UNDISZIPLINIERT «

© Marc Haader

Erhard **Busek**
Institut für den Donauraum und Mitteleuropa

WISSENSCHAFT UND EUROPA BEDINGEN EINANDER

Introduction by Christian Hellmich

CEN.1	Barbara **Laa** E234 Institute of Interdisciplinary Construction Process Management **EXPLORING THE POSSIBILITIES OF URBAN ROOFTOP FARMING IN VIENNA**
CEN.2	Andreas **Rudisch** E206/4 - Institute of Building Construction and Technology **SEISMIC PERFORMANCE OF HISTORICAL FACADE ELEMENTS - HAZARD ASSESSMENT**
CEN.3	Pedro Miguel **Jesus de Sousa Godinho** E202 – Institute for Mechanics of Materials and Structures **A CONTINUUM MICROMECHANICS APPROACH TO THE STRENGTH OF PLANAR FIBER NETWORKS: PAPER MATERIAL APPLICATIONS**

Introduction by Heidrun Halbwirth and Martina Marchetti-Deschmann

CTB.1	Maria **Antoniadou** E164 - Institute of Chemical Technologies and Analytics **CHARACTERIZING THE PERFORMANCE OF THE BARRIER DISCHARGE IONIZATION DETECTOR FOR GAS CHROMATOGRAPHY**
CTB.2	Simone **Spitzer** E166 - Institute of Chemical, Environmental and Biological Engineering **DEVELOPMENT OF BIOGAS UPGRADING PROCESSES FOR DEVELOPING AND EMERGING COUNTRIES**
CTB.3	Stefan **Baudis** E163 - Institute of Applied Synthetic Chemistry **MICROFABRICATED BIOCOMPATIBLE HYDROGELS**
CTB.4	Katarzyna **Zubek** E164 – Institute of Chemical Technologies and Analytics **THE EFFECT OF SMALL AMOUNT OF CATALYSTS ON STEAM GASIFICATION PROCESS**
CTB.5	Marta **Marczak** E164 – Institute of Chemical Technologies and Analytics **ACTIVE METHOD OF MERCURY CAPTURE FROM SUBBITUMINOUS AND LIGNITE COAL COMBUSTION**
CTB.6	M. Josef **Taublaender** E165 - Institute of Materials Chemistry **SOLID-STATE POLYMERIZATION OF HAIRY-ROD POLYIMIDES**
CTB.7	Katalin **Demeter** E166 - Institute of Chemical, Environmental and Biological Engineering **CHARACTERISATION OF THE MICROBIAL WATER QUALITY OF THE DANUBE RIVER AT VIENNA**
CTB.8	Zsolt **Harsfalvi** E166 – Institute of Chemical Engineering **COMPUTATIONAL FLUID DYNAMIC ANALYSIS OF COOLING IN A MIXED VESSEL USING A NON-NEWTONIAN MEDIUM**
CTB.9	Philipp **Lackner** E164 - Institute of Chemical Technologies and Analytics **GEOPOLYMERS AND INORGANIC MULTIBINDER SYSTEMS**
CTB.10	Claudia **Kolm** E166 - Institute of Chemical, Environmental and Biological Engineering **A COMPLEMENTARY ISOTHERMAL AMPLIFICATION METHOD TO THE US EPA qPCR APPROACH FOR THE DETECTION OF ENTEROCOCCI IN ENVIRONMENTAL WATERS**

CTB.11 Thomas **Gundinger**
E166 - Institute of Chemical, Environmental and Biological Engineering

A COMPARATIVE APPROACH TO RECOMBINANTLY PRODUCE THE PLANT ENZYME HORSERADISH PEROXIDASE IN *ESCHERICHIA COLI*

CTB.12 David Johannes **Wurm**
E166 - Institute of Chemical, Environmental and Biological Engineering

TEACHING AN OLD PET NEW TRICKS - EXPRESSION TUNING IN *E. COLI* BL21(DE3)

CTB.13 Victor **Lobanov**
E166 - Institute of Chemical, Environmental and Biological Engineering

PRODUCTION OF HYDROPHOBINS IN THE TWO EXPRESSION SYSTEMS BASED ON *TRICHODERMA*

CTB.14 Katarzyna **Styszko**
AGH University of Science and Technology, Krakow, Poland

EMERGING CONTAMINANTS IN PM10 OF RESIDENTIAL AREA IN KRAKOW

CTB.15 Elisabeth **Fitz**
E166-5 Institute of Chemical, Environmental

OPTIMISING NATURE FOR INDUSTRY: DESIGN OF SYNTHETIC PROMOTERS FOR STRAIN ENGINEERING OF *TRICHODERMA REESEI*

CTB.16 Daniel **Koch**
E166 - Institute of Chemical, Environmental and Biological Engineering

COMPARABILITY OF LIFE CYCLE ASSESSMENTS (LCA) IN PROCESS DESIGN BIOREFINERY PROCESSES

CTB.17 Roland **Martzy**
E166 - Institute of Chemical, Environmental and Biological Engineering

A LOOP-MEDIATED ISOTHERMAL AMPLIFICATION (LAMP) ASSAY FOR THE RAPID DETECTION OF *ENTEROCOCCUS* SPP. IN WATER

CTB.18 Manuel **Spettel**
E163 - Institute of Applied Synthetic Chemistry

QUATERNARY AMMONIUM SALTS AS ALKYLATING REAGENTS IN C-H ACTIVATION CHEMISTRY

CTB.19 David Chan Bodin **Siebert**
E163 - Institute of Applied Synthetic Chemistry

POST-DOCKING DERIVATIZATION REVEALS PYRAZOLOQUINOLINONE BINDING MODE AT THE α+/ γ- $GABA_A$ RECEPTOR INTERFACE

CTB.20 Katarzyna **Szramowiat**
AGH University of Science and Technology, Krakow, Poland

SPATIAL AND SEASONAL VARIABILITY OF MERCURY CONCENTRATIONS IN AEROSOLS FROM MALOPOLSKA REGION, SOUTH POLAND

CTB.21 Clara **Freytag**
E165 - Institute of Materials Chemistry

LOCAL INSTABILITIES IN THE H_2 OXIDATION ON RHODIUM: STRUCTURAL EFFECTS

CTB.22 Johanna **Hausjell**
E166 - Institute of Chemical Engineering

RECOMBINANT PRODUCTION AND PURIFICATION OF CHALCONE-3-HYDROXYLASE (CH3H) FROM YEAST

CTB.23 Thomas **Prochaska**
E164 - Institute of Chemical Technologies and Analytics

POROUS Si_3N_4-BASED SUPPORT MATERIALS WITH TAILORED GAS PERMEABILITY

CTB.24 Clara **Garcia**
E165 - Institute of Materials Chemistry

CATALYTIC ACTIVITY OF THIOLATE-PROTECTED GOLD NANOCLUSTERS SUPPORTED ON TiO_2, SiO_2 AND ZrO_2

CTB.25 Alice **Rassinger**
E166 - Institute of Chemical, Enviromental and Biological Engineering

IMPACT OF INDUCER MOLECULES ON DNA ACCESSIBILITY IN CELLULASE AND XYLANASE EXPRESSION IN *TRICHODERMA REESEI*

CTB.26 Barbara **Roth**
E166 - Institute of Chemical, Environmental and Biological Engineering

RECOMBINANT CORE PROTEINS OF POLYPHENOL OXIDASES ON EXAMPLE OF AURONE SYNTHASE

CTB.27 Markus **Bösenhofer**
E166 - Institute of Chemical Engineering

TOWARDS GENERIC REACTIVE FLOW MODELLING

CTB.28 Tatyana **Yemelyanova**
E166 - Institute of Chemical, Environmental and Biological Engineering

HYDROPHOBINS AS INACTIVE EXCIPIENTS IN THE PHARMACEUTICAL AND FOOD INDUSTRY

CTB.29 Christina **Drechsel**
E164 - Institute of Chemical Technologies and Analytics

A PROCESSING ROUTINE FOR LAYERED Si_3N_4/SiCN STRUCTURES WITH GRADED MULTISCALAR POROSITY

CTB.30 Mateusz **Karczewski**
AGH University of Science and Technology, Krakow, Poland

STEAM GASIFICATION PROCESS ENHANCEMENT WITH ALKALI AND ALKALINE EARTH-RICH WASTE MATERIALS

CTB.31 Magdalena **Maderthaner**
E164 - Institute of Chemical Technologies and Analytics

SELECTIVE OXIDATION AND HOT-DIP-GALVANIZABILITY OF ADVANCED HIGH STREGTH STEELS

CTB.32 Komal **Chenthamara**
E166 - Institute of Chemical, Environmental and Biological Engineering

THE ORIGIN AND ARCHITECTURE OF *TRICHODERMA* HYDROPHOBOME

CTB.33 Olly **Hutabarat**
E166 - Institute of Chemical, Environmental and Biological Engineering

APPLE (*MALUS X DOMESTICA*) AS A MODEL PLANT TO INVESTIGATE THE BIOSYNTHESIS OF 3-HYDROXYPHLORIDZIN

CTB.34 Mohammad Javad **Rahimi**
E166 - Institute of Chemical Engineering

DEGRADATION OF SYNTHETIC POLYMERS BY EPIPHYTIC FUNGI FROM HIGH CANOPY OF THE TROPICAL RAIN FOREST

Introduction by Christoph Lemell and Peter Szmolyan

DMM.1 Fabain **Klute**
E186/1 - Algorithms and Complexity Group
MINIMIZING CROSSINGS IN CONSTRAINED TWO-SIDED CIRCULAR GRAPH LAYOUTS

DMM.2 Thomas **Blazek**
E389 - Institute of Telecommunications
VEHICLE-TO-VEHICLE CHANNEL LOAD BALANCING THROUGH VEHICULAR ROUTING

DMM.3 Taulant **Berisha**
E389 - Institute of Telecommunications
MOVING RELAY NODES ON-BOARD HIGH SPEED TRAINS IN AUSTRIA: IS IT WORTH IT?

DMM.4 Markus **Pöchtrager**
E251 - Institute of History of Art, Building Archaeology and Restoration
AUTOMATED DIGITAL RECONSTRUCTION OF TIMBER STRUCTURES FROM POINT CLOUDS

DMM.5 Johanna **Grames**
E222 - Vienna Doctoral Programme for Water Resource Systems
OPTIMAL INVESTMENT AND LOCATION DECISIONS OF A FIRM IN A FLOOD RISK AREA USING IMPULSE CONTROL THEORY

DMM.6 Mostafa **Fallahnejad**
E370 - Institute of energy systems and electrical drives
LONG-TERM FORECAST OF RESIDENTIAL & COMMERCIAL GAS DEMAND IN GERMANY

DMM.7 Alexander **Czech**
E280 - Center of Regional Science
HOW TO GEOTAG THE WEB?

DMM.8 Maria **Lara**
Institute for Discrete Mathematics and Geometry
TRANSFORMATIONS AND BASE SHAPE ANALYSIS

DMM.9 Antonia **Wagner**
E317 - Institute of Lightweight Design and Structural Biomechanics
EFFICIENT NUMERICAL MODELLING OF MULTILAYER SYSTEMS

DMM.10 Michaela **Nagler**
E317 - Institute of Lightweight Design and Structural Biomechanics
ANALYTICAL TREATMENT OF RESIDUAL STRESSES IN MULTILAYER COATINGS

DMM.11 Lukas **Gnam**
E360 - Institute for Microelectronics
TOWARDS A METRIC FOR AN AUTOMATIC HULL MESH COARSENING STRATEGY

DMM.12 Markus **Schöbinger**
E101 - Institute of Analysis and Scientific Computing

AN EFFICIENT SIMULATION TECHNIQUE FOR THE EDDY CURRENT PROBLEM IN LAMINATED IRON CORES

DMM.13 Michael **Kompatscher**
E185 - Institute of Computer Languages

A COMPLEXITY DICHOTOMY FOR SATISFIABILITY OVER PARTIAL ORDERS

DMM.14 Markus **Wess**
E101 - Institute for Analysis and Scientific Computing

SOLVING RESONANCE PROBLEMS ON UNBOUNDED DOMAINS USING FINITE ELEMENTS AND COMPLEX SCALING

DMM.15 Florian **Thürk**
E354 - Institute of Electrodynamics, Microwave and Circuit Engineering

EVALUATION FRAMEWORK FOR IMAGE RECONSTRUCTION IN ELECTRICAL IMPEDANCE TOMOGRAPHY

DMM.16 Gabriel **Grill**
E188 - Institute of Software Technology and Interactive Systems

NETWORK ANALYSIS ON THE AUSTRIAN MEDIA CORPUS

DMM.17 Matthias **Schartner**
E120 - Department of Geodesy and Geoinformation

MEASURING EARTH ROTATION COMBINING RINGLASER AND VLBI

DMM.18 Nikola **Koutna**
E308 - Institute of Materials Science and Technology

STABILITY AND ELASTICITY OF THE MoN-TaN SYSTEM: AN ATOMISTIC INSIGHT

DMM.19 David **Pollreisz**
Institute of Computer Technology

EMOTION RECOGNITION USING EMPATICA E4 SMART WATCH

DMM.20 Maximilian **Götzinger**
E384 - Institute of Computer Technology

SELF-AWARENESS IN REMOTE HEALTH MONITORING SYSTEMS USING WEARABLE ELECTRONICS

DMM.21 Hassan **Bassereh Moosaabadi**
E101 - Institute of Analysis and Scientific Computing

INTRA- AND EXTRA-CELLULAR STMULATION OF RETINAL BIPOLAR CELLS

Introduction by Michael Getzner and Wolfgang Wimmer

Research Field *Civil Engineering*

Chairs and Reviewer:

Hellmich, Christian
Univ.Prof. Dipl.-Ing. Dr.techn.

E202 - Institute for Mechanics of Materials and Structures
christian.hellmich@tuwien.ac.at

Introduction

Civil engineering enables ever more visionary transportation, bridges, power plants and buildings. Scientific advances in civil engineering shape societies for centuries and millennia to come. Steadily increasing urbanization puts strong requirements on infrastructure.

Current challenges include intelligent transportation systems and smart city concepts, investigation of novel construction materials and improvements to widely used materials such as concrete and wood, improved construction techniques and a smarter use and reuse of available resources.

Due to immediate applications in Austria a focus will also be on hydraulic engineering, water, wood and resource management in general.

EXPLORING THE POSSIBILITIES OF URBAN ROOFTOP FARMING IN VIENNA

Barbara Laa, Maéva Dang and Christoph Achammer

E234 Institute of Interdisciplinary Construction Process Management
Industrial Building and Interdisciplinary Planning

INTRODUCTION

The global trend of urbanization entails major social, economic and ecological challenges at the present and even more in the future. Urban farming is one way to cope with the difficulties ahead. There are numerous studies which show the benefits of urban agriculture, including positive effects on a city's microclimate, urban water management and contribution to food security. [1]

Due to the limitation of available space within the city boundaries, people around the world are beginning to use the existing empty spaces of flat roofs to grow food. A study conducted in Bologna found that the yield of urban rooftop farms would be able to cover 77 % of the vegetable requirements of the city's inhabitants. [2] Thus, such concepts could provide a major contribution to vegetable supply for city dwellers.

The present research is concerned with the possibilities of rooftop farming in the city of Vienna, with a focus on the implementation of different food production systems on existing surfaces.

RESEARCH SUMMARY

The aim of this interdisciplinary work is on the one hand the identification of all roof areas suitable for growing food. On the other hand it seeks to investigate the significant parameters for the installation of farming systems on the scale of an individual building.

According to a study of the MA 22 (viennese municipality department for environmental protection) about the green roof potential in Vienna, there are 1.068 *ha* of roof surfaces which are less than 5° inclined and therefore suited for intensive greening. [3] This represents a high potential for green roofs, but the study does not entail any other factors than surface inclination.

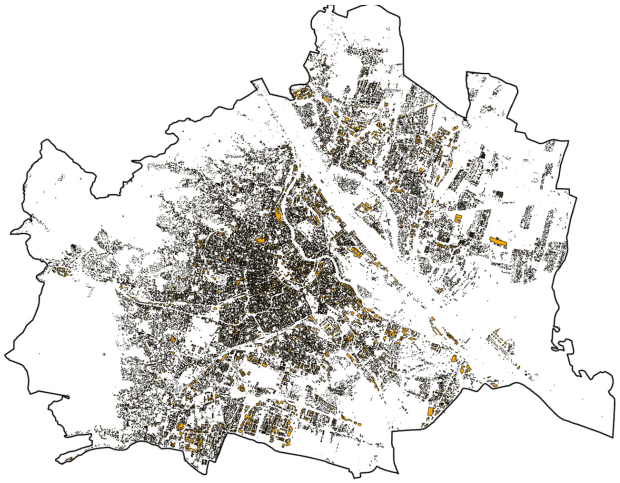

Figure 1: Possible rooftop farming areas in Vienna (data provided by MA 22)

To get a better idea which areas are in fact suitable for the purpose of agriculture, there were following important factors identified: size, supporting structure and roof structure of the building, sunlight exposure, accessibility, infrastructure, legal matters and possible management of the farm. A first analysis with GIS-data was conducted to include some of these parameters. Figure 1 shows for example a visualization of all the roof areas in Vienna, which are less than 5° inclined, bigger than 10 m^2 and receive a minimum of 900 KWh/m^2 solar radiation per year. These surfaces add up to an area of 1.057 *ha*.

All of the above mentioned factors include a number of issues which have to be taken into consideration. In the course of this work the significant parameters in all of these fields were investigated on the basis of a literature review, leading to a guideline for the fundamental requirements regarding the planning and installation of a rooftop farm.

Furthermore there are various ways to produce food on roof areas. For the present research the following systems were considered: conventional farming with soil spread on wide areas of the roof, raised-bed gardening, hydroponics, aeroponics, aquaponics and the combination of any of the mentioned with a greenhouse.

To get further into detail different types of buildings were regarded in connection with the described food production systems. It seems obvious, that an industrial building cannot be treated the same way as a residential building referred to the kind of cultivation. For example a large industrial building with a flat roof offers the possibility to install a lightweight food growing system, which could be managed as a commercial farm. If the building is a supermarket or a shopping mall, the products could even be sold on location. In contrast a conventional apartment building would be probably more suitable for a community garden where residents can rent individual vegetable patches. These could be constructed as raised-beds, placed alongside the beams of the supporting structure.

The examples above show that the existing structure and purpose of the building have a major influence on the feasible food production system. The next step is to find out which systems are suited best for which kind of building and roof type. To this end the strengths and weaknesses of the different growing systems will be investigated and linked with exemplary building typologies.

EXPECTED RESULTS AND CONCLUSION

The main result of the work will be a practical handbook for city planners, real estate owners, companies, associations or otherwise interested individuals. It will entail an overview of what to consider and which steps to take in order to construct a rooftop farm on an existing building in Vienna. In addition the analysis will show the size and location of areas suitable for rooftop agriculture, based on specific parameters.

Furthermore, the work should lead to a better understanding of the opportunities of urban agriculture on top of existing buildings and could serve as a basis for future research in that field.

REFERENCES

[1] Deelstra, T., & Girardet, H. (2000), Urban agriculture and sustainable cities. Bakker N., Dubbeling M., Gndel S., Sabel-Koshella U., de Zeeuw H. Growing cities, growing food. Urban agriculture on the policy agenda. Feldafing, Germany: Zentralstelle fuer Ernaehrung und Landwirtschaft (ZEL), 43-66.

[2] Orsini et al. (2014), Exploring the production capacity of rooftop gardens (RTGs) in urban agriculture: the potential impact on food and nutrition security, biodiversity and other ecosystem services in the city of Bologna.

[3] Nima Vali (2011), Analyse des Dachbegruenungspotentials Wien. Published by MA 22

SEISMIC PERFORMANCE OF HISTORICAL FAÇADE ELEMENTS – HAZARD ASSESSMENT

Andreas Rudisch, Thomas Buchner, Andreas Kolbitsch

E206/4 - Institute of Building Construction and Technology

INTRODUCTION

The conservation of built heritage represents a special area of expertise for civil engineers as well as for restorers. In Vienna, more than 25% of all existing buildings are more than a hundred years old. As a requirement for structural changes to these objects, a reassessment of the existing supporting structure is inevitable in many cases. Due to the risk-based design concept of ÖNORM B 1998-3 and forthcoming B 4008-1 for existing buildings, the awareness for a subsequent earthquake-proof redesign of 19th century buildings was raised in Austria [1]. Yet the consideration of historical façade elements is often neglected [2]. However, in the case of past earthquakes, it has been shown that these nonstrucutral components (NSCs) make up a substantial part of the observed building damages and, in the event of failure, they constitute a significant danger to persons.

PROBLEM DEFINITION

Since the first formal mention about the seismic design of NSCs in the publication of the ATC-03 Report in 1978 [3], slightly different simplified design methods are defined in valid standards at the international level (e.g ASCE-7 [4], EC-8 [5] and DIN [6]) to calculate an inertial horizontal force to design NSCs. Figure 1 shows the respective transmission of the peak ground acceleration (PGA) in case of resonance for a typical historical 5-storey building.

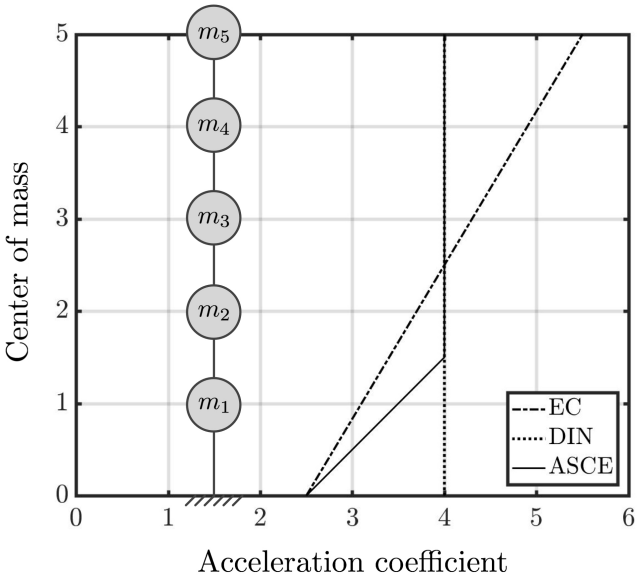

Figure 1: Transmission of the PGA for a 5-storey building in the resonance case – Consideration of selected standards

The application of such simplified methods is not universally valid for all different types of construction [1]. On the one hand, resonance effects are only taken into account with the first mode of the primary structure. If resonance occurs with the second mode, the design forces are underestimated. On the other hand, these simplified standards are just linear methods. This means that if nonlinear material behavior occurs, forces are likely to be overestimated. Numerous research projects have shown that the energy dissipation of the primary structures has a considerable influence on the resultant inertial design forces. In addition to assessing design loads, the prediction of local failure mechanisms of historical NSCs is another challenge, because the provisions of valid standards are primarily concerned with the design of their connections [3]. For these reasons, simplified approaches are often only adequate for a quick pre-design [7].

RESEARCH OBJECTIVES AND METHODOLOGY

Comprehensive numerical simulations are being carried out to determine the maximum peak floor accelereation (PFA) for typical old Viennese masonry buildings, which depends on the PGA and the seismic response of the structure. Therefore, a specially calibrated material model for old masonry walls under cyclic loading is going to be applied in order to take specific failure mechanisms [8] into account. In the future it should be possible to use these determined limit values of the PFA for a suitable assessment, because detailled time history analysis in any individual case is associated with high effort. The next goal is gaining knowledge about the seismic performance and the specific failure mechanisms of typical historical façade elements. For this purpose, model experiments on a one-dimensional shaking table with representative test specimens will be conducted to examine the seismic behavior and the limit state. Figure 2 shows the developed test setup. Finally, the results of the model experiments will be evaluated with non-destructive in situ tests.

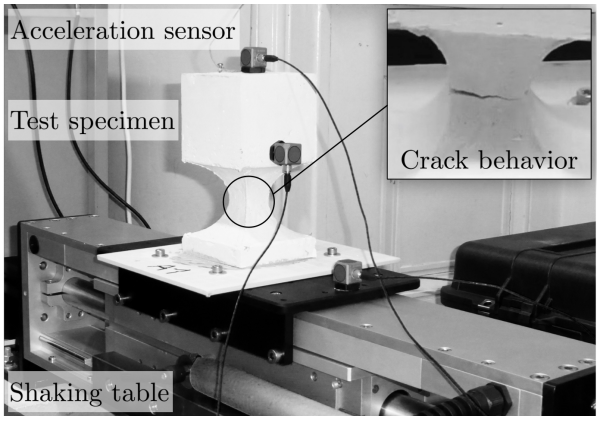

Figure 2: Setup for the limit state test

CONCLUSION

The challenge of the seismic stabilization of historic façade elements is to find an acceptable balance between vulnerability and intervention that reduces the risk of damage [1]. The selection of suitable preventive measures often includes the evaluation of many possibilities. Strengthening such elements to survive future earthquakes might be technically possible, but it involves high costs and often an unacceptable intervention on the built heritage. The assessment depends essentially on the quality of the design parameter identification. The objectives of this research project are to determine design loads on historical façade elements as well as to estimate their seismic performance and limit state. Thereby sustainable and secure retrofitting should be possible in near future.

REFERENCES

[1] Rudisch, A.; Dunjic, V.; Kolbitsch, A.: Historische Zierelemente unter Erdbebenbeanspruchung – State of the Art. Bauingenieur 91, p. 14-22, 2016

[2] Kolbitsch, A.: Assessment and retrofitting of façade elements of 19th century buildings. 15 WCEE Lisboa, 2012.

[3] Singh, M.P.; Moreschi, L.M.: Simplified methods for calculating seismic forces for nonstructural components. ATC-29-1 Seminar Technical Papers, 1998

[4] ÖNORM EN 1998-1: Eurocode 8: Auslegung von Bauwerken gegen Erdbeben - Teil 1: Grundlagen, Erdbebeneinwirkungen und Regeln fr Hochbauten (konsolidierte Fassung). Austrian Standards, 2013

[5] ASCE 7-10: Minimum Design Loads for Buildings and other Structures. ASCE, 2010

[6] DIN EN 1998-1/NA: Nationaler Anhang - National festgelegte Parameter - Eurocode 8: Auslegung von Bauwerken gegen Erdbeben - Teil 1: Grundlagen, Erdbebeneinwirkungen und Regeln für Hochbauten. Deutsches Normungsinstitut, 2011

[7] Moschen, L.; Adam, C; Vamvatsikos, D.: A response spectrum method for peak floor acceleration demands in earthquake excited structures. Probabilistic Engineering Mechanics Vol. 46, p. 94-106, 2016

[8] Dunjic, V.; Rudisch, A.; Kolbitsch, A.: The two-shearfield test – A suitable method for the empirical shear capacity design of masonry. Mauerwerk 20, p. 381-387, 2016

A CONTINUUM MICROMECHANICS APPROACH TO THE STRENGTH OF PLANAR FIBER NETWORKS: PAPER MATERIAL APPLICATIONS

Pedro Miguel Jesus de Sousa Godinho[a], Marina Jajcinovic[b], Thomas Karl Bader[c], Wolfgang Johann Fischer[b], Ulrich Hirn[b], Wolfgang Bauer[b], Christian Hellmich[a,*]

[a]E202 – Institute for Mechanics of Materials and Structures
[b]Graz University of Technology, Graz, Austria
[c]Linnaeus University, Växjö, Sweden

INTRODUCTION

The elastic properties of any micro-heterogeneous material depend on its inherent microstructure. One class of micro-heterogeneous materials are so-called fibrous materials. Their microstructure is made up of fibre networks, in which the individual fibres are connected via fibre-fibre bonds. In the majority of cases, the fibres are more or less parallel to one plane; one speaks of planar fibrous materials. Planar fibrous materials find numerous applications, which range from thermal and sound insulators, tissue templates, as well as gas and fluid fillers, to various paper product applications, including healthcare applications. One particularly widespread planar fibrous material is paper, a network of mechanically and/ or chemically treated wood fibres, so-called pulp fibres. In all the aforementioned applications, as well as in paper production, the mechanical properties, such as elasticity and strength of the planar networks, are of crucial importance. Therefore, it is not surprising that various mathematical models for the mechanical interaction of pulp fibres within the overall material "paper" have been proposed. However, none of these models explicitly accounted for the scale difference between the loads applied to the overall material and those acting on the level of the individual fibre. This motivated our research.

MICROMECHANICS-BASED LINEAR ELASTIC STRENGTH MODEL

In a first research stage, we filled the essential conceptual gap mentioned in the introduction with the development of a new micromechanics-based linear elastic model: We first recalled the fundamental micromechanical concept of the representative volume element and the corresponding stress and strain average rules, before we specified these rules for planar fibre networks such as paper material. Then we introduced elastic material behaviour at the fibre level, and derived so-called concentration relations for upscaling this behaviour to the planar network level. Combination of these relations with matrix-inclusion problems of the Eshelby-Laws type yielded closed-form semi-analytical expressions for the paper stiffness tensor, as a function of fibre stiffness and porosity. The self-consistent linear elastic model, which highlighted the importance of the fibre's anisotropy for the overall elastic behaviour, was confirmed by various multiscale experiments[1]. We here build upon our excellent results for the linear elasticity of planar networks to predict their strength. Given the self-consistent nature of our linear elastic model, stresses in single fibres are stresses in fibre-fibre bonds, and vice-versa. Therefore, we use a self-consistent linear elastic model-adapted Tresca-like function to connect the elastic limits of fibre-fibre bonds (that is of "single fibres") and planar networks. More specifically, we use the concentration relations derived from the linear elastic model, as well as the aforementioned Tresca-like function, to upscale 5-, 50-, and 95%-quantiles of a lognormally distributed sample of ultimate in-plane (mode II) shear strength of "unbeaten" unbleached softwood pulp fibre-fibre bonds to the yield in-plane uniaxial tensile strength of corresponding networks.

RESULTS AND DISCUSSION

Predictions based on the 50%-quantile almost perfectly agree with experiments on the yield in-plane uniaxial tensile strength of laboratory paper sheets of variable porosity (see Figure 1). These results emphasize the role of inter-fibre bond shear strength in the overall strength behaviour of the planar network and suggest that the presented linear elastic strength model may very well constitute an additional support tool in the design of paper production processes.

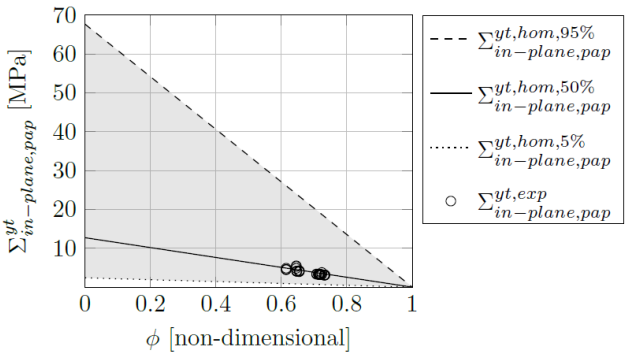

Figure 1: Experimental validation of micromechanics-based linear elastic strength model

CONCLUSION

The excellent agreement between our predictions and the corresponding experiments, strongly indicates that the elastic and strength properties of paper (and more generally of planar fibrous materials, such as thin films), can be accurately, micromechanically predicted from the elastic properties of the fibres leading to their formation, and from the strength properties of bonds between them – respectively. Future research efforts include the expansion of this model to other material classes and related symmetries, as well as to more complex mechanical phenomena.

REFERENCES

[1] P.M.J.S. Godinho, L. Wagner, V. Vass, J. Eberhardsteiner, C. Hellmich: A continuum micromechanics approach to the elasticity of planar fiber networks and its application to paper. In: “CD-ROM Proceedings of the World Conference on Timber Engineering (WCTE 2016)”, J. Eberhardsteiner, W. Winter, A. Fadai, M. Pöll (Eds.); published by: Vienna University of Technology; Grafisches Zentrum HTU GmbH, Vienna, 2016, ISBN: 978-3-903039-00-1 (2016), Paper-Nr. 1074.

Research Field *Chemical technology and Bioscience*

Chairs and Reviewer:

Halbwirth, Heidrun
Assistant Prof. Dipl.-Ing. Dr.techn.

E166 - Institute of Chemical Engineering
heidrun.halbwirth@tuwien.ac.at

Marchetti-Deschmann, Martina
Associate Prof. Mag.rer.nat. Dr.rer.nat.

E164 - Institute of Chemical Technologies and Analytics
martina.marchetti-deschmann@tuwien.ac.at

Introduction

Chemistry, biology and biochemistry are key disciplines of the 21st century matching the ever increasing demand for environmentally-friendly raw materials and bioactive compounds, novel product-specific materials as well as an ever evolving characterization of the materials used with regard to product safety and biological compatibility. Under the influence of limited natural resources and significant signs of climate change, the interface between chemistry and biology is expected to have great potential for solving current problems and developing biologically based innovations.

These research areas have a long tradition at the TU Wien, which goes back to the founding years of the University. Today, the Faculty of Technical Chemistry focuses on networked research in three main research areas (i) CHEMISTRY AND TECHNOLOGY OF MATERIALS, (ii) SUSTAINABILITY, ENERGY AND ENVIRONMENT, and (iii) BIOSCIENCE TECHNOLOGY. Research ranges from knowledge-oriented basic research to developments with high application relevance. In the field of Chemistry and Technology of Materials, the focus is on materials with special physical, chemical and electrochemical functions, on chemical, biochemical and physical processes at biological, organic and inorganic surfaces and interfaces, on sintered and composite materials as well as on a comprehensive material characterization. In the area of Sustainability, Energy and Environment, research at the TU Wien particularly focuses on the developement of viable concepts for the use of biomass for the production of heat and electricity, with sustainable, high-quality use of raw materials within product-oriented or fuel-oriented biorefineries, with environmental chemistry and technology as well as with the development of new catalyst systems for biological transformations and efficient and novel processes in the context of Green Chemistry. In the field of Biosciences Technology, the Technische Universität Wien deals with biochemical, biotechnological and analytical approaches to the production of various bioactive molecules within the framework of white, red and green biotechnology. The focus is on the production as well as structural and functional characterization of proteins, development of bioinstrumentation and innovative bioprocess technology, molecular diagnostics and bioindicators for application in health, hygiene and food safety, as well as the identification, development and production of low molecular weight bioactive substances, in particular from post-growing raw materials.

CHARACTERIZING THE PERFORMANCE OF THE BARRIER DISCHARGE IONIZATION DETECTOR FOR GAS CHROMATOGRAPHY

Maria Antoniadou[a,b], Erwin Rosenberg[a], George A. Zachariadis[b]

[a]E164 - Institute of Chemical Technologies and Analytics
[b]Aristotle University Thessaloniki, Thessaloniki, Greece

INTRODUCTION

The barrier discharge ionization detector (BID) has very recently been introduced as a new detector for gas chromatography (GC-BID). It is based on detecting the electron current formation by the ionization of the analytes eluting from the GC column in a Helium plasma [1]. The dielectric barrier discharge was initially used for industrial purposes [2] and, later, as an excitation source for analytical applications in spectroscopy [3].

The present work focuses on the performance evaluation of the commercial GC-BID instrument, as a systematic study of the analytical capabilities and figures of merit is still missing in the literature [4]. This task was addressed by analysing a large set of standard compounds from several compound classes and evaluating and comparing the results with those of the flame ionization detector (FID). Interesting differences in response behaviour were observed between the BID and the FID.

PROBLEM DESCRIPTION AND EXPERIMENTAL APPROACH

Although the GC-BID system is claimed to be usable with a large variety of analytes, only few studies verify these theoretical assumptions. Most of the studies concentrate on the detection of oxidised gaseous compounds like formic acid, acetic acid [5], CO_2, N_2O [6], where the BID is expected to challenge the FID in sensitivity, as well as a limited number of other compounds including water [7], FAME, ethyl- and pentylbenzene, C_9-C_{10} alkanes and few others [4]. For that reason a complete determination of the instrument's characteristics is important as this will indicate the type of analysis that the instrument is most suitable for.

The experiments consisted of the analysis of various compounds from the following compound classes: anilines, halogens, cyclic compounds, alkanes, aromatics, phenols, esters, alcohols. Standards were prepared in five concentrations ranging from 1 to 0.0001 μg μL^{-1} and were analysed by both GC-BID and GC-FID systems. The analytical methods in both systems were similar. (Restek RTX5-MS column, 30 m×0.25 mm, 0.25 μm film thickness, temperature gradient from 50 to 250 in 10 min; 1 μl automatically injected in split mode (20:1 split) at 250°C; detector at 300°C; 17 min total run time). Additional experiments were performed on the GC-BID instrument to test further characteristics as the dependence of the response on molecular structure. The additional standards used for this task included cyclic ketones, cycloalkanes, PAHs and alcohols, aromatics, alkanes with different solvent.

Analytical characteristics like calibration curve, sensitivity, precision, limits of detection (LOD) and quantification (LOQ) were determined from the above-mentioned measurements. Finally, the effect of the operating conditions like purge flow and discharge gas flow rate were investigated.

RESULTS AND DISCUSSION

The evaluation of GC-BID response demonstrated a generally higher sensitivity in comparison to the FID by a factor of 4.1 on average. Fig.1 shows an example for one compound class. The

calibration curves typically had coefficients of determination higher than 0.999 for both detectors. The precision was investigated for measurements during the same day and the relative standard deviation (RSD%) was less than 5% for the majority of the cases. LODs ranged from 0.043 to 1.47 ng s^{-1} for the GC-BID and 0.08 - 5.1 ng s^{-1} for the GC-FID.

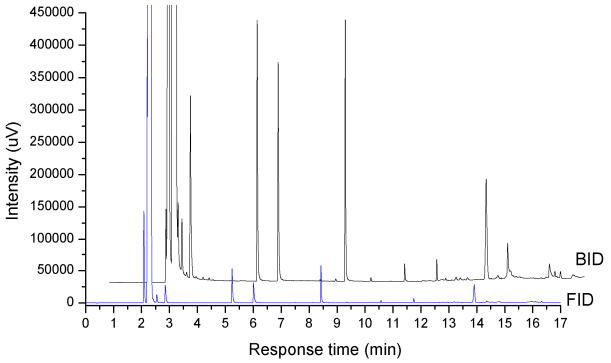

Fig. 1: Chromatogram comparison with BID and FID analysis. Upper: esters-BID, lower: esters-FID.

Fig. 2 shows the evaluation of GC-BID response for n-alkanes with carbon number C10-C17. A clear decrease of peak area response is seen with increasing carbon number. This confirms the concentration dependant behaviour of the BID detector. Also, the operating conditions like purge flow rate and discharge gas flow rate were found to significantly influence the detector response.

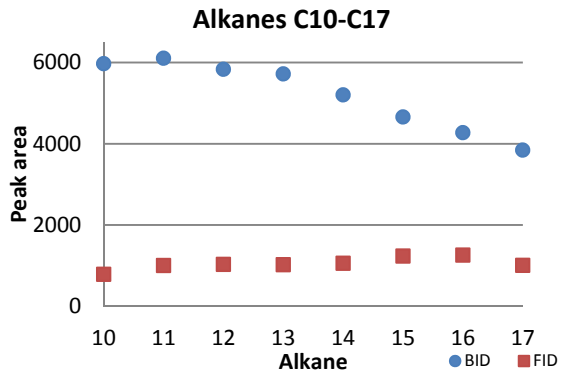

Fig. 2: BID and FID response for an alkane standard C_{10}-C_{17}.

CONCLUSION

The thorough examination of the GC-BID performance in comparison to the GC-FID allowed to better understand its operating principle and optimum operating conditions: As the generation of detector response is more likely achieved by photoionization, rather than the ionization of carbon fragments formed in the combustion of organic compounds in the FID, the response is not mass-flow but rather concentration dependent. Moreover, considerable differences in the specific response of different compound classes exist, while the BID proved to be superior to the FID in terms of sensitivity. These findings will be used to operate the BID under optimum conditions in applications requiring high sensitivity and high time resolution, as achievable by the implementation of a particular modulation technique based on the Hadamard transform.

ACKNOWLEDGMENT

Financial support of this work through the Austrian Research Promotion Agency (FFG) under Project no. 858298 (“DianaBatt”) is gratefully acknowledged.

REFERENCES

[1] Shinada, K., Horiike, S., Uchiyama, S., Takechi, R., Nishimoto, T., Shimadzu Review, 2012.

[2] Kogelschatz, U., Plasma Chem. Plasma Process. 23, 1-46, 2003.

[3] Guo, C., Tang, F., Chen, J., Wang, X., Zhang, S., and Zhang, X., Anal. Bioanal. Chem. 407, 2345-2364, 2015.

[4] Franchina F. A., Maimone, M., Sciarrone, D., Purcaro, G., Tranchida, P. Q., Mondello, L., J. Chromatogr. A 1402, 102–109, 2015.

[5] Ueta, I., Nakamura, Y., Fujimura, K., Kawakubo, S., Saito, Y., Chromatographia 80, 151–156, 2017.

[6] Pascale, R., Caivano, M., Buchicchio, A., Mancini, I. M., Bianco, G., Caniani, D., J. Chromatogr. A 1480, 62-69, 2017.

[7] Frink, L. A., Armstrong, D. W., Food Chem. 205, 23–27, 2016.

DEVELOPMENT OF BIOGAS UPGRADING PROCESSES FOR DEVELOPING AND EMERGING COUNTRIES

Simone Spitzer, Martin Miltner, Michael Harasek

E166 Institute of Chemical, Environmental & Biological Engineering

INTRODUCTION

Farmers in developing and emerging countries could reduce their dependency on fossil energy sources dramatically by producing their own biogas with agricultural waste. In order to use this biogas as fuel, which is the most promising valorisation route in this case, CO_2 and other harmful impurities have to be removed[1]. Usually, farmers in these countries can afford cheap biogas upgrading plants with poor performance at the utmost. Hence, development of alternative upgrading concepts for these countries is important to broaden the usage of renewable and sustainable biogas.

FUNDAMENTALS OF THE PROBLEM

In Brazil, the chosen model region, biogas is typically produced in simple fixed-dome digesters. Investigation on real biogas data from Brazilian farmers showed that the composition of biogas produced in these simple digesters is changing strongly over time. Additionally, hazardous components like H_2S are predominant due to using manure as a major substrate. According to these results, two promising biogas upgrading concepts were developed. Both involve membrane separation technology for CO_2 removal, as this technology has low investment and operation costs, is easy in operation and thus, suitable for biogas upgrading plants in developing and emerging countries.

RESULTS AND DISCUSSION

First concept of a suitable biogas upgrading process comprises membrane based mobile upgrading plants travelling from one biogas plant to another for upgrading the raw biogas. Thereby, investment costs for single farmers are significantly reduced and thus, made affordable for them. For mobile plants various requirements like minimum space and weight demand, fast start up time or vibration resistance due to poor road conditions have to be met. Additionally, the process must be able to deal with the feed quality described above.

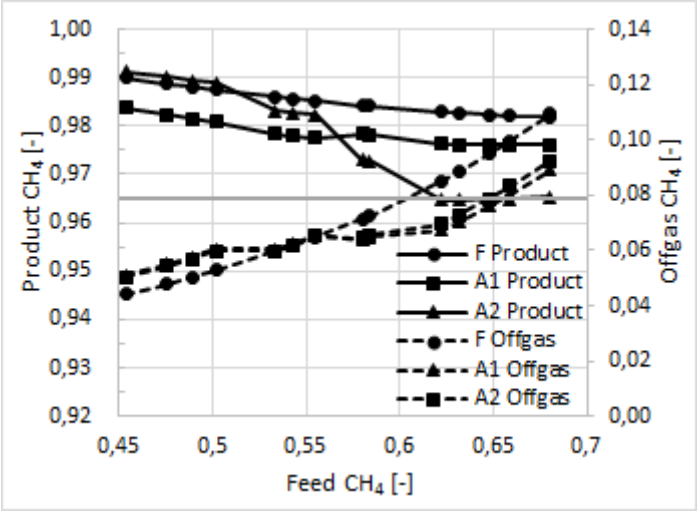

Figure 1: CH_4 concentration in product and off gas stream for different feed compositions at 10 bar. Grey line indicates the biomethane limit of 96.5 %. F = design with fixed membrane area, A1 and A2 = designs with adjustable area

Second concept is based on a hybrid CO_2 removal step for stationary biogas upgrading plants connected by pipelines with several farmers. Therefore, PSA (pressure swing adsorption) and water scrubbers, which are already available as Brazilian technology, are combined with a cheap membrane separation step. Thus, purity of the product stream will be enhanced while methane loss into the off gas will be reduced significantly.

Until yet, research was done primarily for the first concept. Investigation of different upgrading processes for CO_2 removal (scrubbers, PSA, and membrane separation) showed that membrane separation could fulfil the defined requirements at best. Additionally, two pre-treatment steps were defined for removing water and minor impurities like NH_3, H_2S, O_2 and siloxanes. Water and NH_3 are removed by cool-drying. Desulphurization and removal of O_2 and siloxanes are carried out by combining two adsorption steps using iron oxide and activated carbon as adsorbent.

Influence of feed quality and design of the membrane step on the performance was investigated by process simulation in Aspen Plus®. Simulation was carried out for the whole process with focus on the membrane separation step. A model for gas permeation was used based on the solution-diffusion model and validated in several applications[2,3,4]. Performance was investigated for designs with fixed membrane area and with membrane area adjustable to the incoming feed composition. As Figure 1 shows, performance of all designs was high enough for a broad range of incoming biogas compositions to meet the Brazilian biomethane limit of 96.5 %[5] in the product stream. At high CH_4 concentrations in the feed this criterion led to quite high CH_4 loss into the off gas when using designs with fixed membrane area. In comparison, designs with membrane area adjustable to the incoming feed composition were able to reduce the CH_4 loss into the off gas significantly at high CH_4 concentrations in the feed, while product quality remained above the biomethane limit.

CONCLUSION

Equipment for mobile biogas upgrading plants has to cover various requirements. Especially, high product quality has to be achieved for a broad range of feed compositions with the same equipment. Process simulation in Aspen Plus® showed that various designs of membrane based CO_2 removal are applicable for mobile biogas upgrading plants producing biomethane with high quality.

Further investigation of the chosen concepts will be carried out with focus on stationary biogas plants based on hybrid CO_2 removal. Therefore, performance of existing PSA and water scrubber based Brazilian biogas upgrading plants will be evaluated. Process modelling and simulation will be used for investigating and optimizing the performance of various designs for hybrid CO_2 removal.

ACKNOWLEDGEMENT

This work is supported by Vienna Business Agency. The research team is grateful to the project partners SpiritDesign and CIBiogás for supporting the work.

REFERENCES

[1] M. Miltner, A. Makaruk, M. Harasek, Application of Gas Permeation for Biogas Upgrade - Operational Experiences of Feeding Biomethane into the Austrian Gas Grid, 16th European Biomass Conference & Exhibition - Proceedings, 2008.

[2] T. Lassmann, M. Miltner, M. Harasek, A. Makaruk, W. Wukovits, A. Friedl, The purification of fermentatively produced hydrogen using membrane technology: a simulation based on small-scale pilot plant results, Clean Technologies and Environmental Policy, 18, 315–322, 2016.

[3] D. Rodrigues, D. Foglia, W. Wukovits, A. Friedl, Model development of a membrane gas permeation unit for the separation of hydrogen and carbon dioxide, Chemical Engineering Transactions, 21, 1303–1308, 2010.

[4] A. Makaruk, "Numerical modeling, optimization and design of membrane gas permeation systems for the upgrading of renewable gaseous fuels," Dissertation, Institute for Chemical Engineering, Technische Universität Wien, Vienna, 2011.

[5] Agência Nacional do Petróleo Gás Natural e Biocombustíveis, Estabelece a especificação do Biometano contida no Regulamento Técnico ANP nº 1/2015, parte integrante desta Resolução, Resolução ANP Nº 8, 2015.

MICROFABRICATED BIOCOMPATIBLE HYDROGELS

Stefan Baudis[a], Elise Zerobin[a], Zuzana Tomášiková[a], Xiao-Hua Qin[a], Marica Markovic[b], Peter Gruber[b], Jürgen Stampfl[b], Aleksandr Ovsianikov[b], Robert Liska[a]

[a]E163 - Institute of Applied Synthetic Chemistry
[b]E308 – Institute of Materials Science and Technology
stefan.baudis@tuwien.ac.at

INTRODUCTION

Lithography-based additive manufacturing technologies ("3D printing") enable the generation of arbitrary, highly complex 3D structures with very high resolution. This was one of the main aspects, which attracted the interest of modern medicine. The vision is to be able to fill defects in tissues or whole organs with tailor-made, patient-specific, biocompatible polymeric constructs, which promote the regeneration of the tissue or the organ. Hydrogels are an ideal basis for soft tissue regeneration as the mechanical properties match with these of natural tissue and nutrients as well as metabolites can migrate through the constructs easily. The concept is to mimic the extracellular matrix (ECM) by modification of the natural components with crosslinkable groups and to encapsulate cells by spatially resolved photopolymerization using the 2-photon-technology.

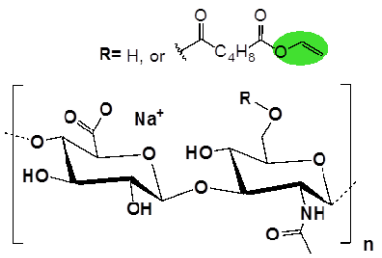

HAVE

Figure 1: Structure of hyaluronic acid vinyl esters (HAVE).

Hyaluronan (HA) is a major component of the ECM. The introduction of double bonds to the back bone of HA enables the production of photocrosslinked, biocompatible hydrogels. Functionalization with (meth)acrylates is not unfavourable due to inherent cytotoxicity. The low cytotoxicity of vinyl esters in combination with the superior photo-reactivity as thiol-ene system makes vinyl esterfunctionalized HA (HAVE, Figure 1) an interesting candidate for biomaterial constructs for tissue engineering.[1]

EXPERIMENTS / FUNDAMENTAL OF THE PROBLEM / EXAMINATIONS

HAVEs were synthesized from HA with different molecular weights by lipase catalyzed transesterification with divinyl adipate (DVA).[1] Formulations with varied macromer contents were prepared and their reactivity was examined by photorheology (Figure 2). Additionally, the influence of the addition of different thiol-based chain transfer agents was investigated. The slope of the storage modulus from rheometric curves was taken as a measure for the reactivity whereas the final storage modulus was used to calculate the mesh size of the hydrogels as reference value for the crosslink density. The swellability of ready-cured hydrogels was determined as complementary parameter. Cell compatibility of HAVEs were assessed by metabolic as well as DNA assay. An exemplary HAVE based formulation was used for the encapsulation of murine fibroblast cells by 2-photon polymerization (2PP) based microfabrication.[2] The viability of the encapsulated cells was assessed by calcein staining.

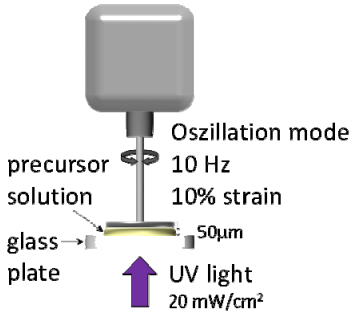

Figure 2: Photorheology (Scheme).

RESULTS AND DISCUSSION

HA can be transformed to biocompatible HAVE by lipase-catalyzed transesterification reaction with DVA in high yields. The degree of substitution (DS) is easily adjusted by variation of reaction time. Macromer content, macromer size, and/or DS determine the material properties on demand (Figure 3).

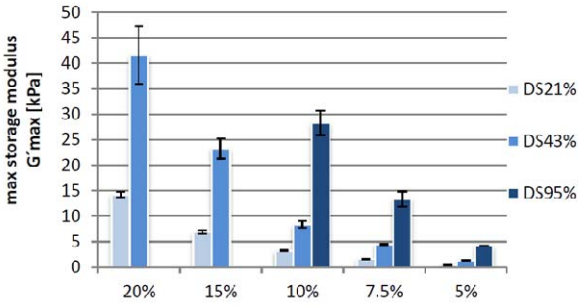

Figure 3: Photorheology results.

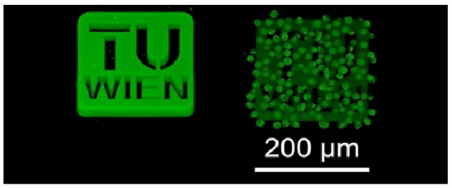

Figure 4: Encapsulated cells in cross-linked HAVE.

Moreover, the variation of the chain length of the thiol component offers an additional adjustment possibility for the properties of the hydrogels.

The cytocompatibility of the synthesized macromeres enables the fabrication of 3D hydrogel constructs with encapsulated cells by laser fabrication using 2PP (Figure 4).

CONCLUSION

HAVEs were found to be a promising modular material platform to engineer 3D hydrogel constructs as environment for living cells. Still, the material is very brittle, therefore ongoing research concentrates on toughening on the hydrogels by reinforcement with collagen fibers.

ACKNOWLEDGEMENT

We kindly acknowledge the financial support by the Austrian Research Promotion Agency (FFG, Project Number 849787, S.B.) and the European Research Council (Starting Grant, Project Number 307701, A.O.).

REFERENCES

[1] X.-H. Qin, P. Gruber, M. Markovic, B. Plochberger, E. Klotzsch, J. Stampfl, A. Ovsianikov, R. Liska (2014) Polym Chem 5, 6523-33.

[2] A. Ovsianikov, V. Mironov, J. Stampfl, R. Liska (2012) Expert Rev Med Devices 9, 613.

THE EFFECT OF SMALL AMOUNT OF CATALYSTS ON STEAM GASIFICATION PROCESS

Katarzyna Zubek[a,b*], Grzegorz Czerski[a], Stanisław Porada[a]

[a]AGH University of Science and Technology
[b]E164 – Institute of Chemical Technologies and Analytics

INTRODUCTION

Gasification is a clean and effective process of gas generation that may be used to produce power and chemicals or converted into synthetic fuel [1]. Because of these advantages numerous works are conducted in order to improve gasification technology, including addition of catalysts. However, in order to use catalyst on an industrial scale, beyond the high catalytic activity it should be characterized by the low price. These conditions are met by catalysts based on alkali and alkaline earth metals that have gained the greatest popularity [2]. However, the manner in which catalyst affects the process depends on many factors, such as type of fuel subjected to gasification, process conditions, type and amount of catalysts etc. [3]. Therefore, there is a necessity to analyse the kinetics of catalytic coal gasification in order to determine their impact on the process. This is important step providing information needed to design gasifiers. The complexity of the gasification intensified by the addition of catalyst makes that kinetics of this process is still a current issue which requires further research. Because of that, the aim of this study was to analyse the kinetics of gasification of 'Janina' coal with small amount of cations of sodium, calcium and potassium and compare the results with those obtained from non-catalytic gasification process.

EXPERIMENT

Bituminous coal from the Polish mine ‘Janina’ was selected as feedstock for the research. Ions of sodium, potassium and calcium, introduced by wet impregnation method were used as catalysts. Obtained samples of coal contained small amount (1% wt) of the corresponding metal. Isothermal measurements of the gasification process were carried out at 800 °C, 900 °C, 950 °C and 1000 °C under elevated pressure of 1 MPa. Weight of the sample fed into the reaction zone was 1 g, steam flow was 0.3 g/min, while the argon flow (carrier gas) was 20 dm^3/min. In the resulting gas the content of CO was continuously controlled by automatic analyser. In addition, the content of H_2 was analysed using gas chromatographs equipped with thermal conductivity detector (TCD). Based on the concentrations of the main components of the resulting gas (CO and H_2) the yields of these gases were determined and kinetics parameters of CO and H_2 formation reaction were calculated. For this purpose the Grain Model (GM) was used, described by equation 1.

$$\frac{dX}{dt} = k_{GM}(1-X)^{\frac{2}{3}} \quad (1)$$

where:

k- kinetic rate constant
X- degree of conversion

RESULTS AND DISCUSSION

The results have shown that the yields of the hydrogen were much higher than CO but this difference decreased with increasing temperature of the process. This effect resulted from the

increasing amount of CO at higher temperatures. The addition of any catalysts increased the yields of both H_2 and CO compared to non-catalytic process, however, only at lower temperatures.

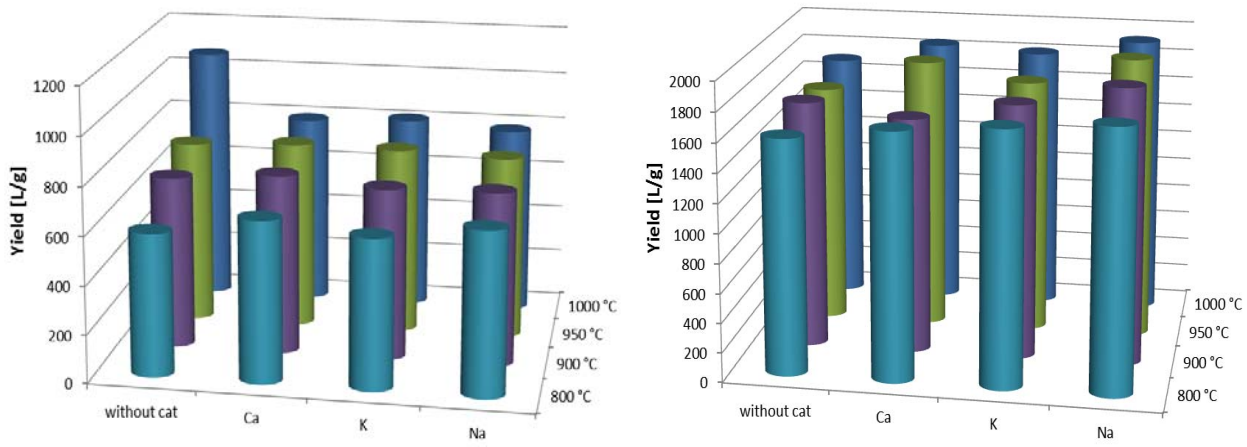

Figure 1 Yield of CO (a) and H_2 (b) from steam gasification process at various temperatures and with/without addition of various catalysts

Activation energies of CO and H_2 formation during non-catalytic coal gasification were the highest and simultaneously very similar. The addition of catalysts caused their significant reduction in a various way. The values of activation energy of CO formation were irrespective of the catalyst used and ranged between 52.1 and 55.2 kJ/mol. In case of E_a of H_2 formation differences were bigger - from 46.9 (Na) to 56.8 (Ca). The results confirmed the catalytic activity of alkali and alkaline-earth metals in the gasification process.

'Janina' coal	CO		H_2	
	A [1/min]	**E_a [kJ/mol]**	**A [1/min]**	**E_a [kJ/mol]**
	Grain Model			
without catalyst:	57.9	80.3	20.2	72.4
with addition of:				
➢ Na^+	2.8	52.1	1.4	46.9
➢ K^+	6.7	55.2	5.0	56.3
➢ Ca^{2+}	3.0	53.1	4.0	56.8

Table 1 Kinetics parameters (activation energy E_a and pre-exponential factor A) of CO and H_2 formation reactions

CONCLUSION

The obtained results have proven that even small amount of properly selected catalyst can improve the gasification process, thus increasing the chances of wider industrial use. Further work will involve examination of 'Janina' coal gasification process with various (greater) amount of catalysts based on alkali and alkaline earth metals.

REFERENCES

1. E. Mostafavi, N. Mahinpey', , M. Rahman, M.H. Sedghkerdar, R. Gupta, High-purity hydrogen production from ash-free coal by catalytic steam gasification integrated with dry-sorption CO_2 capture, Fuel, **178**, 272–282 (2016).
2. L. Zhang, S. Kudo, N. Catalytic effects of Na and Ca from inexpensive materials on in-situ steam gasification of char from rapid pyrolysis of low rank coal in a drop-tube reactor, Fuel Process Technol, **113**, 1-7 (2013).
3. F. Kapteijn, G. Abbel, J. A. Moulijn, CO_2 gasification of carbon catalyzed by alkali metals: reactivity and mechanism, Fuel **63**, 1036-1042 (1984).

ACTIVE METHOD OF MERCURY CAPTURE FROM SUBBITUMINOUS AND LIGNITE COAL COMBUSTION

Marta Marczak[a,b], Piotr Burmistrz[b], Mateusz Karczewski[b]

[a]E164 - Institute of Chemical Technologies and Analytics
[b]AGH – University of Science and Technology, Kraków, Poland

INTRODUCTION

The fossil fuels combustion, in particular coal, is a major source of emissions of pollutants into the environment. Out of many pollutants with the specific threat for the environment, heavy metals, including mercury are of higher importance [1]. Mercury is one of the few elements, on which the human body does not show any physiological requirements. Due to its toxicity, global distribution of emission sources, long residence time in the ambient air, ease of ingress into the aquatic environment and ability to penetrate the trophic chains, mercury and its compounds have been recognized by the US Environmental Protection Agency (US EPA) as a special threat air pollution [1.2].Global research, commissioned by the UNEP (United Nations Environment Programme), confirmed the high impact of mercury on the environment and fully justify taking action on an international scale, which is aimed at reducing its emission [3]. According to estimates [3], in 2010 in the world, approximate 1960 Mg of mercury from anthropogenic sources has been issued, of which 45% accounted for emissions from the combustion of coals [4]. Poland is a country with one of Europe's largest mercury emissions to the atmosphere. The main source of mercury emissions is the burning of fossil fuels, particularly coal. It is the main, by more than 50% of the share, the source of mercury emissions to the atmosphere.

EXPERIMENTS / FUNDAMENTAL OF THE PROBLEM / EXAMINATIONS

The aim of the experiment was to determine the impact of the selected emission reduction process waste sorbents of mercury from the flue gas. For the incineration of selected bituminous coal and lignite-derived from Polish mines. The samples were air-dried into analytical state and were analysed with a mercury content on the DMA-80. Characteristics of selected Polish coals was presented in [5]. Specified fuel parameters (Proximate and ultimate analysis) affecting the behaviour of mercury in coal combustion process were determined. The sorbent with low levels of mercury in the flue gases emitted during the combustion of coals, coke dust was coming from the process of dry coke cooling. Coke dust are macroporous materials. The influence of size faction of the particles on the reduction of mercury emission in flue gases. Dust and coke with a diameter of grains above 0.2 mm, below 0.08 mm were used. The scheme of the mercury emission reduction experiment is shown in Fig. 1. A sample of coal to the furnace was placed at a temperature of 850 °C and was burned in the air stream with the movement of 8 $m^3 \cdot h^{-1}$. The sorbent was placed at the exit of the flue gases. The concentration of mercury measured in the ash was determined in sorbent before and after the process and flue gas going into the air.

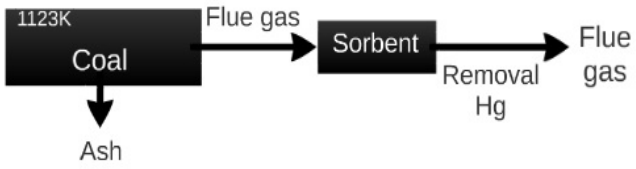

Fig.1: Laboratory scale mercury emission reduction system

RESULTS AND DISCUSSION

Application of coke dust in order to reduce the concentration of mercury in the exhaust gas during combustion of coal turned out to be effective (Table 1). Depending on the diameter of grains, it lowered emissions of Hg by 80-90% for subbituminous coals combustion. Despite the fact that lignite is characterised by much higher mercury levels and unfavourable composition of the example equation, the use of coke dust, in this case, was effective and lowered the concentration of Hg in the flue gas by 60-70% (Table 1).

Table 1. Contents of mercury in the sorbent after the cleanup process, the ashes and the concentration of Hg in the flue gas.

Type of used coal	Coke dust fraction, x [mm]	$\Delta C_{Hg,sorbent\ after\text{-}before}$ [µg·kg^{-1}]	$C_{Hg,coal}$ [µg·kg^{-1}]	$C_{Hg,ash}$ [µg·kg^{-1}]	$C_{Hg,flue}$ [µg·m^{-3}]	Removal [%]
Subbituminous	x > 0,2	85,61	103,70	1,56	1,01	**82,6**
	x < 0,08	95,20	103,70	2,40	0,43	**91,9**
Lignite	x > 0,2	270,20	443,50	2,67	6,96	**61,1**
	x < 0,08	319,5	443,50	1,29	4,92	**72,1**

CONCLUSION

Proposed in the experiment method of application of coke dust to reduce mercury emissions in the exhaust gases as the several tens of times cheaper substitution of commercial activated coal with much less polluting the environment at the production stage and with a very interesting property aspects of its sorptive surface. The results obtained in laboratory studies have shown reduction Hg in the flue gas during combustion of subbituminous and lignite coal respectively level 80 - 90% and 60 - 70 %.

REFERENCES

[1] US EPA, Mercury study report to Congress, EPA-452/R-97-003, US EPA Office of Air Quality Planning and Standards, US Government Printing Office, Washington DC 1997.

[2] US EPA, A study of hazardous air pollutant emissions from electric utility steam generating units. Final Report to Congress, EPA-453/R-98-004a; US EPA Office of Air Quality Planning and Standards, US Government Printing Office, Washington DC 1998.

[3] Burmistrz P., Kogut K., Marczak M., Zwoździak J.: Lignites and Subbituminous Coal Combustion in Polish Power Plants as a Source of Anthropogenic Mercury Emission, Fuel Processing Technology, vol. 152, p. 250–258, 2016.

[4] Burmistrz P., Czepirski L., Kogut K., Strugała A.: Removing mercury from flue gases. A demo plant based on injecting dusty sorbents, Przemysł chemiczny, 93/12, 2014.

[5] Marczak M., Burmistrz P., Kogut K.:. Coal combustion as a source of mercury emission to environment, Rtęć w środowisku : identyfikacja zagrożeń dla zdrowia człowieka pod red. Lucyny Falkowskiej. Wydawnictwo Uniwersytetu Gdańskiego, p. 11–16, 2016.

SOLID-STATE POLYMERIZATION OF HAIRY-ROD POLYIMIDES

M. Josef Taublaender, Daniel Glöcklhofer and Miriam M. Unterlass*

E165 - Institute of Materials Chemistry

INTRODUCTION

Fully aromatic polyimides (PIs), such as poly(*p*-phenylene pyromellitimide) (PPPI; chemical structure see Figure 1 right), show outstanding mechanical, thermal and chemical properties.[1] As a matter of fact, most PIs are practically insoluble in all common solvents and do not melt when heated. Instead, they simply decompose at very high temperatures. These features impart their use *e.g.* in gas separation membranes or aeronautics applications. All of the just mentioned extraordinary properties can be traced back to PIs' molecular structure: Their polymer backbone is entirely stiff. Therefore, PIs belong to the family of rigid-rod polymers.

EXPERIMENTAL PART

However, the aforementioned superior properties of PIs come hand in hand with their major drawback: difficult processability and synthesis under harsh and demanding conditions.[2] Classically, usually stepwise procedures (Figure 1 A) employ high-boiling, toxic solvents, such as dimethylformamide (DMF), and toxic catalysts, such as isoquinoline. Furthermore, long reaction times (t > 8 h) at elevated temperatures (T up to 450 ˚C) are necessary. In a first step an aromatic dianhydride and an aromatic diamine, *e.g.* pyromellitic dianhydride and *p*-phenylene diamine, are converted into a high-molecular weight polymeric intermediate. This soluble poly(amic acid) species allows for processing *e.g.* into fibers, films or coatings. In a subsequent curing step the desired insoluble, infusible PI product (here PPPI) is obtained.

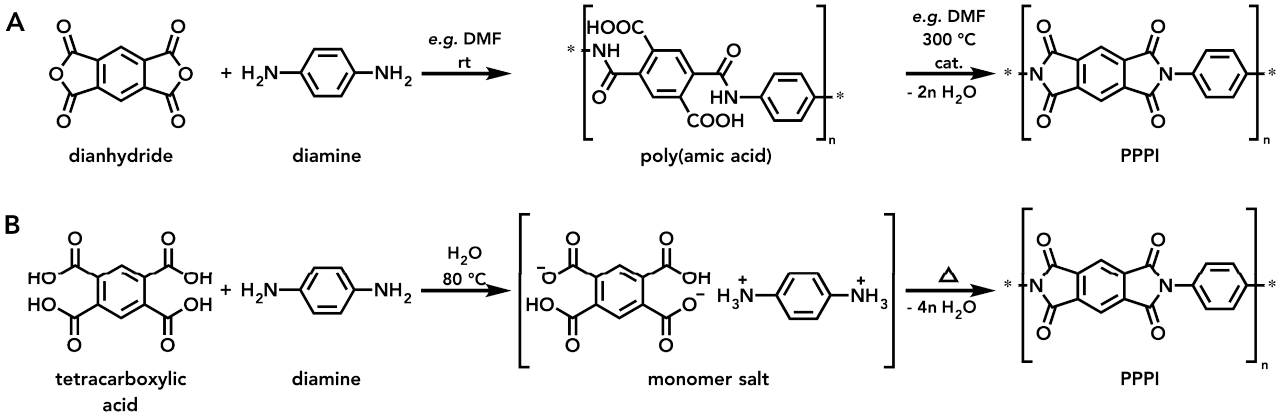

Figure 1: A - Classical two-step procedure to PPPI from pyromellitic dianhydride and *p*-phenylene diamine comonomers. Poly(amic acid) intermediate is soluble and hence solution-processable. B - Solid-state polymerization of PPPI *via* a monomer salt.

In contrast to conventional PI syntheses there are a number of non-classical approaches that avoid the utilization of toxic solvents and catalysts. Hence, such methods can be classified as "green" and are therefore of great scientific, ecological and economic interest. Among these alternative procedures a rather simple one is solid-state polymerization (SSP).[3,4] SSP is a solvent-free polymerization technique that involves heat treatment of appropriate starting materials at temperatures below their melting point. For the SSP of PIs it is advantageous to use monomer salts as starting materials, as they intrinsically provide ideal stoichiometry of comonomers, which is of

the utmost importance in order to obtain high-molecular weight polymers. Furthermore, in contrast to aromatic diamines monomer salts are completely stable under ambient conditions and can be stored without special precautions. Such monomer salts are simply prepared by an acid-base reaction between the comonomers (Figure 1 B, first step). Subsequent heat treatment (Figure 1 B, second step) directly yields the final PI product (in this case PPPI), which is hardly soluble or fusible. In further consequence, this leads to severe processing issues. The goal of the presented project is to improve the processability of PIs by developing a family of potentially malleable monomer salt systems by introducing flexible side chains.

RESULTS AND DISCUSSION

In order to design processable PIs, we attached flexible side chains to PPPI's backbone (Figure 2, R = *n*-alkyl side chain, respectively), so that the rigid-rod nature and hence the high-performance properties are potentially retained. Such a macromolecule - which has a rigid polymer backbone with pendent, flexible side chains - is commonly termed hairy-rod polymer.

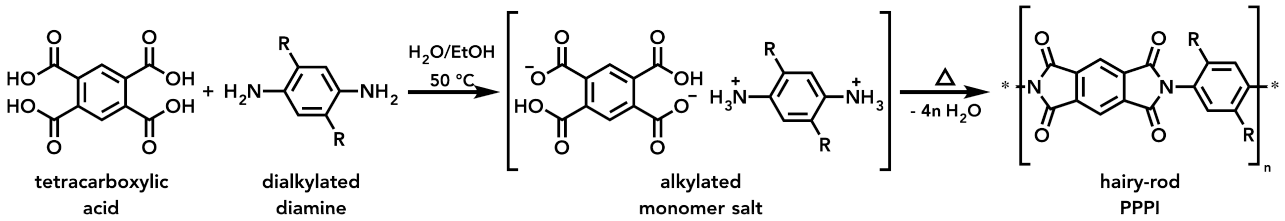

Figure 2: Reaction of pyromellitic acid and a dialkylated aromatic diamine to yield a monomer salt (first step) and subsequent SSP to obtain a hairy-rod polymer (second step). R = *n*-octyl, *n*-decyl, *n*-dodecyl, *n*-tetradecyl side chain.

In this contribution we present our investigation of the influence of aliphatic side chains on *(i)* salt-formation, *(ii)* the ease of SSP, *(iii)* the mechanism of SSP and *(iv)* the resulting hairy-rod PIs' properties and processability. All studied systems were characterized using scanning electron microscopy (SEM), infrared spectroscopy (IR), powder X-Ray diffraction (XRD), *in situ* high temperature XRD (HT-XRD), nuclear magnetic resonance spectroscopy (NMR), thermogravimetric analysis (TGA) and differential scanning calometry (DSC). In contrast to SSPs of all PIs studied to date, it was possible for the first time to observe softening phenomena prior to or during SSP.[4] These phenomena lead to enormous changes in morphology of the polymers as compared to the monomer salts. DSC and HT-XRD measurements reveal several thermal events during elevating the temperature, which might explain these softening phenomena.

CONCLUSION

The hairy-rod PIs' physicochemical properties differ from regular, non-alkylated PPPI. Aside the achieved easier processing, the synthesized hairy-rod PIs are highly interesting for applications in which PIs can conventionally not be applied.

REFERENCES

[1] M. Ballauff, *Angewandte Chemie* **1989**, *28*, 253–267.

[2] P. M. Hergenrother, *High Performance Polymers* **2003**, *15*, 3–45.

[3] K. Kriechbaum, D. A. Cerrón-Infantes *et al.*, *Macromolecules* **2015**, *48*, 8773–8780.

[4] Y. Imai, *Progress in Polyimide Chemistry I* **1999**, Springer, 1–22.

CHARACTERISATION OF THE MICROBIAL WATER QUALITY OF THE DANUBE RIVER AT VIENNA

Katalin Demeter[a,d*], Rita Linke[a,f], Simone Ixenmaier[a,f], Rene Mayer [a,f], Regina Sommer[b,f], Gerhard Lindner[b,f], Christa M. Zoufal-Hruza[c,] Christina Frick[c], Alexander Kirschner[b,f], Julia Derx[f,g], Alfred Paul Blaschke[f,g], Andreas H. Farnleitner[a,e,f]

[a] E166 Institute of Chemical, Environmental and Biological Engineering
[b] Institute for Hygiene and Applied Immunology, Medical University of Vienna, Austria
[c] Municipal Department 39, Laboratories of Environmental Medicine, Vienna City Administration, Austria
[d] Center for Water Resource Systems, TU Wien, Karlsplatz 13, A-1040, Vienna, Austria
[e] Research Unit Water Quality and Health, Karl Landsteiner University of Health Sciences, Krems, Austria
[f] Interuniversity Cooperation Centre for Water and Health, Austria, www.waterandhealth.at
[g] E222 Institute of Hydraulic Engineering and Water Resource Management
* demeter@waterresources.at

INTRODUCTION

Faecal pollution of water resources intended for human use represents a health risk because of the possible presence of pathogens. Monitoring, risk assessment and management of such pollution is therefore imperative. Although detection of pathogens would seem a logical basis to estimate health risk, for practical reasons they are rarely monitored directly. Instead, microbial water quality has traditionally been assessed using faecal indicator bacteria, a selection of general intestinal bacteria that commonly occur across many animal species but do not live or survive in the environment. Viruses have special characteristics that bacterial indicators only represent to a limited extent. This led to the development of viral indicators.

While these general indicators give a good overall picture about microbial water quality, they do not allow the identification of the pollution source. The microbial source tracking (MST) method consists in the genetic detection of intestinal microbes specific to their host species. It may be applied as a forensic tool to identify the pollution sources, it can be integrated into larger environmental investigation designs or into health risk assessment models. In all of these applications MST can give a crucial contribution in terms of the quantitative apportionment of pollution sources.

Comprehensive management of drinking water resources requires a catchment-to-tap principle. A fundamental first step is to gain a deep understanding of the spatial and temporal dynamics of fecal pollution within the catchment. Riverbank filtrate of the Danube serves as the alternative drinking water resource for the City of Vienna (1.8 million inhabitants). Since numerous pressures affect the Danube during its course to Vienna, the characterization of its water quality requires a complex set of tools as well as an extensive spatial and temporal monitoring.

STUDY DESIGN

Five surface water sampling sites were selected to cover the spatial heterogeneity of this river section. Additionally, samples were taken from major wastewater treatment plants in the greater area of Vienna. Standard and alternative fecal indicators (*E. coli*, intestinal enterococci, *Clostridium*

perfringens, somatic coliphages), genetic MST markers (human-, ruminant- and pig-associated *Bacteroidetes* markers), pathogens (enteric viruses) as well as physicochemical parameters were monitored monthly over a 2.5-year period (2013-2015) to determine the characteristics of the raw water resource.

PRELIMINARY RESULTS

Statistical analysis of this multi-parametric data will be performed to reveal the spatial and temporal patterns, to elucidate which environmental parameters drive these patterns and to gain an insight into the interplay among the various indicators, markers and pathogens. Preliminary results show a moderate level of faecal pollution in the Danube River (*E. coli* median concentration 76 CFU/100ml, range 11-4901 CFU/100ml; intestinal enterococci median concentration 24 CFU/100ml, range 2-1901 CFU/100ml). The pollution is predominantly of human origin (95% occurrence of human MST marker); ruminant and pig sources play only a minor role (44% and 25% occurrence, respectively). Detailed analyses will be presented at the conference.

OUTLOOK

Here we will present the comprehensive characterization of the microbial water quality of the Viennese Danube stretch. Results from this long-term study will also serve as a unique basis for further catchment-based modeling using the QMRAcatch approach[1]. Analysis of current and future pollution and risk scenarios by QMRAcatch will allow to guide target-oriented remediation efforts in the catchment and to estimate required water treatment levels to provide safe drinking water.

This is a joint publication within the Interuniversity Cooperation Centre for Water and Health (www.waterandhealth.at). This study was supported by FWF (Vienna Doctoral Program on Water Resource Systems W1219-N22 and P23900-B22) and the Ground Water Resource Systems (GWRS) project (Vienna Water) as part of the "(New) Danube-Lower Lobau Network Project" (LE07-13).

REFERENCE

[1] Schijven *et al.*, QMRAcatch: Microbial Quality Simulation of Water Resources including Infection Risk Assessment, Journal of Environmental Quality, 44(5), 1491-1502, 2016

COMPUTATIONAL FLUID DYNAMIC ANALYSIS OF COOLING IN A MIXED VESSEL USING A NON-NEWTONIAN MEDIUM

Zsolt Harsfalvi, Christian Jordan, Bahram Haddadi, Michael Harasek

E166 – Institute of Chemical Engineering
Technische Universität Wien, 1060 Vienna, Austria

INTRODUCTION

The increasing social and economic importance of food production, in addition to more complex production technologies requires a more detailed investigation as further development in the quality of the food or in the production efficiency. Creating fruit prep for yogurt production especially in large amounts can have lot of pitfalls, which can lead to either an inefficient, long production time or/and a lower level of food quality. The challenge of the process optimization increases with the higher starch, sugar and pectin content of the food prep which has a high impact of the behaviour of the medium. In case of pasteurization, the medium has a final temperature of 90 °C which has to be cooled down fast to 35 °C to make it ready for further operations. The hot medium will be cooled down during a complicated mixing process with built in heat-exchanger where the viscosity of the non-Newtonian (shear thinning) medium strongly increases with decreasing temperature. To investigate the behaviour of the medium, the operating parameters and their influence on the process in complex cooling vessels Computational Fluid Dynamics (CFD) can be applied.

COMPUTATIONAL FLUID DYNAMICS (CFD)

Computer based simulations allow a detailed analysis of fluid systems. This tool is known as Computational Fluid Dynamics or CFD[1] and it is suitable for solving a wide range of industrial and non-industrial applications e.g.: fluid flow, mass transfer, heat transfer, etc. For the presented problem the non-commercial open source software OpenFOAM®[2] was applied.

MATERIAL MODEL

Due to the non-Newtonian behavior and temperature dependent thermophysical properties a complex property model was needed. The temperature dependence of heat capacity, thermal conductivity and density were modelled by the consideration of the Brix number (44,8 °Brix) of the medium using the experimental results from Carbal[3]. The experiment results for 46,1 °Brix were chosen and approached with polynomial functions in the case of specific heat, thermal conductivity and in the case of density. The value of the specific heat were controlled at few points with the help of calorimetry measurements and in the case of density with pycnometer measurements. The experimental data approached with polynomial regression were applied in the material model.

MEASUREMENTS

Although CFD is a powerful tool, it is important, that the user has a proper knowledge regarding the investigated field. For validation reasons it is helpful to accomplish lab scale measurements parallel to the computation to compare and develop the solver, to obtain reliable results. The CFD simulations and measurements were accomplished on a small mixed vessel, called macro-viscosimeter developed by TU Wien[4]. This device was initially developed to measure viscosity of mediums with large particles and filaments. It has a 10 L volume, a heating/cooling jacket and a simple mixer blade in the centre. This was considered as an ideal device to test and later validate the CFD model. To obtain as much information as possible about the cooling process 8 pieces of

PT 100 temperature sensors were installed into the vessel to investigate the temperature field. The temperature sensors were placed at different wall positions and also in the medium at different heights and radius. An additional help to support the validation process was the torque measurement of the mixer blade during the cooling using a Viscopakt measurement device.

RESULTS AND DISCUSSION

Considering the inefficient mixer blade and the weak cooling power the process time is longer as in industrial cases[5]. Because of the high computational need and relatively small time steps the simulation was calculated only for 25 minutes real time. The result of the comparison of the torque and selected contour plots of the results are shown in Figure 1. The streamlines of the velocity field in the vessel show that the medium is sucked in at the top and at the bottom of the rotating blade and it is pushed out in radial direction at the middle of the blade. This makes it possible that the colder medium at the bottom and at the top reaches the core of the vessel. This progress is clearly visible in the temperature field. The heat exchange and the gradient near to the wall can be also seen as expected. The non-Newtonian rheology can be recognised in the viscosity field - the shear thinning in the vicinity of the mixer blades adversely affects the mixing behaviour.

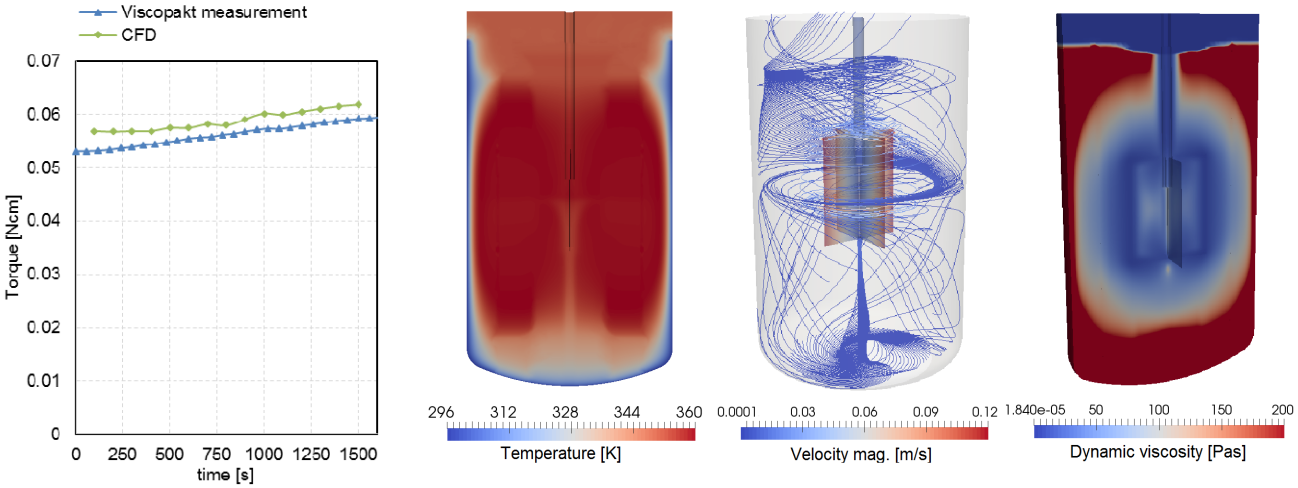

Figure 1 Comparison of the calculated and measured value of the torque (left), selected contour plots[6] of the CFD simulation at t = 1500 s (righ)

CONCLUSION

The comparison of the simulation and the measurement showed promising results using the created material model. To control the reliability of the model, the computation should continue until the end of the cooling process. If the function of the torque and the temperature show the same agreement as in the first 25 minutes, the material model can be used with confidence in other more complicated cooler mixed vessels.

REFERENCES

[1] Fletcher, C.A.J., Computational techniques for fluid dynamics 1, 1988
[2] *OpenCFD Ltd*. <www.openfoam.org> accessed 20.02.2017
[3] Carbal R.A.F., Orrego-Alzate C.E., Gabas A.L., Telis-Romero J., 2007,Rheological and thermophysical properties of blackberry juice, Food Science Technology, 589-596
[4] Pohn S., Kamarád L., Kirchmayr R,. Harasek M., Design Calibration and numerical investigation of a macroviscosimeter. Czech Society of Chemical Engineering (ČSCHI), 1099–1100, 2010
[5] Scargiali F., Busciglio A., Grisafi F., Brucato A., Influence of Viscosity on Mass Transfer Performance of Unbaffled Stirred Vessels, Chemical Engineering Transaction, 32, 1483-1489, 2013
[6] Paraview.org <www.paraview.org> accessed 20.02.2017

GEOPOLYMERS AND INORGANIC MULTIBINDER SYSTEMS

Philipp Lackner[a,b], Roland Haubner[a], Peter Geiderer[b]

[a]E164 - Institute of Chemical Technologies and Analytics, TU Wien
[b]Murexin GmbH

INTRODUCTION

Geopolymers are large 3D molecules that are formed of aluminates and silicates. The term "geopolymer" was invented by Joseph Davidovits as a consequence of combining inorganic monomers ("geo") to a large molecule ("polymer") [1].

As raw materials silicon and aluminum containing materials like fly ash, metakaolin or blast furnace slag are used. Aluminates and silicates have to be dissolved, which is done by high alkaline sodium or potassium silicate solutions and/or sodium or potassium hydroxide solutions. The monomers in the solution poly-condensate to the 3D structure and build up mechanical strength.

Fly ash is obtained at flue gas treatment of coal power stations. Blast furnace slag is a side product of iron production. Metakoalin is formed from kaolin by a thermal treatment at about 750°C [2]. These materials are more environmentally friendly than Portland cement because the materials are waste products and/or need less energy for production (CO_2 footprint) [3].

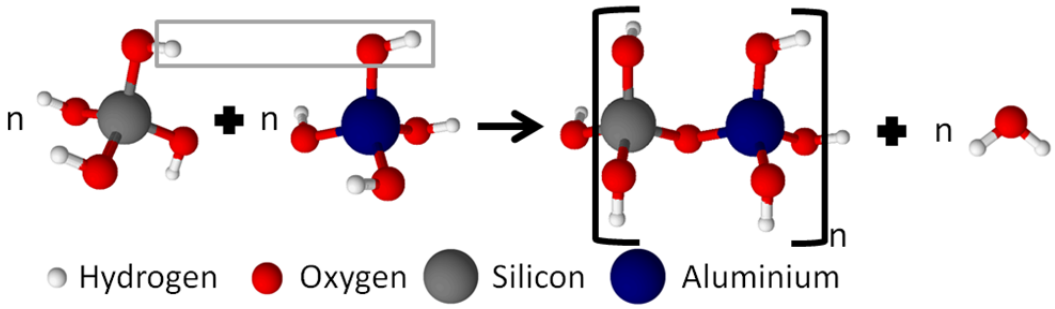

Fig. 1: Condensation reaction

Aluminate and silicate have a tetrahedral structure and react in a condensation reaction to a chain of geopolymer (Fig. 1). In this reaction water is a side product. This is contrary to cementitious reactions were water is chemically fixed in hydrates ("hydration") [4]. As a result of that, one big disadvantage is the high drying shrinkage and crack formation of geopolymer mortars. But geopolymers also have a lot of advantages. They have a high final strength, a heat resistance up to 1200°C and a very good chemical resistance. It is possible to immobilize toxic and radioactive materials in geopolymers because the 3D-structure of the geopolymer confines the harmful substance [5].

The goal of this work is to produce a geopoylmer based on metakaolin, because of its good working performance and to characterize it by TGA-DSC and IR spectroscopy. An additional aim is to improve the geopolymer mortar by combining it with other inorganic binders.

RESULTS

Different metakaolines and activator solutions have been tested. According to a fast strength development, a geopolymer mortar produced from metakaolin, potassium silicate solution with a pH of about 13,5 and a solid content of 45% and quartz sand 0,1-0,7 mm was chosen allowing comparison with other inorganic binders. Fig. 2 shows the drying shrinkage through water evaporation of the geopolymer mortar as a function of different onset times under a poly-ethylene

(PE) sheet. It shows that there is a nearly constant drying shrinkage after the geopolymer reaction has finished.

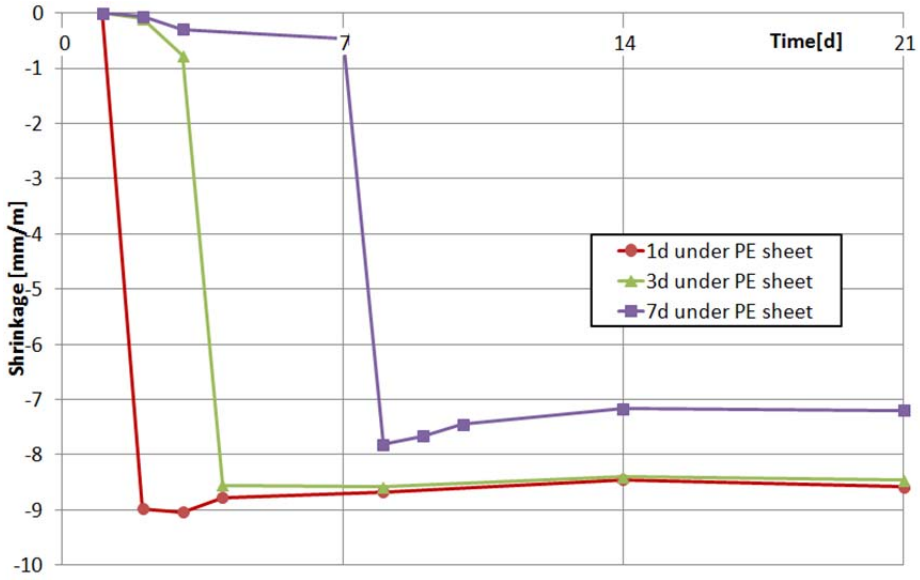

Fig. 2: Shrinkage of a geopolymer mortar during drying after onset times of 1, 3 and 7 days under a PE sheet

The Infrared wavenumber-shift of the asymmetric stretch bond of Si-O-T (T...Si or Al) is characteristic for the geopolmer formation [3][6]. By means of FTIR-spectroscopy with ATR cell, the geopolymer formation was measured. With addition of blast furnace slag to the mortar the shrinkage could be lowered. This can be explained by forming calciumsilicatehydrates C-S-H with the CaO from the slag and the silicate from the activator solution. Also gypsum was added which result in a very fast hardening. Probably this is due to formation of syngenite ($K_2Ca(SO_4)_2 \cdot H_2O$) as a reaction-product of gypsum with potassium from the activator solution.

DISCUSSION AND FORECAST

It was possible to produce a metakaolin based geopolymer and to characterize it by IR spectroscopy. The shrinkage during drying can be reduced by adding blast furnace slag. In the next steps other inorganic binders will be tested.

REFERENCES

[1] Joseph Davidovits, Properties of Geopolymer Cements, published in Proceedings First Internationl Conferece on Alkaline Cements and Concretes, Kiev, 1994, pp. 131-149.

[2] Christine Pélegris, Axel Compere, Ralph Davidovits, „Indirect 3D-printing of MK-750-based geopolymer ceramic“, Geopolymer Camp 2016, St. Quentin.

[3] E. Gasparini *et al.*, “Geopolymers from low-T activated kaolin: Implications for the use of alunite-bearing raw materials,” *Appl. Clay Sci.*, vol. 114, pp. 530–539, Sep. 2015.

[4] Verein Deutscher Zementwerke e.V. (Hrsg.), Zement-Taschenbuch, 51. Auflage, Verlag Bau+Technik GmbH, 2008.

[5] Martin Leute, Präsentation, Geopolymer eine neue Generation zementfreier Bindemittel, Wöllner Austria GmbH, 8111 Gratwein-Strassengel.

[6] P. Rovnaník, “Effect of curing temperature on the development of hard structure of metakaolin-based geopolymer,” *Constr. Build. Mater.*, vol. 24, no. 7, pp. 1176–1183, Jul. 2010.

A COMPLEMENTARY ISOTHERMAL AMPLIFICATION METHOD TO THE U.S. EPA qPCR APPROACH FOR THE DETECTION OF ENTEROCOCCI IN ENVIRONMENTAL WATERS

Claudia Kolm[a,g], Roland Martzy[a,g], Kurt Brunner[a], Robert L. Mach[b], Rudolf Krska[c], Georg Heinze[d], Regina Sommer[e,g], Georg H. Reischer[a,b], Andreas H. Farnleitner[b,f,g]

[a] E166 – Institute of Chemical, Environmental & Biological Engineering, Molecular Diagnostics Group, Department IFA-Tulln

[b] E166 – Institute of Chemical, Environmental & Biological Engineering, Research Group of Environmental Microbiology and Molecular Diagnostics

[c] University of Natural Resources and Life Sciences, Vienna (BOKU), Department IFA-Tulln, Center for Analytical Chemistry, Tulln, Austria

[d] Medical University Vienna, Center for Medical Statistics, Informatics and Intelligent Systems, Section for Clinical Biometrics, Vienna, Austria

[e] Medical University Vienna, Institute for Hygiene and Applied Immunology, Water Hygiene, Vienna, Austria

[f] Karl Landsteiner University of Health Sciences, Research Unit Water Quality and Health, Krems, Austria

[g] ICC Interuniversity Cooperation Centre Water & Health, Vienna, Austria (www.waterandhealth.at)

INTRODUCTION

Faecal indicator bacteria such as intestinal enterococci are used around the globe to assess the microbiological quality of environmental waters. In this respect, quantitative polymerase chain reaction (qPCR) has become powerful detection tool within the last decade to monitor the levels of enterococci more rapidly. Despite high sensitivity and specificity, however, qPCR is limited to specialized laboratories having access to high-end instruments and extensively trained personnel to perform the method, as well as to analyze and interpret the obtained data. Isothermal amplification methods – such as helicase-dependent amplification (HDA) – represent a novel group of DNA-based detection techniques that mainly differ from PCR-technology in the temperature conditions needed to amplify a specific DNA target region. Unlike qPCR, HDA can be performed at a constant temperature (~ 65 °C) and thus offers considerable advantages especially for resource-limited settings. Furthermore, HDA is a promising technique for incorporation into portable, battery-operated devices and microfluidic systems (lab-on-a-chip).

AIM OF THE WORK

The aim of this work was to design and develop an HDA assay that is complementary to existing qPCR assays of the United States Environmental Protection Agency (US EPA) for the detection of enterococci. To that end, the qPCR US EPA Method 1611 [1] – targeting the 23S rRNA gene as a marker for fecal pollution – was translated into the HDA reaction format. The performance of the developed *Enterococcus* HDA assay was evaluated and compared to reference qPCR with respect to specificity, sensitivity, limit of detection, and analysis of environmental isolates, as well as its applicability to environmental water samples.

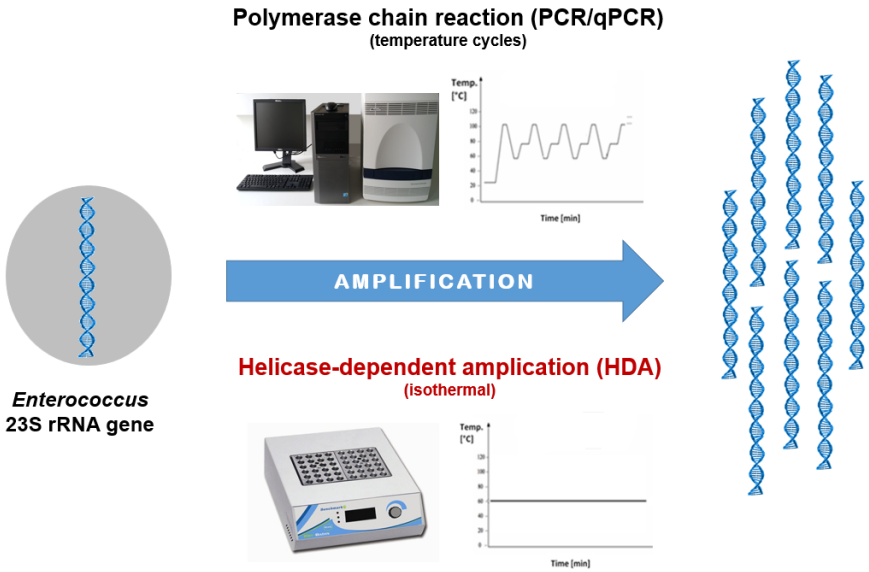

Figure 1: Schematic representation of instrument complexity and temperature requirements for polymerase chain reaction (PCR) and helicase-dependent amplification (HDA) technology

RESULTS AND DISCUSSION

The developed *Enterococcus* HDA assay successfully discriminated 15 enterococcal from 15 non-enterococcal reference strains and reliably detected 48 environmental isolates of enterococci. The limit of detection determined by analyzing a dilution series of *Enterococcus faecalis* genomic DNA was 25 target copies per reaction, only three times higher than that of qPCR. The applicability of the assay was tested on 30 environmental water samples, simulating a range of fecal pollution. Despite the isothermal nature of the reaction and the use of simple instruments, the HDA results were consistent with those of the qPCR reference.

CONCLUSION

This novel HDA assay targets the same *Enterococcus* 23S rRNA gene region as the existing qPCR assays of the US EPA but can be entirely performed on a simple heating block. Given the performance, we conclude that the developed *Enterococcus* HDA assay has great potential as a complementary screening method to the qPCR. This amplification platform can broaden the applicability of molecular methods (e.g., for high-throughput analysis) and greatly increase their overall accessibility (e.g., in resource-limited settings or developing regions).

ACKNOWLEDGEMENTS

This study was part of the Life Science Call 2013 project LSC13-020 funded by the Niederösterreichische Forschungs- und Bildungsgesellschaft (NFB) and supported by the Austrian Science Fund (FWF) project P23900. This study was a joint collaboration of the Interuniversity Cooperation Centre Water & Health (www.waterandhealth.at).

REFERENCES

[1.] USEPA *Method 1611: Enterococci in Water by TaqMan quantitative polymerase chain reaction (qPCR) assay*; EPA-821-R-12-008; U.S. Environmental Protection Agency, Office of Water, Washington, D.C.: 2012

A COMPARATIVE APPROACH TO RECOMBINANTLY PRODUCE THE PLANT ENZYME HORSERADISH PEROXIDASE IN *ESCHERICHIA COLI*

Thomas Gundinger and Oliver Spadiut*

E166 - Institute of Chemical, Environmental and Biological Engineering

INTRODUCTION

Horseradish peroxidase (HRP, EC 1.11.1.7, Figure 1) represents an important heme-containing oxidoreductase that catalyses the oxidation of a variety of organic and inorganic substrates using hydrogen peroxide as oxidizing agent (H_2O_2). HRP is used in many biotechnological and medical applications, such as immunoassays (Figure 2) or targeted cancer treatment[3, 4]. Currently, HRP is still isolated from plant, though linked to several disadvantages. These comprise a quite expensive isolation and purification procedure, low production yields as well as the fact that final preparations describe a mixture of heterogeneously glycosylated HRP isoenzymes rather than a well-defined enzyme preparation[4, 5].

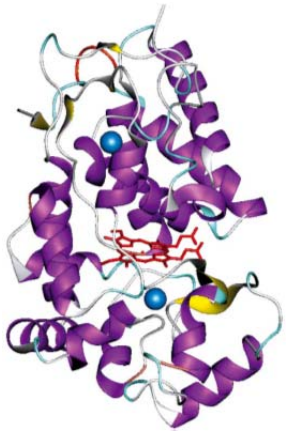

Figure 1. Three-dimensional image of the X-ray crystal structure of HRP isoenzyme C. The heme group (center region) is located between the two domains which each contain one Ca2+-ion (spheres)[1].

Thus, recombinant expression of HRP in the bacterium *Escherichia coli* was investigated to overcome these hurdles. However, production of HRP resulted in the formation of insoluble inclusion bodies (IBs) in the cytoplasm of *E. coli*, which have to be refolded to give active HRP. Up to now, obtained refolding yields are quite low, giving a final concentration of only 10 mg HRP per litre cultivation broth[6]. Alternatively, attempts were made to produce active HRP by translocation into the periplasm of *E. coli*. Although production was successful, obtained final yields did not exceed 0.5 $mg \cdot L^{-1}$ cultivation broth[6]. Consequently production of HRP in *E. coli* is currently not competitive and traditional isolation from plant still prevails.

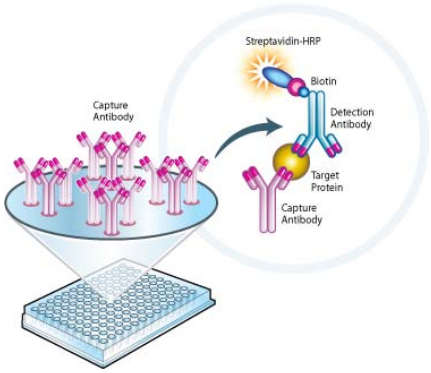

Figure 2. Visualization of HRP-conjugated antibodies used for immunoassays. (Conjugation is performed by Biotin-Streptavidin interaction.)[2]

EXPERIMENTAL APPROACH

In this study, we revisited the production of HRP in *E. coli* and investigated and compared both strategies, A) the production of HRP as IBs and subsequent refolding, as well as B) the production of active HRP in the periplasm. The latter strategy was examined by an integrated approach, investigating various variables along the process by performance of two design of experiments (DoE). An overview graphic of the experimental principle is shown in Figure 3.

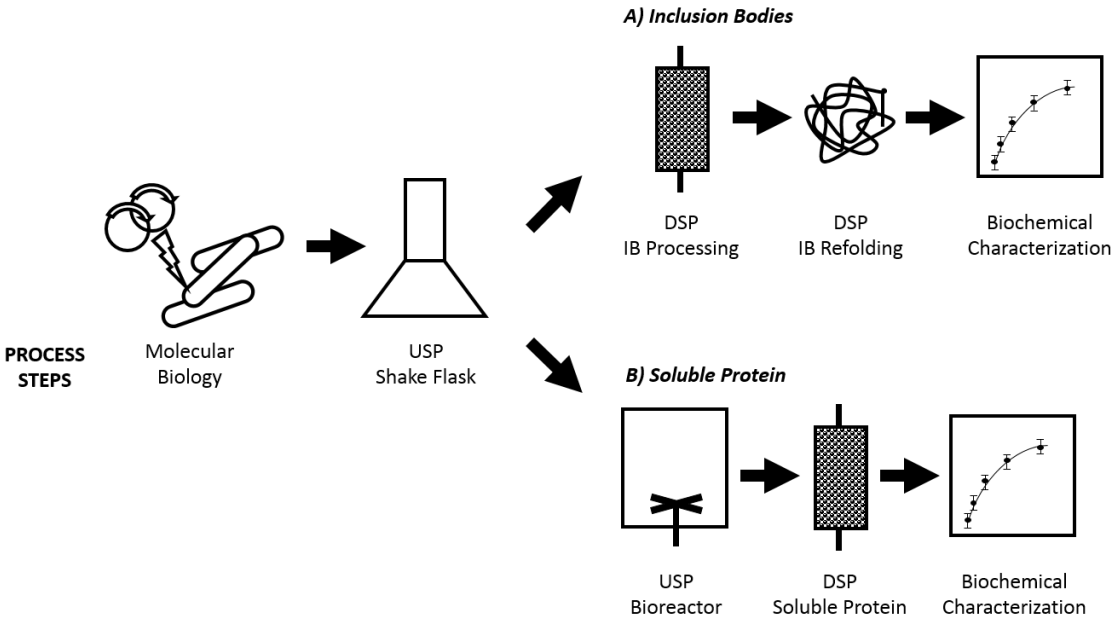

Figure 3. Overview – Experimental principle of the study

RESULTS AND DISCUSSION

In fact, we were able to produce HRP in *E. coli* via both strategies. On the one hand we obtained a refolding yield of 10 % from IBs resulting in a final production yield of 100 mg active HRP per litre cultivation broth, and on the other hand we were able to produce 48 mg active enzyme per litre cultivation broth in the periplasm (both titres are based on a biomass concentration of 60 g DCW·L^{-1} cultivation broth). Regarding biochemical properties, catalytic activity and thermal stability of soluble HRP were highly reduced, which may be caused by the impact of the fused DsbA protein, needed for translocation into the periplasm. Refolded HRP showed comparable substrate affinity, but a 9-fold reduced catalytic activity and 2-fold reduced thermal stability compared to plant HRP. However, the reduced kinetic properties can be compensated by protein engineering.

CONCLUSION

In conclusion, the combination of both production strategies describes a promising toolbox for HRP engineering and production. Thereby, HRP can be engineered by directed evolution or semi-rational protein design and expressed in the periplasm of *E. coli* allowing straight forward screening for improved variants, which are finally produced as IB in high amounts and subsequently refolded.

REFERENCES

[1] Veitch, N.C., *Horseradish peroxidase: a modern view of a classic enzyme.* Phytochemistry, 2004. **65**(3): p. 249-59.

[2] Mitosciences®. Available from: http://www.mitosciences.com/sandwich_elisa_assay_overview.html.

[3] Krainer, F.W. and A. Glieder, *An updated view on horseradish peroxidases: recombinant production and biotechnological applications.* Appl Microbiol Biotechnol, 2015. **99**(4): p. 1611-25.

[4] Spadiut, O. and C. Herwig, *Production and purification of the multifunctional enzyme horseradish peroxidase.* Pharm Bioprocess, 2013. **1**(3): p. 283-295.

[5] Lavery, C.B., et al., *Purification of peroxidase from Horseradish (Armoracia rusticana) roots.* J Agric Food Chem, 2010. **58**(15): p. 8471-6.

[6] Grigorenko, V., et al., *New approaches for functional expression of recombinant horseradish peroxidase C in Escherichia coli.* Biocatalysis and Biotransformation, 1999. **17**(5): p. 359-379.

TEACHING AN OLD PET NEW TRICKS – EXPRESSION TUNING IN *E. COLI* BL21(DE3)

David J. Wurm, Christoph Herwig, Oliver Spadiut*

E166 - Institute of Chemical, Environmental & Biological Engineering, TU Wien

INTRODUCTION

Escherichia coli is the most widely used host organism for recombinant protein production due to its well-studied genome, the existence of numerous cloning vectors and engineered strains, as well as the possibility of cheap and straight-forward cultivation to high cell densities yielding high product titers [1,2]. Strong induction of recombinant protein production in *E. coli* can lead to agglomeration of inactive product, so called inclusion bodies (IBs), and also imposes a high metabolic burden which can result in cell death [3].

CHALLENGE

To reduce metabolic burden and increase product quality it is important to tailor the induction level of recombinant protein expression. Within this project the goal was to tune recombinant protein expression by supplying different limiting amounts of the inducer lactose. A prerequisite thereof is to characterize the strain regarding the maximum specific uptake rate of lactose ($q_{s,lac}$) to know the possible feeding ranges and prevent sugar accumulation as this can lead to osmotic stress [4].

RESULTS AND DISCUSSION

First the correlation between the lactose and the glucose uptake were evaluated by conducting several experiments and fitting the obtained data by a mechanistic model [5,6] (open circles and black line in Figure 1). Afterwards we investigated the impact of $q_{s,lac}$ on the formation of soluble protein and inclusion bodies. We decoupled growth from recombinant protein expression in a series of controlled bioreactor cultivations of *E. coli* expressing the model protein enhanced green fluorescent protein (eGFP) at a constant $q_{s,glu}$ and varied $q_{s,lac}$ (Figure 1). Furthermore we performed induction with the very commonly used inducer IPTG.

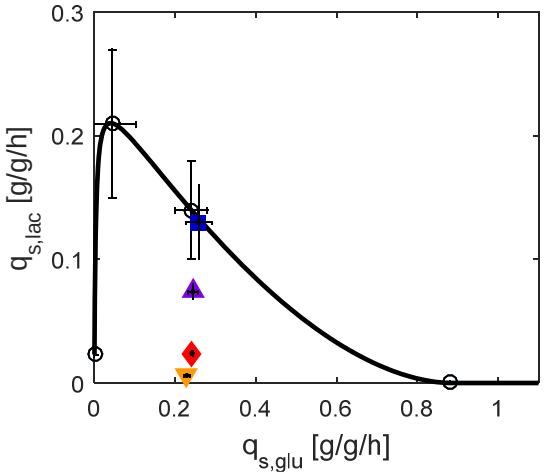

Figure 1: Black line indicates maximum specific uptake rate of lactose ($q_{s,lac}$) as a function of specific uptake rate of glucose ($q_{s,glu}$) for *Escherichia coli* BL21(DE3) strain producing enhanced green fluorescent protein (eGFP). Data points (open circles) were obtained from several batch and fed-batch cultivations and fitted by the mechanistic model according to our previous study[10]. Filled symbols indicate performed experiments

We found that by varying the specific uptake rate of the inducer lactose we were able to tune the induction level. Both soluble protein and inclusion bodies formation were strongly impacted by the induction conditions.

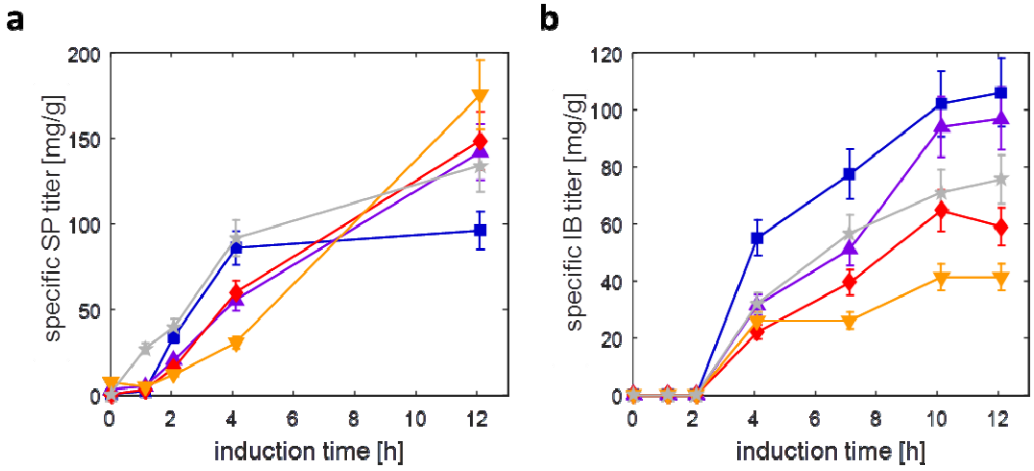

Figure 2: Specific titers of soluble product (SP; Figure 2a) and inclusion bodies (IB; Figure 2b) in the different cultivations over time.

CONCLUSION

We found that induction at high $q_{s,lac}$ and IPTG gave a high specific titer of soluble product in the early phases of induction, but for prolonged production times induction a low $q_{s,lac}$ is favourable and leads to higher product titers. For the inclusion body formation rate we saw a clear correlation between specific uptake rate of the inducer lactose and the specific inclusion body titer throughout the whole induction phase and we were able to obtain higher production rates with the inducer lactose compared to IPTG.

Our developed method of feeding limiting amounts of the inducer lactose allows tuning the recombinant protein expression rate. This might pave the way for obtaining “difficult-to-expressed proteins” and to increase product titers as well as product quality.

REFERENCES

[1] Jia B., Jeon C.O., High-throughput recombinant protein expression in *Escherichia coli*: current status and future perspectives, Open Biology, 6, 160196, 2016

[2] Huang C.J. *et al.*, Industrial production of recombinant therapeutics in *Escherichia coli* and its recent advancements, Journal of Industrial Microbiology and Biotechnology, 39, 383-399, 2012

[3] Joseph B.C. *et al.*, An Overview of the Parameters for Recombinant Protein Expression in *Escherichia Coli*, Journal of Cell Science, 6, 1-7, 2015

[4] Wurm D.J. *et al.*, The *E. coli* pET expression system revisited—mechanistic correlation between glucose and lactose uptake, Applied Microbiology and Biotechnology, 100, 8721-8729, 2016

[5] Wurm D.J. *et al.*, How to Determine Interdependencies of Glucose and Lactose Uptake Rates for Heterologous Protein Production with *E. coli*, accepted for publication in Methods in Molecular Biology

[6] Wurm D.J. *et al.*, Mechanistic platform knowledge of concomitant sugar uptake in *Escherichia coli* BL21(DE3) strains, accepted for publication in Scientific Reports

PRODUCTION OF HYDROPHOBINS IN THE TWO EXPRESSION SYSTEMS BASED ON *TRICHODERMA*

Victor Lobanov[a], Feng Cai[a,b], Agnes Przylucka[a], Lizaveta Sidarenka[a], Qirong Shen[b], Irina Druzhinina[a]

[a]E166 - Institute of Chemical, Environmental and Biological Engineering, Research Area Biochemical Technology, Microbiology Group, TU Wien, Vienna, Austria
[b]Jiangsu Collaborative Innovation Center for Solid Organic Waste Resource Utilization, Nanjing Agricultural University, Nanjing, China

INTRODUCTION

Genetically modified organisms have grown to play an integral role in modern day industry, visible from the substantial amount of research currently pursued on the topic. Strain modification is a process compromising of screening for ideal traits and transforming designed gene vectors into the chosen host organism. Such vectors may be optimised depending on the host and secretion product. Due to their versatility and high secretory capacity, filamentous fungi are common in the production of proteins for industrial applications. Certain species, e.g. *Trichoderma reesei* QM 6a, are regarded as model organisms. Extensive research and optimisation of fermentations using *T. reesei* allow industrial bioreactors to secrete products in excess of 100 gL^{-1} (1), part of a global multibillion euro market (2). *Trichoderma* are ubiquitous worldwide, finding niches in saprotrophic as well as mycotrophic settings, enabled by a highly complex cocktail of enzymes and auxiliary proteins. One class of small molecular weight proteins, hydrophobins (HFB), is particularly interesting. These amphipathic proteins are known for their acute surface activity and spontaneous layer formation. The tertiary structure is marked by a conserved α-helix barrel with peripheral β-sheets defining largely the variability across hydrophobins (3).

Hydrophobins offer potential solutions and improvements to numerous industrial needs, largely based around the exploitation of their amphipathic and sheet-forming properties as agents to functionalise material surfaces (4). HFBs may be loosely distinguished into two classes differentiated by their layer formation (robust or transient), thus ideal for diverse material coatings (5). Furthermore, their application in water significantly decreases surface tension (6), thereby increasing wettability. HFBs are safe for ingestion and trigger no immune response (7-9), rendering them relevant for biomedical as well as food industries (10, 11). Ironically, the very properties of hydrophobins so desired for industrial use, e.g. the surface activity, mire potential production upscaling. Assuming improvement in the purification of hydrophobins from the bioreactor medium, the potential for strain optimisation remains nonetheless open. In light of this, the current study presents a case comparison of the recently discovered *T. guizhouense* NJAU 4742 (12) as a potential replacement of the traditional cell factory *T. reesei* for overexpression of *Trichoderma* class II hydrophobins, namely HFB4 and HFB7.

METHODS

As a platform for comparison between the two species, several gene constructs for heterologous and homologous overexpression were designed and transformed into both organisms. Initially, the hydrophobin encoding genes* $hfb4_{vir}$ and likewise $hfb7_{vir}$, both originating from *T. virens* Gv 29-8, were overexpressed in *T. reesei* QM 6a using a pUC19 plasmid containing a *cdna1* promoter, *cbh1* terminator, and 6His cassette. Concurrently, the homologous expression of $hfb4_{gui}$ in *T. guizhouense*

using a *cdna1* promoter and native terminator were investigated. The *cdna1*P*hfb4*$_{vir}$6His*cbh1*T construct, as well as its *hfb7*$_{vir}$ counterpart, were transformed into *T. guizhouense*. Furthermore, *hfb4*$_{gui}$ was transformed into *T. reesei* QM 6a first with the original *cdna1*P*hfb4*$_{gui}$*hfb4*$_{gui}$T construct and with a *cdna1*P*hfb4*$_{gui}$6His*cbh1*T construct.

RESULTS AND DISCUSSION

By manipulating both strain and gene overexpression construct, the initial comparison of *T. reesei* and *T. guizhouense,* whereby the overexpression mutants from *T. guizhouense* outproduced their *T. reesei* counterparts, may be expanded in a meaningful way. Shake flask fermentations provide an initial summary as to which organism and construct combination allows greater hydrophobin secretion. Regardless, this will necessitate further bioreactor fermentations as well as extensive optimisation of the fermentation set-up to study how the cell factories may permit further upscaling of hydrophobin production.

CONCLUSION

Given the demand for an effective production mechanism for large-scale hydrophobin production, it is imperative that not only well-known organisms be tested, but also those more recently discovered. In line with this, the current study has focused on the potential of *T. guizhouense* as a viable candidate for this task. This was explored by comparing overexpression mutants from the newcomer candidate against the traditionally used *T. reesei* using various hydrophobin overexpression cassettes.

* To differentiate orthologous hydrophobin genes, the first three letters of the respective species name is appended to the gene; i.e. *hfb4*$_{vir}$, *hfb4*$_{gui.}$

REFERENCES

1. Druzhinina I, Kubicek C. Chapter Two-Familiar Stranger: Ecological Genomics of the Model Saprotroph and Industrial Enzyme Producer Trichoderma reesei Breaks the Stereotypes. Advances in applied microbiology. 2016;95:69-147.

2. Nevalainen KM, Te'o VS, Bergquist PL. Heterologous protein expression in filamentous fungi. Trends Biotechnol. 2005;23(9):468-74.

3. Wosten HA, Scholtmeijer K. Applications of hydrophobins: current state and perspectives. Appl Microbiol Biotechnol. 2015;99(4):1587-97.

4. Espino-Rammer L, Ribitsch D, Przylucka A, Marold A, Greimel KJ, Acero EH, et al. Two novel class II hydrophobins from Trichoderma spp. stimulate enzymatic hydrolysis of poly (ethylene terephthalate) when expressed as fusion proteins. Applied and environmental microbiology. 2013;79(14):4230-8.

5. Linder MB, Szilvay GR, Nakari-Setälä T, Penttilä ME. Hydrophobins: the protein-amphiphiles of filamentous fungi. FEMS Microbiology Reviews. 2005;29(5):877-96.

6. Wosten HA, de Vocht ML. Hydrophobins, the fungal coat unravelled. Biochim Biophys Acta. 2000;1469(2):79-86.

7. Giles SS, Dagenais TR, Botts MR, Keller NP, Hull CM. Elucidating the pathogenesis of spores from the human fungal pathogen Cryptococcus neoformans. Infection and immunity. 2009;77(8):3491-500.

8. Hakanpää J, Paananen A, Askolin S, Nakari-Setälä T, Parkkinen T, Penttilä M, et al. Atomic resolution structure of the HFBII hydrophobin, a self-assembling amphiphile. Journal of Biological Chemistry. 2004;279(1):534-9.

9. Hohl TM, Van Epps HL, Rivera A, Morgan LA, Chen PL, Feldmesser M, et al. Aspergillus fumigatus triggers inflammatory responses by stage-specific β-glucan display. PLoS Pathog. 2005;1(3):e30.

10. Fischer G, Dott W. Relevance of airborne fungi and their secondary metabolites for environmental, occupational and indoor hygiene. Archives of Microbiology. 2003;179(2):75-82.

11. Bimbo LM, Makila E, Raula J, Laaksonen T, Laaksonen P, Strommer K, et al. Functional hydrophobin-coating of thermally hydrocarbonized porous silicon microparticles. Biomaterials. 2011;32(34):9089-99.

12. Li Q-R, Tan P, Jiang Y-L, Hyde KD, Mckenzie EH, Bahkali AH, et al. A novel Trichoderma species isolated from soil in Guizhou, T. guizhouense. Mycological progress. 2013;12(2):167-72.

EMERGING CONTAMINANTS IN PM10 OF RESIDENTIAL AREA IN KRAKOW

Anna Korzeniewska[a], Katarzyna Styszko[a*], Katarzyna Szramowiat[a], Klaudia Kubisty[a], Magdalena Kistler[b], Anne Kasper-Giebl[b], Janusz Gołaś[a]

[a]AGH University of Science and Technology, Faculty of Energy and Fuels, Department of Coal Chemistry and Environmental Sciences, Krakow, Poland
[b]E164 – Institute of Chemical Technologies and Analytics *styszko@agh.edu.pl

INTRODUCTION

Emerging contaminants (ECs) are a group of chemicals that show the adverse impact on ecosystems and human health but their concentration has been not regulated in environmental legislation yet, as their presence has been not well-known so far. They might have a synthetic origin or might be derived from natural sources. There are several types of known existing ECs such as antibiotics, pesticides, pharmaceuticals, effluents, certain naturally occurring contaminants and more recently nanomaterials. The identification and the knowledge about the origination, fate and processes of transport and transformation of ECs are still sparse. However, these issues are of high importance due to the strong toxicological impact of ECs [1]. Polycyclic aromatic hydrocarbons (PAHs), however alreasdy included in legislation (Directive 2008/50EC) are a class of organic compounds that consists of two or more aromatic rings in their structure. PAHs are a group of ubiquitous and widespread semi-volatile hydrocarbons. Some of them are classified by International Agency for Research on Cancer (IARC) as probable or possible carcinogenic and mutagenic, like benzo[a]pyrene or dibenzo[a,h]anthracene. PAHs are mainly formed during natural and anthropogenic combustion processes of fuels like wood, coal, peat, oil, fossil fuels, waste, crop/agricultural waste, animal dung and biomass. In the atmosphere PAHs occur in both, gas and particulate-bound phase [2]. Phenols are characterized as volatile organic compounds that are released to the ambient air during the manufacturing processes of many phenolic resins and organic solvents. The biggest amount of phenols are emitted to the atmosphere from petroleum refineries, petrochemical, steel mills, coke oven plants, coal gas, synthetic resins, pharmaceuticals, paints, plywood industries and mine discharge [3].

The goal of the study was to determinate the concentration of benzo(a)pyrene and alkylphenols, as representatives for PAHs and phenols respectively, in PM10 fraction of aerosols collected in the residential area in Krakow.

EXPERIMENT

Samples were collected during the short (21-day) sampling period in January and February 2016. PM10 samples were collected on 47 mm quartz fibre filters (Pallflex). The mass of particulate matter per filter was gravimetrically measured as 3.96 mg on average. Averagely, 55 m^3 of ambient air was aspirated by the particulate matter impactor. PM10 samples were analysed for the presence of BaP, bisphenol-A and phenol with an application of the gas chromatography equipped with mass spectrometer. The analytical method was similar to that one presented in previous works [4].

RESULTS AND DISCUSSION

The average concentration of PM10 during the sampling period was equal to 73.2 $\mu g \cdot m^{-3}$ and ranged between 17.7 and 201 $\mu g \cdot m^{-3}$. In 15 days out of 21-day sampling period the concentration of

PM10 was higher than the limit value for PM10 according to 2008/50EC. The presence of benzo[a]pyrene, bisphenol-A, phenol was confirmed in all analysed samples.

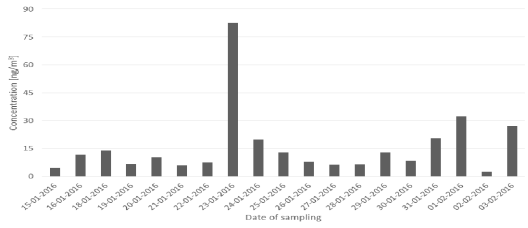

Fig. 1 The concentration of benzo[a]pyrene in analysed samples

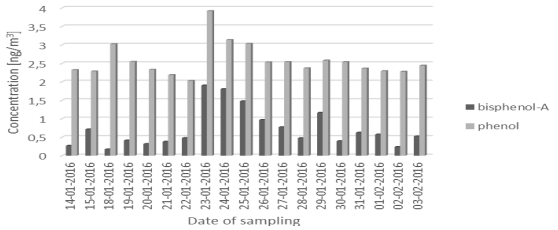

Fig. 2 The concentration of bisphenol-A and phenol in analysed samples

It showed that the average concentration of benzo[a]pyrene was estimated at 15.83 ng·m^{-3} and 2.56 ng·m^{-3} respectively for phenol while average concentration of bisphenol-A was estimated at 0.69 ng·m^{-3} . The concentrations measured for benzo[a]pyrene were in the range of 2.46 ng·m^{-3} to 82.5 ng·m^{-3} and 2.03 ng·m^{-3} to 3.91 ng·m^{-3}, respectively for phenol. The concentrations measured for bisphenol-A were in the range of 0.15 ng·m^{-3} to 1.9 ng·m^{-3}. The mass of benzo[a]pyrene contributes to the 0.025 % of PM10 mass, while phenol and bisphenol-A to 0.005 % and 0.005%, respectively. The highest level of BPA was observed in PM10 aerosols from Chennai and Mumbai, India. In Chennai, the concentration range was 200 - 17.4 pg·m^{-3} (average 4550 pg·m^{-3}) [5]. One of the significant emission sources of od atmospheric BPA could be the open burning of domestic plastic wastes [6].

CONCLUSION

The relation between emitted ECs and the source still needs to be identified. That is why the samples of PM 10 were collected in the residential area of Krakow, which is mainly affected by air pollution originating from combustion processes like biomass or coal combustion. Recognition of the sources of emission of ECs is extremely important, therefore in the following part of the study authors will focus on the ECs emission from combustion processes for the production of heat.

ACKNOWLEDGEMENTS

This work was partially supported by AGH University Grant. The authors acknowledge the financial support of OeaD and of the Ministry of Science and Higher Education (Poland) in the frame of project WTZ (Wissenschaftlich–Technische Zusammenarbeit), No. PL09/2015.

REFERENCES

[1] “Emerging contaminants in the environment: Risk-based analysis for better management” R. Naidu, V. A. Arias Espana, Y. Liu, J. Jit, Chemosphere 154 (2016), pp. 350-357

[2] “A review on polycyclic aromatic hydrocarbons: Source, environmental impact, effect on human health and remediation”, H.I. Abdel-Shafya, M.S.M. Mansour, Egyptian Journal of Petroleum, Vol. 25, Issue 1, March 2016, pp. 107–123

[3] “The treatment of waste air containing phenol vapors in biotrickling filter” G. Moussavi , M. Mohseni, Chemosphere 72 (2008) , pp. 1649–1654

[4] “Polycyclic aromatic hydrocarbons and their nitrated derivatives associated with PM10 from Kraków city during heating season” K. Styszko, K. Szramowiat, M. Kistler, A. Kasper Giebl, S. Socha, E. E. Rosenberg and J. Gołaś, E3S Web of Conferences 10, 00091 (2016)

[5] (2010) “Ubiquity of bisphenol A in the atmosphere” P. Fu, K. Kawamura, Environmental Pollution, Vol. 158, Issue 10, October 2010, pp. 3138–3143

[6] “Comparison of abundances, compositions and sources of elements, inorganic ions and organic compounds in atmospheric aerosols from Xi'an and New Delhi, two megacities in China and India” J. Li, G.Wang, S.G. Aggarwal, Y. Huang, Y. Ren, B. Zhou, K. Singh, P.K. Gupta, J. Cao, R. Zhang, Science of The Total Environment, Vol. 476–477, April 2014, pp. 485–495

OPTIMISING NATURE FOR INDUSTRY: DESIGN OF SYNTHETIC PROMOTERS FOR STRAIN ENGINEERING OF *TRICHODERMA REESEI*

Elisabeth Fitz[a], Robert Bischof[a], Bernhard Seiboth[a,b]

[a]acib GmbH, Graz, Austria, c/o E166-5 Institute of Chemical, Environmental & Biological Engineering, TU Wien
[b]Molecular Biotechnology Group, Institute of Chemical, Environmental & Biological Engineering, TU Wien, Gumpendorferstrasse 1A, 1060 Wien, Austria

INTRODUCTION

Over the recent years a lot of efforts and research have been made to develop the fuel-based chemical industry towards a bio-based industry. A common approach is the production of biochemicals and enzymes via microbial production hosts.

Trichoderma reesei is a filamentous fungus that is well established for the production of biorefinery enzymes[1,2], mostly cellulases and hemicellulases. Due to its capability to produce high amounts of proteins that are secreted directly into the medium it is also used increasingly to express heterologous proteins. To optimise their production, different genetic tool are necessary to obtain high yields. One of the limiting factors is the transcription levels of the heterologous target genes[3]. Therefore, we develop synthetic promoters with a high basal expression level.

EXPERIMENTS / FUNDAMENTAL OF THE PROBLEM / EXAMINATIONS

The promoter of the uncharacterized gene *cdna1* (P*cdna1*) is one of the strongest promoters that is active during growth on glucose[4]. Although even stronger promoters exist, they are often repressed on glucose or require activation by specific inducers. Our goal was to rationally design a promoter, which is as strong as an inducible promoter but active during growth on glucose.

The project was divided into two parts and focuses on the design of a 200 bp long **core promoter** and an about 1000 bp long **proximal promoter**, which can be combined to a full length promoter. Using RNAseq data from glucose-grown cultures, we analysed 50 highly expressed genes towards their core promoter structure[5]. As references we used the core promoters from *cdna1* and from a strongly expressed phosphatase. Based on the findings we established a box structure system: 6-20 bp long sequences (boxes) were arranged on a 200 bp long either completely artificial or modified natural backbone.

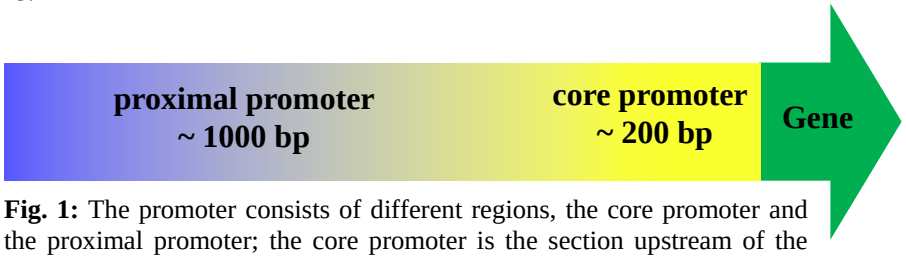

Fig. 1: The promoter consists of different regions, the core promoter and the proximal promoter; the core promoter is the section upstream of the start ATG

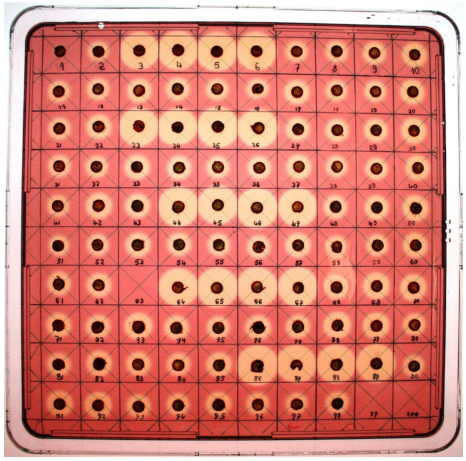

Fig. 2: Cellulose containing agar plate with strains expressing CEL12A under the control of the different synthetic core promoters, stained with a Congo Red solution; CEL12A degrades the cellulose around the gel plug and therefore the dye cannot bind anymore and forms the “clearing zones”;

RESULTS AND DISCUSSION

Six novel core promoters were generated and fused to the endoglucanase CEL12A. The expression strength of the core promoters was tested via a colorimetric plate assay in *T. reesei*: the strains were grown on a cellulose containing agar medium. The agar was then dyed with a Congo Red solution, which led to a discoloured “clearing zone” were the fungi secreted a lot of the cellulase CEL12A. The amount of secreted cellulase is proportional to the expression.

We found that two of the new synthetic core promoters surpassed the expression strengths of the native P*cdna1* and the phosphatase by 175% and 20% respectively. Both of these synthetic core promoters were based on the artificial backbone, whereas the inserted boxes where arranged as in a natural core promoter. The activity occurred solely from the used boxes, including already known sequences like TATA-boxes, GC-boxes or CT-rich regions, but also newly found boxes from our sequence analysis.

CONCLUSION

This work demonstrates that the ration engineering of a core promoter using the box structure can be a tool to further improve the expression strength of already strong core promoters. The next step is the development of a synthetic proximal promoter that further enhances the strength of a synthetic promoter.

This system offers the possibility to combine different characteristics to get the optimised synthetic promoter for different applications.

REFERENCES

1 Ferreira NL, Margeot A, Blanquet S, Berrin JG (2014). “Use of cellulases from *Trichoderma reesei* in the twenty-first century part I: current industrial uses and future applications in the production of second ethanol generation.” In: Gupta VK, Schmoll M, Herrera-Estrella A, Upadhyay RS, Druzhinina I, Tuohy MG (eds) Biotechnology and biology of Trichoderma. Elsevier, Oxford, pp 245–261

2 Paloheimo M, Thomas Haarmann T, Mäkinen S, Vehmaanperä J. “Production of Industrial Enzymes in *Trichoderma reesei*” In: Schmoll M, Dattenböck C(eds.), Gene Expression Systems in Fungi: Advancements and Applications, Fungal Biology; pp 23-57

3 Dehli T, Solem C, Jensen PR (2012) “Tunable promoters in synthetic and systems biology.” Subcell Biochem 64:181–201

4 Nakari-Setälä, T, and M Penttilä. “Production of Trichoderma Reesei Cellulases on Glucose-Containing Media.” *Applied and Environmental Microbiology* 61.10 (1995): 3650–3655.

5 Ries L, Pullan ST, Delmas S, Malla S, Blythe MJ, Archer DB. “Genome-wide transcriptional response of *Trichoderma reesei* to lignocellulose using RNA sequencing and comparison with Aspergillus niger.” BMC Genomics. 2013;14:541

COMPARABILITY OF LIFE CYCLE ASSESSMENTS (LCA) IN PROCESS DESIGN BIOREFINERY PROCESSES

Daniel Koch, Anton Friedl, Bettina Mihalyi

E166 - Institute of Chemical, Environmental and Biological Engineering at TU Wien

INTRODUCTION

The incremental growing of human population and technological advancement is leading to a shift in the priorities of decision makers. Challenging topics are gaining attention such as the increasing energy demand, resources availability and the mitigation of emissions. To tackle these, the concept of sustainable development is widely promoted. Presently its common definition is, that the needs of today's generation are to be fulfilled without hindering the freedom and possibilities of future generations to fulfil their own needs. [1] Assessing a given system on sustainable development is highly complex and often does not yield one simple and clear solution. A task like this is also described as a wicked problem.

Life Cycle Assessment LCA has proven to be a powerful method to analyse the environmental impacts of a product, a service or a process. Broad areas of the LCA methodology are standardized through the ISO standards 14040 and 14044. The idea is a holistic approach, including all life cycle stages with its inventories (material and energy flows) from raw material extraction to the end of life scenario, cradle-to-grave. The informative value of a LCA result depends heavily on the quality of available data, chosen methodologies (e.g. allocation for multi-product systems), as well as the defined scope and goal of the assessment. [2]

FUNDAMENTAL OF THE PROBLEM

At the beginning LCA was focused on established product systems but for the application of the precautionary principle it should already be implemented in an early stage process design phase, in addition to classic process simulation tools. It is essential for a technical realisation of environmental sustainability to include life cycle thinking already in process development.

In order to increase independence from fossil resources, biomass based refineries are the centre of interest for many research groups. This innovative technology also is intended to support a sustainable development and to minimise the environmental load. Even within the different concepts for biomass based refineries there are a selection of process paths to obtain the so called platform chemicals in a certain quality. But looking at different impact categories of the whole life cycle, not all of them have a better environmental footprint than the conventional process.

This study investigates how LCA can help to find the most ecological respectively the sustainable process paths in an early stage of process design using a case study on the issue "lignocellulosic biorefinery". To yield the different products in this biorefinery the lignocellulosic biomass has to be pretreated to provide the various fractions, cellulose, hemicellulose and lignin, for downstream upgrading (further refining procedures). Through this study two common research questions should be answered: "Is it possible to make profound decisions from an LCA documentation in the literature without conducting one exclusively with the specific application and frameworks?" and "How far are LCA results from different assessments about the same process principle comparable?"

METHODOLOGY

An extensive literature research is carried out to find answers for the research questions. Results of different life cycle calculations are analysed in detail. The recently most assessed lignocellulosic biomass pretreatment method, the dilute acid process, was selected for this case study. It is commonly used for second generation bioethanol biorefineries.

Important aspects of the LCA methodology were precisely investigated to have a good basis of comparison, including: goal and scope definition, functional unit, land use change, biogenic carbon sequestration, allocation of products and feedstock. All recognised differences and shortcomings are evaluated, eventually recalculated and documented.

RESULTS AND CONCLUSION

Process development also involves choosing one of many different process chains to reach the desired outcome. The environmental impacts need to be assessed for these decisions to promote a sustainable development.

Analysing the environmental implications for a specific process from different LCAs in literature comes with a large number of uncertainties and a high variation range. Comparing two different process path possibilities only through LCA results from the literature is hardly helpful. Life cycle calculations that can be found are remotely comparable to exactly the same two process paths of interest. There are usually many varieties for the goal, the scope and the data quality. Each process development has unique goals which cannot be ignored when trying to transfer a life cycle calculation result with different unique aspects onto it. Taking a selection of more than one life cycle calculation result from the literature into account, comes with a lot of detail work for each process and a higher deviation of the results. The variation of the results in all steps, setting goal and scope, choosing the methodologies, data quality of the life cycle inventory (LCI), timeframe and more aspects of the LCAs either lead to incomparability of the results or to no significant recommendation. Trying to understand the variations and looking into the calculations in detail to take deviations in each level into account comes with a very high effort, even if the LCA is done with ISO compliance there are certain presumptions, boundary conditions and calculations which are not exposed.

While it is already challenging to compare the environmental impact of different commercial processes by consulting the literature, it is even more increasingly unfeasible for processes in the design phase where even more uncertainties, flexible parameters and a larger number of assumptions are present. Therefore it is imperative to apply an exclusive LCA as decision support along with each process development. Ideally it is done together with the engineers developing the process.

REFERENCES

[1] Brundtland G. H., “Report of the World Commission on Environment and Development: Our Common Future.” 1987

[2] Curran M. A. „Life Cycle Assessment: a review of the methodology and its application to sustainability.” Current Opinion in Chemical Engineering, 2:1-5, 2013

A LOOP-MEDIATED ISOTHERMAL AMPLIFICATION (LAMP) ASSAY FOR THE RAPID DETECTION OF *ENTEROCOCCUS* SPP. IN WATER

Roland Martzy[a,g], Claudia Kolm[a,g], Kurt Brunner[a], Robert L. Mach[b], Rudolf Krska[c], Hana Šinkovec[d], Regina Sommer[e,g], Andreas H. Farnleitner[b,f,g], Georg H. Reischer[a,b]

[a] E166 - Institute of Chemical, Environmental & Biological Engineering, Molecular Diagnostics Group, Department IFA-Tulln
[b] E166 - Institute of Chemical, Environmental & Biological Engineering, Research Group of Environmental Microbiology and Molecular Diagnostics
[c] University of Natural Resources and Life Sciences, Vienna (BOKU), Department IFA-Tulln, Center for Analytical Chemistry, Vienna, Austria
[d] Medical University Vienna, Center for Medical Statistics, Informatics and Intelligent Systems, Section for Clinical Biometrics, Vienna, Austria
[e] Medical University Vienna, Institute for Hygiene and Applied Immunology, Unit Water Hygiene, Vienna, Austria
[f] Karl Landsteiner University of Health Sciences, Research Unit Water Quality and Health, Krems, Austria
[g] ICC Interuniversity Cooperation Centre Water & Health, Vienna, Austria (www.waterandhealth.at)

INTRODUCTION

Microbial pollution of water resources through faecal input is a threat to public health in developing as well as in industrialised countries. According to the WHO, 9% of the world's population are without access to safe drinking water [1], which is why the improvement of drinking water quality and sanitation is one of the United Nations Sustainable Development Goals [2]. The microbiological quality of water used for drinking, bathing, or irrigation can be determined by the detection of standard faecal indicator bacteria (SFIB) such as *Escherichia coli* or certain *Enterococcus* species. The major shortcomings of the conventional detection methods include the requirement for a microbiological laboratory and that SFIB can only be identified and quantified with certainty after up to 48 hours of growth. Therefore, molecular detection methods based on quantitative polymerase chain reaction (qPCR) are nowadays being used extensively for routine water quality monitoring. However, expensive equipment and computer software are required for their application and the interpretation of the results. To overcome these drawbacks, isothermal amplification methods have recently become a useful alternative to the molecular detection method of qPCR, allowing molecular diagnostics directly at the point-of-care with simple or no instrumentation and without the need for highly trained personnel [3].

AIM OF THE WORK

The aim of this study was the development of a novel method for the rapid molecular detection of *Enterococcus* spp. in water by loop-mediated isothermal amplification (LAMP) and its comparison to the qPCR method 1611 recommended by the US Environmental Protection Agency [4].

RESULTS AND DISCUSSION

The developed LAMP assay can be completely performed at 65 °C and does not require any temperature changes throughout the 45 minute reaction. Therefore, a simple heating block is

sufficient to fulfil the requirements for the implementation of the *Enterococcus* LAMP. The sensitivity and specificity tests were performed using a set of 30 *Enterococcus* and non-target bacterial reference strains, which showed that the developed LAMP assay is equally sensitive and specific as the reference qPCR assay. The LAMP method had a limit of detection (95% probability of detection) of 130 DNA target molecules per reaction. Additionally, enterococci isolated from Austrian surface water bodies as well as a set of DNA extracts from environmental waters were tested. Contingency analysis demonstrated a highly significant correlation between the results of the developed LAMP assay and the reference qPCR method. The simple naked-eye identification of the LAMP products was achieved within one minute by the addition of a DNA-intercalating fluorescence dye.

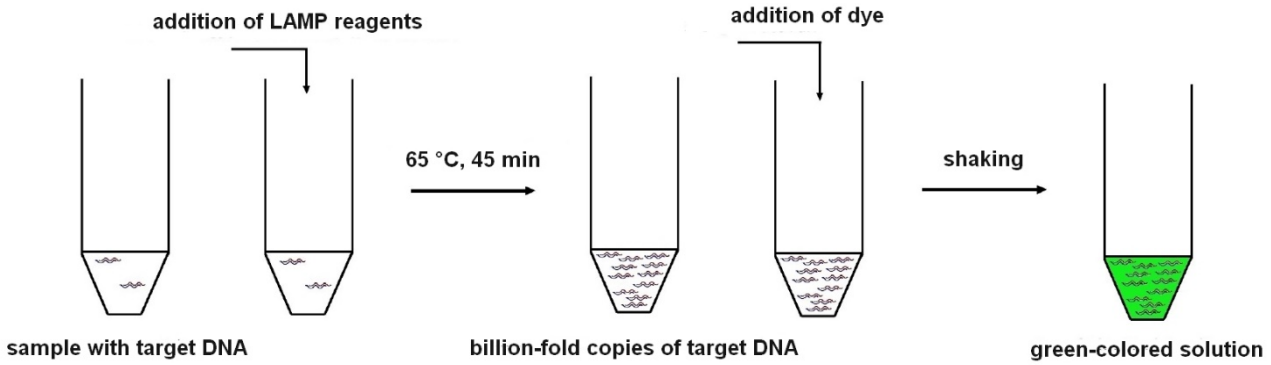

Figure: LAMP detection scheme.

CONCLUSION

In our study, a novel loop-mediated isothermal amplification (LAMP) assay for the molecular detection of enterococci in water samples was developed. The LAMP assay does not require expensive instrumentation and can be performed in less than one hour. In conclusion, this method represents an essential component for the efficient screening and testing of water samples in low-resource settings without sophisticated laboratory equipment and highly specialised personnel, e.g. in developing countries. In order to provide an entire on-site applicable workflow for the assessment of water quality, our future work will focus on simple filtration methods as well as on the development of a user-friendly and time-saving DNA extraction protocol for bacterial DNA from water.

ACKNOWLEDGEMENTS

This study was part of the Life Science Call 2013 project LSC13-020 funded by the Niederösterreichische Forschungs- und Bildungsgesellschaft (NFB) and supported by the Austrian Science Fund (FWF) project P23900. This study was a collaboration with the Interuniversity Cooperation Centre Water & Health (http://www.waterandhealth.at).

REFERENCES

[1] WHO. *Key Facts from JMP 2015 Report*. 2015. http://www.who.int/water_sanitation_health/monitoring/jmp-2015-key-facts/en/.

[2] UN. *Transforming our world: the 2030 Agenda for Sustainable Development.* 2015. https://sustainabledevelopment.un.org/post2015/transformingourworld.

[3] Notomi, T., et al., *Loop-mediated isothermal amplification of DNA.* Nucleic acids research, **28**(12): E63. 2000.

[4] USEPA. *Method 1611: Enterococci in Water by TaqMan® Quantitative Polymerase Chain Reaction (qPCR) Assay*. 2012. https://www.epa.gov/sites/production/files/2015-08/documents/method_1611_2012.pdf.

QUATERNARY AMMONIUM SALTS AS ALKYLATING REAGENTS IN C-H ACTIVATION CHEMISTRY

Manuel Spettel, Michael Schnürch

E163 - Institute of Applied Synthetic Chemistry, TU Wien, Vienna, Austria

INTRODUCTION

Selective C-C bond-forming reactions are very fundamental and often used reactions in organic chemistry. Yet, such reactions often require functionalized starting materials. Therefore, in recent years, transition-metal-catalyzed C-H activation reactions have gained lots of attraction and are an important tool in organic chemistry.[1-3] This reactions generally use less functionalized starting materials, and are therefore more step- and atom efficient.[4, 5] Also, they tolerate a wide area of functional groups. Thus, in recent years, C-H activation processes for assembly and functionalization of organic molecules could greatly simplify the synthesis of pharmaceuticals, natural products and general feedstock chemicals.[6-8] Amongst the transformations which can be carried out via C-H activation methods, alkylation reactions are tremendously important and frequently used in the organic lab. Conventional approaches use primarily either alkyl halides or olefins as alkylation agents, whereas both alkyl sources have their advantages and disadvantages. The goal of the present work was to find an alternative alkyl source which combines the best features of the two aforementioned reagents.

FUNDAMENTAL OF THE PROBLEM

Sideproduct formation is a major drawback when using alkyl halides. On the other hand, transition-metal-catalyzed C-H activation reactions using olefins as alkylating reagents are highly potent C-C bond-forming reactions and have been used successfully in numeruous examples in the last two decades.[9, 10] However, short chained olefins such as ethylene, propylene or butylene are gaseous at room temperature and highly flammable, therefore not a desired alkylating agent in the lab. Thus, herein we tried to overcome the disadvantages of using gaseous olefins, by using solid quaternary ammonium salts as alkylating agents. An *in-situ* Hofmann elimination delivers the olefin which is then used by a Rh(I)-catalyzed reaction towards the desired alkylated product.

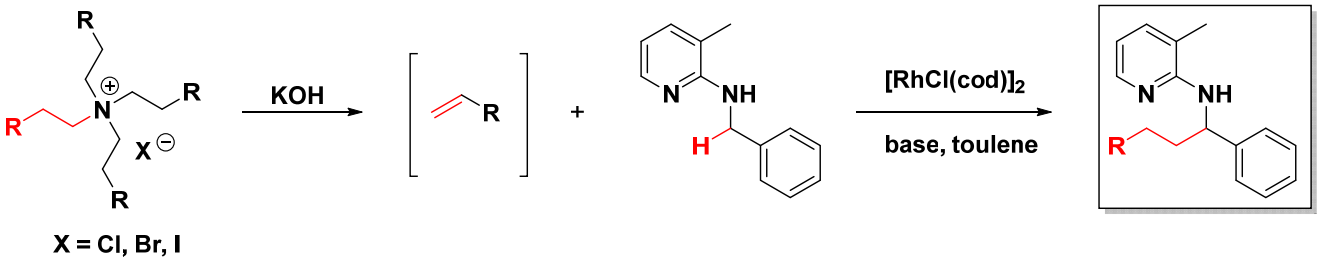

Scheme 1: Reaction scheme for C-H alkylation with quaternary ammonium salts

We started the development of direct alkylation of benzylic amines using the conditions optimized for our direct alkylation reactions with olefins[10], but employing quaternary ammonium salts as alkyl source. Initial experiments using potassium carbonate as base showed only good results for the ethylation protocol but where quite slow (28h). Longer alkyl chains dropped to nearly no conversion immediately. We realized that the rate limiting step for the reaction seems to be the formation of the olefin *via* Hofmann elimination. After intensively screening for optimal conditions

to accelerate the elimination step, potassium hydroxide was found as crucial reagent for this reaction. With optimized conditions in hand, also longer alkyl chains could be introduced with good efficiency.

RESULTS AND DISCUSSION

With the optimized protocol in hand, we performed alkylation reactions with different quartenary ammonium salts on a number of different substrate to demonstrate the scope of the present transformation. We used different quaternary ammonium salts in order to obtain products with alkyl chains up to C8. Also we changed substitution patterns at our starting material leading us to a variation of products with different moieties.

CONCLUSION

Benzylic amines were alkylated using quaternary ammonium salts as alkyl source. The Hofmann elimination was found to be the crucial step in order to obtain effective conversion to the product. Kinetic studies towards a fast Hofmann elimination have led to a universal and handy protocol for alkylating C-H activation reactions, especially since gaseous olefins can be substituted for solid quaternary ammonium salts.

REFERENCES

[1] Moselage, M., J. Li, and L. Ackermann. *ACS Catalysis*, **2016**. 6(2): p. 498-525.

[2] Luo, C.-Z., et al., *ACS Catalysis*, **2015**. 5(8): p. 4837-4841.

[3] Verma, S., et al., *ACS Sustainable Chemistry & Engineering*, **2016**. 4(4): p. 2333-2336.

[4] Bond, G.C., *Metal-Catalysed Reactions of Hydrocarbons*. **2005**.

[5] Dyker, G., *Handbook of C–H Transformations: Applications in Organic Synthesis*. **2005**.

[6] Wencel-Delord, J. and F. Glorius, *Nat Chem*, **2013**. 5(5): p. 369-375.

[7] Schipper, D.J. and K. Fagnou, *Chem. Mater*., **2011**. 23: p. 1594.

[8] Yamaguchi, J., A.D. Yamaguchi, and K. Itami, *Angew. Chem., Int. Ed*., **2012**. 51: p. 8960.

[9] Murai, S., et al., *Nature,* **1993**. 366(6455): p. 529-531.

[10] Pollice, R., et al., *ACS Catalysis*, **2015**. **5**(2): p. 587-595.

POST-DOCKING DERIVATIZATION REVEALS PYRAZOLOQUINOLINONE BINDING MODE AT THE α+/ γ- $GABA_A$ RECEPTOR INTERFACE

David Chan Bodin Siebert[a], Marcus Wieder[b], Lydia Schlener[b], Margot Ernst[c], Thierry Langer[b], Gerhard Ecker[b], Michael Schnürch[a], Lars Richter[b*]

[a]E163 - Institute of Applied Synthetic Chemistry, TU Wien, Vienna, Austria
[b]Department of Pharmaceutical Chemistry, University of Vienna, Vienna, Austria
[c]Department of Biochemistry and Molecular Biology, Center for Brain Research, Medical University of Vienna, Vienna, Austria

INTRODUCTION

gamma – Aminobutyric acid (GABA) is a wide-spread transmitter which binds to two pharmacologically diverging GABA receptors, $GABA_A$ and $GABA_B$. $GABA_A$ receptors ($GABA_A$Rs) are transmembrane pentameric ligand-gated chloride ion channels and represent an important target of many clinically relevant drugs (e.g. benzodiazepines, barbiturates, etc.). These receptors consist of different subunits (e.g. α,β,γ, etc.), which are drawn from nineteen subunit isoforms that are grouped into classes (e.g. α1-α6, β1-β3, etc.).[1-4] Each $GABA_A$ receptor possesses several extracellular and transmembrane small molecule binding sites – such as the high affinity benzodiazepine binding site (BZ site) at the α+/γ- interface.[5] This interface represents the allosteric binding site of the eponymous compound class of the benzodiazepines which exert anxiolytic, muscle-relaxant, sedative- hypnotic and anticonvulsant effects. Until today, benzodiazepines are widely used for medical treatments as well as in pharmaceutical research. To antagonize their effects various chemotypes have been introduced, e.g. the pyrazoloquinolinones (PQs).[6] However, all chemotypes possess partly overlapping and partly distinct *in vitro* and *in vivo* effects. This ambiguous behaviour might be based on the lack of knowledge regarding their binding sites and modes respectively.

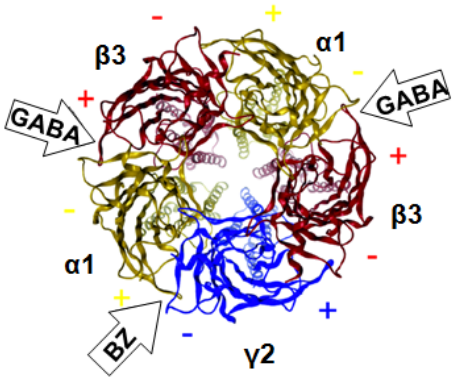

Figure 1: Homology model of a hetero-pentameric α1β3γ2 $GABA_A$ receptor (top view).

EXPERIMENTS

In order to determine the binding mode of pyrazoloquinolinones at the extracellular α+/γ- interface (BZ site) a homology model based on the crystal structure of the human $GABA_A$ β3 homopentamer was created consisting of two α1, two β3 and one γ2 subunits.[7] Flexible Molecular Docking was then performed using the PQ CGS8216 to get 100 different binding poses. For each pose an array of seven selected derivatives were built using the initial coordinates of CGS8216 to expand the dataset up to 800 poses in total (Figure 2). From the 7 analogues, four were classified as active (pKi > 8) while three were classified as inactive (pKi < 7). To validate the poses, the

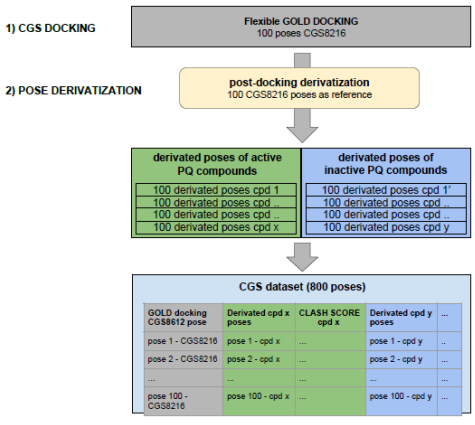

Figure 2: First part of the workflow outlining the Flexible Molecular Docking and the Post-docking Derivatization.

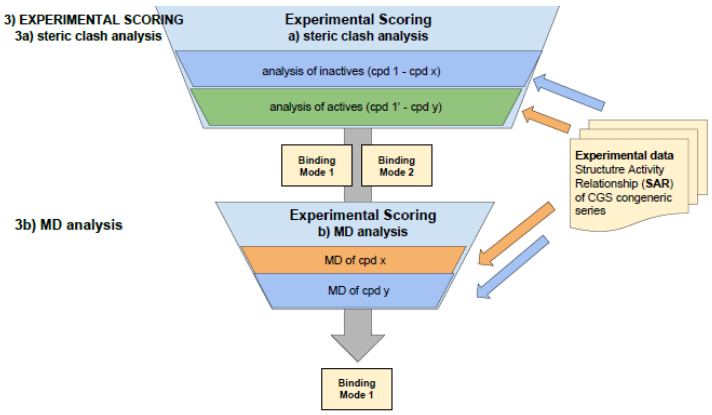

Figure 3: Second part of the workflow outlining the experimental/clash analysis and the MD analysis.

derivative analogue placements were analyzed for steric clashes and their compliance with Structure Activity Relationships (Experimental Scoring). The evaluation led to two reasonable binding modes which were further differentiated by Molecular Dynamic Simulations. Analysis of the variation of RMSD (root-mean-square deviation) and the occurring protein - ligand interactions resulted in one consistent binding hypothesis (Figure 3).

RESULTS AND DISCUSSION

We were able to identify a binding hypothesis for the pyrazoloquinolinones at the benzodiazepine binding site (α+/γ- interface) that is in great accordance with known SAR data (Figure 4). The filtering of potential binding poses was undertaken with a novel methodology termed "post-docking derivatization". This methodology makes use of SAR information for validation of docking poses to narrow down reasonable binding modes. On top of this analysis we performed Molecular Dynamic Simulations that corroborated the binding hypothesis with the greatest SAR accordance.

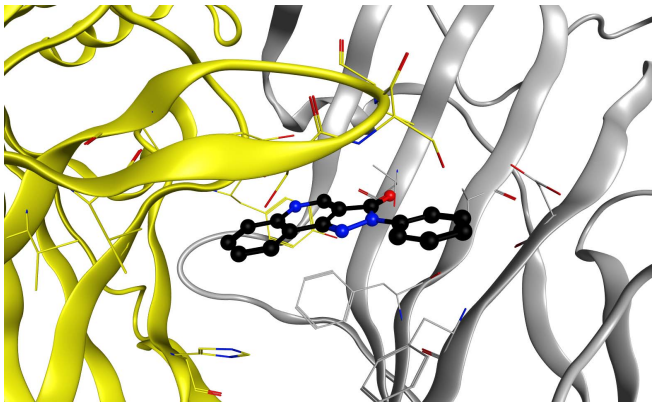

Figure 4: Final binding hypothesis of pyrazoloquinolinones at the the extracellular α+/γ- interface.

CONCLUSION

The binding hypothesis of the pyrazoloquinolinones will simplify the structure guided optimisation in the retrieval of required antagonists for the BZ site of the $GABA_A$ receptor. Furthermore, the binding hypothesis will positively influence ongoing research at homologous binding site of the $GABA_A$ receptor, e.g. the α+/β- interface (low affinity allosteric binding site of PQs).[8] In addition, the post-docking derivatization methodology represents a useful tool to easily cluster reasonable docking poses including important biological information.

REFERENCES

[1] Sieghart W, *Pharmacol Rev*, 181-234, **1995**.

[2] Siegl E, *Curr Top Med Chem*, 833.839, **2002**.

[3] Ernst *el at.*, *Neuroscience*, 933-943, **2003**.

[4] Olsen RW and Sieghart W, *Pharmacol Rev*, 243-260, **2008**.

[5] Puthenkalam, R. *et al., Front Mol Neurosci,* **2016**.

[6] Czernik *et al.*, *Life Sci.*, **1982**.

[7] Miller and Aricescu, *Nature*, **2014**.

[8] Ramerstorfer *et al.*, *J. Neuoscience*, **2011**.

SPATIAL AND SEASONAL VARIABILITY OF MERCURY CONCENTRATIONS IN AEROSOLS FROM MALOPOLSKA REGION, SOUTH POLAND

Katarzyna Szramowiat[a], Katarzyna Styszko[a*], Magdalena Kistler[b], Łukasz Uruski[a], Anne Kasper-Giebl[b], Janusz Gołaś[a]

[a]AGH University of Science and Technology, Faculty of Energy and Fuels, Department of Coal Chemistry and Environmental Sciences, Krakow, Poland
[b]E164 – Institute of Chemical Technologies and Analytics
*styszko@agh.edu.pl

INTRODUCTION

The ubiquity of mercury in the environment became one of the most frequently discussed topics in the environmental science. Its presence is strictly linked to the energy production and coal combustion processes as well as incineration of other fossil fuels, mining and smelting [1]. Atmospheric Hg have three main forms: gaseous elemental mercury (GEM), gaseous oxidized mercury (HgII) compounds (GOM), and mercury associated with particulate matter (denoted also as total particulate mercury – TPM or $Hg_{(P)}$ [2, 3]. Bad ambient air quality in the South Poland (Malopolska Voivodeship) is continuously a matter of concern of local authorities and researchers, but most of all it poses a problem for the inhabitants of Poland's second largest and most PM10 polluted city – Krakow [4]. This study is a part of larger measurement campaign, aiming to describe the chemical composition of aerosols in Krakow agglomeration. The concentrations of mercury in atmospheric aerosols in Krakow agglomeration were not a matter of research so far. This study is a continuation of at the results described by Styszko et al. [3].

EXPERIMENTS

The concentrations of total particulate mercury (TPM) have been measured during heating and non-heating seasons of 2013 in South Poland (Malopolska). All samples were collected on quartz fibre filters (Pallflex, Pall Life Sciences) with a diameter of 47 mm. An automatic Hg analyser, MA-3000 (NIC, Japan) with autosampler was applied for determination of the particle-bound mercury in the collected samples. Measurements were conducted with calibration curve linear (r^2 = 0.9984) in the range 0.045-1.000 ng. Limit of detection was determined as 0.015 ng, while limit of quantification 0.045 ng. PM10 and PM2.5 were collected at three locations representing the urban (Krakow), industrial/residential (Skawina) and rural/residential (Bialka) environment.

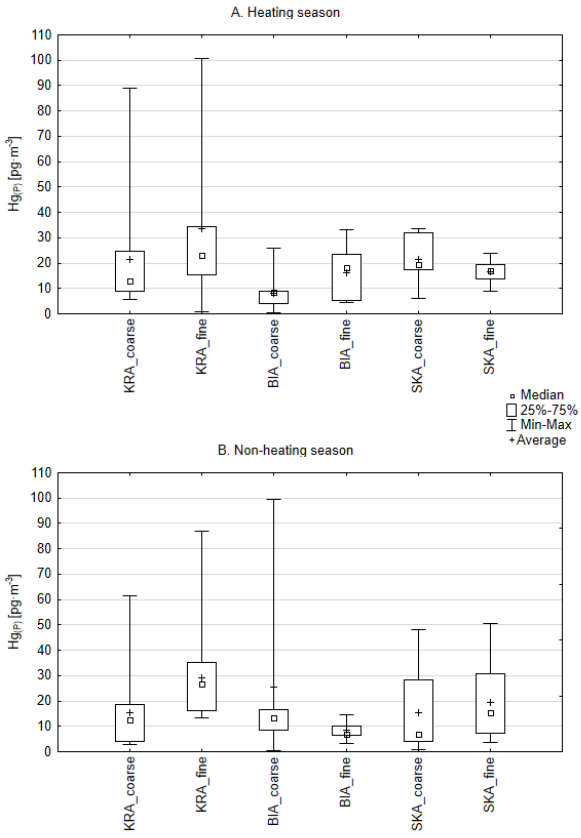

Fig.1. Hg(P) concentration in PM10 and PM2.5 [pg·m^{-3}] during the whole study period.

RESULTS AND DISCUSSION

The results referring the particulate mercury concentration in three regions of the Malopolska Voivodeship are the continuation of works presented before [5]. The presented study aims at the comparison of the total particulate mercury concentration variations at three chosen measuring stations in Malopolska region, Poland. The data obtained in Krakow, Skawina and Bialka were used to estimate the coarse and fine particulate mercury concentrations, showed that up to 71% of the mercury present in PM10 was present in the PM2.5 fraction. The measured mass concentrations of PM10 and PM2.5 fractions in heating season were in the range of 30 to 128 $\mu g \cdot m^{-3}$ and 9 to 75 $\mu g \cdot m^{-3}$, respectively. In the non-heating season those concentrations were in the range of 6 to 40 $\mu g \cdot m^{-3}$ and 0.3 to 36 $\mu g \cdot m^{-3}$. The average concentration of mercury (Hg_{coarse}) in coarse fraction (PM2.5-10) during the heating season ranged from 8.0±7.1 $pg \cdot m^{-3}$ to 21.3±21.7 $pg \cdot m^{-3}$. In the non-heating season, the average Hg_{coarse} ranged from 15.2±16.4 $pg \cdot m^{-3}$ to 25.6±31.8 $pg \cdot m^{-3}$. The average concentration of mercury Hg_{fine} in fine fraction (PM2.5) were between 16.3±10.4 $pg \cdot m^{-3}$ and 33.4±31.8 $pg \cdot m^{-3}$ in the heating season and between 8.5±3.7 $pg \cdot m^{-3}$ and 28.6±16.7 $pg \cdot m^{-3}$ in the non-heating season. Occurrence of mercury in particulate matter is mainly caused by the local sources (like emission from coal-fired power plants), long-range transportation of fine particles and processes of particles transformation: like absorption, coagulation and agglomeration favoured additionally by mild weather conditions, higher relative humidity of air and low wind velocities.

CONCLUSION

TPM was present in the samples from the rural area (Bialka) in concentrations only slightly lower than those observed in the city (Krakow, Skawina) during the heating and non-heating seasons. The higher concentrations of TPM in Skawina and Krakow are believed to be caused both by local emission sources like coal-heated power plants and by a long-range transport of fine particles. This is confirmed by pHg values and particulate mercury deposition rates. The relation between origination of fine mercury from power plants and long-range transport needs to be still identified. This creates the justification for further research on the particulate mercury fate. Recognition of the mercury speciation is extremely important for identification of the mercury emission sources. Hence, in the following part of the study authors will focus on the mercury partitioning between solid and gas phase.

ACKNOWLEDGEMENTS

This work was partially supported by AGH University Grant. The authors acknowledge the financial support of OeaD and of the Ministry of Science and Higher Education (Poland) in the frame of project WTZ (Wissenschaftlich–Technische Zusammenarbeit), No. PL09/2015.

REFERENCES

[1] K.T. Whitby, Atmos. Environ. (1967) 12 (1978) 135-159.
[2] W.H. Schroeder, J. Munthe, Atmos. Environ. 32 (1998) 809-822.
[3] K. Styszko, K. Szramowiat, M. Kistler, A. Kasper-Giebl, L. Samek, L. Furman, J. Pacyna, J. Gołaś, C. R. Chim. 18 (2015) 1183-1191.
[4] K.M. Markowicz, P.J. Flatau, M.V. Ramana, P.J. Crutzen, V. Ramanathan, Geophys. Res. Lett. 29 (2002) 21-24.
[5] K. Szramowiat, K.Styszko, M. Kistler, A. Kasper-Giebl, J. Gołaś, Particulate matter alert in South Poland, in: e.a. Richard Zemann (Ed.), Vienna young Scientists Symposium, TU Wien. — Gumpoldskirche, Vienna, 2015.

LOCAL INSTABILITIES IN THE H_2 OXIDATION ON RHODIUM: STRUCTURAL EFFECTS

Clara Freytag, Martin Datler, Yuri Suchorski*

E165- Institute of Materials Chemistry, TU Wien

MOTIVATION

The catalytic H_2 oxidation is the deciding process in the energy conversion in hydrogen fuel cells. The only product of the reaction is water, therefore the importance of such "green" energy production increases continuously. To improve the efficiency of future generation fuel cells, a deeper understanding of the H_2 oxidation is desirable and thus, intensive theoretical and experimental studies are necessary. Until now, the H_2 oxidation was mainly studied on smooth single crystal surfaces of metals such as Pt, Pd, Rh[1], whereas industrial catalysts are made of noble metal nanoparticles exhibiting different high Miller-index facets on their surface. It is therefore reasonable to create model systems with stepped (high Miller-index) surfaces. Recently, a self-sustained oscillating behaviour of the H_2 oxidation reaction was observed on a Rh foil exhibiting µm-sized stepped domains[2]. However, the observed turbulent-like spatiotemporal behaviour is complexly coupled over the whole sample. Therefore, to simplify the model system, we confine the stepped Rh surface, which seems to be necessary for oscillating reaction behaviour, to a small ca. 30 µm wide furrow-like region on a smooth Rh(111) single crystal surface.

EXPERIMENTAL

For the present studies, a Photoemission Electron Microscope (PEEM) was used as a flow reactor for the H_2 oxidation reaction. In PEEM, the electrons photo-emitted from the studied surface as a result of the UV-light illumination create a strongly magnified, real-time image of the surface. This allows an *in situ* visualisation of surface processes on a µm-scale and a monitoring of ongoing catalytic reactions[3,4]. Recently, the novel "kinetics by imaging" approach was developed[5], which links the catalytic activity of the imaged surface to the PEEM image brightness. This approach allows studying of the local kinetics on a µm-scale and thus revealing of structural effects.

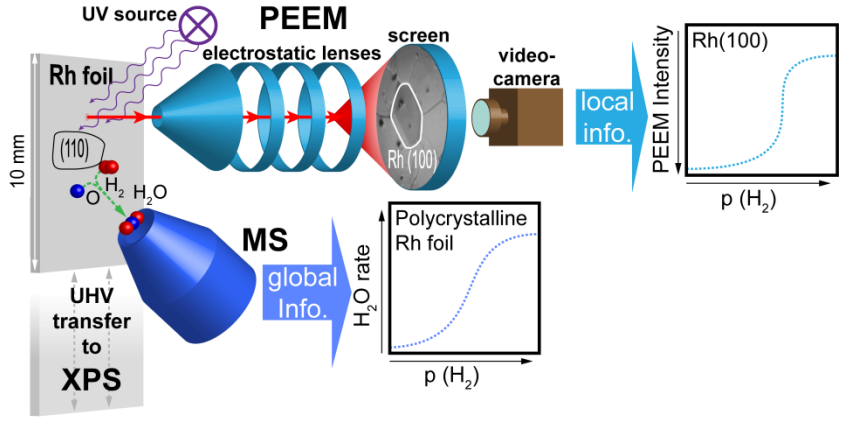

Fig. 1: Schema of the experiment: The PEEM is used as a flow reactor in the 10^{-6} mbar pressure range. Apart of PEEM, the multipurpose UHV apparatus is equipped with XPS for chemical information and allows fast transfer of the Rh sample between XPS and PEEM under the reactive atmosphere. The MS is used for global kinetic measurements simultaneously to local kinetic measurements by PEEM.

The contrast mechanism of the PEEM is based on the work function of the imaged surface: low work function allows electrons to escape more easily and the PEEM image is bright, a high work function leads to a dark image. Since adsorbed H and O atoms change the work function, the state of the Rh surface (O or H covered, dark or bright, correspondingly) can be monitored by PEEM. In the experiment, the PEEM image is video-recorded and the digitized video-files are analyzed in order to collect the local kinetic information (Fig.1). The Rh sample was a 10x10 mm^2 Rh(111)

single crystal which was cleaned with Ar^+ ion bombardment and annealed at 1177 K in UHV and at 777 K in $5x10^{-7}$ mbar of O_2.

RESULTS AND DISCUSSION

The hydrogen oxidation reaction might exhibit self-sustaining oscillations of the reaction rate under stationary conditions. Since the reaction rate depends on the surface coverage, this should also oscillate between the O covered (low activity) and H covered (high activity). Such periodic changes are accompanied by surface pattern formation such as expanding spirals in the reaction front propagation[4]. In the present study, we focused on a furrow-like defect (Fig. 2a) exhibiting stepped Rh surfaces on its flanks. After the conditions were set where the polycrystalline Rh foil exhibited oscillating behaviour, variations in the image intensity could be observed within the furrow. When setting ROIs inside the furrow (Fig. 2a) and evaluating the image intensity within the ROIs over time, periodic changes in the local image intensity were detected (Fig.2b). At the same time, the ROIs set outside the furrow ("ROI top" and "ROI bottom") did not register any intensity variation (Fig. 2b).

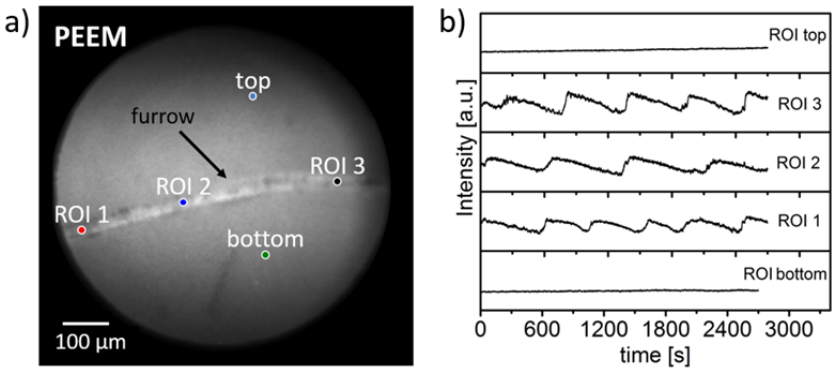

Fig. 2: a) PEEM snapshot during ongoing H_2 oxidation at p_{O2} = 1.1 x 10^{-6} mbar, p_{H2} = 8.4 x 10^{-7} mbar and T = 433 K. Regions of interest (ROIs) are marked where the local intensity was evaluated; **b)** Local intensity in marked ROIs over time. Oscillations are registered within the furrow but not on the smooth surface outside.

Since the observed oscillating behaviour is confined to the furrow, it seems like the stepped surface plays a decisive role in the appearance of oscillations. The oscillations can occur if two steady states are possible and a feedback mechanism switching between these steady states is provided. The steady states are the oxygen-covered (inactive) and the hydrogen covered (active) state of the surface. As the feedback mechanism, we assume the incorporation of oxygen under the Rh surface, i.e. formation of the subsurface oxygen. Such a periodic formation and depletion of the subsurface oxygen governs the sticking of oxygen and hydrogen and thus modulates the adsorption and the reaction in an oscillating way. However, the highly stepped Rh surface is necessary to form the subsurface oxygen. This is available on the flanks of the furrow, but not around the furrow where solely the smooth Rh(111) surface is located. In this way the oscillations are confined to the furrow.

SUMMARY

We show that the oscillations in the H_2 oxidation only occur within the mesoscopic furrow on the smooth Rh(111) surface. The furrow contains highly stepped surfaces on its flanks and it seems that these steps and defects are necessary for the appearance of oscillations, at least under present conditions. Periodic formation and depletion of subsurface oxygen on the stepped surface is assumed to serve as a feedback mechanism for the observed oscillating behaviour, but further studies are necessary to prove this assumption.

REFERENCES

[1] V. Gorodetskii, A. Sametova, A. Matveev, V. Tapilin, Catalysis Today, **144**, 219, 2009 and references therein
[2] M. Datler, I. Bespalov, S. Buhr, J. Zeininger, G. Rupprechter, Y. Suchorski, to be published, 2017
[3] D. Vogel, C. Spiel, Y. Suchorski, A. Urich, R. Schlögl, G. Rupprechter, Surface Science, **605**, 1999, 2016
[4] G. Ertl, Nobel Prize Lecture, Angew.Chem.Int.Ed., **47**,3524, 2008
[5] Y. Suchorski, G. Rupprechter, Surface Science, **643**, 52, 2016.

RECOMBINANT PRODUCTION AND PURIFICATION OF CHALCONE-3-HYDROXYLASE (CH3H) FROM YEAST

Johanna Hausjell, Julia Weissensteiner, Heidi Halbwirth, Oliver Spadiut*

E166 Institute of Chemical Engineering, TU Wien

INTRODUCTION

Cytochrome P450ies make up one of the largest and most diverse known protein family and are present in all kingdoms of life. Their name results from a characteristic absorption band at 450 nm which they exhibit when complexed with carbon monoxide. P450ies are responsible for catalysis of essential reactions including carbon source assimilation, hormone-synthesis, generation of structural compounds, carcinogenesis and degradation of xenobiotics [1]. Due to their ability to hydroxylate complex carbohydrates very specifically, attainment of high amounts of P450ies is also relevant in regard to biotransformation and industrial applications [2]. Isolation of P450ies from native plant or animal tissues often results in humble yields which is why recombinant production is a striking alternative. However, eukaryotic P450ies are in most cases membrane bound which makes recombinant production and subsequent purification challenging [3]. As a result there is also only little known about the structure and substrate conversion mechanisms of membrane bound P450ies.

EXPERIMENTS AND EXAMINATIONS

We are currently working on the recombinant expression and subsequent purification as well as characterization of chalcone-3-hydroxylase, a membrane bound P450 enzyme. CH3H is involved in the biosynthesis of anthochlor pigments in plants, which are important for yellow colorization, formation of UV-honey guides and exhibit health beneficial effects [4-6].

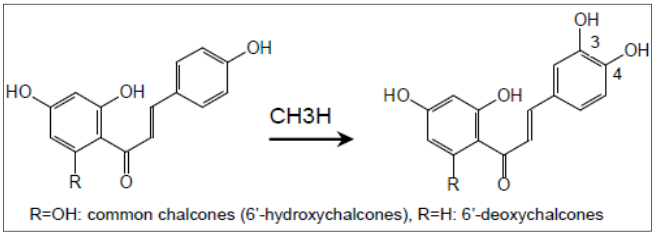

Figure 1: Reaction catalysed by CH3H

In order to shed light on the substrate conversion mechanisms and to elucidate the stringent substrate-specificity the enzyme needs to first be produced in large quantities. Yeasts were chosen as production host as they are able to both perform post translational modifications and quickly grow on inexpensive media up to high cell densities [7]. Subsequent attainment of CH3H involves cell disruption, solubilization of the membrane as well as isolation and purification of the protein.

This project involves bioprocess engineering for establishment of an up- and downstream process in order to attain high amounts of purified CH3H. Up- and downstream process development is the main focus of the integrated bioprocess development working group. Characterization of substrate specificity will then be performed in the division of photochemistry. Further disciplines involved include protein crystallography for structure elucidation and analytical chemistry for increased process understanding in up- and downstream process development.

RESULTS AND DISCUSSION

Recombinant CH3H was actively produced with a strep tag in *S. cerevisiae* strain INVSc1 under control of the CUP1 promoter, where expression of the enzyme is induced by addition of copper

sulfate. The producing strain was characterized in terms of uptake and production rates as well as yields and growth rate. Subsequently it was physiologically compared to the wild type strain.

A downstream process for purification of CH3H was established: After cell disruption, the membrane was solubilized in different detergents with varying concentrations to screen for suitable conditions. The enzyme was first purified using affinity chromatography and then the suitability of detergents for solubilization was evaluated by size exclusion chromatography. Based on the obtained chromatograms, the most appropriate detergent was selected and applied for large-scale purification.

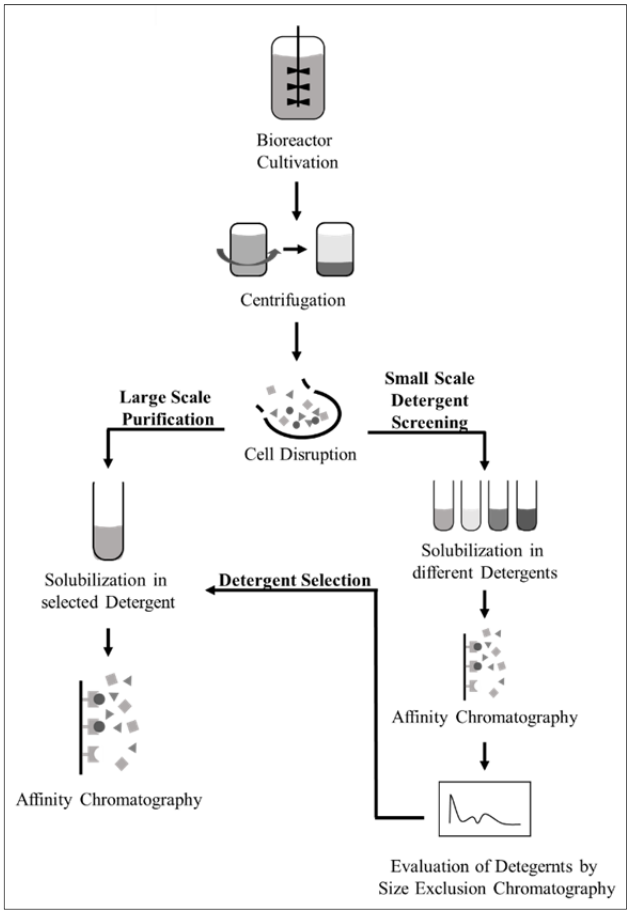

Figure 2: Scheme of cultivation and experimental design for establishment of the downstream process.

CONCLUSION

CH3H was actively expressed in *S. cerevisiae* and a downstream process for large scale purification was established.

Future experiments will involve investigations regarding substrate specificity and crystallization to elucidate the structure of the enzyme, and through correlation of both results shed light on the reaction mechanism. Furthermore protein engineering is ongoing to develop a soluble version of CH3H for facilitated downstream processing.

ACKNOWLEDGEMENTS

The authors acknowledge financial support from the Austrian Science Fund (FWF): P 29552-B29.

REFERENCES

[1] Werck-Reichhart D., Feyereisen R., Cytochromes P450: a success story, Genome Biology, 2000

[2] Ullrich R., Hofrichter, M. Enzymatic hydroxylation of aromatic compounds, Cellular and Molecular Life Sciences, 271-293, 2007

[3] Zelasko S., Palaria A., Das A., Optimizations to achieve high-level expression of cytochrome P450 proteins using Escherichia coli expression systems, Protein Expression and Purification, 77-87, 2013

[4] Miosic S., Knop K., Hölscher D., Greiner, J., Gosch, C., Thill, J., Kai, M., Shrestha,B. K., Schneider, B., Crecelius, A. C., Stich, K. & Halbwirth, H. 4-Deoxyaurone Formation in Bidens ferulifolia (Jacq.) DC. PloS one, 2013

[5] Harborne J. B., Comparative Biochemistry of Flavonoids, Academic Press, 1967

[6] Yadav V. R., Prasad S., Sung, B., Aggarwal, B. B., The role of chalcones in suppression of NF-κB-mediated inflammation and cancer, International Immunopharmacol, 295-309, 2011

[7] Rosano G.L., Ceccarelli E.A., Recombinant protein expression in microbial systems, Frontiers in Microbiology, 2014

POROUS Si_3N_4-BASED SUPPORT MATERIALS WITH TAILORED GAS PERMEABILITY

Thomas Prochaska, Roland Haubner and Thomas Konegger

E164-CT - Institute of Chemical Technologies and Analytics, TU Wien

INTRODUCTION

Porous silicon nitride ceramics can be used for gas separation, also at high temperatures. Silicon nitride has the advantage of chemical stability up to high temperatures and good mechanical properties.[1] For its use as support material in gas separation, gas permeabilities $>10^{-14}$ m^2 are necessary.

The objective of this work was an investigation of the influence of various processing parameters on the permeability behaviour of porous silicon nitride tubes generated via slip-casting.

EXPERIMENTAL PROCEDURES

For all experiments the samples were manufactured via slip casting. The slip contained Si_3N_4, powder (UBE Industries), sintering aids, a dispersing agent and water. As sintering aids Al_2O_3 (Almatis) and Y_2O_3 (H.C. Starck) were used, and Dolapix A88 (Zschimmer & Schwarz) was used as dispersion aid. After casting into plaster moulds, the green bodies were dried overnight at 105 °C followed by sintering at 1600 °C in N_2 atmosphere. Three different Si_3N_4 sources were used; each of them had a different α-Si_3N_4 to β-Si_3N_4 ratio and particle size (Table 1). Mercury porosimetry (Pascal P140 and P440, Porotec), He-pycnometry, water immersion testing, and an air flow test bench were used to investigate porosity, skeleton density, bulk density and air permeability.

Table 1: Particle size and α/β contents of the used powders

	$d_{0.5}$ /µm	α - Si_3N_4 /%	β - Si_3N_4 /%
Si_3N_4-A	1.1	99.4	0.6
Si_3N_4-B	1.6	99.9	0.1
Si_3N_4-C	1.4	88.3	11.7

RESULTS AND DISCUSSION

As a first step, the impact of different concentrations of sintering aids was investigated. As Si_3N_4 source Si_3N_4-A was used. The mass fractions of the sintering aids were reduced subsequently. Starting with the highest amounts of 2.5 % of Al_2O_3 and 2.5 % of Y_2O_3 with respect to silicon nitride, three samples were prepared and sintered at 1600°C. The same was done with mass fractions of 1.0%, 0.5% and 0.2 % of each sintering aid.

Decreasing the amount of sintering aids yielded a higher permeability but reduced mechanical stability. To ensure sufficient stability of the samples, mass fractions of 2.5% of the sintering aids were chosen for subsequent investigations.

To evaluate the impact of Si_3N_4 source, samples made of Si_3N_4-B and Si_3N_4-C powders were sintered at 1500 °C, 1550 °C and 1600 °C. A difference in the morphology of the microstructure depending on the powder type was observed using scanning electron microscopy. According to the literature [2], this is caused by the different amounts of β-Si_3N_4 in the starting materials.

A lower sintering temperature leads to a higher permeability. For Si_3N_4-C sintered at 1500 °C and 1550 °C, a high scattering of permeability values was observed. The samples made of Si_3N_4-C and sintered at 1600 °C yielded a higher permeability than the samples made of Si_3N_4-B regardless of the sintering temperature.

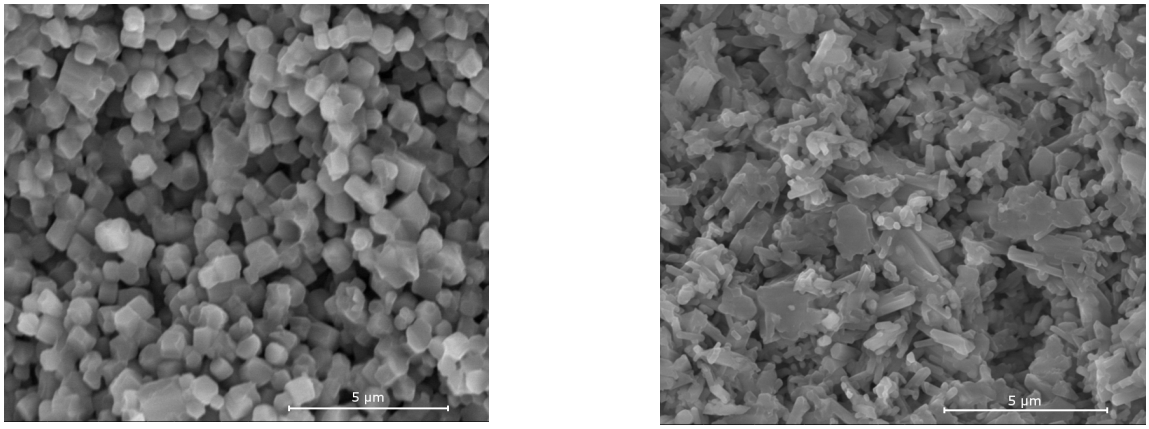

Fig. 1: left: fracture surface of Si_3N_4-B with equiaxed grains, 0.1 % β-Si_3N_4 in the starting powder; right: fracture surface of Si_3N_4-C with anisotropic rod-like grains, 11.7 % β-Si_3N_4 in the starting powder

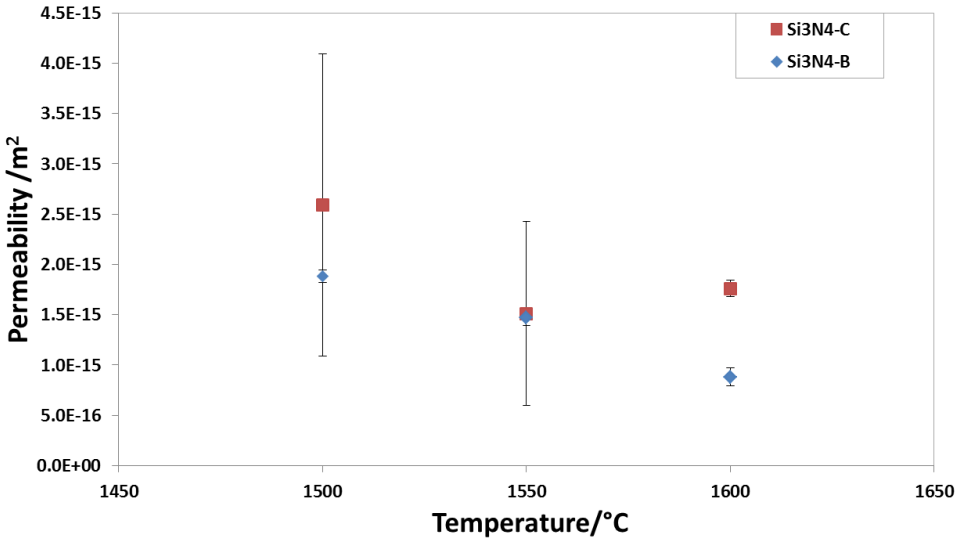

Fig. 2: Permeability as a function of sintering temperature for Si_3N_4-B and Si_3N_4-C. Each point is the mean value of four samples.

CONCLUSIONS

The impact of different processing parameters on porosity and permeability was shown. Based on the data at hand, a sintering temperature of 1600 °C with 2.5 % of both Al_2O_3 and Y_2O_3 as sintering aids with Si_3N_4-C as Si_3N_4 source was most promising. At the moment the desired permeability of 10^{-14} m^2 could not yet be achieved, thus requiring further work.

REFERENCES

[1] Konegger, T., et al. (2016). "Asymmetric polysilazane-derived ceramic structures with multiscalar porosity for membrane applications." Microporous and Mesoporous Materials **232**: 196-204.

[2] Kalemtas, A., et al. (2013). "Mechanical characterization of highly porous β-Si3N4 ceramics fabricated via partial sintering & starch addition." Journal of the European Ceramic Society 33(9): 1507-1515.

CATALYTIC ACTIVITY OF THIOLATE-PROTECTED GOLD NANOCLUSTERS SUPPORTED ON TiO_2, SiO_2 AND ZrO_2

Clara García, Noelia Barrabés, Günther Rupprechter

E165 - Institute of Materials Chemistry, TU Wien

INTRODUCTION

Thiolate-protected gold nanoclusters are an interesting emerging class of materials due to their stability, optical and electronic properties. Since the first report in 1994 by Brust et al. [1], atomically precise synthesis and separation protocols and final chemical and structure determination have been widely studied. This made possible to treat $Au_n(SR)_m$ clusters as well-defined nanostructures. Their stability and electronic states were found to be related to the highly symmetrical metallic core, which is protected by multiple gold-thiolate staples (-SR-Au-SR-), monomeric in case of $Au_{144}(SC_2H_4Ph)_{60}$) and dimeric staple bands in $Au_{25}(SC_2H_4Ph)_{18}$

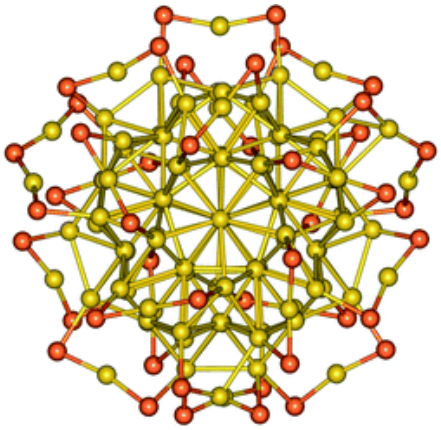

Picture 1: $Au_{144}(SC_2H_4Ph)_{60}$

Heterogeneous catalysis by metal nanoparticle supported on oxides, are often limited in their activity/selectivity, due to variations in metal particle size, surface structure and bonding to the support. Thiolate-protected Au nanoclusters had shown enhancement catalytic activity in several processes in comparison with the common nanoparticles catalysts. Atomically designed metal clusters offer the possibility to design well-defined and truly homogeneous surfaces leading to optimal catalysts for reaction mechanism studies. Although, the stability of the cluster structure and type of interaction with the support during the thiolate ligands removal treatments and under reaction conditions represent key understanding for their catalytic application.

EXPERIMENTS

Therefore, an in-depth investigation of the effect of the cluster size (Au_{25} vs Au_{144}), the staple configuration (short vs long staple) and the ligand interactions depending on the material support nature (TiO_2, SiO_2 and ZrO_2) is the focused on the present work, key information for their catalytic studies.

In order to evaluate the influence and effect of each parameter (size, staple, and support), the catalytic activity of the supported clusters is studied in Water-gas shift reaction (WGS). WGS reaction is an important industrial chemical process for the production of hydrogen and plays an important role in the production of methanol, each of which may be directly used as a fuel for various applications. The current conventional low-temperature catalysts have important drawbacks, as the deactivation of Cu-ZnO when it is exposed to air and /or water condensation[2]. Due to the enhancement of the catalytic performance by supported nanoclusters, the studied systems represents also an alternative in this process.

RESULTS AND DISCUSSION

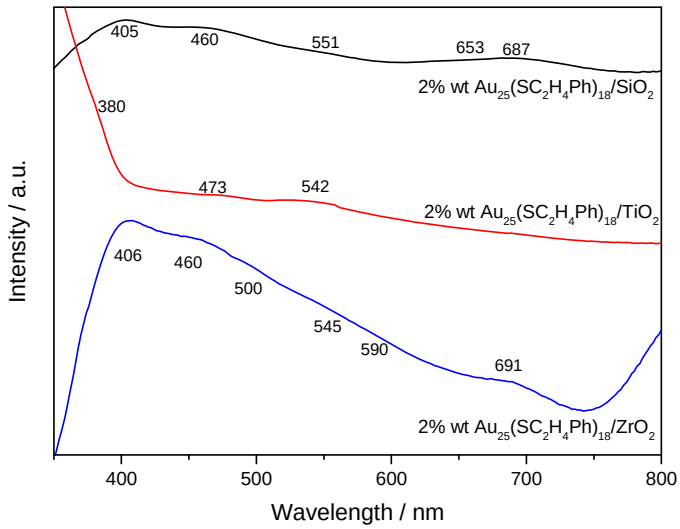

Chart 1: UV-Vis solids spectra

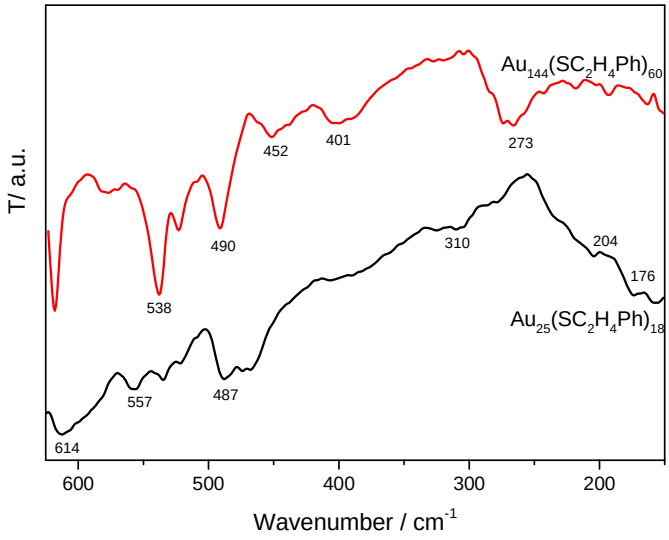

Chart 2: Far-Infrarred spectra

$Au_{25}(SC_2H_4Ph)_{18}$ and $Au_{144}(SC_2H_4Ph)_{60}$ clusters has been synthesized and isolated based on reported studies. The cluster purity and properties have been characterized by UV-Vis, FTIR and MALDI[3]. Each clusters has been supported on the different oxide materials (SiO_2, TiO_2 and ZrO_2) with a 2% wt by impregnation. The cluster characterization have been performance using optical spectroscopy (UV-vis) and infrared spectroscopy (FIR and MIR). By means of V-Vis solids it has been shown that there are different kinds of interactions denoted with the changes of the bands in the UV-Vis spectra depending on the supports. It is also confirmed the presence of the clusters without decomposition. Vibrational spectroscopy also showed the characteristic bands for both clusters.

CONCLUSION

Thermogravimetrical studies (TG), X-ray diffraction studies and XPS will be applied. The catalytical behavior will be measured via mass spectrometry. In terms of scientific community this study represent a bridge between the model catalysis and the real catalysis, due that with supported cluster catalysis it is possible to obtain structure-resolved active sites with 100% homogeneity (completely defined surface) normally just obtain by single crystals. In model catalysis, ultra-high vacuum conditions are required in all the studies whereas we operated at real conditions (atmospheric pressure).

REFERENCES

[1] Brust, M, J Chem Soc Chem Comm, 801, 1994

[2] J. A. Rodriguez, J. Phys. Chem. C, 116, 2012

[3] Huifeng Q. Rongchao J; Chem. Mater, 23, 2011

IMPACT OF INDUCER MOLECULES ON DNA ACCESSIBILITY IN CELLULASE AND XYLANASE EXPRESSION IN *TRICHODERMA REESEI*

Alice Rassinger, Thiago Mello-de-Sousa, Katharina Regnat, Christian Derntl, Robert Mach, Astria Mach-Aigner

E166 - Institute of Chemical, Enviromental and Biological Engineering at TU Wien

INTRODUCTION

Trichoderma reesei is a filamentous ascomycete, which exerts a saprotrophic lifestyle [1]. It gains its nutrients by degradation of plant cell wall material. For this purpose, it secretes various cellulases and hemicellulases to break down complex polysaccharides. The most naturally abundant plant-based biomass is cellulose, followed by hemicellulose (*e.g.* xylan) as second most abundant. Synergistic action of *T. reesei's* secreted enzyme cocktail leads to a degradation of the plant biomass.

These enzymes are industrially used [2]. Especially cellulases are highly secreted in the fungal strain Rut-C30, which is the ancestor of industrial strains. Their expression is regulated by the interplay of transcription factors (TFs) in response to different carbon sources or specific inducers.

AIM OF STUDY

In *Trichoderma*, the transactivator Xyr1 (encoded by *xyr1*) [3], the repressor Cre1 (encoded by *cre1*) [4], and gene-specific transcription factors regulate the expression of two major cellulases (encoded by *cbh1* and *cbh2*) and xylanases (encoded by *xyn1* and *xyn2*). Inducer substances such as sophorose (a transglycosylation product of cellobiose) and D-xylose achieve an induction of gene expression of these enzymes. On D-glucose, Cre1 mediates carbon catabolite repression (CCR), which leads to a down-regulation of expression of *xyr1* and of both cellulase and xylanase-encoding genes.

Transcription factors do not regulate gene expression exclusively, the chromatin packaging and other DNA-protein interactions add an additional layer in gene regulation. Therefore, the chromatin status as well as differences in protein-DNA interactions on TF binding motifs were investigated by chromatin accessibility real-time PCR (CHART-PCR) and *in vivo* footprinting in the wild-type strain and in the CCR-released industrial ancestor strain Rut-C30.

RESULTS AND DISCUSSION

For the cellulase-encoding genes (*cbh1* and *cbh2*) no remarkable changes in chromatin on repressing and inducing conditions in both strains were observed, whereas changes were detected for the xylanase-encoding genes (*xyn1* and *xyn2*). Together with *in vivo* footprinting analyses differences in protein-DNA interactions were detected, particularly for *xyn2*, depending on the inducer applied in the wild-type strain. Using sophorose, the protein-DNA interactions on the functional TF motifs of *xyn2* were similar in the wild-type strain and Rut-C30.

CONCLUSION

Both methods, the CHART-PCR and the *in vivo* footprinting, contribute to a deeper understanding of an important aspect in gene regulation. Besides that, the chromatin status of cellulase and xylanase-encoding genes react differently to applied inducers. It can be therefore concluded that

additional regulatory mechanisms are involved that shape the final promoter architecture in response to different inducers.

REFERENCES

[1] Kuhls et al, Proceedings of the National Academy of Science of the United States of America 93, 7755–7760, 1996

[2] Vikari et al, Biomass and Bioenergy *46*(0), 13-24, 2012

[3] Stricker et al, Eukaryotic Cell 5, 2128–2137, 2006

[4] Strauss et al, FEBS Letters 376, 103–107, 1995

RECOMBINANT CORE PROTEINS OF POLYPHENOL OXIDASES ON EXAMPLE OF AURONE SYNTHASE

Barbara Roth, Christian Molitor, Heidi Halbwirth*

E166 - Institute of Chemical, Environmental & Biological Engineering, TU Wien

INTRODUCTION

Aurone synthases belong to the family of polyphenol oxidases (PPOs), which contain a dinuclear (type III) copper center. PPOs catalyze the *o*-hydroxylation and the oxidation of phenolic compounds and are found in almost all plants[1]. Even though PPOs are involved in enzymatic browning reactions of e.g. fruits and vegetables, their involvement in the secondary plant metabolism, except for few cases, still remains unclear[2]. Plant PPOs are expressed as latent (inactive) pro-enzymes (~ 60 kDa) in which the catalytically active domain (~ 40 kDa) is shielded by its C-terminal domain (~ 20 kDa)[3]. However, the latent pro-enzymes can be activated *in vitro* by sodium dodecyl sulfate (SDS)[4]. During the maturation, the C-terminal domain is cleaved proteolytically, resulting in active enzyme[1]. Aurone synthases are specialized plant PPO involved in the formation of the yellow coloured flower pigments aurones from chalcones[5] (Fig. 1). In petals of *Coreopsis grandiflora* two candidate aurone synthases, *AUS1* and *AUS2*, are found to be expressed[6]. As the natural substrates of these PPOs are known the availability of fully active recombinantly expressed aurone synthases is of high importance in order to get insights into the substrate specificity of plant PPOs on a molecular level.

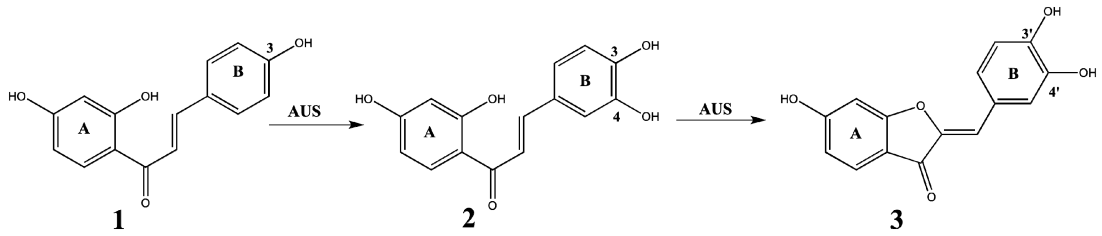

Figure 1: Excerpt of the secondary metabolism leading from the chalcone isoliquiritigenin **(1)** to the aurone sulfuretin **(3)** via butein **(2)**

EXPERIMENTAL

The aurone synthases *AUS1* and *AUS2* were cloned into the pGEX-6P-1 expression vector in both variants, to obtain (i) the full-length latent pro-enzyme as well as (ii) the shorter active enzyme. The *AUS* variants were expressed as fusion proteins containing glutathione S-transferase (GST) at the N-terminus. The protein purification was performed by fast protein liquid chromatography (FPLC) using affinity chromatography and ion exchange chromatography and confirmed by SDS-polyacrylamide gel electrophoresis (SDS-PAGE). The GST-tag of the fusion protein was removed proteolytically using PreScission™ protease. The substrate specificity of the purified enzymes was examined using high-performance liquid chromatography (HPLC) and UV/VIS spectroscopy.

RESULTS AND DISCUSSION

To date, we successfully expressed the latent pro-enzymes as soluble proteins. A high purity of the aurone synthases was achieved by affinity and ion exchange chromatography as confirmed by SDS-PAGE. After *in vitro* activation with SDS, both isoenzymes showed the expected enzymatic activity (Fig. 2) revealing that the proteins are correctly folded and functionally active.

Also the core sequences of *AUS1* and *AUS2* were expressed as soluble fusion proteins, as verified by SDS-PAGE. Furthermore, the proteins remained soluble after proteolytic removal of the GST-tag, however, they did not show any enzymatic activity, neither with nor without SDS. These results probably indicate that the proteins are folded correctly, but the incorporation of the copper atoms within the active site was not successful. An incubation with copper also did not result in enzymatic activity. Therefore, further experiments are necessary in order to obtain aurone synthases in their active forms.

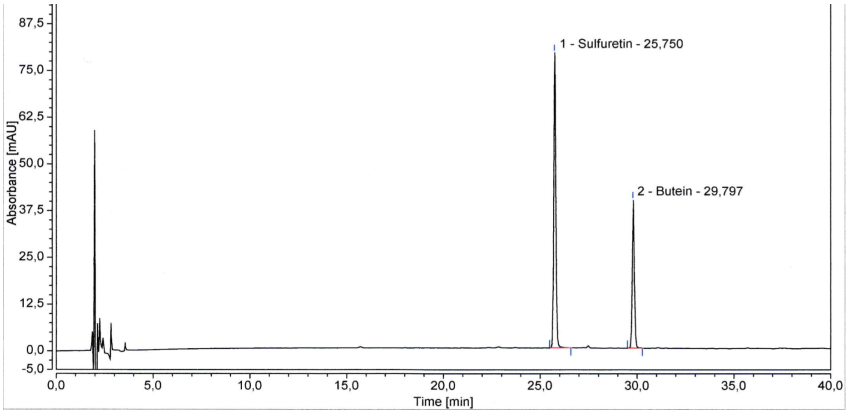

Figure 2: Chromatogram of an enzymatic assay of an active aurone synthase e.g. *AUS1* (substrate: butein; product: sulfuretin)

CONCLUSION

This work evidenced that it is possible to recombinantly express latent *PPO*s, which were functionally active after *in vitro* activation. However, the production of the catalytically active main core resulted in soluble but inactive protein, maybe due to a lack in copper incorporation.

A successful *in vitro* incorporation of the copper atoms within the active site would enable us to investigate the substrate specificity of plant polyphenol oxidases. Furthermore, the co-crystallization of aurone synthase (loaded with copper and/or zinc) with substrates and inhibitors will provide novel insights into the mechanism of plant PPOs.

ACKNOWLEDGMENT

The research is funded by the Austrian Science Fund (FWF): P28795.

REFERENCES

[1] L. T. Tran, J. S. Taylor, C. P. Constabel, *BMC Genomics* **2012**, *13*, 395.

[2] M. L. Sullivan, *Front Plant Sci* **2014**, *5*, 783.

[3] C. M. Marusek, N. M. Trobaugh, W. H. Flurkey, J. K. Inlow, *J. Inorg. Biochem.* **2006**, *100*, 108-123.

[4] A. M. Mayer, *Phytochemistry* **2006**, *67*, 2318-2331.

[5] S. Miosic, K. Knop, D. Hölscher, J. Greiner, C. Gosch, J. Thill, M. Kai, B. K. Shrestha, B. Schneider, A. C. Crecelius, U. S. Schubert, A. Svatos, K. Stich, H. Halbwirth, in *PLoS ONE, Vol. 8*, 2013/05/15 ed., **2013**, p. e61766.

[6] C. Kaintz, C. Molitor, J. Thill, I. Kampatsikas, C. Michael, H. Halbwirth, A. Rompel, *FEBS Lett.* **2014**, *588*, 3417-3426.

TOWARDS GENERIC REACTIVE FLOW MODELLING

Markus Bösenhofer[a,b], Christian Jordan[a], Michael Harasek[a]

[a]E166/2 - Institute of Chemical Engineering at TU Wien
[b]K1-MET GmbH, Linz, Austria

INTRODUCTION

Simulation of reacting flows relies heavily on sub-models for chemistry and turbulence-chemistry interaction. The main problem employing these models is their, usually, limited range of validity [1-4]. Therefore, sub-models have to be thoroughly chosen and tested prior to employing them. However, complex reactive flows featuring different flow and chemistry regimes would need generic models capable of adapting to the occurring regimes. Such generic models might also improve the predictions for classical combustion problems. According to literature, generic models could be based on local flow and chemistry time scales [4]. Determining flow time scales is straight forward, while determining chemistry time scales is problematic [5-6]. Therefore, as a first step towards a more generic reactive flow modelling, a critical evaluation of the chemical time scales is done. Well known definitions of the chemical time scale (τ_c) were proposed e.g. by Rehm et al. [5] and Prüfert et al. [6]. Rehm et al. proposed two definitions, Rehm I (Eq. 1) is defined as the maximum of the inverse reaction rate Jacobian (J). Rehm II (Eq. 2), defines the chemical time scale as the maximum of the inverse of the real parts of the reaction rate Jacobian eigenvalues (λ_i). Prüfert et al. [6] (Eq. 3) defined the chemical time scale as the inverse Euclidean matrix norm of the weighted reaction rate Jacobian. The weighting is done by the reaction rate ($\omega,\dot{}$).

$$\tau_c = max\left(\frac{1}{J}\right) \quad (1) \qquad \tau_c = max\left(\frac{1}{|\Re(\lambda_i)|}\right) \quad (2) \qquad \tau_c = \left\| J_{ij} \frac{\dot{\omega}_i}{\|\dot{\omega}_{ij}\|} \right\|^{-1} \quad (3)$$

TIME SCALE EVALUATION

The influences of the turbulence-chemistry interaction model, the reaction mechanism and the time scale definition on the chemical time scale are investigated. Therefore, the Eddy Dissipation Concept [1] (EDC) interaction model and two modifications (Gran [2] & modMag [3]), the comprehensive GRI [10] mechanism and a global reaction as well as the time scale definitions of Rehm et al. [5] and Prüfert et al. [6] were employed to model the well-known Sandia Flame D [7]. All 18 test cases were modelled with customized solvers based on the open source library OpenFOAM®. The chemical time scales were evaluated 0.1 m upstream of the burner tip. Figure 1 indicates the evaluation point (0.2 m axial direction) of the evaluation point and shows the methane consumption rate.

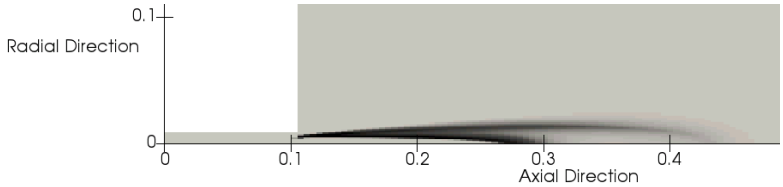

Figure 1: Reaction layer of the Flame D indicated by the methane consumption rate for the global reaction (black: high, grey: low; axial and radial direction in meters)

Figure 2 and Figure 3 compare the time scale dependencies on the reaction mechanism and the chemistry-turbulence model, and the time scale definitions, respectively. Reaction mechanism and time scale definition show a significant influence on the calculated time scales, while the chemistry-turbulence model has a minor influence.

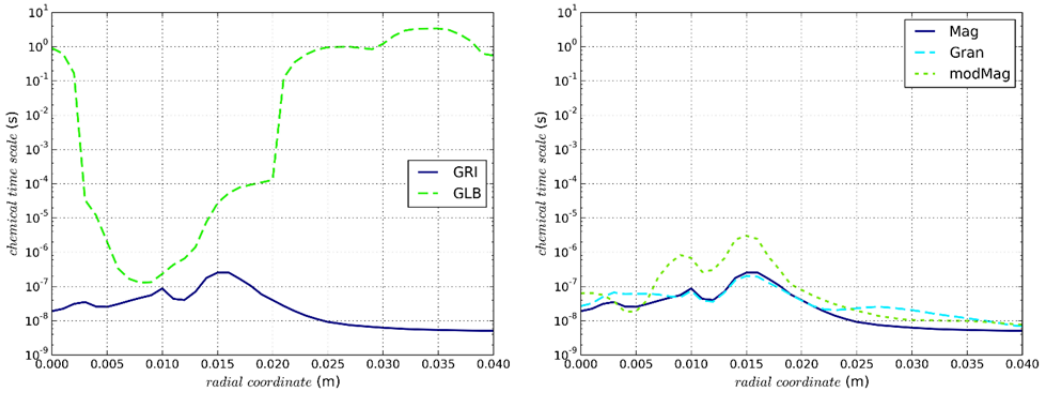

Figure 2: Chemical time scale for different chemical reaction mechanism (left) and turbulence-chemistry interaction models (right) 0.1 m upstream the Sandia Flame D [8, 9] burner tip; Time scale according to Prüfert et al. [7]

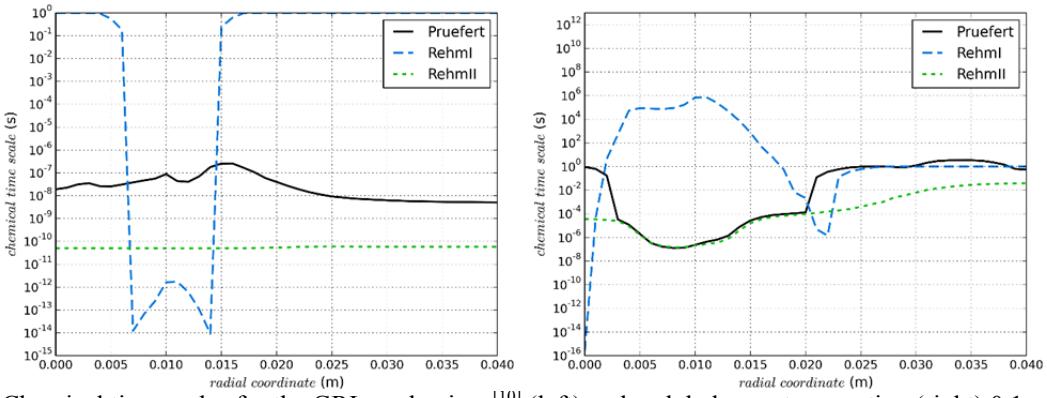

Figure 3: Chemical time scales for the GRI mechanism [10] (left) and a global one-step reaction (right) 0.1 m upstream the Sandia Flame D [8, 9] burner tip; Time scale definitions by Rehm et al. [6] and Prüfert et al. [7]

CONCLUSION

The assessment of the chemical time scale dependencies revealed a high influence of the reaction mechanism and the time scale definition. Differences are in the range of several orders of magnitude and the predicted time scale profiles along the radial coordinate feature different characteristics. Since generic modelling of reactive flows requires a reliable and consistent time scale prediction, further research effort has to be put on the definition of robust and reliable chemical time scale definitions. If these are available, reactive flow modelling might get improved by more generic models, especially, for complex multi-scale applications.

REFERENCES

[1] B. F. Magnussen, On the structure of turbulence and a generalized eddy dissipation concept for chemical reaction in turbulent flow, 19th Aerospace Sciences Meeting, St. Louis, Missouri, USA, January 12-15, 1981.

[2] I.R. Gran and B.F. Magnussen, A Numerical Study of a Bluff-Body Stabilized Diffusion Flame. Part 2, Combustion Science and Technology, pp. 191-217, 1996.

[3] B. F. Magnussen, The Eddy Dissipation Concept, ECCOMAS Thematic Conference on Computational Combustion, Lisboa, Portugal, 21-24 June, 2005.

[4] A. Parente, M.R. Malik, F. Contino, A. Cuoci, B.B. Dally, Extension of the Eddy Dissipation Concept for turbulence/chemistry interactions to MILD combustion, Fuel, pp. 98–111, 2016.

[5] M. Rehm, P. Seifert, B. Meyer, Theoretical and numerical investigation on the EDC-model for turbulence–chemistry interaction at gasification conditions, Computers & Chemical Engineering, pp. 402-407, 2009.

[6] U. Prüfert, F. Hunger, C. Hasse, The analysis of chemical time scales in a partial oxidation flame, Combustion and Flame, pp. 416-426, 2014.

[7] R. Barlow, J. Frank, A. Karpetis, J. Chen, Piloted methane/air jet flames, Combustion and Flame, pp. 433–449, 2005.

[8] G.P. Smith, D.M. Golden, M. Frenklach, N.W. Moriarty, B. Eiteneer, M. Goldenberg, C.T. Bowman, R.K. Hanson, S. Song, W.C. Gardiner Jr., V.V. Lissianski & Z. Qin, “GRI-MECH 3.0”, http://combustion.berkeley.edu/gri-mech/

HYDROPHOBINS AS INACTIVE EXCIPIENTS IN THE PHARMACEUTICAL AND FOOD INDUSTRY

Tatyana Yemelyanova[a], Vladimir Berezhinskiy[a], Agnes Przylucka[a], Feng Cai[a,b], Günseli Bayram Akcapinar[a,e], Hinrich Grothe[c], Erik Reimhult[d], Irina S. Druzhinina[a]

[a]E166 - Institute of Chemical, Environmental and Biological Engineering
[b]Nanjing Agricultural University, Nanjing, China
[c] Institute of Materials Chemistry, TU Wien, Vienna, Austria
[d]University of Natural Resources and Life Sciences, Vienna, Austria
[e]Department of Statistics and Medical Informatics, Acibadem University, Istanbul, Turkey

INTRODUCTION

The pharmaceutical and food industries require not only bioactive ingredients but also inactive excipients in formulation development. Pharmaceutical excipients are substances other than the pharmacologically active drug, which are included in the manufacturing process or are contained in a finished pharmaceutical product dosage form. They may be important for keeping the drug from being released too early in the assimilation process or protect the product's stability so that it will be at maximum effectiveness at time of use. Class II hydrophobins (HFBs) from *Trichoderma* spp. can be potentially used as such inactive excipients. In this study, the class II HFB4 proteins from different *Trichoderma* spp. were heterologously produced in *Pichia pastoris*. The extracellular hydrophobins obtained from the fermentation process were purified and their antioxidant properties tested.

EXPERIMENTS / FUNDAMENTAL OF THE PROBLEM / EXAMINATIONS

Filamentous fungi produce a diversity of hydrophobins, a family of low molecular weight amphiphilic surface-active proteins containing four disulfide bridges and a large conserved and exposed hydrophobic patch [Picture 1] [1]. Hydrophobins are traditionally split into class I and class II, by their solubility and hydropathy plots of their amino acid sequences. Class I hydrophobins are not soluble in water whereas the proteins from class II are easily dissolved in the aqueous phase. The large potential of class II hydrophobins in clinical applications has been described in recent literature[1-8]. It was reported that class II HFBs (HFB4 and HFB7) of *Trichoderma* can enhance the rate of enzymatic hydrolysis of aromatic-aliphatic polyesters such as PET [2]. Furthermore, class II hydrophobins have been successfully used for generating stabilized foams in foam-rich products where control of the air phase is especially important [3]. In contrast, the formation of stabilized CO_2 nanobubbles by class II hydrophobins have been reported to induce gushing and are considered to be a negative property of this protein in the carbonated beverages industry [4].

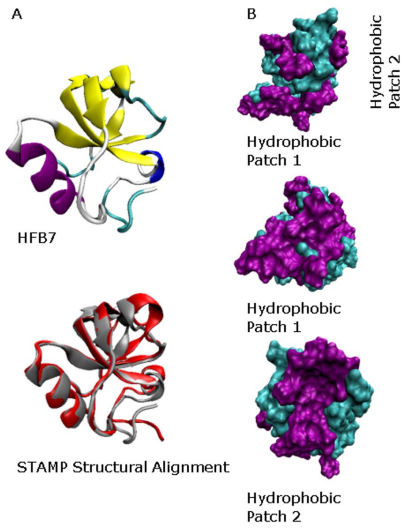

Picture 1: 3D-structure of HFB7. A: structure HFB7 at the end of MD simulations. B:surface representation of HFB7 coloured by hydrophobicity[1].

Przylucka et al. (2017) have proposed the role a novel HFB7 from T. virens in the protection against oxidative stress[1]. The antioxidant activity and ACE-inhibitory of class II HFB2 from *Trichoderma reesei* was reported Khalesi et al. (2016) who

demonstrated the reduction of free radicals of ABTS in the environment [5]. Currently, there are only several antioxidants which are used in industrial applications, such as BHT (Butylated Hydroxy Toluene), BHA (Butylated Hydroxy Anisol), sodium metabisulfite and ascorbic acid. Some of these antioxidants have a negative impact on human health. As hydrophobins have been shown to be immunologically inert [6-7], in this study, we test the antioxidant potential of a collection of class II HFB4 proteins from *Trichoderma* and discuss the possibility of their use as pharmaceutical excipients.

RESULTS AND DISCUSSION

Hydrophobins were originally detected because they enable fungi to grow at the interphase of solids or water and air, which was brought about by their assembly into amphiphilic structures on the outer fungal cell wall. In a previous study, an extended repertoire of class II HFBs was identified in *Trichoderma* species. Among them, HFB4 from 160 different species of *Trichoderma* were studied in detail. In some infrageneric groups of Trichoderma, these HFBs are under positive selection pressure, and some of their residues are positively selected during their evolution. A set of numerous HFB4 genes with different biochemical properties such as pI and hydrophobicity from different *Trichoderma* species were expressed in *P. pastoris* [8]. Subsequently, the antioxidant activity of different HFBs at certain concentrations was determined. The results of this study allowed to detect a few particular HFB4 proteins that significantly reduce the presence of ABTS+ radicals in the solution in comparison with other HFB4s from *Trichoderma* species. The structural analysis of these proteins will be presented and discussed. To test the interaction between HFB4 proteins and industrially, pharmaceutically, and biologically relevant enzymes were assessed using quartz crystal microbalance with dissipation monitoring (QCM-D). For this purpose, quartz crystal sensors, coated with a homogeneous film of either borosilicate or polyethylene terephthalate presenting a hydrophilic and a hydrophobic surfaces, respectively, were used.

CONCLUSION

Class II HFB4 can be potentially used as an inactive excipient in the pharmaceutical or food industry. Its unique amphiphilic properties are promising for the use as antioxidants and stabilizing agents. The interaction between industrially important enzymes and HFBs is the major focus of future investigations as well as their emulsifying properties.

REFERENCES

[1] Agnes Przylucka et al. “HFB7 – A novel orphan hydrophobin of the *Harzianum* and *Virens* clades of *Trihoderma*, is involved in response to biotic and abiotic stresses”, Fungal Genetics and Biology, article in press, 2017

[2] Liliana Espino-Rammer et al. “Two Novel Class II Hydrophobins from Trichoderma spp. Stimulate Enzymatic Hydrolysis of Poly (Ethylene Terephthalate) when Expressed as Fusion Proteins”, Applied and Environmental Microbiology, Pages 4230-4238, 2013

[3]] Basheva E.S. et al. “Unique properties of bubbles and foam films stabilized by HFBII hydrophobin”, Langmuir 27, Pages 2382–2392, 2011

[4] Cox A.R., F. et al. “Surface properties of class II hydrophobins from *Trichoderma reesei* and influence on bubble stability”, Langmuir 23, Pages 7995–8002, 2007

[5] Mohammadreza Khalesi et al. “Antioxidant activity and ACE-inhibitory of Class II hydrophobin from wild strain *Trichoderma reesei*”, International Journal of Biological Macromolecules, Volume 91, Pages 174–179, 2016

[6] Tatyana V. Yemelyanova et al. “Hydrophobin-functionalized poly-lactide-co-glycolide nanoparticles for drug delivery”, BIOTRANS 2015, Page 554, 2015

[7] Mirkka Sarparanta et al. “Intravenous Delivery of Hydrophobin-Functionalized Porous Silicon Nanoparticles: Stability, Plasma Protein Adsorption and Biodistribution”, Journal of Molecular Pharmaceutics, Pages 654–663, 2012

[8] Günseli Bayram Akcapinar et al. “Hydriphobins of *Trichoderma* as immobilizers of enzymes on polymeric surfaces for biocatalyses”, BIOTRANS 2015, Page 525, 2015

A PROCESSING ROUTINE FOR LAYERED Si_3N_4/SiCN STRUCTURES WITH GRADED MULTISCALAR POROSITY

Christina Drechsel, Roland Haubner and Thomas Konegger

E164 - Institute of Chemical Technologies and Analytics, TU Wien

INTRODUCTION

Porous non oxide ceramics are interesting materials for uses in energy and environmental related fields such as catalysis and separation. The excellent mechanical and thermal properties and also the chemical stability make ceramics very effective. Especially the use of preceramic polymers opens up new processing methods and leads to flexibility in shaping, enabling the manufacturing of layered structures and coatings.

Layered ceramic structures with multiscalar porosity can be used as membranes for gas separation at high temperatures. They generally consist of a microporous selective layer responsible for the separation, and a macro-porous support providing the mechanical stability. Usually, there has to be an intermediate layer bridging the difference in pore size and possible chemical variations between selective layer and support.[1] The aim of this work is to find a processing routine for layered structures with multiscalar porosity solely consisting of Si_3N_4 and comparable polymer-derived materials.

EXPERIMENTS & EXAMINATIONS

Two types of support structures were prepared, serving as substrates for the following layers. A composite intermediate layer was deposited via dip coating, onto which a selective layer was applied.

Support structures: Type A supports were prepared using a poly(vinyl)silazane as polymer precursor and UHMW-PE as sacrificial filler, resulting in amorphous silicon carbonitride with a porosity of about 42 % after pyrolysis.[2] [3] Type B supports were prepared via slip casting and partial sintering of silicon nitride yielding a porosity of about 50 %.

Intermediate layer: The intermediate layer was prepared using a combination of preceramic polymer and silicon nitride particulates (the same materials as for the supports). The poly(vinyl)silazane serves as a binder for the particulates, yielding a composite layer after pyrolysis. The layer was deposited using dip coating of slurry containing both the polymer and the particulates (in a ratio of 1:1.4). To achieve sufficient slurry stability, the particulates were modified by a silanization treatment using 3-aminopropyltrimethoxysilane. Through variation of solvent content in toluene, a slurry composition yielding a satisfactory intermediate layer was found. The use of two different slurries were necessary due to filtration effects caused by the different pore structures of the two support types.

Selective layer: The selective layer was deposited via dip coating using a solution of the poly(vinyl)silazane used for the previous layers in toluene/hexane. Preliminary optimization tests were carried out on glass plates and the results compared to a model from Landau and Levich.[4] To avoid infiltration of the substrate, an additional masking with polystyrene was conducted. After crosslinking, the selective layer was stable and the polystyrene was burnt out during pyrolysis.

RESULTS AND DISCUSSION

A layered structure with multiscalar porosity was achieved on both of the support types. The scanning electron microscopy pictures of each processing step can be seen in figure 1.

The type A supports have a porosity of approximately 42 % with ink bottle type pores, type B supports 50 % with uniform pores. For the preparation of the intermediate layer, a higher solvent concentration of the slurry was necessary for the slip cast supports than for the polymer derived (PDC) supports due to the previously mentioned filtration effects. Using 91 wt.% toluene for the slip cast and 80 wt% toluene for the PDC supports, a crack-free, continuous composite intermediate layer with approximately 30 µm in thickness could be prepared. Under use of the masking step (polystyrene), it was possible to prepare a thin (approximately 1 µm) selective layer on top of the intermediate layer, whilst preserving the porosity of the underlying layers.

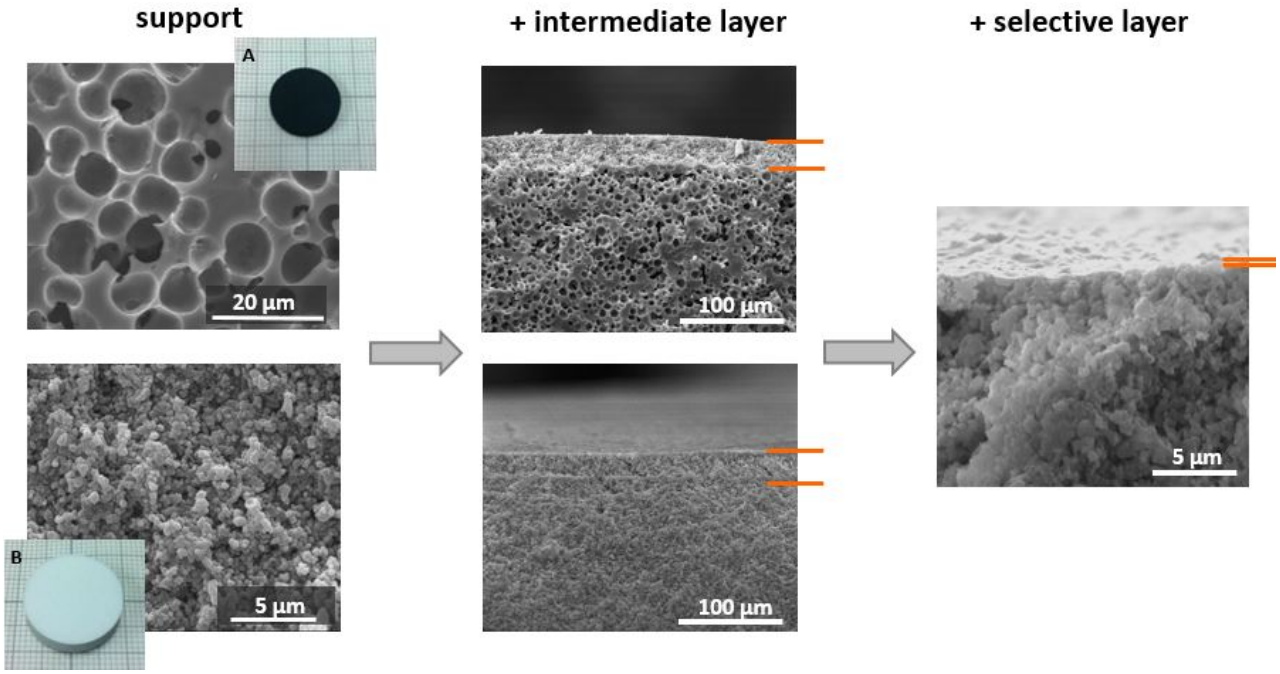

Figure 1: SEM micrographs of the layered silicon (carbo)nitride structures in every processing step

CONCLUSION

Using preceramic polymers, it is possible to prepare layered structures with multiscalar porosity using dip coating processes. A practicable routine was developed, but further optimization is necessary. Since these structures are proposed for high temperature gas separation membranes, the generation of microporosity in the selective layer and their stability have to be characterized and optimized.

REFERENCES

[1] Verweij, H., et al., Microporous Silica and Zeolite Membranes for Hydrogen Purification, MRS Bulletin, 756-764; 2006

[2] Konegger, T., et al., *Planar, Polysilazane-Derived Porous Ceramic Supports for Membrane and Catalysis Applications.* Journal of the American Ceramic Society, 3047-3053, 2015

[3] Konegger, T., et al., *A novel processing approach for free-standing porous non-oxide ceramic supports from polycarbosilane and polysilazane precursors*, Journal of the European Ceramic Society, 2679-2683, 2015

[4] Konegger, T., et al., *Preparation of polymer-derived ceramic coatings by dip-coating.* Materials Science Forum,, 645-652, 2015

STEAM GASIFICATION PROCESS ENHANCEMENT WITH ALKALI AND ALKALINE EARTH-RICH WASTE MATERIALS

Mateusz Karczewski[a,b*], Stanisław Porada[a], Marta Marczak[a,b]

[a]AGH University of Science and Technology
[b]E164 – Institute of Chemical Technologies and Analytics

INTRODUCTION

Among various methods to resolve the problem of process optimisation, the enhancement by use of catalytic materials seems to have noticeable potential in the field. The addition of various elements in their compound of metallic form in low amounts is reported to influence such process parameters as the process kinetics and syngas composition. Among all possible elements from which several like noble metal[1] s and alkali or alkaline earth metals[2] have been already confirmed to have such influence, the latter seems to be the most promising due to not only to resulting high process efficiency[3] but also due to their lower prices. This work aims to adjust this discovery into the application-ready product by proposing a cheap waste-based additive for steam coal gasification. A comparison between the use of the additive and the process without it have been presented.

EXPERIMENT

The experiment was performed with bituminous coal obtained from Janina mine. Rich in potassium, sodium and calcium waste material was obtained from industrial sector that in normal utilisation procedure performs its onsite incineration. Both samples were air-dried and ground 0.2 mm in diameter size. The proper fuel blend of coal and waste material was prepared based on data on best possible alkali presence with sodium and potassium as a priority due to their best influence[4]. As a result, fuel blend with waste addition no bigger than 10% was created (labelled as JB).

Both samples were steam gasified in laboratory scale gasifier in two different temperatures (800 and 900ºC) and under the stable pressure of 10 bars. The gasifier used argon as a carrier gas with a flow of 2l·min^{-1} and distilled water as a steam source with intake of 0,3 ml/min. The composition of resulting syngas was measured by NDIR flue gas analyser. Total syngas yield was determined by calculating the yield of each product from the area under curve dV·dt^{-1}=f(t). The carbon conversion degree was also evaluated with use of the volume of carbon-based gaseous products with given equation (1):

$$X(t) = \frac{(V_{co}(t)+V_{CO2}(t)+V_{CH4}(t))\cdot M_C}{V_{mol}\cdot m\cdot C^{daf}} \cdot 100\ \% \qquad (1)$$

where:

$V_{CO(t)}$, $V_{CO2(t)}$, $V_{CH4(t)}$ - volume of released gas component at standard conditions as a function of time, dm^3*g^{-1}
V_{mol} - volume of one mole of gas at temperature of 273 K and pressure of 101325 Pa, dm^3*mol^{-1}
M_c- molar mass of carbon, g*mol^{-1}
m – sample mass, g
C^{daf}- dry ash free carbon content, -

RESULTS AND DISCUSSION

The results have shown a noticeable increase in carbon conversion degree after addition of the additive. Depending on the temperature its conversion degree rose from 60.7% and 74.7 to 73.5 and 94.3%. Such results mean that the presence of additive increased the selectivity of the process into gaseous products instead of undesired tar side products. Fig 1. Also shows that hydrogen and carbon oxides which are the most important constituents of syngas were recorded to have the highest yield increase after utilisation of the additive.

Carbon to syngas conversion [wt%]		
RT[°C]	**Coal**	**J blend**
900	74.7	94.3
800	60.7	82.8

Table 1 Degree of carbon conversion to gaseous products

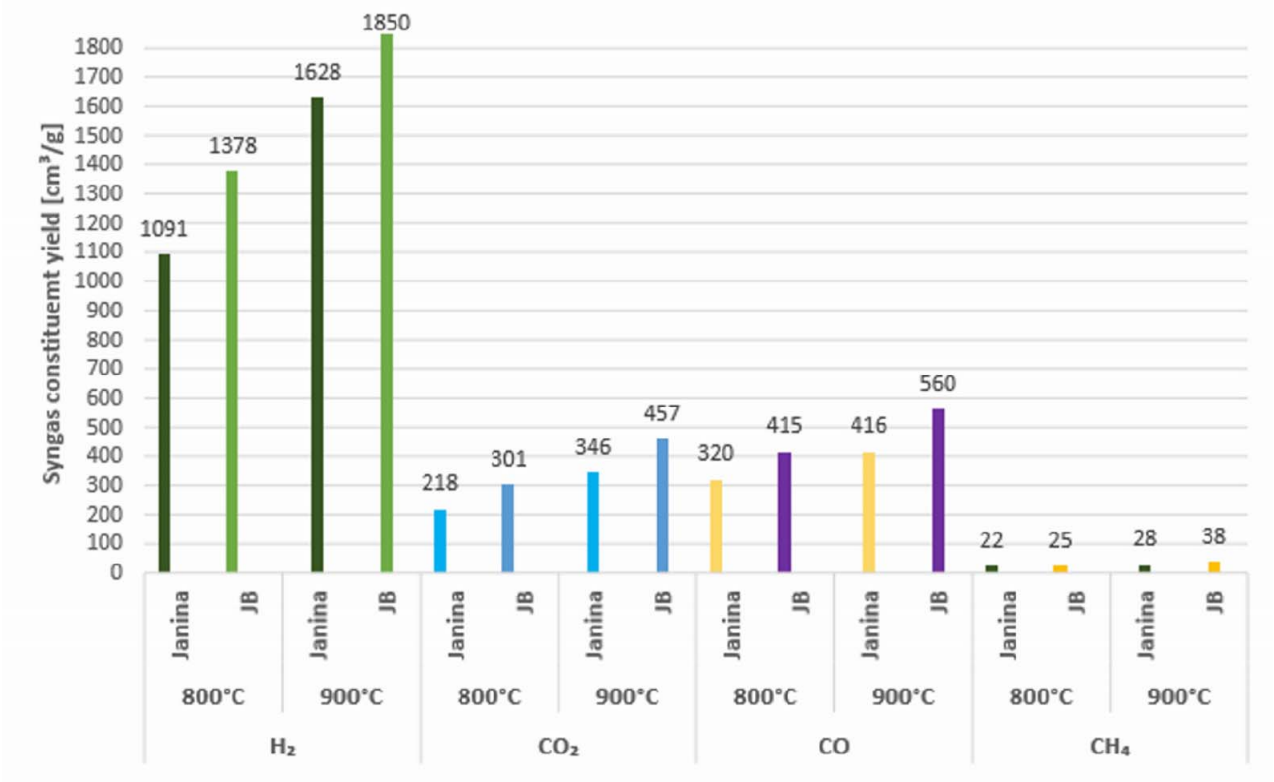

Figure 1 Yield of syngas of syngas produced from additive-free coal and from tested fuel blend during steam gasification process in different temperatures

CONCLUSION

This experiment has proven that it is still possible to greatly enhance already well-researched processes like steam gasification with both simple and cheap approaches. The next step in the popularization of this method will be an analysis of additive influence on low-quality hard coals, which are main feedstock of choice for this type gasification processes.

REFERENCES

1. K. Otto, M. Shelef, Catalytic steam gasification of graphite: Effects of intercalated and externally added Ru, Rh, Pd and Pt., Carbon **15(5)**, 317–325 (1977)
2. F. Huhn, J. Klein, H. Jüntgen, Investigations on the alkali-catalysed steam gasification of coal: Kinetics and interactions of alkali catalyst with carbon, Fuel **62(2)**, 196–199 (1983)
3. J. Tang J. Wang, Fuel Processing Technology, Catalytic steam gasification of coal char with alkali carbonates: A study on their synergic effects with calcium hydroxide. **142**, 34-41 (2016)
4. S. Porada, A. Rozwadowski, K. Zubek, Studies of catalytic coal gasification with steam. Polish Journal of Chemical Technology, **18(3)**, 97-102 (2016).

SELECTIVE OXIDATION AND HOT-DIP-GALVANIZABILITY OF ADVANCED HIGH STRENGTH STEELS

Magdalena Maderthaner[a,b], Alexander Jarosik [b], Roland Haubner[a]

[a]E164 - Institute of Chemical Technologies and Analytics, TU Wien
[b]voestalpine Stahl GmbH, Linz, Austria

INTRODUCTION

There is a growing demand for Advanced High Strength Steels (AHSS) in the automotive industry owing to their high specific strength and good formability. The mechanical properties satisfy the demands for improved passenger safety and decreased vehicle weight due to thinner cross sections. Hot-dip galvanizing is a common procedure to prevent corrosion of steels, galvanized steel forms the basis for further processing as organic coating.

Galvanizing of AHSS is troublesome because of the selective oxidation of the oxygen-affine alloying elements Mn and Si during annealing at 840 °C in 5%H_2 in N_2 at a dew point (DP) of -30 °C (which is equivalent to 380 ppm H_2O or pO2 = 3,16 · 10^{-22} atm). Although the annealing conditions are reducing for Fe, the ignoble elements are oxidized. Due to the resulting concentration difference, ignoble elements segregate from the bulk to the surface and form an amorphous, vitreous, Si-rich oxide layer. The covering oxides show a poor wetting behaviour when the steel strip immerses in the Zn(Al, Fe)-bath, resulting in bare spot defects and bad Zn-adhesion.

EXPERIMENTS

The effect of DP (and therefore oxygen partial pressure) during annealing of 2.5Mn-1.5Si-AHSS on subsequent hot dip galvanizing is evaluated. DP is set to 0 °C (6056 ppm H_2O, humidified), -30 °C (380 ppm H_2O, general industrial conditions) and -60 °C (14 ppm H_2O, dry). Annealed specimens are analysed by Scanning Electron Microscopy (SEM), depth profiles are generated by Glow Discharge Optical Emission Spectroscopy (GD-OES). Galvanized specimens are judged by coating quality (lack of bare spot defects) and Zn-adhesion during forming.

RESULTS AND DISCUSSION

The more oxygen containing an annealing atmosphere is, the more oxides are formed. According to Wagner's theory of selective oxidation, internal oxides are formed, when the mass flow of oxygen into the substrate is superior to the mass flow of ignoble elements from the substrate to the surface[1]. At DP 0 °C, the surface consists of finely dispersed Mn-rich oxides, uncovered Fe is visible. The grain boundaries are severely oxidized up to a depth of 3 µm. At DP -30 °C, the surface is completely covered by Mn-Si-mixed oxides. The grain boundaries are partly oxidized to a depth of 2 µm. At DP -60 °C, the oxygen content is very low. Nearly no internal oxidation occurs, as the flow of ignoble elements to the surface exceeds the offered oxygen. Metallic Fe is apparent on the surface, the formed oxides consist mainly of Si.

Best Zn-coating quality is observed at DP 0 °C, DP -60°C is only slightly better than DP -30 °C. Zn-adhesion during forming is poor for DP 0 °C, as the massive grain boundary oxidation weakens the integrity of the surface region, corn breakouts may occur.

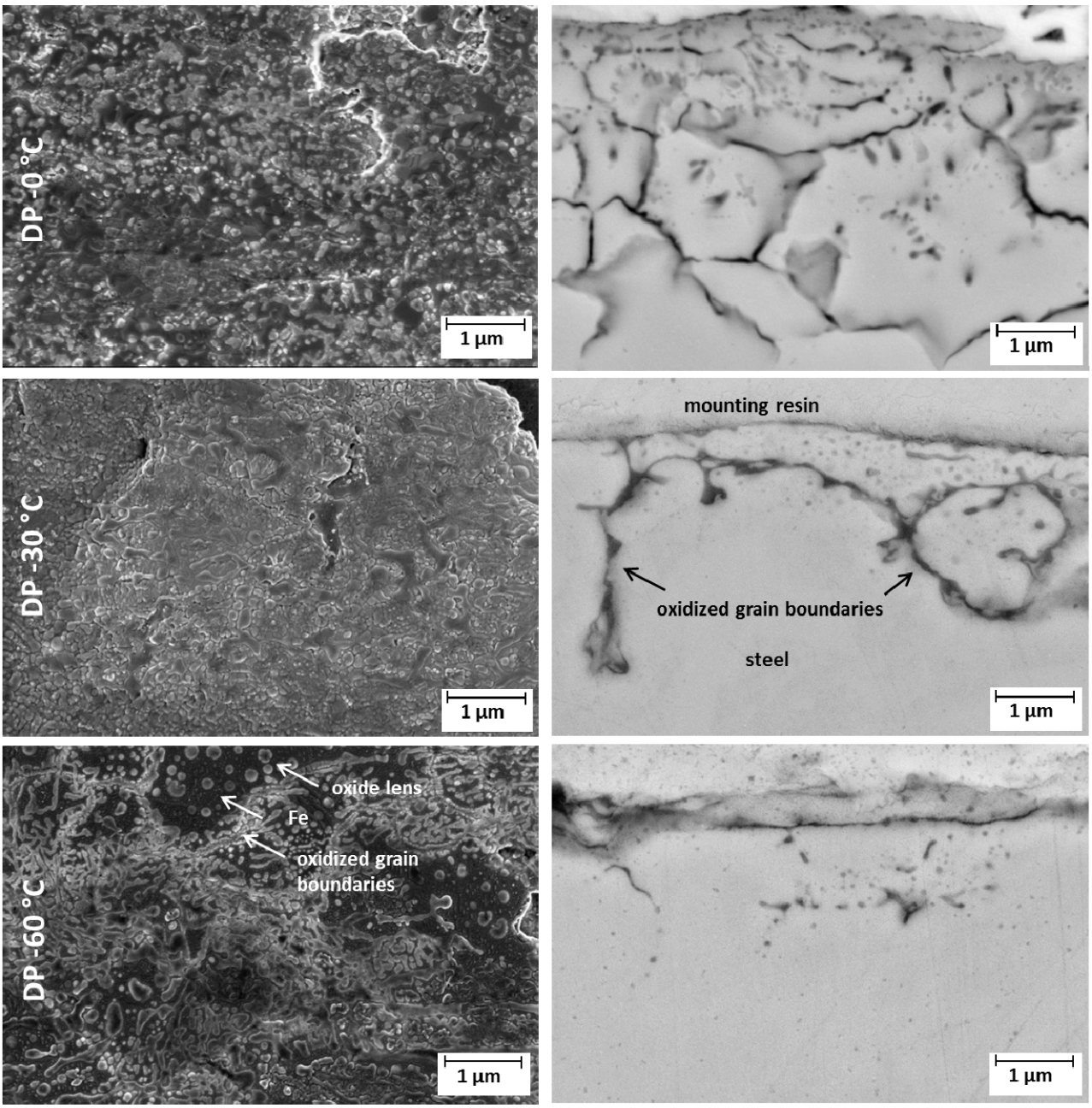

Picture 1: SEM-micrographs of the annealed surface (left) and cross-section (right) of 2.5Mn-1.5Si-AHSS, annealed at DP 0 °C (top), DP -30 °C (middle), -60 °C (bottom).

CONCLUSION

Although there is metallic Fe on the surface to enable good reactive wetting with the Zn(Al, Fe)-bath at DP -60°C, there are also plenty Si-oxides at the surface, which are known to a have a deteriorating effect on galvanizing[3].

AHSS cannot currently be satisfactory galvanized by adjusting the annealing atmosphere. Further research is necessary.

REFERENCES

[1] Wagner, Carl. "Reaktionstypen bei der Oxydation von Legierungen." Berichte der Bunsengesellschaft für physikalische Chemie 63.7 (1959): 772-782.

[2] Marder, A. R. "The metallurgy of zinc-coated steel." Progress in materials science 45.3 (2000): 191-271.

THE ORIGIN AND ARCHITECTURE OF *TRICHODERMA* HYDROPHOBOME

Komal Chenthamara[a], Feng Cai[a,b], Agnes Przylucka[a], Qirong Shen[b], Günseli Bayram Akcapinar[a,§], Irina Druzhinina[a]

[a]E166 - Institute of Chemical, Environmental and Biological Engineering, Research Area Biochemical Technology, Microbiology Group, TU Wien, Vienna, Austria
[b]Jiangsu Collaborative Innovation Center for Solid Organic Waste Resource Utilization, Nanjing Agricultural University, Nanjing, China
[§]present address: Department of Statistics and Medical Informatics, School of Medicine, Acibadem University, Istanbul, Turkey

INTRODUCTION

Higher filamentous fungi (subkingdom Dikarya) are commonly known as moulds, mushrooms or toadstools. Their vegetative body, *mycelium*, can be described as an apically growing branching tube (the *hypha*), which in macroscopic species aggregates into large structures such as fruiting bodies. To facilitate their reproduction, dispersal, and survival in unfavourable conditions these organisms (fungi *sensu stricto*) form various spores that can be produced on a diversity of hyphal structures such as conidiophores or sporocarps. Vegetative hyphae usually grow inside their food and feed by secreting digestive enzymes into their environment and absorbing dissolved small molecules. Therefore, a hyphal organisation of the body provides high surface area-to-volume ratio that is a key adaptation for the efficient extraction of nutrients while growing on or in solid substrates or germinating as spores in a liquid. Hyphae are specifically adapted for efficient attachment to a diversity of solid surfaces; they can also invade substrates and tissues due to large penetrative mechanical forces that they can also exert because of efficient attachment abilities. The development of many fungi includes interchanges between penetration of tissues/substrates for nutrition and growing out of them for dispersal. Undoubtedly, fungi have unique molecular adaptations that emerged in the course of the evolution of their distinctive life style. Hydrophobins are the small amphiphilic surface active proteins containing eight conserved cysteine residues that are produced only by filamentous fungi[1–3]. Some mushrooms (Basidiomycota) have a rich arsenal of hydrophobins that are required for the formation of their fruiting bodies and spore distribution, while the rest of them and the majority of Ascomycota have only a few hydrophobin-encoding genes. In this respect, the mycoparasitic genus *Trichoderma* (Hypocreales, Pezizomycotina), which also includes several cosmopolitan generalist species with high environmental opportunistic potential[4], is as an exception as genomes of these fungi have expanded the number of hydrophobins. Previous studies have revealed that most of *Trichoderma* hydrophobins are the orphan genes that have no homologues in related organisms, while other Pezizomycotina fungi share their hydrophobins. The first genome-wide studies of *Trichoderma* provided the evidence for the operation of purifying natural selection pressure for *Trichoderma* hydrophobins that results in "birth-and-death" evolution of these proteins[5].

In this study, we investigate the evolution of hydrophobin-encoding genes in the genus *Trichoderma* and compare it to other fungi from the order Hypocreales and beyond.

METHODS

First, the genomes of 11 *Trichoderma* spp. and 12 genomes of other Hypocreales fungi were mined for hydrophobin-encoding genes. Then, the resulting library amino acid sequences (~140 OTUs)

was subjected to sequence alignment and phylogenetic analysis by Bayesian methods. Best fit substitution model was selected based on BIC criterion using Smart Model Selection tool. Evolutionary analysis using two independent runs of 5 million MCMC generations resulted in reliable diagnostic parameters estimated based on potential scale reduction factor, effective sample size and average standard deviation of split frequencies. The hypothesis of gene loss, gene duplication, and horizontal gene transfer (HGT) events were tested using NOTUNG 2.9, HGT was also verified by TRex. The operation of positive selection pressure was tested using the K_a/K_s ratio and Tajima *D*-test as implemented in DnaSP v5. The expression analysis for hydrophobin-encoding genes has been performed by mining available transcriptomic databases for *T. reesei*. As the former species has the smallest hydrophobome (HFBome) in *Trichoderma*, an *in vitro* analysis of the expression of hydrophobin-encoding genes was performed for *T. virens, T harzianum* and *T. guizhouense* that have the largest *Trichoderma* HFBomes to date. Physical-chemical properties of individual hyprophobins have been calculated based on such parameters as the surphace hydrophobicity, hydropathy plots, pI, and others.

RESULTS AND DISCUSSION

This study provides the exhaustive evolutionary survey of hydrophobin-encoding genes and respective proteins in *Trichoderma* and other Hypocreales fungi. Phylogenetic analysis revealed at least 14 monophyletic clades containing active individual hydrophobin-encoding genes in *Trichoderma*. In several cases, the events of gene loss and duplication have been confirmed statistically. The analysis of the selection pressure revealed a highly heterogeneous pattern when individual genes in some species appeared to be under the strong pressure of either purifying or positive selection while the respective homologous genes evolved neutrally in the other taxa.

CONCLUSION

Our study demonstrates that the expansion of HFBome in the genus *Trichoderma* and its unique architecture are closely linked to the ecological adaptations of this genus. The phylogenomic analysis allowed to differentiate evolutionary old (plesiomorphic) from the newly emerged (apomorphic) hydrophobins. We show that the evolution of the entire HFBome most likely contributes to the fitness of an individual species, while individual genes may emerge and get lost relatively quickly. Thus, our study points to the importance of the expression regulation of hydrophobins and the important role of hydrophobin-hydrophobin interactions for the survival of *Trichoderma*. We also propose a model that explains the role of HFBome in the emergence of superial environmental opprtunism of this fungus.

In this work, the nomenclature of class II hydrophobins of Ascomycota fungi has been developed.

REFERENCES

1.Linder, M. B., Szilvay, G. R., Nakari-Setälä, T. & Penttilä, M. E. Hydrophobins: the protein-amphiphiles of filamentous fungi. FEMS Microbiol. Rev. 29, 877–896 (2005).

2.Wösten, H. A. Hydrophobins: multipurpose proteins. Annu. Rev. Microbiol. 55, 625–646 (2001).

3.Ruocco, M. et al. Multiple roles and effects of a novel Trichoderma hydrophobin. Mol. Plant-Microbe Interact. MPMI 28, 167–179 (2015).

4.Druzhinina, I. S. et al. Trichoderma: the genomics of opportunistic success. Nat. Rev. Microbiol. 9, 749–759 (2011).

5.Kubicek, C. P., Baker, S., Gamauf, C., Kenerley, C. M. & Druzhinina, I. S. Purifying selection and birth-and-death evolution in the class II hydrophobin gene families of the ascomycete Trichoderma/Hypocrea. BMC Evol. Biol. 8, 4 (2008).

APPLE (*MALUS* X *DOMESTICA*) AS A MODEL PLANT TO INVESTIGATE THE BIOSYNTHESIS OF 3-HYDROXYPHLORIDZIN

Olly Hutabarat [a], Christian Haselmair-Gosch[a], Silvija Miosic[a], Andreas Spornberger[b], Karl Stich[a], and Heidi Halbwirth[a,*]

[a]Institute of Chemical, Environmental and Biological Engineering, Technische Universität Wien, 1060 Vienna, Austria

[b]Department of Crop Science, University of Natural Resources and Life Sciences, 1180 Vienna, Austria

INTRODUCTION

Dihydrochalcones (Figure 1) are phenolic compounds which are discussed as defence mechanism against pathogens in apple [1]. However, studies on their physiological relevance are impeded by unknown biosynthetic steps like the formation of 3-hydroxyphloridzin. Polyphenol oxidases (PPO) and cytochrome P450 dependent enzymes could be involved. Although PPOs from apple have repeatedly been reported to produce 3-hydroxyphloretin as intermediates in the phloretin oxidation [2,3], their physiological relevance for the 3-hydroxyphloridzin biosynthesis in apple leaves has not yet been demonstrated. However, the involvement of such an unspecific enzyme which produces a spectrum of cell-toxic compounds in the biosynthesis of the constitutively in *Malus* sp. present 3-hydroxyphloridzin is unlikely. Hydroxylation of phloretin in position 3 has high similarity to the B-ring hydroxylation of flavonoids catalysed by the well-known flavonoid 3'-hydroxylase (F3'H). Recently we demonstrated that the dihydrochalcone phloretin is accepted as substrate *in vitro* by F3'H and the closely related chalcone 3-hydroxylase (CH3H) from the ornamental plant *Coreopsis grandiflora*. The acceptance of phloretin as substrate was also confirmed *in planta* via overexpression of *CH3H* in apple [4]. Transgenic plants showed increased contents of 3-hydroxyphloridzin and reduced susceptibility against fire blight and apple scab. We isolated *F3'H* cDNA clones from *M.* x *domestica* leaves to investigate the involvement of F3'H in the pathway leading to 3-hydroxyphloridzin.

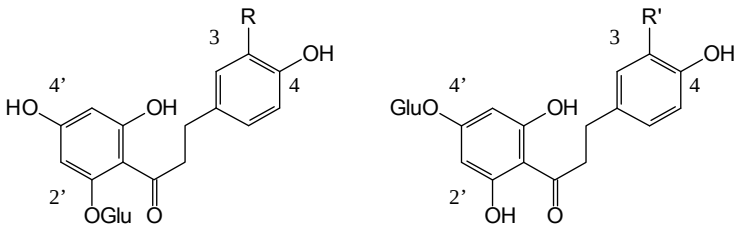

Figure 1: Main phloretin derivatives found in *Malus* species. R=H: Phloretin. R=OH: 3-Hydroxyphloretin. R'=H: Trilobatin. R'=OH: Sieboldin

EXPERIMENTS

Young leaves of *M.* x *domestica* (cv. Golden Delicious on rootstock M9) were harvested in spring 2014 in the experimental orchard of the University of Natural Resources and Life Sciences in Vienna, frozen in liquid nitrogen and stored at -80 °C. *M.* x *domestica* cv. Rebella leaves were obtained from Julius Kühn Institut Dresden-Pillnitz, Germany. mRNA was extracted with the µMACS mRNA Isolation Kit (Miltenyi Biotec, Germany). cDNA was synthetized using the SuperScript II Reverse Transcriptase (Invitrogen, Carlsbad, CA) and an oligo-dT primer. Based on the NCBI sequence information for *F3'H* (FJ919633 and FJ919631) [5], full size *F3'H* cDNA

* heidrun.halbwirth@tuwien.ac.at

clones were isolated. Heterologous expression in yeast and enzyme assays were performed as described previously [4].

RESULTS AND DISCUSSION

To investigate whether F3'H of apple could be a part of the 3-hydroxyphloridzin biosynthesis, we isolated two *F3´H* cDNA clones from apple leaves. The cDNA clones had a length of about 1.6 kb and an open reading frame of 511 amino acids. They showed sequence identity of 94% at the amino acid level to each other and of 72-74% to the F3'H of *Cosmos sulphureus* (NCBI No FJ216426). In comparison to the published sequences [5] only two exchanges at the amino acid level were observed in each of the clones. Heterologous expression in yeast resulted in functionally active F3'H only in one of the cases, despite the high sequence homology and several heterologous expression attempts. The functionally active recombinant enzyme accepted flavanones, dihydroflavonols, and flavonols as substrates. Phloretin, however, was not accepted as substrate, irrespective of the assay conditions applied. Inspection of the apple genome [6] at www.rosaceae.org did not reveal the presence of further *F3'H* copies that could be alternatively involved. Therefore, our investigations indicate that *F3'H* is not a part of the pathway leading to constitutively present 3-hydroxyphloridzin in apple leaves.

CONCLUSION

We isolated two flavonoid 3'-hydroxylase (*F3´H*) cDNAs from young leaves of *Malus* x *domestica* and heterologously expressed it in yeast. One F3´H was functionally active, but phloretin was not accepted as a substrate, thereby indicating that F3'H is not involved in the formation of 3-hydroxyphloridzin in apple leaves.

ACKNOWLEDGMENT

This work was supported by the Austrian Science Fund FWF [Project P25399-B16]. Olly Hutabarat gratefully acknowledges Hasanuddin University (Agricultural Engineering Department, Makassar, South Sulawesi, Indonesia), the Ministry of Education and Culture of the Republic of Indonesia (DIKTI), and the Austrian Agency for International Cooperation in Education and Research (OeAD-GmbH) for enabling the performance of the PhD studies abroad.

REFERENCES

[1] C Gosch et al, *Phytochemistry*, 2013, *150*, 142.

[2] PW Goodenough et al, *Phytochemistry*, 1983, *22*, 359.

[3] M Haruta et al, *Bioscience, Biotechnology, and Biochemistry*, 1998, *62*, 358

[4] OS Hutabarat et al, *Planta*, 2015, *243*, 1213.

[5] Y Han et al, *Plant Physiol.*, 2010, *153*, 806.

[6] R Velasco et al, Nature Genetics, 2010, *42*, 833.

DEGRADATION OF SYNTHETIC POLYMERS BY EPYPHYTIC FUNGI FROM HIGH CANOPY OF THE TROPICAL RAIN FOREST

Mohammad Javad Rahimi[a], Marica Grujic[a], Carina Pleha[a], Ana Forte[a], Komal Chenthamara[a], Carina Pretzer[a], Alexey Kopchinskiy[a], Shadi Pour Mehdi[a], Linda Lim[b], Gunseli Bayram Akcapinar [a,c] and Irina S. Druzhinina[a]

[a] Vienna University of Technology, Institute of Chemical Engineering, Research Area Biotechnology and Microbiology, Gumpendorferstraße 1a, 1060 Vienna, Austria
[b] Universiti Brunei Darussalam, Chemistry Programme, Jalan Tungku Link, Bandar Seri Begawan, BE 1410, Brunei Darussalam
[c] present address: Department of Statistics and Medical Informatics, School of Medicine, Acibadem University, Istanbul, Turkey

In the second half of the 20 century, our society developed new technologies and processes for the mass production of quality products. The technological explosion of knowledge in the petrochemical industry and the resulting synthesis of diverse plastics has had a profound effect on humankind. Polyesters such as Terylene or Dacron are used in textile industry; Mylar is most frequently used for building insulation; drinking water and beverages are packed in convenient plastic bottles made of poly(ethylene terephthalate), or PET. This ubiquitous material is the fourth most common plastic in the world today, following polyethylene, polypropylene and polyvinyl chloride. Along with numerous advantages, such as low-cost production, versatility, lightweight and ease to shape, the important property of most suitable plastics is their resistance to biodegradation. However, it is linked to the acute ecological threat of the utilization of plastic waste. Nowadays our society faces the massive amount of plastic waste accumulated in the environment [1, 2].

Some synthetic polymers such as PET and many others have a structural resemblance to the natural polyester polymer cutin, a wax that covers aerial parts of plants and consists of interlinked omega hydroxy acids. Thus, it is possible to assume that microorganisms living on cutin-rich parts of plants may also be capable of biological degradation of plastic waste [3]. The phyllosphere, or aerial parts of plants, is an ecosystem that hosts a vast and diverse microbial community. Such microbiomes are especially rich in canopies of tropical rain forests where trees do not shed leaves annually. The adaptation of epiphytic and/or endophytic microorganisms to their habitat requires the development of such specialized functions as an efficient attachment to the leaf surface, resistance to oxidative stress and survival in the oligotrophic environment. To solve these challenges, phyllosphere microorganisms produce enzymes that hydrolyze not only lignocellulose but also cutin [4].

In this study, we identified and tested 300 of epi- and endophytic fungi isolated from the high canopy of a tropical rainforest and detected at least a dozen of strains that are capable of degrading polycaprolactone, a biodegradable polyester that has numerous biomedical and industrial applications. Many active strains are known as plant pathogens (*Lasiodiplodia theobromae*, *Fusarium* sp., *Clonostachys* sp., *Colletotrichum acutatum*), but there are also common generalists (*Trichoderma guizhouense*, *Pestalotiopsis* sp. and *Penicillium* sp.). Strains were tested for the activity of their cutinases and ability to degrade lignocellulose. For *Trichoderma* and Fusarium, the expression analysis revealed the set of most potent enzymes putatively involved in polycaprolactone degradation.

REFERENCES

[1] Sinha V, Patel MR, Patel JV. Pet waste management by chemical recycling: A review. J Polym Environ. 2010; 18, 8-25.

[2] Müller RJ, Kleeberg I, Deckwer WD. Biodegradation of polyesters containing aromatic constituents. J. Biotechnol. 2001; 86, 87-95.

[3] Murphy CA, Cameron JA, Huang SJ, Vinopal RT. Fusarium polycaprolactone depolymerase is cutinase. Appl Environ Microbiol. 1996;62(2):456-60.

[4] Chen S, Su L, Chen J, Wu J. Cutinase: characteristics, preparation, and application. Biotechnol Adv. 2013;31(8):1754-67.

Research Field *Data, Models and Mathematics*

Chairs and Reviewer:

Lemell, Christoph
Associate Prof. Dipl.-Ing. Dr.techn.

E136 - Institute of Theoretical Physics
christoph.lemell@tuwien.ac.at

Szmolyan, Peter
Univ.Prof. Dipl.-Ing. Dr.techn.

E101 - Institute of Analysis and Scientific Computing
peter.szmolyan@tuwien.ac.at

Introduction

Technological progress has expanded the data-collection capabilities enormously and continues to do so. Clearly, it is not the data per se that create value. What really matters is the ability to derive from them new insights, to recognize relationships, and to make increasingly accurate predictions.

To this end, mathematical methods have been and are being developed making them an integral and essential component of basic and applied research in science, technology, industry, and economy. This involves the integration of mathematics, statistics, and computation in the broadest sense, and the interplay of these areas with applications.

Computing is often the means by which the mathematical sciences are applied to other fields. For example, mathematicians collaborate with scientists working in fluid dynamics, material science, molecular biology, quantum physics, or semiconductor physics to develop new models and simulation software to understand complex phenomena.

The common goal is to capture pertinent features of a problem by abstract structures through the process of modeling, performing formal reasoning on these abstract structures or using them as a framework for computation, and then reconnecting back to make predictions. Clearly, this is an inherently iterative process.

Therefore, a new algorithm can be as powerful an enhancement to resolution as a new instrument. Additionally, the data that can be measured are not always the data that one ultimately wants. This results in what is known as an inverse problem: the process of collecting data imposes a very complicated transformation on the data one wants, and a computational algorithm is needed to invert the process.

Not all data are numerical – they may be, e.g., categorical, qualitative or visual describing shape. Hence perspectives and techniques for dealing with such data and with their uncertainties are also of interest.

This part of the Vienna young Scientists Symposium will give an overview of the manifold activities at TU Wien related to the interplay of data, models, and mathematics. We interpret the topic in the wide sense sketched above including experiments, representation and analysis of various types of data, modeling, mathematical analysis, and computation. In addition the minisymposium aims at stimulating the exchange of ideas between different research fields.

MINIMIZING CROSSINGS IN CONSTRAINED TWO-SIDED CIRCULAR GRAPH LAYOUTS

Fabian Klute[a], Martin Nöllenburg[a]

[a]E186/1 - Algorithms and Complexity Group at TU Wien

INTRODUCTION

Node-link diagrams are a classical way to visualize data which is represented as a graph. Graph drawing aims to find algorithms which automate the layouting. Of course one needs criteria for what a good layout is. One of the most used ones is the number of crossings between single edges in the drawing. This is not only intuitively a good criteria, but was also confirmed by e.g. Purchase [5].

We focus on a particular drawing style called circular layouts. In such a layout vertices are positioned on a circle, while the edges are drawn as straight-line chords of said circle, see Figure 1a. Finding a vertex order that minimizes the crossings is NP-hard [3] making it unlikely that an exact and efficient algorithm exists. Heuristics and approximation algorithms have been studied in numerous papers, see, e.g., Baur and Brandes [4].

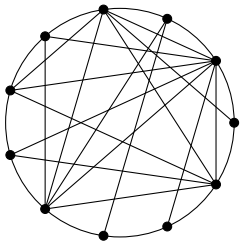

(a) One-sided layout

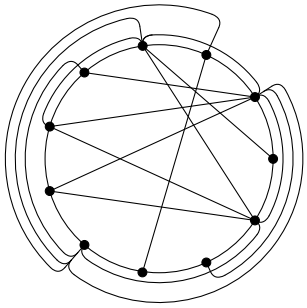

(b) Two-sided layout for $k = 1$

Figure 1: Circular graph layouts

Gansner and Koren [1] presented an approach to compute improved circular layouts for a given input graph $\mathscr{G} = (\mathscr{V}, \mathscr{E})$ in a three-step process. The first step computes a vertex order of $\mathscr{V}$ that aims to minimize the overall edge length of the drawing, the second step determines a crossing-free subset of edges that are drawn outside the circle to reduce edge crossings in the interior, and the third step introduces edge bundling to save ink and reduce clutter in the interior.

Inspired by their approach we take a closer look at the second step of the above process, which, in other words, determines for a given cyclic vertex order an outerplane subgraph to be drawn outside the circle such that the remaining crossings of the chords are minimized. We generalize the problem from outerplane graphs to outer k-plane graphs, i.e., we ask for an edge set to be drawn outside the circle such that none of these edges has more than k crossings. For $k = 0$ this is the same problem considered by Gansner and Koren [1]. An example for $k = 1$ is shown in Figure 1b.

EXPERIMENTS/FUNDAMENTAL OF THE PROBLEM/EXAMINATIONS

We show how the previously described problem can be transformed into an equivalent problem on a more restricted graph class. The first tool we use is the circle graph $G = G_{\pi,\mathscr{G}} = (V,E)$ derived from $\mathscr{G}$ with an order π on the vertices. This graph has a vertex for every chord and two vertices $u, v \in V$ are connected, if the corresponding chords cross.

The problem of finding an optimal set of edges such that the exterior part has at most k crossings per edge can be modeled as a special case of a more general weighted version of the maximum

constrained-degree subgraph problem.

Definition 1 *Given a weighted graph $G = (V,E)$ and $k \in \mathbb{N}$ find a set $V' \subset V$ such that the induced subgraph $G[V'] = (V',E')$ has $d(G[V']) \leq k$ and maximizes the weight*

$$W = W(G[V']) = \sum_{v \in V'} w(v) - \sum_{(u,v) \in E'} w(u,v).$$

Setting the weight of vertices to their degree and the edges to constant one or two will yield the correct version for our purpose. This is the case since we want to find a set of vertices which eliminate a lot of crossings in the original layout of $\mathscr{G}$ and the degree of a vertex $v \in V$ corresponds to the number of crossings of the original chord. The weight on the edges can be used to count the crossings moved to the exterior or not.

RESULTS AND DISCUSSION

The general problem as defined in Definition 1 is NP-hard making it unlikely to find a time-efficient algorithm solving it. For fixed k we present an algorithm running in $O((k\gamma)^{2k}\ell)$, where ℓ is the so called cord length of the circle graph, i.e. the sum of the length of all chords, γ is the maximum degree of the circle graph G and k is the maximum number of crossings allowed for an exterior edge. For $k = 0,1,2$ this yields a still practical usable algorithm for medium sized graphs.

The algorithm itself is an extension of the independent set algorithm for circle graphs presented by Valiente [2] and uses a dynamic programming approach. For $k = 1$ it can be described rather simple, once you observed that the set of chords can be split along sets of one single chord or two intersecting ones into independent parts.

CONCLUSION

In summary we showed how a crossing-optimal two-sided circular layout can be found for the case that each exterior edges can have at most k crossings. We prove that the problem is NP-hard for general k, but can be solved in polynomial time for fixed k.

For practical application of our algorithm we aim to integrate bundling of the edges into our algorithm and evaluate the visualization against other circular layouts, especially Ganser and Korens algorithm [1].

REFERENCES

[1] E. R. Gansner and Y. Koren. Improved circular layouts. In Graph Drawing (GD06), volume 4372 of LNCS, pages 386398. Springer, 2007.

[2] G. Valiente. A new simple algorithm for the maximum-weight independent set problem on circle graphs. In Algorithms and Computation (ISAAC03), volume 2906 of LNCS, pages 129137. Springer, 2003.

[3] S. Masuda, T. Kashiwabara, K. Nakajima, and T. Fujisawa. On the NP-completeness of a computer network layout problem. In Circuits and Systems (ISCAS87), pages 292295. IEEE, 1987.

[4] M. Baur and U. Brandes. Crossing reduction in circular layouts. In Graph-Theoretic Concepts in Computer Science (WG04), volume 3353 of LNCS, pages 332343. Springer Berlin Heidelberg, 2004.

[5] Purchase, Helen C., Robert F. Cohen, and Murray James. Validating graph drawing aesthetics. In International Symposium on Graph Drawing, pp. 435-446. Springer Berlin Heidelberg, 1995.

VEHICLE-TO-VEHICLE CHANNEL LOAD BALANCING THROUGH VEHICULAR ROUTING

Thomas Blazek

E389 - Institute of Telecommunications

INTRODUCTION

With the advent of self-driving cars, the need for inter-car communication, as well as vehicle-to-infrastructure communication arises. This is necessary to provide information across the Vehicular Ad-Hoc Network (VANET), to mitigate dangerous situations and avoid accidents. However, dense urban traffic poses a challenge to communication systems due to the large amount of communication nodes within range, leading to high channel loads. We demonstrate that usage of the communication channel can be drastically improved by cooperative road routing of the vehicles.

ROAD ROUTING AND NETWORK FORMULATION

In [1], the authors demonstrated that routing vehicles cooperatively through a city brings an almost unanimous speed gain for all cooperating vehicles. The simulations took among others, the city of Linz in Upper Austria, and gave 3000 vehicles start and endpoint, and let them drive, once egoistically (*unrouted*) and once using a routing algorithm (*routed*).

We take the generated traces, and now assume that all traffic nodes are equipped with a wireless communication system. This communication system will detect the presence of a signal, if the received signal power P_{rx} is above a given threshold. Combined with a given transmit power, and the pathloss encountered in the urban environment, we get a maximum distance where node i is aware of node j transmitting. For simplicity, we assume this distance to be the same in all directions, regardless of the obstructions. We now define all nodes that are within this range of each other as being connected by an edge $e(i,j)$, and thus construct the communication graph $G = (V,E)$ from the set of all nodes V and the set of all edges E. We then define the distance $d(i,j)$ as the minimal path length from i to j, that is the minimal number of hops required to get from i to j. Then, we introduce the set of neighbors of i as the set of all nodes with $N(i) = \{j | d(i,j) = 1\}$, and the order of that set is given as $|N(i)|$.

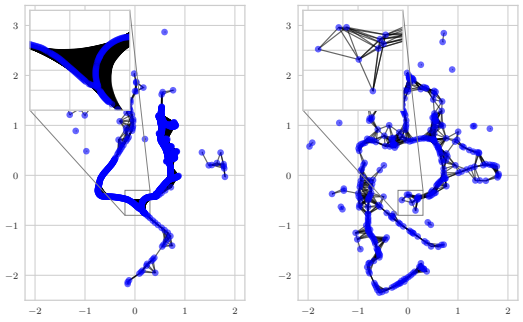

(a) Unrouted **(b)** Routed

Figure 1: Network graph of the vehicular traffic for multiple communication ranges.

Figure 1 demonstrates these graphs for a snapshot time and a communication range of 300 m, both for routed and unrouted scenarios. This was chosen because communication ranges of up to 300 m have been demonstrated for vehicular standards [2] in measurements. When assuming Non-Line-of-Sight conditions (NLOS), ranges of at least 100 m were measured [3]. We therefore use these values as optimistic and pessimistic estimates for our further analysis.

RESULTS AND DISCUSSION

Figure 2 depicts the size N below which 5, 50 and 95 % of the orders of the neighbor sets lie as a function of simulation time. The figure shows the results for routed and unrouted, as well as the two given communication ranges. As can be seen, the unrouted scenarios produce traffic jams very quickly, and the traffic nodes see large amounts of neighbors. The routed scenario, on the other hand, avoids this completely, staying at small sizes throughout the simulation. We now assume that

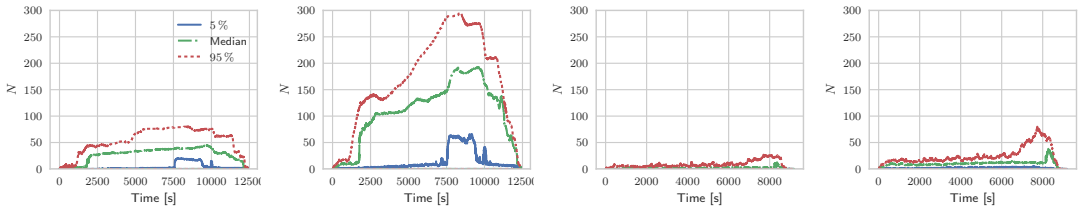

(a) 100m, unrouted **(b)** 300m, unrouted **(c)** 100m, routed **(d)** 300m, routed

Figure 2: Time evolution of the cluster sizes for 100 and 300 m, routed and unrouted simulations.

every vehicle communicates $P_s = 10$ times per second, with an average duration of $l = 667\,\mu$s. This corresponds to typical signaling communication for safety messages in vehicular standards. Then, we can introduce the channel load as the expected value of the product $\mathrm{E}(NP_s l)$. Figure 3 shows that the unrouted scenario sees heavily loaded communication channels, while routing completely eliminates the excessive channel load.

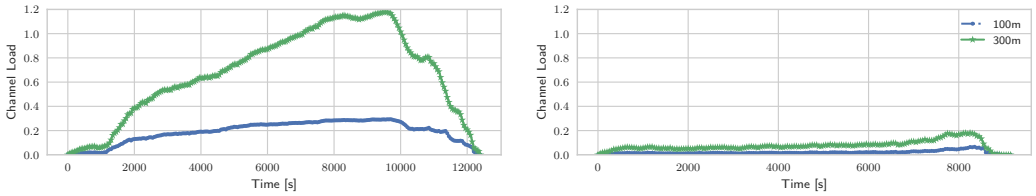

(a) Unrouted **(b)** Routed

Figure 3: Channel load as a function of time for the unrouted and routed scenarios.

CONCLUSION

Cooperative driving effectively mitigates the problem of high perceived channel load and ensures that safety communication is able to be transmitted without experiencing excessive delays. Very important in this context is the fact that the routing was not aiming to achieve this, but the target geometric spread of the routing algorithm aligns very well with a similar target for low channel loads.

REFERENCES

[1] C. Backfrieder, G. Ostermayer, and C. Mecklenbräuker, *Increased Traffic Flow Through Node-Based Bottleneck Prediction and V2X Communication,* IEEE Transactions on Intelligent Transportation Systems, 99, pp. 1-15, 2016.

[2] J. Karedal, N. Czink, A. Paier, F. Tufvesson, and A. F. Molisch, *Path Loss Modeling for Vehicle-to-Vehicle Communications,* IEEE Trans. Veh. Technol., vol. 60, no. 1, pp. 323-328, 2011.

[3] T. Mangel, O. Klemp, and H. Hartenstein, *A validated 5.9 GHz Non-Line-of-Sight pathloss and fading model for inter-vehicle communication,* in Proc. 11th Int. Conf. ITS Telecommun., pp. 75-80, 2011.

MOVING RELAY NODES ON-BOARD HIGH SPEED TRAINS IN AUSTRIA: IS IT WORTH IT?

Taulant Berisha

E389 - Institute of Telecommunications TU Wien

INTRODUCTION

A large number of passengers in Austria commute on a daily basis by using High Speed Trains (HSTs). Nowadays, a large amount of passengers can be considered active mobile phone users. Due to increased numbers of mobile users, the capacity problem is considerably introduced. To deal with this issue, the railway company in Austria (ÖBB) has implemented Wi-Fi on-board the railjet high speed trains. However, this solution is able to minimize only the issues on last-hop. The main problem is the deployment of base stations along a specific railway track. To deal with coverage issues, the signal strengths for all User Equipments (UEs), 2G/3G/4G, should be increased by minimizing the vehicular penetration loss. For this purpose we take the advantage of using two inter-connected multi-band multi-operator amplify-and forward Moving Relay Nodes (MRNs).

The use of relay nodes in mobile networks is common. They have gained more attention to be applied not only in fixed locations but on moving vehicles as well. By implementing the MRNs on-board the HSTs we gain on both capacity and coverage. I focus in this work on the coverage results of 4G user equipments along the railway that connects the two Austrian cities Vienna and Salzburg.

MEASUREMENTS

A large number of simulations consider installing different MRNs on-board trains such as in [1–3]. The authors show the performance improvement and the potential of MRNs. However, there are no available experiments performed in Austria.

One of the main challenges to conduct measurements and to evaluate the network performance for mobile users is how the measurement setup is established. We build such a setup which is able to evaluate the performance of MRNs as well as the mobile network itself (see Figure 1). This setup is used in our previous work in [4, 5]. The evaluation of 4G network is based on real-world measurements and the UEs used in this setup reflect the quality of experience for end user. On the left upper part of Figure 1 commercial UEs are shown, which are used during the measurement campaign. Along with UEs, we use various mini PC devices (Banana Pi) which enable us to monitor the measurement process at different positions on-board the HST. We distribute the UEs on different positions in the HST, because the MRNs are equipped with leaky cable antennas and the performance decays with increased distance from the MRN.

Figure 1: The measurement setup.

RESULTS AND DISCUSSION

One of the ways of showing the possible improvements in coverage for the whole route is by using descriptive statistics. Figure 2 shows a quantile-quantile plot for the Reference Signal Received Power (RSRP) of the UEs located strategically in the middle carriage of the HST. The gain for different operators can be read by drawing a vertical line from the red-dashed line to the scatter curve. The improvement in 4G is 17 dB and 10 dB for operator A and operator B, respectively. The green lines (trapezoid-like shape constructed by parameters such as minimum amplifier sensitivity, maximum gain, maximum output power, and red-dashed line) is the proposed model to optimize the gain and the output power of MRNs, in order to power them on-demand depending on radio-frequency conditions. Coverage increase does not necessary imply data rate improvement, but the MRNs employed here are particularly promising to boost the performance for cell edge scenarios.

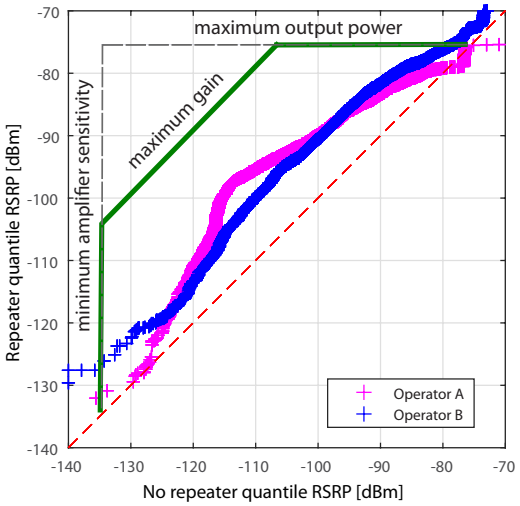

Figure 2: The estimated quantile-quantiles in RSRP 4G [5].

CONCLUSION

In this work, the effect of amplify-and-forward MRNs on coverage under high mobility scenarios is investigated. UEs are measured on-board railjet HSTs under realistic conditions. The obtained results are promising especially for the network areas where the received signal is normal, a gain of 17 dB in RSRP is achieved with MRN. In addition, MRNs can be powered-up on demand. The future work is likely to be towards optimizing different scenarios such as urban, sub-urban and rural scenarios.

REFERENCES

[1] Sui Y., Papadogiannis A and Svensson T.: *"The Potential of Moving Relays - A Performance Analysis"*. Vehicular Technology Conference (VTC-Spring), p. 1-5, May 2012.

[2] Sui Y., Guvenc I and Svensson T.: *"On the deployment of moving networks in ultra-dense urban scenarios"*. International Conference on 5G for Ubiquitous Connectivity (5GU), p. 240-245, Nov. 2014.

[3] Müller M., Taranetz M. and Rupp M.: *"Performance of remote unit collaboration schemes in High Speed Train scenarios"*. Vehicular Technology Conference (VTC-Fall), Sept. 2015.

[4] Berisha T., Svoboda P., Ojak S. and Mecklenbräuker, C.: *"SegHyPer: Segmentation- and Hypothesis based Network Performance Evaluation for High Speed Train Users"*. International Conference on Communications (ICC), May 2017.

[5] Berisha T., Svoboda P., Ojak S. and Mecklenbräuker, C.: *"Cellular Network Quality Improvements for High Speed Train Passengers by on-board Amplify-and-Forward Relays"*. International Symposium on Wireless Communication Systems (ISWCS), p. 325-329, Sept. 2016.

AUTOMATED DIGITAL RECONSTRUCTION OF TIMBER STRUCTURES FROM POINT CLOUDS

Markus Pöchtrager[a,b], Gudrun Styhler-Aydın[a], Marina Döring-Williams[a], Norbert Pfeifer[b]

[a] E251 - Institute of History of Art, Building Archaeology and Restoration, TU Wien
[b] E120 - Department of Geodesy and Geoinformation, TU Wien

INTRODUCTION

The analysis of historic timber constructions is an important task for the planning of adaptive reuse of buildings or for maintenance and restoration issues. Current approaches in analysis of timber structures consists of several consecutive stages, including surveying and modelling, that need to be done manually or in semi-automatic routines. A new concept for a fully automated analysis of timber constructions was developed to increase efficiency and put the focus on the data analysis rather than on data processing.

METHOD

As laser scanner data initially only consists of millions of single points that do not contain much information about the structure of the scanned objects (see Picture 1), we need processing methods that give a link between single points and create connected objects with known geometrical and structural properties.

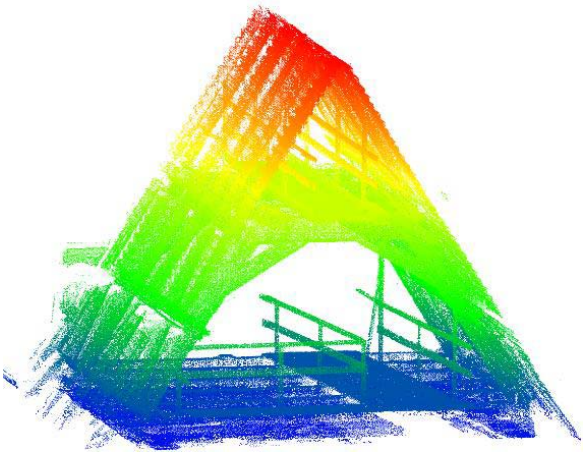

Picture 1: Point cloud of a historic roof construction in the Vienna Imperial Palace

For an automated modelling of wooden beams with rectangular cross section a workflow was developed, consisting of following stages: 1) Calculate normal vector information for each point, 2) Segmentation of the point cloud, 3) Classify segments and identify beam segments, 4) Identification of adjacent beam segments, 5) Fit cuboids to beams, 6) Intersection of beams and analysis of the structure.

The major tasks in this analysis are the segmentation of the point cloud and subsequently the classification of segments into beam segments and other segments (e.g. walls, roof tiles, etc.). To achieve proper segments of points, representing the faces of the wooden beams, a segmentation is performed using the seeded region growing approach[1] including normal vector information. The angle between normal vectors of neighbouring points is used as a local homogeneity criterion to get segments of flat surfaces. Thereby, two neighbouring points belong to the same segment if the difference between their normal vectors is below a given threshold.

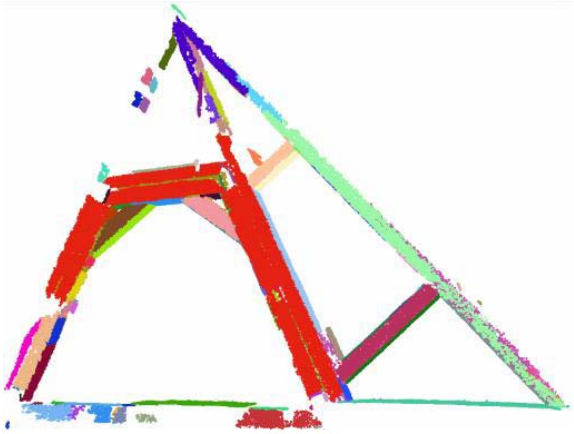

Picture 2: Segmentation results on a roof construction; Different colours represent different segment ids

The classification of segments requires information about two geometric properties of the segment points, namely the planarity and the linearity. As all the beams have a more or less flat surface, only planar segments are taken into account for the further analysis. Non-planar segments are split up using a RANSAC algorithm[2] for plane fitting, if they contain planar sub-segments. In the next step, the 2-D shape of the segments plays a major role in the identification of beam segments. Only segments of linear shape represent a single beam object. To get decisive shape factors the minimum bounded rectangle (MBR) and the α-shape representation can be calculated and used. On the side faces of the beams, where the transition between different beams is smooth enough (see Picture 2 – red segment), the segmentation results in segments containing several beams. A combination of different shape factors indicate to classify the segment as beam segment, discard the segment or to split it into multiple sub-segments again.

Based on the list of classified beam segments, the next step is to detect and join adjacent segments that form a wooden beam together. The association of adjacent planar segments results in a first rough 3-D modelling of the beams (see Picture 3). If at least two sides of a beam are covered by planar segments, it is possible to even go a step further and fit a cuboid to the segment points.

The difficulties in the final processing stage are the modelling of the beams in their correct dimension as well as the detection and modelling of woodworking joints, which are important for structural analysis. The original point cloud can be used as a reference data for the completion of the construction modelling.

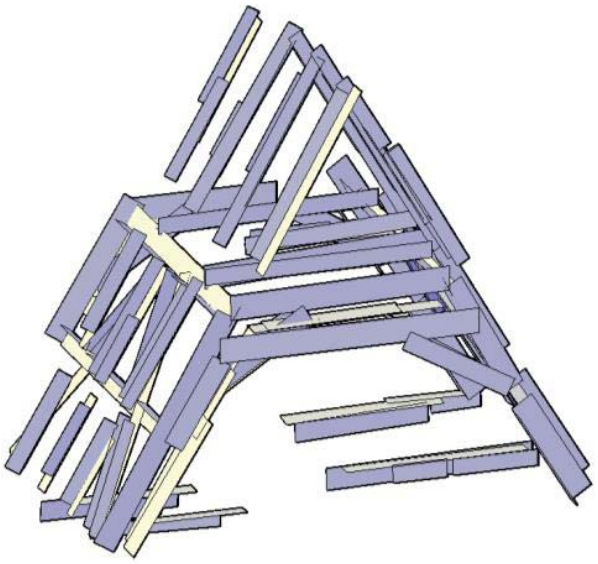

Picture 3: Automatically reconstructed beams represented by their planar segments (MBR)

RESULTS AND DISCUSSION

As the results showed, the developed workflow is heavily dependent on the results of the segmentation. The difficulty of finding an optimal homogeneity criterion is caused by cracks and damages in the beams of the historic timber structures. While cracks in the wood should not break up the element into multiple segments, the gap between two wooden elements should be identified as such.

CONCLUSION

As the results in Picture 3 show, the proposed method is feasible for the automated reconstruction of timber structures. A high degree of automation is enabled for the modelling of beams with rectangular cross section. The quality issues regarding segmentation and further processing results in an incomplete automated detection of beams, which in turn requires an intense global analysis of the structure in order to produce a complete documentation of the construction.

REFERENCES

[1] Adams, R., & Bischof, L. (1994). Seeded region growing. *Pattern Analysis and Machine Intelligence, IEEE Transactions on, 16*(6), 641-647.

[2] Fischler, M. A., & Bolles, R. C. (1981). Random sample consensus: a paradigm for model fitting with applications to image analysis and automated cartography. *Communications of the ACM*, *24*(6), 381-395.

OPTIMAL INVESTMENT AND LOCATION DECISIONS OF A FIRM IN A FLOOD RISK AREA USING IMPULSE CONTROL THEORY

Johanna Grames[a,b], Dieter Grass[c], Peter Kort[d,e], Alexia Prskawetz[b,f]

[a]E222 - Vienna Doctoral Programme for Water Resource Systems

[b]E105 - Institute of Statistics and Mathematical Methods in Economics, Research Group Economics

[c]E105 - Institute of Statistics and Mathematical Methods in Economics, Research Group Operations Research and Control Systems

[d]Tilburg School of Economics and Management, Econometrics and Operations Research, Tilburg University, Tilburg, The Netherlands

[e]Department of Economics, University of Antwerp, Antwerp, Belgium

[f]Wittgenstein Centre (IIASA, VID/AW, WU), Vienna Institute of Demography, Vienna, Austria

INTRODUCTION

Climate change puts increasing environmental pressure on coastal zones and on areas around lakes and rivers. On top of the list of potential impacts of climate change are effects of sea level rise on coastal cities and effects of extreme events on built infrastructure like floods from heavy precipitation events ([1]). Floods and other extreme weather events increase economic losses ([2]). Large-scale flood disasters from recent years gained attention among decision makers (e.g. businesses). Implementing actions to reduce disaster risks and build flood resilience facing limited resource needs decision support tools ([3]).

The aim of this paper is to understand investment decisions of firms and their implications on businesses in flood risk areas. [4] developed a conceptual descriptive model to understand the feedbacks of flood risk reduction (i.e. investments in flood defense and moving away from the river) and flood damage from a societal perspective. [5] introduced an optimal decision framework to investigate the interaction of a society's investment in flood defense and productive capital.

FUNDAMENTAL OF THE PROBLEM

In this paper we look at a partial equilibrium model and try to understand the firm's investment decisions in its interrelations with the hydrological system. A representative firm can have multiple choices: First, it can choose the optimal investment in capital used for production, second the optimal investment in flood risk reduction measures and third, the optimal location for its production plant.

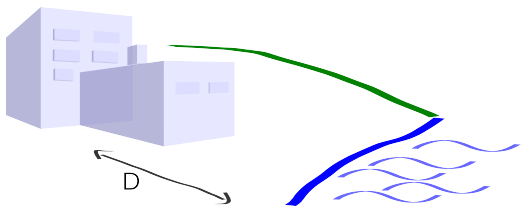

Figure 1: The firm chooses where to build its production plant by choosing the distance to the water.

Our qualitative model helps to understand feedback mechanisms between the firm's decisions and the hazard of flooding. We apply Impulse Control Theory (see [6]) and develop a continuation algorithm to solve the model numerically. We provide analytical and numerical solutions and analyse variations of these solutions under different parameterizations of the model[1].

[1]Please find more details in the full working paper version [7].

RESULTS AND DISCUSSION

We find that, the higher the flood risk and the more the firm values the future, i.e. the more sustainable the firm plans, the more the firm will invest in flood defense. Investments in productive capital follow a similar path. Hence, planning in a sustainable way leads to economic growth. Sociohydrological feedbacks are crucial for the location choice of the firm, whereas different economic settings have an impact on investment strategies. If flood defense is already present, e.g. built up by the government, firms move closer to the water and invest less in flood defense, which allows firms to accrue higher expected profits. Firms with a large initial productive capital surprisingly try not to keep their market advantage, but rather reduce flood risk by reducing exposed productive capital.

CONCLUSION

This paper provides the investment behaviour and location choice of a firm in a flood risk area within an optimal decision framework. Sustainable investment planning of the firm leads not only to a safer environment with less flood risk, but also to economic growth both in the short and the long run. If the area is already protected against floods, firms still invest in flood defense, but less. And if the firm is more capital intensive potential damage is larger, but the timing and amount of impulse investments do not change.

Anthropogenic flood risk reduction can affect the environment resulting in changes of the water system and consequently again increase flood risk due to negative feedbacks. In this case, production output is much less and the firm decides to build its production far away from the water.

REFERENCES

[1] A. Hunt and P. Watkiss, "Climate change impacts and adaptation in cities: a review of the literature," *Climatic Change*, vol. 104, no. 1, pp. 13–49, 2011.

[2] D. R. Easterling, J. L. Evans, P. Y. Groisman, T. R. Karl, K. E. Kunkel, and P. Ambenje, "Observed variability and trends in extreme climate events: A brief review," *Bulletin of the American Meteorological Society*, vol. 81, no. 3, pp. 417–425, 2000.

[3] R. Mechler, J. Czajkowski, H. Kunreuther, E. Michel-Kerjan, W. Botzen, A. Keating, C. McQuistan, N. Cooper, and I. O'Donnell, "Making communities more flood resilient: The role of cost benefit analysis and other decision-support tools in disaster risk reduction.," *White Paper, Zurich Flood Resilience Alliance*, 2014.

[4] A. Viglione, G. Di Baldassarre, L. Brandimarte, L. Kuil, G. Carr, J. L. Salinas, and G. Blschl, "Insights from socio-hydrology modelling on dealing with flood risk - roles of collective memory, risk-taking attitude and trust," *Journal of Hydrology*, vol. 112, 2014. doi:10.1016/j.jhydrol.2014.01.018.

[5] J. Grames, A. Prskawetz, D. Grass, A. Viglione, and G. Blschl, "Modeling the interaction between flooding events and economic growth," *Ecological Economics*, vol. 129, pp. 193 – 209, 2016.

[6] M. Chahim, R. Brekelmans, D. den Hertog, and P. Kort, "An impulse control approach to dike height optimization," *Optimization Methods and Software*, vol. 28, no. 3, pp. 458–477, 2013.

[7] J. Grames, D. Grass, P. Kort, and A. Prskawetz, "Optimal investment and location decisions of a firm in a flood risk area using impulse control theory," *Working Paper TU Wien ECON*, no. 1, 2017.

LONG-TERM FORECAST OF RESIDENTIAL & COMMERCIAL GAS DEMAND IN GERMANY

Mostafa Fallahnejad[a,*], Benedikt Eberl[b], Maik Günther[c]

[a]E370 - Institute of energy systems and electrical drives
[b]Forschungsstelle für Energiewirtschaft mbH, Munich, Germany
[c]Stadtwerke München, Munich, Germany

ABSTRACT

Natural gas demand of non-daily metered customers (residen-tial and commercial sectors) in Germany can be calculated using Standard Load Profiles (SLPs) and temperature forecasts. SLPs were generated with historic data and represent the actual situation. But they are not helpful for the calculation of daily gas demand in long-term. Better insulation of buildings and more efficient heating systems will change the SLPs in the future. Thus, in this paper a LP model was developed to create SLPs for the future. The model is executed for one- and two-family dwellings, apartments and the commercial sector for the years 2016, 2025 and 2040. The obtained SLPs demonstrate that year by year, the heating phase will be started at colder temperatures. Moreover, the new SLPs are used to calculate the daily gas demand. The demand profiles reveal that in future, the reduction of the gas demand in colder months is higher than in warmer months.

Keywords*: Standard Load Profile; Natural Gas Demand; Residential Sector; Commercial Sector; LP*

INTRODUCTION

Standard Load Profiles (SLPs) are used to forecast the daily consumption of natural gas by small customers. In general, there are two categories of natural gas consumers: non-daily metered consumers (or SLP customers) and real-time metered customers (or RLM customers). SLP customer is referred to a customer with an annual consumption of less than 1,500 MWh and an installed power of less than 500 kW per hour.

The gas utility companies were in the past involved in the determination of gas consumption of non-daily metered customers. In 2000, these measurements were centrally recorded and organized by the Federal Association of German Gas and Water Industries (in German: Bundesverband der deutschen Gas- und Wasserwirtschaft; BGW) and the Association of Local Utility Companies (in German: Verband Kommunaler Unternehmen; VKU). In addition, further measurements were supplemented with respect to the customer groups and temperature ranges in order to obtain sufficient data for statistical analyses [1]. Based on these measurements, the Department for Energy and Application Technology at Technical University of Munich (TUM) was commissioned by BGW and VKU to derive tem-perature-dependent load profiles for the gas supply [2]. In 2002, eight different load profiles for the residential customers and fourteen different load profiles for the commercial sector were developed [3], [4]. Based on the experiences gained, the primary SLPs were modified in 2005. In these regards, within the residential sector a profile for the one- and two-family dwellings and a profile for the apartments were introduced. With-in the commercial sector, on the other hand, the number of profiles was reduced to eleven. Additionally, one general profile representing the whole commercial sec-tor was presented [5].

The SLPs generated at TUM established a standard in this field. The primary SLPs have been continuously revised and updated in order to match to the current situations and provide a better

forecast. A summary of the revisions made to the SLPs can be found in [2]. The synthetic SLPs were used by more than 83% of the operators in 2014. According to the Federal Network Agency (in German: Bundesnetzagentur; BNetzA), nearly all exit point operators (98%) used SLPs when delivering to household or small business customers [6]. In June 2015, the most recent revision of SLPs was published by Federal Association of Energy and Water (in German: Bundesverband der Energie- und Wasser-wirtschaft e.V.; BDEW) in cooperation with VKU and the European Association of Business and Distribution Organizations for Energy (GEODE). From 1st October 2015, all network operators can use the new profiles [7]. In the recent revision, the so called SigLinDE profiles were introduced. These profiles are composed of a sigmoid term and a linear term. The aim for adding the linear term was to adjust the profiles for the cold tem-peratures and review the profiles at the high tempera-tures.

Stadtwerke München GmbH (SWM) operates the worldwide gas market model WEGA to analyze gas prices and trade flows till 2040 [8]. An input parameter for the model is the daily gas demand from 2016 to 2040. Actual SLPs are based on historic data and they are not helpful to calculate the daily demand of SLP customers in long-term. It is expected that in the future buildings better thermal insulations and more efficient heating systems are employed, and also the family structures and the floor space per person will change. No research could be identified in which creation of SLPs for the future is discussed. Thus, new SLPs are created in this paper for one- and two-family dwellings (EFH), apartments (MFH) and the commercial sector (GHD) for the years 2016, 2025 and 2040. For this purpose, the linearization concept SigLinDE is used in a LP model in GAMS environment. Based on these new SLPs for the future the daily demand for 2016, 2025 and 2040 is calculated.

REFERENCES

[1] BGW, and VKU, “Praxisinformation P 2006/8 Gastransport/Betriebswirtschaft. Abwicklung von Standardlastprofilen zur Belieferung nicht-leistungsgemessener Kunden”, 2006.

[2] S. von Roon, T. Gobmaier, K. Wachinger, and M. Hinterstocker, „Statusbericht zum Standardlastprofilverfahren Gas“, 2014.

[3] B. Geiger, and M. Hellwig, „Entwicklung von Lastprofilen für die Gaswirtschaft - Gewerbe, Handel und Dienstleistung“, 2002.

[4] M. Hellwig, „Entwicklung und Anwendung parametrisierter Standard-Lastprofile“, PhD thesis, TU Munich, 2003.

[6] BNetzA, „Monitoring report 2015“, 2016.

[5] U. Wagner, and B. Geiger, „Gutachten zur Festlegung von Standardlastprofilen Haushalte und Gewerbe für BGW und VKU“, 2005.

[7] BDEW, VKU, and GEODE, “Abwicklung von Standardlastprofilen Gas”, 2015.

[8] M. Günther, “Practical Application of a Worldwide Gasmarket Model at Stadtwerke München”, in Operations Research Proceedings 2015, in press, 2016.

HOW TO GEOTAG THE WEB?

Alexander Czech

E280 - Center of Regional Science at Vienna University of Technology

Spatial information guides people's activities in space. In the last decades the World Wide Web has also become a widely used source for this kind of information. People use web search engines to query spatial information, for example to look up the best French restaurant, a still open grocery store, or a scenic hiking route.

Most research around "Neogeography" or "Big Geo-Data" focuses on already geotag data originating on social media. But in comparison to the web, this is only a small portion of all the data, and it can be skewed by a vocal minority [1]. To leverage a big corpus of web data, this corpus needs to be geotagged and the relation between geotag and data needs to be proven.

In previous work a geotag on a website was defined as a human readable postal address. The study was done for a select subset of HTML documents belonging only to the .at top-level domain and the address pool was restricted to addresses from the inner Viennese districts (1.-9. and 20.) [2]. This work resulted in an information distribution landscape that can be seen in **Figure 1**.

The current spatial area of interest is the urban system of Randstad in the Netherlands. The Website dataset will again be sourced from the Common Crawl Project, who provides semimonthly raw crawled websites data. One crawl of which is about 81 terabyte in compressed archives [3].

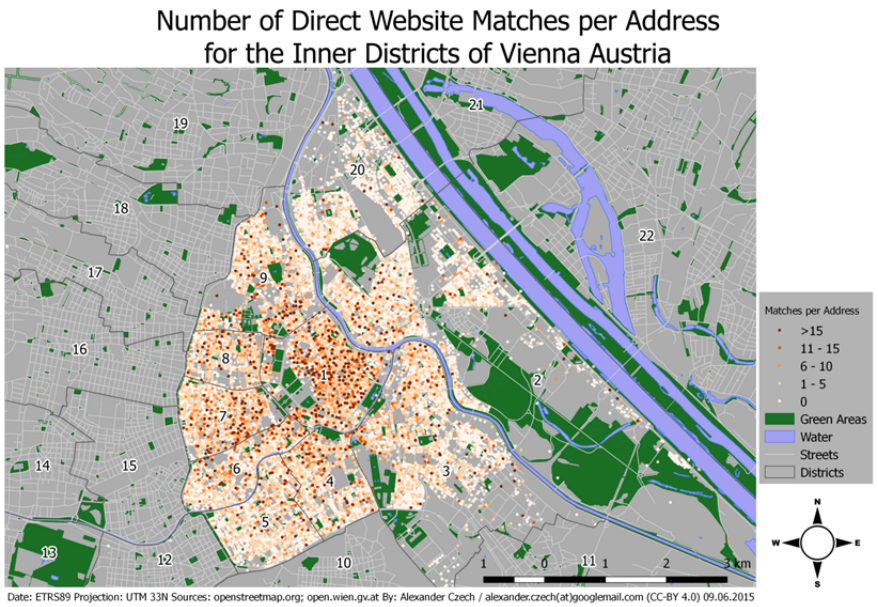

Figure 1 Distribution of addresses joined to HTML documents [2].

The apache spark cluster frame work is used to process this dataset. After preprocessing the data an address matching routine, will be employed to find addresses within HTML documents.

The next step is to show that the data that was geotagged is related to the addresses. Tools from the natural language processing and information retrieval domain are used to achieve this. All documents related to the addresses are transformed into vector representations. The paragraph vector distributed bag of words (PV-DBOW) method is applied for here [4], it builds conceptually upon the skip-gram model to represent words in a vector space [5]. Four models for each language, Dutch, English, French and German are trained on respective Wikipedia corpora. These models are then used, to infer document vectors for documents in the corresponding language, which have been geotagged to an address. This approach was selected because PV-DBOW has been shown to perform robustly in similarity tasks when trained on external corpora [6].

To test the relation between data and address the average similarity between documents geotagged to the same address is calculated through cosine similarity of the document vectors [7] and compared to the cosine similarity of a random sample. The expectation being that the documents matched to the same addresses are more similar to each other than a random sample of documents to each other, thus showing that there is a relation of documents and address.

To further verify this relation, all addresses are grouped into predefined address group (e.g. schools, stores, hotels, and so on). All documents related to all addresses of one group are then compared to each other similar to the process above. The expected results again being that documents in one group are more similar to each other than compared to a random sample.

After being able to proof the relation between data and geotag, the idea is to use this new source of data to support the research on urban spaces and urban systems. As an example the web can be seen as a force of globalization. These have very different and uneven effect on space[8] and **Figure 1** already suggests such uneven effects, because a spatial pattern in the distribution can be observed. Further the concept of relational (Urban-)spaces can be explored through the relation of data and space [9]. Also the research on city networks and urban systems that focuses on the connection between cities [10, 11, 12] could be improved by examining the connection of cities through the webgraph. There is already research around identifying, measuring and quantifying communities through the webgraph structure that could be adapted to such a task [13, 14].

REFERENCES

[1] J. W. Crampton, M. Graham, A. Poorthuis, T. Shelton, M. Stephens, M. W. Wilson, and M. Zook, “Beyond the geotag: situating ‘big data’ and leveraging the potential of the geoweb,” *Cartogr. Geogr. Inf. Sci.*, vol. 40, no. 2, pp. 130–139, 2013.

[2] A. Czech, “Geospatial Information Retrieval for POIs with the use of a Data Mining System,” 2015.

[3] Common Crawl, “Common Crawl.” Mar-2012.

[4] Q. Le and T. Mikolov, “Distributed Representations of Sentences and Documents,” *Int. Conf. Mach. Learn. - ICML 2014*, vol. 32, pp. 1188–1196, 2014.

[5] T. Mikolov, G. Corrado, K. Chen, and J. Dean, “Efficient Estimation of Word Representations in Vector Space,” *Proc. Int. Conf. Learn. Represent. (ICLR 2013)*, pp. 1–12, 2013.

[6] J. H. Lau and T. Baldwin, “An Empirical Evaluation of doc2vec with Practical Insights into Document Embedding Generation,” in *ACL*, 2016, pp. 78–86.

[7] C. D. Manning, P. Raghavan, and H. Schütze, *An Introduction to Information Retrieval*. 2009.

[8] S. Sassen, *The global city*. 1991.

[9] P. Weichhart, *Entwicklungslinien der Sozialgeographie*. Steiner, 2006.

[10] J. V. Beaverstock, R. G. Smith, and P. J. Taylor, “A roster of world cities,” *Cities*, vol. 16, no. 6, pp. 445–458, 1999.

[11] J. H. Choi, G. A. Barnett, and B. S. Chon, “Comparing world city networks: A network analysis of Internet backbone and air transport intercity linkages,” *Glob. Networks*, vol. 6, no. 1, pp. 81–99, 2006.

[12] H. Kramar and J. Kadi, “Polycentric city networks in central-eastern Europe: Existing concepts and empirical findings,” *Geogr. Pol.*, vol. 86, no. 3, pp. 183–198, 2013.

[13] J. M. Kleinberg, “Hubs, authorities, and communities,” *ACM Comput. Surv.*, vol. 31, no. 4es, p. 5, 1999.

[14] G. Flake, S. Lawrence, L. Giles, and F. Coetzee, “Self-Organization of the Web and Identification of Communities,” *IEEE Comput.*, vol. 35, no. 3, pp. 66–71, 2002.

TRANSFORMATIONS AND BASE SHAPE ANALYSIS

María Lara Miró

Institute for Discrete Mathematics and Geometry at TU Wien

INTRODUCTION

Principal aim of this topic is to investigate a novel approach to the base shape analysis of a given shape, that is, a decomposition of the shape into geometrically meaningful "base shapes" that provides geometric insight and hence lends itself to an intuitive refinement of a design while preserving geometric structure. This will greatly facilitate design processes that involve free-form shapes and transitions between physical and computational modelling.

FUNDAMENTAL OF THE PROBLEM

Darboux-Bäcklund-transformation and cross-ratio are two key points which I have had to become familiar with. Darboux-Bäcklund-transformations of curves are a kind of transformations which have helped to preserve the defining geometric features of their respective base surface classes [1]. They are considered a special type of Ribaucour transformation which is formed by two curves $x, \hat{x} : I \to \mathbb{R}^n$ if tangents at corresponding points $x(s)$ and $\hat{x}(s)$ are tangent to a common circle $c(s)$, i.e., if its tangent cross-ratio

$$cr = x'(\hat{x}-x)^{-1}\hat{x}'ds(\hat{x}-x)^{-1}$$

is real.

From three non-collinear points q_1, q_2, q_4 and a real number, there exists a fourth point on a circle such that

$$cr = (q_1-q_2)(q_2-q_3)^{-1}(q_3-q_4)(q_4-q_1)^{-1}$$

holds.

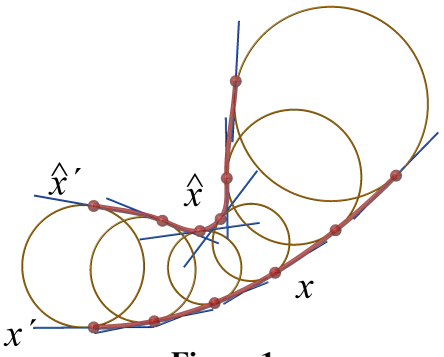

Figure 1: Darboux-Bäcklund-transformation

Thus, repeated transformations via cross-ratio generate new curves in the space.

We explore the relation between analogous smooth and discrete theories in a setting to analyze if the interplay between them becomes tangible.

From a given discrete curve, we analyze new Darboux transforms by observing how the cross-ratio, the initial point and the number of points in which the initial curve is divided affect them.

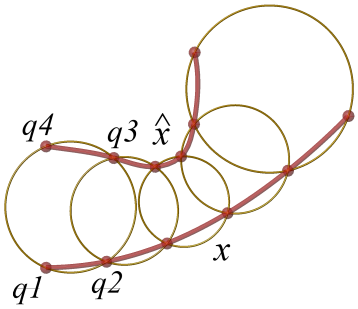

Figure 2: Cross-ratio-transformation

Our next mission is to compose some Möbius transformations [2] in order to get specific curves in the space. This is possible because the composition of two Möbius transformations is again a Möbius transformation [3].

$$z = f_2^{-1}(f_1(z)) = p_2$$

Interfacing areas between my research and the research fields of my institute are Transformation theory of curves and surfaces, Discrete differential geometry, Geometric modelling and Architectural geometry.

RESULTS AND DISCUSSION

From the same value of cross-ratio, the transformation of a smooth curve will be different from the same curve discretized. Likewise, two different discretizations will have different transformations. These differences will be null in transformations of the initial point and will increase as we move away from it.

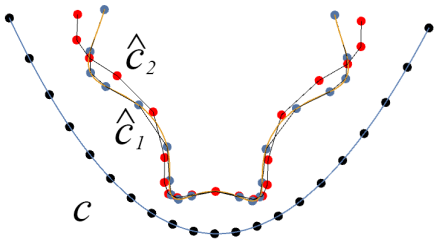

Figure 3: Smooth-discrete curves

Using Darboux-Bäcklund-transformation, it is possible to get any curve c from another one c' divided into the same number of segments if and only if c is transformed the same number of times than the number of segments have and the value of cross-ratio in every transformation will be prescribed for all the segments (r,s,t) belonging to that curve.

In the same way, a curve c can be transformed being prescribed the initial and final points p_0, p_n of the transformation. The cross-ratio will be prescribed for all the segments, except for the last two ones $p_n, pn-1, p_{n-2}$, because cross-ratio in p_n, p_{n-1} and p_{n-1}, p_{n-2} shall ensure that p_{n-1} will coincide in both transformations.

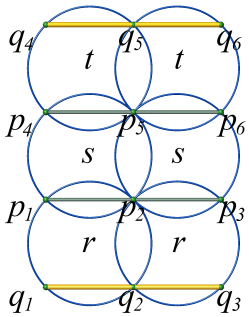

Figure 4: Composition Möbius transformations

CONCLUSION

As transformations are intimately related to the generation of discrete and semi-discrete surfaces, the control of developed methods will not only apply to smooth surfaces used in design, but also to faceted and panelled surfaces that lend themselves more easily to modelling and physical construction. The next steps will be to analyze the advantages over other forms of design [4].

REFERENCES

[1] F Burstall, U Hertrich-Jeromin, C Müller, W Rossman: *Semi-discrete isothermic surfaces*; Geom. Dedicata 183 (2016) 43-58, June 2015.

[2] H Pottmann, A Asperl, M Hofer, A Kilian: *Architectural geometry*; Bentley Institute Press, 2007.

[3] U Hertrich-Jeromin: *Introduction to Möbius differential geometry*; London Math Soc Lect Note Ser 300, Cambridge University Press, 2003.

[4] E Colabella: *Generative Art*; Domus Argenia Publ, Proc GA2008, Milan, 2008.

EFFICIENT NUMERICAL MODELLING OF MULTILAYER SYSTEMS

Antonia Wagner[a], Michaela Nagler[a], Matthias Bartosik[b], Helmut Böhm[a], Melanie Todt[a]

[a]E317 - Institute of Lightweight Design and Structural Biomechanics
[b]E308 - Institute of Materials Science and Technology

INTRODUCTION

The multilayer systems considered in this study consist of a substrate and a coating formed by several hundred bi-layers with a thickness of a few nanometers each, deposited via PVD (physical vapor deposition), see Fig.1. After the manufacturing process residual stresses in the range of GPa can be observed in the multilayers [1]. These stresses are induced primarily by two effects. When cooling down the multilayer system from deposition to room temperature a bending moment is induced due to the mismatch between the thermal expansion coefficients of the substrate and the bi-layers. Furthermore stresses originating from the film growth process contribute to the overall residual stress state. The aim of the present study is to develop an efficient finite element model (FEM) allowing to estimate the residual stresses in such multilayer systems and to gain further insight into experimental results and facilitate interpretation. Compared to analytical approaches the FEM simulation provides details on the three-dimensional behaviour of multilayer systems and enables implementing plastic yielding in the layers as well as damage in the interfaces between the layers.

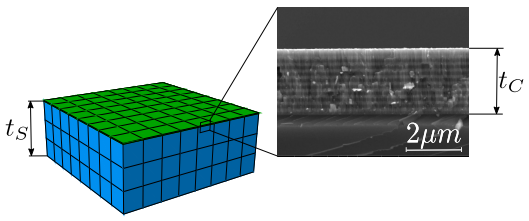

Figure 1: FEM-model and scanning electron microscopy image of a multilayer system

MODELLING APPROACH

The modelling of the multilayer system is realized using the FEM software package ABAQUS. Due to the fact that the layers are only a few nanometers thick and thus much thinner than the substrate (Fig.1), modelling both, the substrate and the bi-layers, with FEM using standard continuum elements leads to a high number of degrees of freedom (DOF). This results in excessive simulation times. To overcome this limitation the layers are discretized by conventional shell elements. The modelling of the substrate material is done with continuum elements. The connection between the substrate material and the individual layers is realised with cohesive zone elements. To further increase computational efficiency when considering a system with up to hundreds of bi-layers a unit cell is modelled and 2D-periodic boundary conditions (PBC) are applied. In finite element models the PBCs can be implemented by means of equations relating the displacement of the corner, edge and surface nodes to initially defined master nodes. Unlike standard PBCs which describe periodicity in all directions, for the present purpose the top and bottom faces are allowed to deform freely. With these boundary conditions a representative unit cell of an infinite plate with periodicity in two dimensions is simulated. Since the interfaces between the layers do not intersect a free surface, damage in the interfaces is not considered in the current model. When applying periodic boundary conditions to an FE-model consisting of a combination of continuum and shell elements, the difference in formulation has to be considered. Whereas continuum elements have only the three translational DOFs, for the shell elements the rotational DOFs have to be restricted additionally.

APPLICATION EXAMPLE

To demonstrate the present modelling approach the compressive residual stress originating from the film growth process is treated in the following. For testing the algorithm, the coating, which is actually deposited layer by layer, is modelled as a homogenized coating represented by one single layer. The considered bilayer system consists of TiN and CrN of equal thickness. For the simplified model the elastic properties are calculated with the rule of mixture. For the substrate a thickness t_s of 380 μm is chosen and four different materials are considered: Ti6Al4V, Si (100), Austenite and WC-Co (in ascending order of their Young's moduli). With this model a parameter study is carried out by varying the thickness of the coating t_c ranging from 0.5 to 5 μm in order to investigate its effect on the residual stresses. Moreover the influence of different substrate materials can be observed by changing the elastic properties. To simulate the compressive growth stresses, the shell elements representing the layers are removed in the first step of the FE-analysis. Then a compressive stress is applied to the coating and the shell elements are added in a second step. The equilibrium which is restored by stress redistribution returns the results for the residual stresses of the substrate and the coating, see Fig.2.

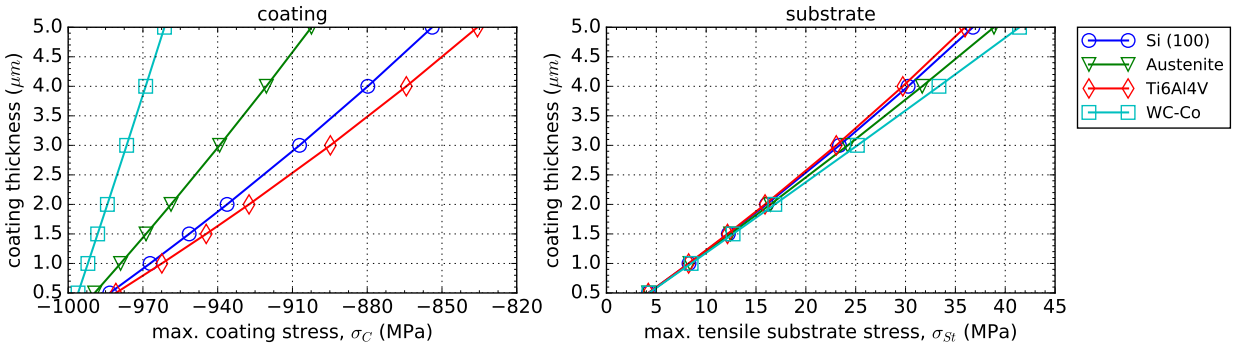

Figure 2: Maximum in-plane residual stresses of the homogenized coating and maximum residual stresses of the substrate as a function of coating thickness and substrate material for a coating preload of 1GPa

The side of the substrate closer to the coating is subjected to compression and the opposite to tensile stress. The coating is exposed to compressive stress over the entire thickness. Extending the coating thickness reduces the magnitude of the compressive stress in the coating, but increases the maximum tensile stress in the substrate as shown in Fig.2. Using a substrate material with a high Young's modulus leads to an increase of the total value of maximum stress in the coating and the substrate.

CONCLUSION AND OUTLOOK

In this study an efficient FE-model for a multilayer system with hundreds of bi-layers was developed by means of implementing periodic boundary conditions and choosing shell elements to discretize the individual layers. The next step of this work is to simulate the cooling down from deposition temperature of a multilayer arrangement and to consider the influence of damage in the interfaces. To do so the boundary conditions of the model have to be modified such that one of the lateral surfaces is left free to deform. An accurate prediction of the residual stresses in a multilayer coating obtained from the FEM model will be used to provide initial conditions for further simulations and can consequently improve the final results.

REFERENCES

[1] F.Lomello,Temperature dependence of the residual stresses and mechanical properties in TiN/CrN nanolayered coatings processed by cathodic arc deposition, Surf.Coat.Technol. 238(2014) 216-222

ANALYTICAL TREATMENT OF RESIDUAL STRESSES IN MULTILAYER COATINGS

Michaela Nagler[a], Antonia Wagner[a], Matthias Bartosik[b], Helmut Böhm[a], Melanie Todt[a]

[a]E317 - Institute of Lightweight Design and Structural Biomechanics
[b]E308 - Institute of Materials Science and Technology

INTRODUCTION

Multilayers on substrates have extensive applications in optical, microelectronic and structural components as well as for protective coatings [1]. The multilayer systems are strongly influenced by residual stresses (in range of GPa [2]) which directly affect the mechanical behaviour of the substrate and the coating. These stresses occur because of 1) different coefficients of thermal expansions (CTEs) when the multilayer system is cooled down from its production temperature to room temperature and 2) film growth stresses (e.g., atomic and ionic peening during film growth generating lattice defects). The multilayer system which is considered in this study consists of a substrate and a few hundred nanometer-thick bi-layers deposited by PVD (physical vapor deposition), see Fig. 1. The aim of the present study is to develop an analytical approach for predicting residual stresses in multilayer systems. The advantage of an analytical model, in contrast to the Finite Element approach, lies in providing for efficient parameter studies.

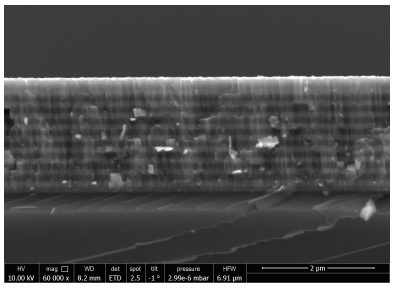

Figure 1: Cross-section of a PVD nitride multilayer system

MODELING CONCEPT

The analytical approach is based on Euler-Bernoulli beam theory where a one dimensional linear elastic stress state is considered. The influence of growth-induced stresses is estimated by adding a prestressed layer to a system consisting of a substrate of n layers that is self equilibrated, but not stress free. The equilibrium of this modified system is estimated by the force and moment balances for a beam in the absence of external forces and moments using:

$$N = \int_0^{t_S} \sigma_{x,S}(z)dA + \sum_{j=0}^{n} \int_{t_j}^{t_{j+1}} \sigma_{x,j}(z)dA + \int_{t_n}^{t_{n+1}} \sigma_{D,n}(z)dA = 0 \tag{1}$$

$$M = \int_0^{t_S} \sigma_{x,S}(z) \cdot z dA + \sum_{j=0}^{n} \int_{t_j}^{t_{j+1}} \sigma_{x,j}(z) \cdot z dA + \int_{t_n}^{t_{n+1}} \sigma_{D,n}(z) \cdot z dA = 0 \tag{2}$$

In Eqs. (1) and (2) $\sigma_{x,S}(z)$ denotes the stress distribution in thickness direction in the substrate, $\sigma_{x,C}(z)$ denotes the stress distribution in the coating consisting of an compressive prestress $\sigma_D(z)$ in the layer $n+1$ because of growth stresses. A is the integration area, t_S is the thickness of the substrate and t_j denotes the thickness of the j-th layer.

APPLICATION EXAMPLE

As a test case a configuration is considered that consists of a substrate and a coating with the smeared-out properties of multiple CrN and TiN layers of identical thickness. The elastic properties of the

simplified coating are calculated via the rules of mixture.
With this approach a parametric study of the multilayer system is carried out with regard to the influence of different substrate materials. Furthermore different thickness parameters of the coating and a varying compressive preload in layer $n+1$ of 1, 3 and 5GPa are taken into account. For the substrate two different materials are considered: Si(100) and WC-Co, which has a four times greater Young's modulus. The substrate thickness t_S is chosen to be $380\mu m$. The thickness of the coating t_C ranges from $0.5\mu m$ to $5\mu m$.

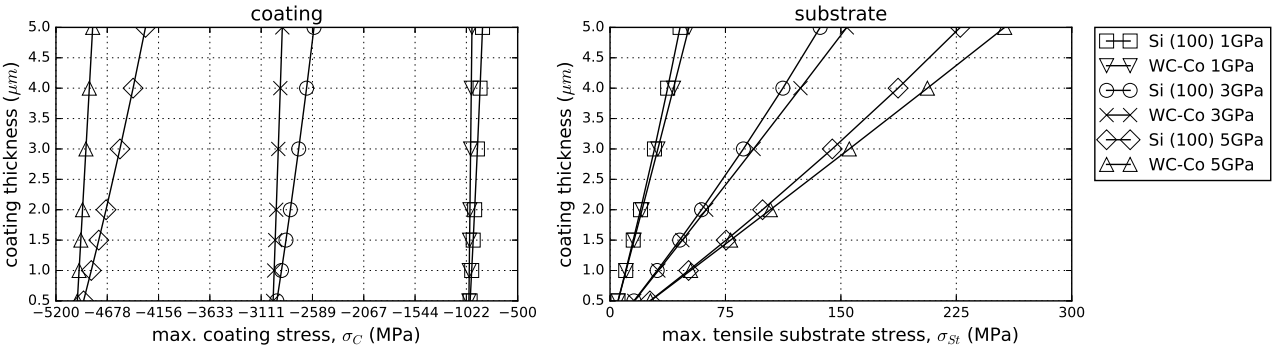

Figure 2: Maximum residual stress in the homogenized coating (left) and substrate (right) depending on substrate materials, coating thickness and compressive preload

When a compressive preload is applied to the coating, the residual stress in the coating appears as a compressive stress, see Fig. 2. The substrate is subjected to compressive stress near the film and to tensile stress on the opposite side. Due to the fact that the maximum tensile stress is greater than the maximum compressive stress in the substrate, only the tensile stress in the substrate is depicted in Fig.2. Increasing the total coating thickness leads to a reduction of the magnitude of the residual stress in the coating. Furthermore the magnitude of the stress increases in the substrate and the coating with an increasing Young's modulus of the substrate. Additionally the influence of a variation of the applied coating prestress can be observed. A comparison between the resulting residual stress values for the substrate and the coating for compressive preloads of 1, 3 and 5GPa shows a stress increase by a factor of five in the coating and the substrate.

CONCLUSION

Within this work an analytical approach to determining residual film growth stresses in an elastic multilayer system was presented. The advantage of an analytical model is the low computational effort when a parametric study is executed. The next stage of the project should include a cooling process after the deposition of the pre-stressed coating on the substrate. Instead of a homogenized coating a multi-layer arrangement, with alternating pre-stressed bi-layers will be considered. Consequently the thickness, the material data and the compressive preload of each single layer can be adjusted.

REFERENCES

[1] C.H.Hsueh, Thermal stresses in elastic multilayer systems, Thin Solid Filsm 418 (2002) p. 182-188.

[2] F. Lomello, Temperature dependence of the residual stresses and mechanical properties in TiN/CrN nanolayered coatings processed by cathodic arc deposition, Surface and Coatings Technology 238 (2014) p. 216-222.

TOWARDS A METRIC FOR AN AUTOMATIC HULL MESH COARSENING STRATEGY

Lukas Gnam[a,b], Josef Weinbub[a,b], Andreas Hössinger[c], Siegfried Selberherr[b]

[a]Christian Doppler Laboratory for High Performance TCAD at the
[b]E360 - Institute for Microelectronics
[c]Silvaco Europe Ltd., St. Ives, United Kingdom

INTRODUCTION

In numerical simulations of various areas of science and engineering, e.g., biomechanical engineering [1] or ray tracing [2], the discretization of objects in physical space is an integral step. In particular for three-dimensional cases, where a volume mesh generation is required, the mesh generation is rather critical for the robustness, stability, and accuracy for the subsequent simulation steps. One common approach to generate a volume mesh utilizes the Advancing Front method [3, 4]. This approach uses a two-dimensional hull mesh (i.e., a closed surface) as starting point, which potentially consists of an unnecessary large amount of mesh elements. Obviously, the properties of the hull mesh (e.g. the number of triangles and their quality) heavily influence the quality and the execution time of the volume mesh generation process and the subsequent simulations. The aim of this work is to introduce a novel combined comparison metric to compare the quality of the coarsened mesh to its original input. This work paves the way for an automatic domain- and mesh-specific hull mesh coarsening method to aid subsequent volume meshing steps.

COARSENING ALGORITHM

Within this work, CGAL's Triangulated Surface Mesh Simplification [5] has been utilized to coarsen two widely used and representative geometries. The first geometry, the *bunny*, consists originally of 69 451 triangles and the second geometry, the *elephant*, consists originally of 5 558 triangles (see Figure 1). One important parameter which can be set using CGAL's algorithm is the *stop ratio*, denoting the desired number of remaining triangles in the coarsened mesh.

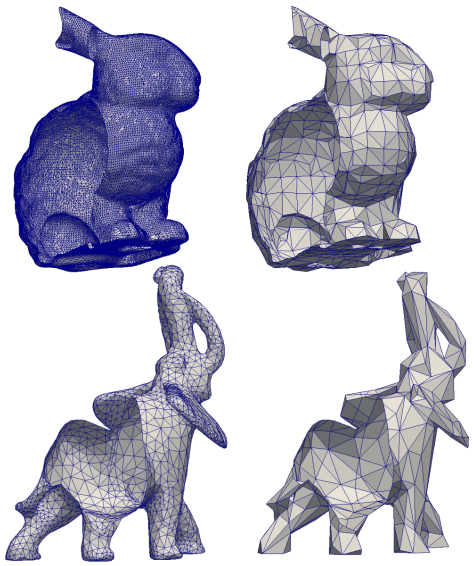

Figure 1: Cross-sections of the original and exemplary coarsened meshes of the two test geometries. The *bunny* in the top row was coarsened from 69 451 to 1 513 triangles, the *elephant* from 5 558 to 554.

DEVISED METRIC

To evaluate the coarsening algorithm, we selected four widely used metrics to capture various aspects of the coarsening process. We picked the triangle shape quality T, the geometric distance to the original mesh H, the differences in curvature C, and the surface area deviation A [6–8]. Using these metrics we devised a combined quality metric M, which maps all aspects to a single scalar-valued metric:

$$M = \alpha(1-T) + \beta H + \gamma C + \delta A, \quad \alpha,\beta,\gamma,\delta \in \mathbb{R}, \quad M \in [0,\infty). \tag{1}$$

Here α, β, γ, and δ denote the weighting factors which have to be determined with respect to the actual application of the considered mesh [1, 2]. Note that two exactly equal meshes yield $M = \alpha/2$, since in this case H, C, and A are equal to 0 and $T = 0.5$.

However, coarsening can lead to enhanced triangle quality, which subsequently results in $M < \alpha/2$.

RESULTS AND DISCUSSION

For coarsening the test geometries, we investigated different stop ratios in the range of $[0.004, 0.75]$. We computed the four different metrics T, H, C, and A for each coarsened mesh. As expected, our studies show that the values for H, C, and A vary up to an order of magnitude of 2 (e.g., $H = 0.00064$ to $C = 0.07377$). Since we wanted to attribute each geometric feature the same level of importance and to preserve various prominent geometric features (i.e., curvatures), we empirically chose the ratio of the weighting factors β, γ, and δ. Due to the fact that a poor quality of one single triangle in the coarse mesh heavily influences not only the volume mesh generation process, but also the subsequent numerical simulations, we had to ensure that the triangle shape metric T was of the same level of importance as the three geometric features. Therefore, we chose its weighting factor α such that the first term in Equation 1 is of the same order of magnitude as the sum of the other three terms. By considering all these demands, we found a suitable choice of absolute weighting factors as shown in Table 1. These factors vary for each geometry, because the difference of each of the four metrics T, H, C, and A between the original and coarse mesh depends on the number of removed triangles which is mesh specific. Additionally, our investigations show that by applying these absolute factors a coarsened mesh can be judged as *good*, if the condition $M < 0.4$ holds. Above this threshold either the triangle shape metric or the geometric feature metrics tend to become unreasonably high.

Model	α	β	γ	δ	M_{equal}	M_{max}
Bunny	0.34	11.5	1.15	0.92	0.17	13.91
Elephant	0.18	8.82	0.88	0.70	0.09	10.58

Table 1: Weighting factors and ranges of M in Equation 1 obtained in this study for the considered geometries. M_{equal} denotes the value for two exactly equal meshes and M_{max} the worst-case maximum.

CONCLUSION

The investigated algorithm together with the presented quality metric is the first step towards devising an automatic hull mesh coarsening work flow. Future work will focus on analyzing the domain-specific weighting factors and on devising an automatic method to compute those factors to ultimately guide a coarsening work flow via the combined scalar-valued quality metric.

ACKNOWLEDGMENT

The financial support by the Austrian Federal Ministry of Science, Research and Economy and the National Foundation for Research, Technology and Development is gratefully acknowledged as is the support by the TU Wien IP project *"Parallel 3D Mesh Generation for Bio-Micro- & Nanoelectromechanical Systems"*.

REFERENCES

[1] D.H. Pahr *et al.*, J. Mech. Behav. Biomed. **33**, 76-83, 2014.
[2] P. Manstetten *et al.*, Proc. of ICCS, 2017, submitted.
[3] S. H. Lo, Int. J. Numer. Meth. Eng. **21**, 1403-1426, 1985.
[4] P. L. George *et al.*, Int. J. Numer. Meth. Eng. **37**, 3605-3619, 1994.
[5] http://www.cgal.org
[6] L. Zhou *et al.*, Proc. of SPIE **4302**, 99-110, 2001.
[7] T.D. Gatzke *et al.*, Int. J. Shap. Model. **4302**, 99-110, 2001.
[8] P. Cignoni *et al.*, Comp. Graph. Forum **17**, 1-28, 2006.

AN EFFICIENT SIMULATION TECHNIQUE FOR THE EDDY CURRENT PROBLEM IN LAMINATED IRON CORES

Markus Schöbinger[a], Joachim Schöberl [a], Karl Hollaus [a]

[a]E101 - Institute of Analysis and Scientific Computing

INTRODUCTION

Laminated iron cores are an essential part of many electrical devices, for example transformers. Their property to be composed of a large number of thin iron laminates is essential to decrease the losses caused by eddy currents. From a numerical point of view this property poses a great challenge, since simulating the behavior of the iron core requires models incorporating each single laminate. In the classical finite element setting this causes the resulting equation system to become unfeasibly large. Therefore different methods have to be developed to calculate an approximated solution in a reasonable amount of time.

EXPERIMENTS/FUNDAMENTAL OF THE PROBLEM/EXAMINATIONS

The main topic of interest is the eddy current problem, which follows from the Maxwell equations. For the quasi-static magnetic field the weak formulation is given as: Find the magnetic vector potential $\vec{A}$ so that

$$\int_\Omega \mu^{-1}(\vec{A})\,\mathrm{rot}\vec{A}\,\mathrm{rot}\vec{v}\,d\Omega + \frac{\partial}{\partial t}\int_\Omega \sigma\vec{A}\vec{v}\,d\Omega = \int_\Omega \vec{J}\vec{v}\,d\Omega + \int_{\Gamma(\Omega)} \vec{K}\vec{v}\,d\Gamma$$

for every suitable test function $\vec{v}$ where μ is the magnetic permeability, σ the electric conductivity and the right hand side variables $\vec{J}$ and $\vec{K}$ allow the prescription of current densities in the volume and on the boundary of the domain, respectively.

For ease of presentation a simplified setting will be considered where μ is assumed to be independent of $\vec{A}$ (resulting in a linear equation) and the time harmonic solution is calculated, which allows to eliminate the time dependency by using complex numbers. Furthermore only a two dimensional cross section is considered and the problem is assumed to be independent of the third dimension. Prescribing only the boundary current, this leads to the two dimensional equation

$$\int_\Omega \mu^{-1}(\vec{A})\,\mathrm{rot}\vec{A}\,\mathrm{rot}\vec{v}\,d\Omega + i\omega\int_\Omega \sigma\vec{A}\vec{v}\,d\Omega = \int_{\Gamma(\Omega)} \vec{K}\vec{v}\,d\Gamma \tag{1}$$

with the angular frequency ω and the imaginary unit i.

Figure 1 shows the solution in the iron domain of an academic example featuring only ten laminates. One can observe, that the solutions in each laminate admit little variance compared to each other. This encourages the idea that it might be sufficient to calculate the behavior of the solution in a single laminate and then propagate this

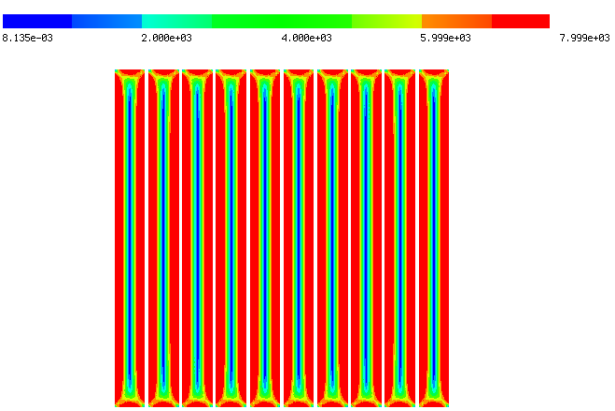

Figure 1: Absolute value of the solution in iron

result accordingly. These so called cell problems
give rise to many classical homogenization methods [1].

Here a slightly different ansatz will be used. The idea is to write the solution as a superposition of a mean value with local so called micro-shape functions to account for the behavior in each laminate. In the simplest form the ansatz

$$\vec{A} = \vec{A_0} + \varphi \begin{pmatrix} 0 \\ A_1 \end{pmatrix} + \nabla(\varphi w) \tag{2}$$

is used where the functions $\vec{A_0}$, A_1 and w are calculated on a much cheaper mesh which treats the iron core as a bulk. φ is the micro-shape function, which in this case is chosen to be a piecewise linear spline on each laminate. The approximation can be improved by adding additional micro-shape functions of higher order to (2) in a similar fashion. The ansatz (2) is then used in (1) together with averaging methods for the resulting coefficients to generate the new set of equations, as shown for example in [2].

RESULTS AND DISCUSSION

The presented method allows for the calculation of efficient approximation for the eddy current problem in laminated materials. In an example with one hundred laminates the meshes shown in figure 2 were used for calculations and for finding a reference solution to estimate the error. While the reference mesh has about 200 times more elements, the difference between the solutions measured in the L^2 norm is only 0.3%

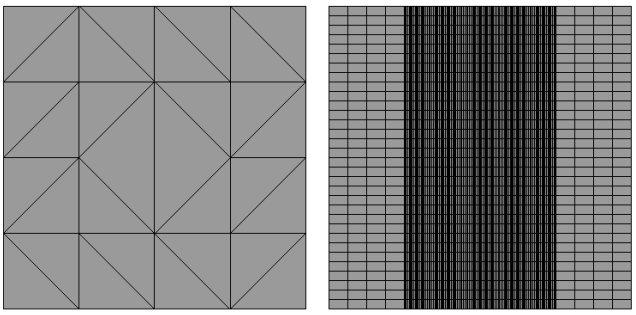

Figure 2: Cheap calculation mesh and reference mesh for 100 laminates

CONCLUSION

Simulating laminated materials using micro-shape functions has proven to be an efficient method for the linear eddy current problem. Future research will deal with generalizing this approach to the nonlinear case in the time domain.

ACKNOWLEDGMENT

This work was supported by the Austrian Science Fund (FWF) under Project P 27028-N15.

REFERENCES

[1] A. Bensoussan, J. Lions, and G. Papanicolaou, *Asymptotic Analysis for Periodic Structures*. North-Holland, 2011.

[2] K. Hollaus and J. Schöberl, "Homogenization of the eddy current problem in 2d," ser. 14th Int. IGTE Symp., Graz, Austria, Sep. 2010, pp. 154–159.

A COMPLEXITY DICHOTOMY FOR SATISFIABILITY OVER PARTIAL ORDERS

Michael Kompatscher[a], Trung Van Pham [a,b]

[a]E185 - Institute of Computer Languages, TU Wien
[b]Institute of Mathematics, Hanoi, Vietnam

INTRODUCTION

Reasoning about temporal data is a common task in various areas of computer science, including Artificial Intelligence, Computational Linguistics and Operations Research. A typical computational problem in this context is Scheduling: Given a set of events and a set of temporal constraints on them, is there a time assignment of the events that satisfies all the constraints?
Usually time in such problems is modeled by linear orders. But for instance to model distributed and parallel computing, partial orders are more suitable, see Lamport [3]. We classify the computational complexity of all scheduling problems, where time is modeled by a partial order. Depending on the type of constraints, we show that such a problem is always either in P or NP-complete [4].

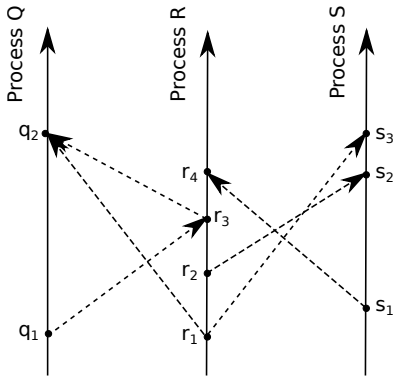

Figure 1: An example of parallel processing modeled as partial order; arrows denote the order/precedence relation

THE PROBLEMS

Let Φ be a finite set of quantifier-free formulas over the relational symbol $\leq$. The formulas in Φ determine the types of constraints that we allow as input. Then we define Poset-SAT(Φ) as the following computational problem:

Poset-SAT(Φ):
INPUT: Variables $\{x_1,\ldots,x_n\}$ and a set of formulas $\phi_i(x_{i_1},\ldots,x_{i_k})$, where $\phi_i \in \Phi$;
QUESTION: Is there a partial order $(A;\leq)$ such that the set of formulas is satisfied in A, i.e., are there $a_1,\ldots,a_n \in A$ such that $\phi_i(a_{i_1},\ldots,a_{i_k})$ holds in A for all ϕ_i?

Our aim is to give a complete classification of the complexity of such problems. It is easy to see that Poset-SAT(Φ) can be always solved in nondeterministic polynomial time. We show that an analogue to Schafer's famous dichotomy for Boolean satisfiability problems [5] holds: Poset-SAT(Φ) can be solved either in P or is NP-complete, depending on the allowed constraints Φ.

PROOF STRATEGY

In proving our result, the main problem is not to identify the complexity for single instances of Φ, but to determine *all* possible sources of NP-completeness or tractability. To do so we use a variety of methods from complexity theory, universal algebra and model theory that were developed by Bodirsky and Pinsker to tackle the analogous problem for graphs [2].

Every Poset-SAT problem can be restated using the *random partial order* $(P;\leq)$, a well-known structure in model theory that can be defined as the unique countable partial order that is homogeneous and contains an isomorphic copy of every finite partial order. By this universality property, the question if there is a solution to an input formula of Poset-SAT(Φ) is equivalent to the question if there are

elements of $(P;\leq)$ satisfying this formula.

Hence our strategy is to investigate the random partial order $(P;\leq)$ respectively the structure P_Φ defined on P by the formulas in Φ. The nice model-theoretical properties of the random partial order allow us to do so by studying the *polymorphism clone* of P_Φ instead, i.e. the set of all functions from P^n to P that preserve all relations of P_Φ; in fact the complexity of Poset-SAT(Φ) only depends on this polymorphism clone. Hence the classification of Poset-SAT(Φ) problems translates directly to the investigation of polymorphism clones of structures P_Φ; the smaller the clone, the harder the induced problem. The so called *method of canonical functions* that relies on Ramsey theoretic properties of $(P;\leq)$ helps us to perform this analysis and draw the line between small NP-complete clones and big clones of tractable structures.

RESULTS AND DISCUSSION

Every problem of the form Poset-SAT(Φ) can be either solved in polynomial time or is NP-complete. We can further precisely describe the border between problems in P and NP-c: Either a relation from a given finite list (Low, Betw, Cycl, Sept...) is primitive positive definable in P_Φ and the problem is NP-complete, or the problem is in P.

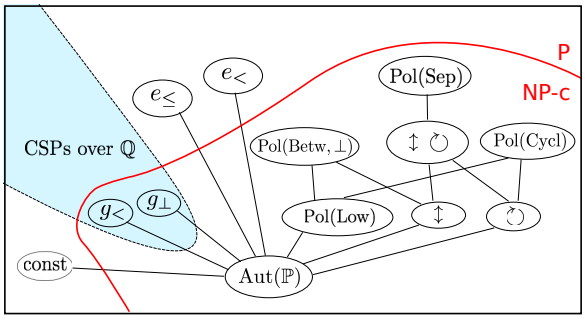

Figure 2: Dichotomy on polymorphism clones

This dichotomy corresponds to an algebraic dichotomy: Either the polymorphism clone of P_Φ contains a function that satisfies some non-trivial equation, and Poset-SAT(Φ) is in P, or the problem is NP-complete [4].

CONCLUSION

In studying constraint satisfaction problems over infinite structures, on one hand we can make statements about computation problems that appear naturally, in this case scheduling problems in distributed computing. On the other hand, the methods that we use to prove such results give us new deep insights about model-theoretic and algebraic properties of the underlying structures, in this case the random partial order and the structures which are first-order definable on it. This exchange between basic research and applications forms new connections between complexity theory, universal algebra and Ramsey theory and is subject of current and ongoing research [1].

REFERENCES

[1] Barto L. Kompatscher M., Olšak M, Pinsker M., Pham T. V.: *Equations in oligomorphic clones and the Constraint Satisfaction Problem for ω-categorical structures*. Preprint arXiv:1612.07551, 2017.

[2] Bodirsky M., Pinsker M.: *Schaefer's theorem for graphs*. Journal of the ACM 62(3), p. 19ff, 2015.

[3] Lamport, L.: *Time, clocks, and the ordering of events in distributed systems*. Communications of the ACM, 21(7), p. 558-565, 1978.

[4] Kompatscher M., Pham T. V.: *A complexity dichotomy for poset constraint satisfaction*. accepted for STOCS' 17, Preprint arXiv:1603.00082

[5] Schaefer, T. J.: *The complexity of satisfiability problems.* Proceedings of the tenth annual ACM symposium on Theory of computing. ACM, 1978.

SOLVING RESONANCE PROBLEMS ON UNBOUNDED DOMAINS USING FINITE ELEMENTS AND COMPLEX SCALING

Lothar Nannen[a], Markus Wess[a]

[a]E101 - Institute for Analysis and Scientific Computing at TU Wien

INTRODUCTION

A variety of waves, for example acoustic, elastic or electromagnetic waves can be modelled using partial differential equations. In general wave phenomena can be considered non-local, in a sense, that a local perturbation can lead to changes in distant regions. Therefore, a genuinely non-local problem cannot straightaway be reduced to a bounded one without altering it fundamentally. The Finite Element Method is a popular choice for solving Partial Differential Equations numerically. However, since this method bases on the decomposition of the computational domain into finitely many bounded subdomains it is not right away suitable for solving non-local problems on unbounded domains. To overcome these difficulties, we use the method of complex scaling or perfectly matched layers [1], [2]. This method introduces an artificial non-reflecting damping layer which is cut-off after a sufficiently large thickness. In this work we are concerned with using some varieties of this method to solve resonance problems.

PROBLEM SETTING

As a model problem we consider the Helmholtz equation on unbounded domains. The real part of an eigenfunction of the associated resonance problem can be interpreted as the amplitude of a time-harmonic acoustic wave. If the domain in question is not the whole space suitable boundary conditions have to be imposed. To ensure physical meaningful resonances an additional radiation condition, the pole condition is stated.

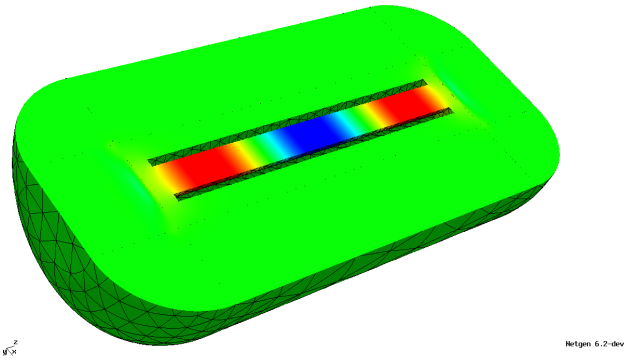

Figure 1: Cross section of an approximated resonance function of a pipe shaped domain using a cylindrical scaling

COMPLEX SCALING

To overcome the problem of the given infinite domain and realize the aforementioned radiation condition, we introduce complex scaling. This technique can be described in three steps. At first the initial domain is split up into a bounded *interior* and an unbounded *exterior* domain, such that all inhomogeneities of the geometry and (if given) the potential are located in the interior domain. Next a transformation of the initial equation in the exterior domain is introduced, such that the solution of the transformed equation coincides with the sought for solution in the interior domain. Moreover, only solutions that satisfy the radiation condition are exponentially decreasing in the exterior domain. Because of this decrease, the error arising from truncating the exterior domain in the last step can be shown to be small for a sufficiently thick exterior domain.

Since the truncated complex scaled equation is now stated on a bounded domain, the finite element

method can be applied for discretization leading to a finite dimensional generalized eigenvalue problem, which can be solved using standard numerical methods. This is done using the high order finite element library Netgen/NGSolve.

RESULTS AND DISCUSSION

Theoretical analysis of the method shows, that the complex scaling has several effects on the spectrum of the initial problem including the appearance of an essential spectrum and spurious resonances. Numerical experiments show a heavy dependence of the essential spectrum and the spurious resonances on the numerous parameters of the complex scaling such as the shape of the scaling layer and the damping profile. Moreover the theoretical convergence rates [4], [5] are only achieved for sufficiently small mesh sizes $h \leq h_0$, where h_0 also depends on the parameters of the complex scaling and the resonance itself. In our work discuss these dependencies and how they can be reduced using frequency dependent complex scalings [3].

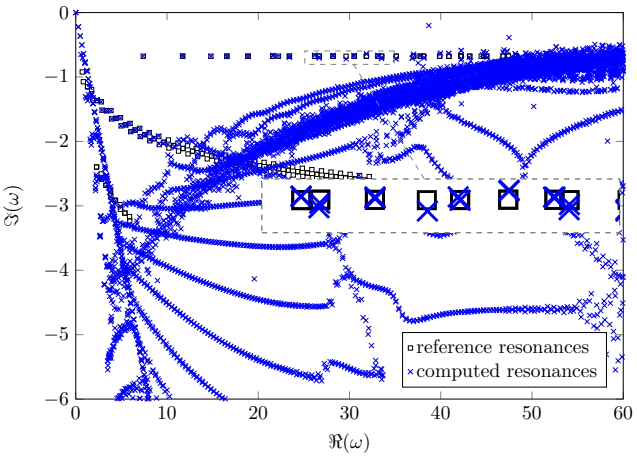

Figure 2: Spectrum of the discretized problem including correct resonances, the essential spectrum and spurious resonances

ACKNOWLEDGEMENT

The authors acknowledge support from the Austrian Science Fund (FWF): P26252.

REFERENCES

[1] Kim, S. and Pasciak, J. E., The computation of resonances in open systems using a perfectly matched layer, *Math. Comp.*, **78** (2009), pp. 1375–1398.

[2] Kim, S. and Pasciak, J. E., Analysis of the spectrum of a Cartesian perfectly matched layer (PML) approximation to acoustic scattering problems *J. Math. Anal. Appl* **361** (2010), pp. 420–430.

[3] Nannen, L. and Wess M., Spurious modes of the complex scaled Helmholtz Equation, *ASC Report, TU Wien*, **15** (2016).

[4] Karma, O., Approximation in eigenvalue problems for holomorphic Fredholm operator functions. I, *Numer. Funct. Anal. Optim.*, **17** (1996), pp. 365–387.

[5] Karma, O., Approximation in eigenvalue problems for holomorphic Fredholm operator functions. II, *Numer. Funct. Anal. Optim.*, **17** (1996), pp. 389–408.

EVALUATION FRAMEWORK FOR IMAGE RECONSTRUCTION IN ELECTRICAL IMPEDANCE TOMOGRAPHY

Florian Thürk, Eugenijus Kaniusas

E354- Institute of Electrodynamics, Microwave and Circuit Engineering

INTRODUCTION

The life of patients undergoing surgery under full anesthesia or recovering in intensive care units depends on mechanical ventilation of the lungs. While this procedure is vital in clinical routine, artificial and unphysiological pressure conditions within the lungs can damage the lungs and cause severe complications. The detection of related injuries currently relies mostly on the associated changes of hemodynamic parameters, like blood pressure or oxygen saturation, which respond only indirectly to adverse pulmonary events. In order to accurately determine the state of the lungs, high resolution imaging techniques like computed tomography (CT) are typically utilized. Sophisticated medical imaging, however, can only be applied with the drawback of radiation exposure and laborious transportation effort.

In this context, a novel imaging modality, electrical impedance tomography (EIT), has the potential for radiation-free lung function monitoring directly at the bedside. Small currents are injected and the resulting voltages are measured via multiple surface electrodes (usually 16 or 32) attached around the thorax. From these measurements, 2D-images can be reconstructed, visualizing the impedance distribution inside the thorax at high temporal resolution (about 50Hz). The mathematical formulation behind this reconstruction is highly ill-posed, resulting in virtually infinite solutions. In order to identify reasonable impedance distributions, forward solvers (e.g., finite element models) and regularization are applied. Therefore, the resulting images vary based on prior assumptions and the specific algorithms, limiting the objective diagnostic power of EIT.

In this work, a framework is described, which allows for a thorough validation of algorithms based on well-established parameters which can be derived from (i) simulations, (ii) image analysis and (iii) comparison to gold standard modalities. The purpose of this evaluation is to demonstrate the high influence of reconstruction settings on EIT-images and their derived clinical parameters.

METHOD

As forward model, a finite element model (FEM) was created based on piglet CT data, freely available within the open source framework EIDORS [1]. In order to identify the influence of thorax shape on the reconstruction, the original contours were filtered by exclusion of Fourier descriptors (FD), which represent higher spatial frequencies [2]. In total, 6 FEMs were created including all, 15, 5, 3 and 1 FDs and, in addition, an independent model based on a circular shape. Based on these FEMs, GREIT [3] reconstruction matrices (**RM**) were created, see Fig.1.A.

In GREIT, the EIT problem is linearized based on figures of merit that describe the performance of reconstruction after simulated training targets are inserted into FEM, i.e., the forward model. In this work, we generated **RM**s with different training target size *ts*, weighting radius *rw* (i.e., point spread function), and noise figure *nf* (describing the noise amplification of the reconstruction). In addition, lung and heart regions inside FEMs were weighted with different conductivity assumptions $w_{1\text{-}4}$. This results in a set of 9600 different **RM**s (Fig. 1.B). For FEM generation and the definition of forward and inverse solvers, NETGEN and EIDORS framework was used.

Simulation: **RM**s were first described using established figures of merits derived from FEM simulations, i.e., amplitude response *AR*, position error *PE*, resolution *Res*, shape deformation *SD* and ringing *R* [1] (Fig. 2.A).

Image analysis: A single voltage measurement was then reconstructed with all **RM**s and physiological parameters, i.e., center of ventilation *CoV*, right-left ratio *RL*, and global inhomogeneity index *GI*, were calculated (Fig. 2.B).

Gold standard validation: Using CT images, a comparison of these physiological parameters, e.g., root mean square error *RMSE*, can then be performed for each **RM** (Fig. 2.C).

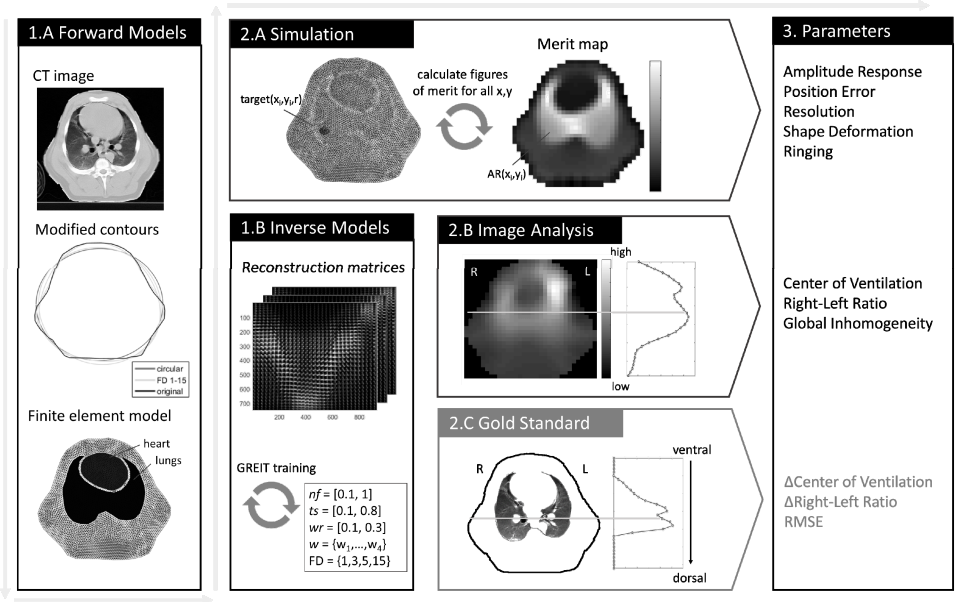

Figure 1 Framework for thorough evaluation of the influence of different reconstruction settings in EIT.

RESULTS AND DISCUSSION

For all output parameters, a strong variability between different **RM**s could be observed. In simulation, values for *AR, PE, Res, SD* and *R* ranged from 0.47 to 2.12; 0.02 to 0.14; 0.21 to 0.50; 0.06 to 0.38; and 0.07 to 0.96. Similar variations were observed during image analysis in *CoV, RL* and *GI* with ranges of 33.8% to 55.2%; 0.29 to 0.70; and 0.77 to 4.72.

CONCLUSION

In this work, a novel framework was proposed, which allows a thorough evaluation of EIT reconstruction models, ranging from simulations to image analysis and to final validation. Even though a first evaluation showed a significant influence of reconstruction settings, further evaluation is crucial to describe interrelations and reasonable ranges of output parameters in more detail. In order to provide guidelines for specific EIT applications (e.g., lung monitoring), the validation against a gold standard method will be essential.

REFERENCES

[1] A. Adler and W. R. B. Lionheart, "Uses and abuses of EIDORS: an extensible software base for EIT.," *Physiol. Meas.*, vol. 27, no. 5, pp. S25–S42, 2006.

[2] B. Grychtol, W. R. B. Lionheart, M. Bodenstein, G. K. Wolf, and A. Adler, "Impact of model shape mismatch on reconstruction quality in electrical impedance tomography," *IEEE Trans. Med. Imaging*, vol. 31, no. 9, pp. 1754–1760, 2012.

[3] A. Adler, J. H. Arnold, R. Bayford, et.al., "GREIT: a unified approach to 2D linear EIT reconstruction of lung images.," *Physiol. Meas.*, vol. 30, no. 6, pp. S35–S55, 2009.

NETWORK ANALYSIS ON THE AUSTRIAN MEDIA CORPUS

Gabriel Grill[a], Julia Neidhardt [a], Hannes Werthner [a]

[a] E188 - Institute of Software Technology and Interactive Systems

INTRODUCTION

The role and influence of media in society has been a much debated topic in the last several months, in particular with respect to populist political movements. On the one hand they supposedly benefit from sensational media reporting [1], while on the other hand claiming that media outlets report strongly biased against them, a technique for instance implemented by the Pegida movement [2]. In order to contribute to the study this kind of complex reciprocal interplay, this work aims to develop a theoretical framework that enables scholars to examine media reporting using network-based methods. Thereby revealing central entities, topics and statistical connections between extracted entities of interest in news articles. The comparison of different media outlets based on these results may yield insights into the study of media bias [3]. This work may encourage creators of media to reflect on their reporting and the public to be more informed on underlying systematics of news coverage. The framework is evaluated based on a case study focusing on last year's Austrian presidential election. This is the first research effort applying a network-based approach onto the Austrian Media Corpus [4], a complete and unique collection of over 33 million articles encompassing the last three decades of Austrian media coverage. The project is conducted in cooperation between the Electronic Commerce Group, Institute of Software Technology and Interactive Systems, TU Wien and the Austrian Centre for Digital Humanities, Austrian Academy of Sciences. Work on semantic annotation of entities and relations as well as network analysis is carried out in an internship at the National Institute of Informatics in Tokyo, Japan.

FUNDAMENTAL OF THE PROBLEM

This work specifically focuses on a case study encompassing reporting on the Austrian presidential elections in 2016. We expect insights related to the following research questions:

- Are we able to detect central entities, topics or key words in the extracted networks?
- What can we infer about structural properties of the networks and are we able to identify communities?
- How can we capture differences in reporting in respect to variant news publishers and time spans?

METHODOLOGY

In order to generate, analyse and visualize different types of networks, methods from the fields Natural Language Processing, Network Analysis and Data Mining are applied. First, an expressive subset of stemmed nouns, verbs and adjectives as well as co-occurrence-based relations between them are extracted from news articles. All words are stored with corresponding metadata. This includes a reference to the container sentence, paragraph and article as well as information on the article such as the

publishing date, news outlet and associated department. Nouns are also assigned different class labels (e.g. person, location) using a Named Entity Recognition framework. Networks are made of nodes representing selected nouns, referred to as entities in this work, and edges modelling relationships between them. Co-occurrence Networks consist of edges representing co-occurrence of entities in a sentence, paragraph or document. Emotion Networks contain up to eight types of edges representing either one of seven emotions or neutrality. Emotion labels are assigned based on the amount of words, included in an emotions dictionary [5], associated with a co-occurrence relation between two entities. Sentiment Networks consist of edges between co-occurring entities and can either indicate a positive, negative or neutral valence. Sentiment labels are either assigned based on the strength of the valence and amount of words associated with a co-occurrence, or the valence of a verb between a subject and an object in a sentence [6]. Valence is determined based on a dictionary [7]. Social Networks are Sentiment Networks comprised only of entities classified as person or organisation.

EXPECTED RESULTS

The expected results of this work belong to two different levels. By studying network models and measures, we gain insights to develop a theoretical framework for different types of co-occurrence relationships. By conducting empirical analyses, we obtain concrete statements about the Austrian presidential election in 2016. Concrete results may open up discussion in the public or other fields. Results will be presented at the Vienna young Scientific Symposium in more detail.

CONCLUSION

In this work, a network-based approach is applied on the Austrian Media Corpus. This will help to determine whether such an approach is indeed well suited for the study of Austrian news reporting and whether statistical connections can be revealed that otherwise would not be easy to detect. The case study on the Austrian presidential election in 2016 will provide insights whether there are differences in reporting across news publishers, time spans and ballots. In a next step the classification of extracted entities and relations will be enriched using available semantic databases.

REFERENCES

[1] Robert G. Picard, “Are Journalists Reporting - Or Publicising - Populism?”, European Journalism Observatory - EJO, 28-Oct-2016.

[2] K. Holt and A. Haller, “The Populist Communication Paradox of PEGDIA: Between ‘Lying Press‘ and Journalistic Sources”, 66th annual ICA conference “Communicating with power”. Fukuoka, Japan, 9-13 june. Preconference: Populism in, by, and Against the Media, 2016.

[3] W. L. Bennett, “News: The Politics of Illusion”, Tenth Edition. University of Chicago Press, 2016.

[4] M. Durco, K. Moerth, H. Pirker, and J. Ransmayr, “Austrian Media Corpus 2.0”, 2014.

[5] R. Klinger, S. S. Suliya, and N. Reiter, “Automatic Emotion Detection for Quantitative Literary Studies - A case study based on Franz Kafkas ‘Das Schloss‘ and ‘Amerika‘ ”, Digital Humanities 2016: Conference Abstracts, Krakw, Poland, 2016, pp. 826-828.

[6] S. Sudhahar, G. A. Veltri, and N. Cristianini, “Automated analysis of the US presidential elections using Big Data and network analysis”, Big Data Soc., vol. 2, no. 1, Feb. 2015.

[7] Remus, Robert, Uwe Quasthoff, and Gerhard Heyer. “SentiWS-A Publicly Available German-language Resource for Sentiment Analysis”, LREC. 2010.

MEASURING EARTH ROTATION COMBINING RINGLASER AND VLBI

Matthias Schartner[a], Johannes Böhm[a], Sigrid Böhm[a]

[a]E120 - Department of Geodesy and Geoinformation

INTRODUCTION

Precise knowledge of Earth orientation parameters (EOP) is indispensable for any kind of positioning and navigation on Earth and in space. Errors as large as one milliarcsecond cause positioning errors on the Earth surface of three centimetres and kilometres at distances like those to Mars when navigating spacecrafts.

The orientation of the Earth in space is usually described by five EOP which describe the deviation from a uniform rotation in 24 hours and the variations of the rotation axis with respect to Earth (polar motion) and space (nutation). It is necessary to regularly observe these variations, which are caused by different excitations and occur at different time scales from sub-diurnal to years.

STATUS QUO - VLBI

Very Long Baseline Interferometry (VLBI) is the only technique that can estimate the full set of five EOP. Normally, these parameters are measured with daily resolution and models are used to describe the diurnal and sub-diurnal variations, mostly caused by ocean tides and luni-solar torques. Many studies, however, detected deficiencies in these models [1] which need further improvement.

In geodetic VLBI, globally distributed radio telescopes observe the radiation from quasars billions of light years away. It can be assumed that they are fixed points on the sky and that the radiation arrives in plane wavefronts, thus being observed by one telescope earlier than by the other one. This difference in arrival time is the primary observable in geodetic VLBI.

Figure 1: Station Wettzell (Germany) with the new twin radio telescope

Since the telescopes observe at data rates like Gbits/sec, the huge amount of data has to be saved on hard disks which are then shipped to one common location where the signals are correlated. Usually these VLBI observations last 24 hours and are carried out twice or three times a week.

These observations can then be used for the determination of a variety of different parameters, such as the realisation of terrestrial and celectial reference frames and for the estimation of EOP.

IMPROVEMENTS USING RINGLASER

Ringlasers represent an elegant and alternative measurement technique. They can measure Earth rotation in an absolute sense, independently of an external reference frame like quasars used by VLBI. However, the demands on such instruments are extremely high and cannot be met by existing com-

mercial devices [2].

Up to now, there is only one ringlaser with sufficient precision, located in Wettzell, Germany. The ringlaser is sensitive enough to measure changes in Earth rotation. Actually, ringlasers measure rotations via the Sagnac effect, which means that two identical light beams travel around a closed ring on exactly the same path in opposite directions. If the ringlaser rotates, the path length is changing causing a phase shift. This phase shift is then translated into a frequency difference, the so-called Sagnac frequency [2].

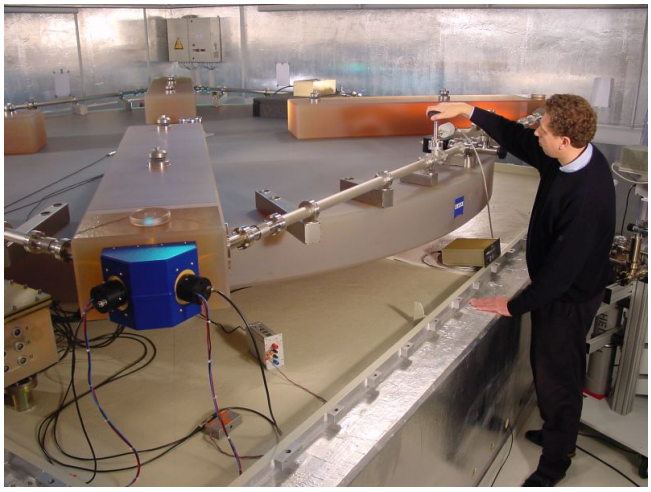

Figure 2: Ringlaser at Wettzell (Germany)

If the ringlaser is connected to the Earth, changes in the Earth rotation can be measured. The main advantage of ringlasers compared to VLBI is, that they measure Earth rotation directly in real-time with a high sampling rate. Therefore, they are sensitive to the sub-diurnal frequency changes. To get the complete information about orientation of the Earth, at least three different ringlasers at different positions on the Earth are needed.

COMBINATION

At the moment there is only one ringlaser for measuring Earth rotation. This means that it is not possible to estimate the whole orientation of the Earth, however, it is possible to combine ringlaser data and VLBI observations to improve the solution, mostly for the sub-diurnal variations. At the moment the accuracy of EOP from ringlaser data is one order of magnitude worse than the results from VLBI, but it is assumed that the accuracy gets better with further investigations as proposed in this project.

To perform a combination, great care must be taken that the same models are applied and all additional measurement influences are corrected correctly.

CONCLUSION

We plan to combine observations from VLBI and ringlaser to improve the quality of the estimated Earth orientation parameters. We have access to improved ringlaser data from Wettzell, so that we are optimistic to enhance the present approach of Earth rotation determination.

The main advantage of using ringlaser data is the they are very sensitive to sub-diurnal changes and they provide an independent measurement opportunity.

REFERENCES

[1] Combining VLBI and ring laser observations for determination of high frequency Earth rotation variation, Journal of Geodynamics, Vol. 62, pp. 69-73.

[2] The Large Ring Laser G for Continuous Earth Rotation Monitoring, Pure and Applied Geophysics, Vol. 8(166), pp. 1485-1498.

STABILITY AND ELASTICITY OF THE MoN–TaN SYSTEM: AN ATOMISTIC INSIGHT

Nikola Koutná[a,d], David Holec[b], Martin Friák[c, d], Mojmír Šob[c, d, e], and Paul H. Mayrhofer [a]

[a] E308 - Institute of Materials Science and Technology, TU Wien
[b] Department of Physical Metallurgy and Materials Testing, Montanuniversität Leoben, Austria
[c] Central European Institute of Technology (CEITEC), Masaryk University, Brno, Czech Republic
[d] Institute of Physics of Materials, Czech Academy of Sciences, Brno, Czech Republic
[e] Department of Chemistry, Faculty of Science, Masaryk University, Brno, Czech Republic

Transition metal nitrides (TMNs) represent a prominent class of materials possessing numerous outstanding physical properties, such as excellent chemical and thermal stability, incompressibility and strength, high melting point and good thermal and electronic conductivity or superconductivity. Therefore, considerable efforts have been devoted to investigate the possibility of enhancing performance of exceptional TMNs by designing ternary or multinary TMN systems. MoN and TaN have attracted significant attention owing to their beneficial properties in functional thin film applications spanning from electronics to protective coatings. Up to date, however, there has been only one first-principles study [1] on the MoN–TaN ternary system.

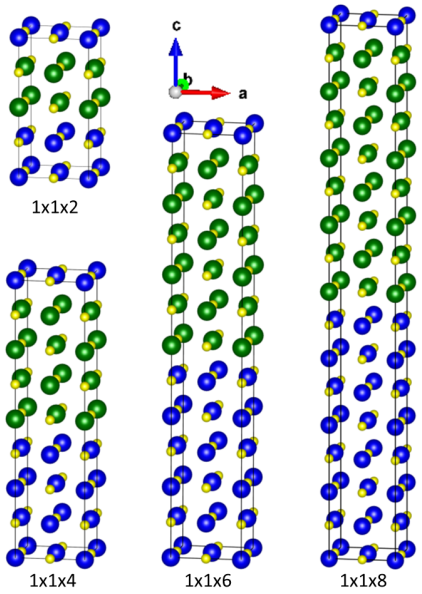

Figure 1: Computational models for MoN/TaN superlattices.

To gain a deep insight into chemical, mechanical, and dynamical stability of MoN–TaN, it is desirable to employ density functional theory (DFT), as a state-of-the-art method of quantum-mechanical modelling. Thanks to its high reliability, DFT has become a powerful tool of computational materials science and an important counterpart to experiment. In the present study, the $Mo_{1-x}Ta_xN$ solid solutions are assumed to adopt the cubic structure with NaCl prototype ($Fm\bar{3}m$, #225, B1-type), often referred to as rocksalt (rs) structure, and the hexagonal structures with NiAs ($P6_3/mmc$, #194), WC ($P\bar{6}m2$, #187), and TaN ($P\bar{6}2m$, #189) prototypes, respectively. Besides, we consider cubic-like MoN/TaN superlattices, as another materials design concept (Fig. 1).

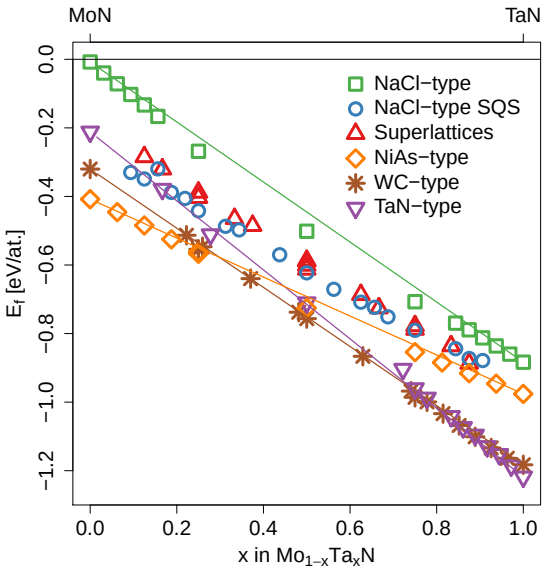

Figure 2: Energy of formation, E_f, of various $Mo_{1-x}Ta_xN$ systems as a function of Ta content.

Our calculations (Fig. 2) clearly demonstrate that hexagonal-type $Mo_{1-x}Ta_xN$ solid solutions based on low-energy modifications of MoN and TaN are the most stable over the whole compositional

range. Despite being metastable, the disordered cubic polymorphs are energetically significantly preferred over their ordered counterparts. An in-depth analysis of atomic environments in terms of bond lengths and angles (Fig. 3) reveals that the chemical disorder results in (partially) broken symmetry, i.e., the disordered cubic structure relaxes towards a hexagonal NiAs-type phase, the ground state of MoN.

Surprisingly, superlattice architecture is also clearly favored over the ordered cubic solid solution. We show that the bi-axial coherency stresses in superlattices break the cubic symmetry beyond simple tetragonal distortions and lead to a new tetragonal ζ-phases (P4/nmm, #129) exhibiting a lower formation energy than the symmetry-stabilized cubic structures of MoN and TaN. Unlike the cubic TaN, the ζ-TaN is predicted elastically and vibrationally stable, while the ζ-MoN is stabilized only by the superlattice structure.

To analyse compositional trends in the elastic response of various $Mo_{1-x}Ta_xN$ systems, we establish their mechanical stability and find the closest high-symmetry approximants of the elastic tensors. The disordered cubic and all the hexagonal systems are mechanically stable (though the TaN-type MoN is nearly unstable); on the contrary, the ordered cubic systems and superlattices are stabilized only above some critical Ta content of $\sim 25\%$ and $\sim 50\%$, respectively. The estimated polycrystalline elastic moduli shown in Fig. 4 suggest than the hexagonal NiAs- and WC-phases of $Mo_{1-x}Ta_xN$ are significantly harder that the other modifications. According to the Pugh's criterion and Poisson's ratio, the cubic polymorphs and the sublattices are predicted to be ductile. The trends in stability based on energetics and elasticity are corroborated by density of electronic states.

Finally, our systematic and in-depth study provides information on stable and metastable phases in quasi-binary MoN–TaN system, and as such can guide experimental search for functional thin films with complex chemistry and/or architecture.

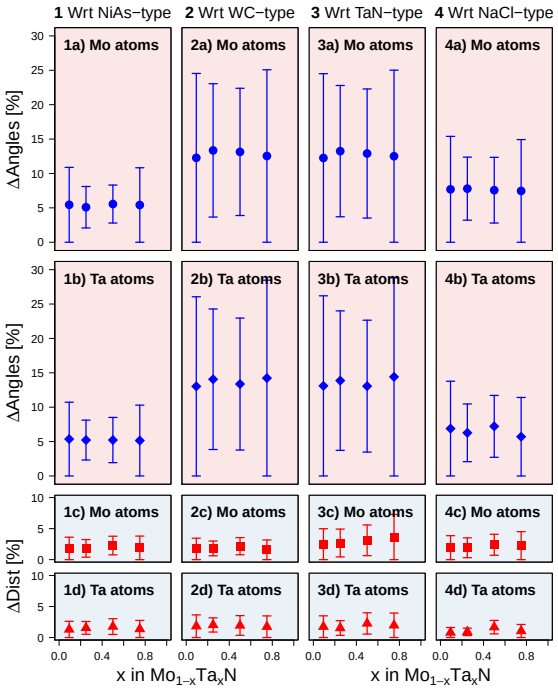

Figure 3: Analysis of local environments in disordered $Mo_{1-x}Ta_xN$ systems.

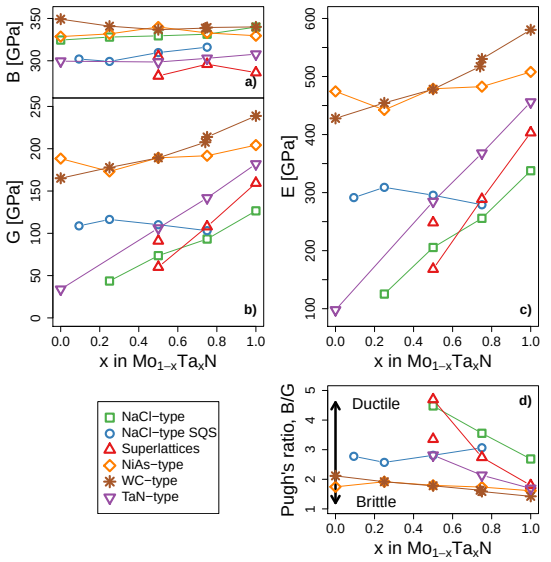

Figure 4: (a) Bulk modulus, (b) shear modulus, (c) Young's modulus, and (d) Pugh's ratio of various $Mo_{1-x}Ta_xN$ systems.

REFERENCES

[1] K. Bouamama, P. Djemia, and M. Benhamida, Journal of Physics: Conference Series **640** (2015) 012022.

EMOTION RECOGNITION USING EMPATICA E4 SMART WATCH

David Pollreisz and Nima TaheriNejad

Institute of Computer Technology, TU Wien, Austria

INTRODUCTION

For some individuals, e.g., autistic children, it is harder or not possible to express their feelings for reasons such as speech impairment or atypical facial expressions [1]. They are often misunderstood and which negatively affects their social lives. Therefore, help of an emotion recognition software could improve the quality of the interaction between their them and people in their social environment [2].

In this work, the smart watch E4 from Empatica was used to measure three different body signals: Heart rate, Skin temperature, and Skin conductance. We then tried to evaluate the correlation between these bio-signals and four different emotions; namely, Happiness, Sadness, Anger, and Pain. An important factor is that this watch is versatile and yet can be integrated to the daily life of these individuals without causing any impediment in their normal life.

DATA COLLECTION

For this work ten participants, all male and between 20 to 25 years old, took part in the experiment. They had to do watch six different short video clips and their reaction to them was measured in terms of their heart rate, skin temperature and skin conductivity. The experiment itself was divided into five phases. In each phase a different emotion of the following was measured: happiness, sadness, anger or pain. Each phase had the same procedure, the participant had to sit still for one minute so that his baseline could be measured. After the one minute was over the video started playing. At the end of each phase, the participant had to fill out a self-assessment form, about which emotion he just experienced and how strong he felt that emotions. Last, the participants got pinched in the arm to simulate pain.

DATA PROCESSING

In total 60 videos were shown to participants and ten samples of pain were solicited. Out of these data, 16 were marked with the emotion happy, 15 with sad, 8 with angry and 8 with pain. These marked data were analysed in two different ways: Continuous analysis and peaks statistics.

Continuous analysis This method analysed each second of the three measured signals. First, a mean value was calculated from ten seconds before the video started and then compared to each value after the start of the video. Every time the measured value was above the baseline a counter was increased. The same was done if the value was below the baseline but with a different counter. In this fashion, we could measure if the signal has shown more increase or decrease.

Peak Statistics Only the Electrodermal activity signals have rapid changes in it, therefore, only for thwsw signals the peaks were analysed. Although the Electrodermal activity values are in a range from 0.1μS to 12μS, all the peaks have the same absolute height. Therefore, the peaks were characterised in three different sizes, small peaks from 0.1μS up to 0.4μS, medium peaks started from 0.4μS to 0.8μS and big peaks started at 0.8μS. An example of these three different heights is shown in figure 1.

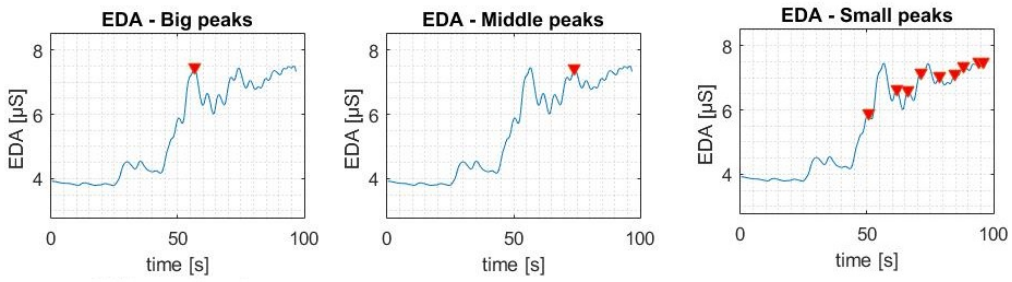

Figure 1: example of the peak detection

Result Table 1 summarizes the result of these analysis. With the information obtained through these analysis, an algorithm was created that could detect emotions out of these three bio-signals. The algorithm labeled 65% of the emotions with its first choice and 84% with the second choice right.

Table 1: Summary of the emotion of the data analysis

Emotion	Heart rate	Electrodermal activity	Electrodermal activity Peaks	Skin temp.
Happiness	slight increase	increase	small & few	slight decrease
Sadness	decrease	increase	small & many , big & few	slight decrease
Anger	slight decrease	increase	medium & some	slight decrease
Pain	no change	increase	medium & few	no change

References

[1] R. B. Grossman *et al.*, "Emotional facial and vocal expressions during story retelling by children and adolescents with high-functioning autism," *Journal of Speech, Language, and Hearing Research*, vol. 56, no. 3, pp. 1035–1044, 2013.

[2] R. Brewer *et al.*, "Can neurotypical individuals read autistic facial expressions? atypical production of emotional facial expressions in autism spectrum disorders," *Autism Research*, vol. 9, no. 2, pp. 262–271, 2016.

SELF-AWARENESS IN REMOTE HEALTH MONITORING SYSTEMS USING WEARABLE ELECTRONICS

Maximilian Götzinger[ab], Nima Taherinejad[b], Amir M. Rahmani[bc],
Pasi Liljeberg[a], Axel Jantsch[b], Hannu Tenhunen[a]

[a]Department of Information Technology, University of Turku, Finland
[b]E384 - Institute of Computer Technology at TU Wien
[c]Department of Computer Science, University of California Irvine, USA

INTRODUCTION

Predicting patient's health deterioration is nowadays done by healthcare professionals with the help of Early Warning Score (EWS) systems. Vital signs such as heart rate, blood pressure, oxygen saturation, and body temperature are monitored and abstracted to an EWS. To help people who are currently not in the hospital, portable devices that monitor the patient's vital signs, calculating the EWS, and alarm (if a health deterioration is predicted) are needed [1]. However, such an automated device needs to monitor vital signs and calculate the EWS accurately. Noisy or faulty data can lead to a wrong calculation of the EWS, which can result in false, or - even worse - in missing alarms. Therefore, we propose a modified EWS (MEWS) system that is inspired by the concept of self-awareness. It provides a data reliability validation to correct the sensory data in case of faulty readings.

EXPERIMENTS/FUNDAMENTAL OF THE PROBLEM/EXAMINATIONS

Data Reliability is a meta-data which consists of accuracy and precision of sensory data [2]. It provides additional knowledge and perspective to the data. For example, a body temperature sensor that is detached from the patient's body provides accurate and precise data, but it is not valid in the context of the EWS system. Therefore, a reliable system must not consider such invalid values. For examining the reliability of the input data, our system uses consistency, plausibility, and cross-validation.

Consistency: Are the changes in the value consistent? For example, in our study, changes in the body temperature are not very fast; a change of several degrees per minute is impossible [3]. Whereas, a sensor failure or its detachment of the patient's body can lead to these fast signal changes that are not valid and, therefore, they should not affect the EWS.

Plausibility: Is the absolute value itself plausible? For example, an oxygen saturation outside 0 to 100 is not plausible, and regardless of the cause, it should not be considered for score evaluation of the EWS. The same goes for extremely high or low temperature. For instance, a sensory value of 60 or 70°C is highly unlikely anywhere in Europe.(if not impossible)

Cross-validity: Could data be plausibly valid or not, given some other (complementary) data and given certain conditions? For example, a body temperature of few degrees is valid only if the subject does not have any other vital signs (and is practically deceased). Otherwise, it shows a discrepancy and the data cannot be trusted.

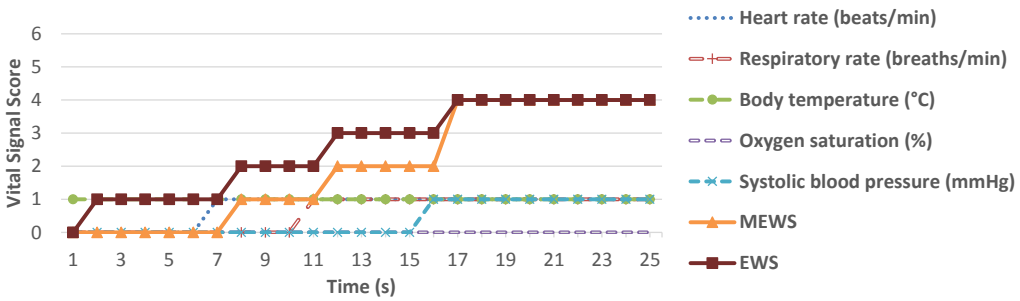

Figure 1: Calculation of the MEWS and EWS with the same data set. Body temperature is manually set to 32°*C* (score 1) and the other input signals are time-displaced (one after the other) to non-zero score values.

RESULTS

The data set that we applied is from experiments carried out by Azimi et al. [1], and contains records of heart rate, systolic blood pressure, respiratory rate, and oxygen saturation of a 35 years old healthy male subject. The measured temperature was replaced by a faulty temperature data to assess the system's behavior during a malfunction. Three different scenarios were simulated. For the evaluation of the first two validation steps, temperature data was introduced such that, firstly, was out of plausible range and, secondly, had an impossible slope (in the context of the body temperature). For the evaluation of the cross-validity, the body temperature was set to a non-perfect score but in a valid range without changes that are implausible. For the sake of brevity, only the cross-validation experiment is explained here in details. While the body temperature was set to 32°*C*, which implies a non-zero score, the rest of the vital signs were score 0. Time-displaced, these input signals also changed to non-zero score, one input after the other. As shown in Figure 1, the conventionally calculated EWS (without cross-validity check) is higher because of the invalid body temperature. Such a case, nonetheless, is physiologically not possible and hence, the EWS should not be considered. On the other hand, MEWS is changing only when more than 50% (3 out of 4) of the input variables reach a non-zero score (that is, at 17s).

CONCLUSION

We show that it is possible to check the reliability of the input data with our modular solution based on self-awareness. The proposed system allows processing both the data and their meta-data, such as the reliability assessment. The modularity of our system and its good match of the data processing flow from lower to higher abstraction levels showed to be a promising architecture for EWS or similar systems. In future, we want to expand the system by a fuzzy logic reliability classification that is not just binary anymore. Instead of the input data is just reliable or not, it will have a grade of reliability.

REFERENCES

[1] I. Azimi, A. Anzanpour, A. M. Rahmani, P. Liljeberg, and H. Tenhunen, "Self-aware early warning score system for iot-based personalized healthcare," in *Proceedings of international conference on IoT and big data technologies for healthCare*, 2016.

[2] A. J. N. TaheriNejad and D. Pollreisz, "Comprehensive observation and its role in self-awareness; an emotion recognition system example," in *the Federated Conference on Computer Science and Information Systems (FedCSIS)*, sep 2016.

[3] M. Pasquier, P.-A. Moix, D. Delay, and O. Hugli, "Cooling rate of 9.4 °C in an hour in an avalanche victim ," *Resuscitation*, vol. 93, pp. e17 – e18, 2015.

INTRA- AND EXTRA-CELLULAR STMULATION OF RETINAL BIPOLAR CELLS

Hassan Bassereh Moosaabadi[a], Paul Werginz[a,b], Frank Rattay[a]

[a]E101 - Institute of Analysis and Scientific Computing
[b]Department of Neurosurgery, Massachusetts General Hospital, Harvard Medical School, Boston, USA

INTRODUCTION

Retinal implants use an array of electrodes to generate visual perceptions in blind people that have lost their photoreceptor cells [1]. Some types of retinal implants aim for stimulating the bipolar cells (BC) electrically whereas in healthy conditions BCs receive inputs from photoreceptors. The aim of the Switch Board Marie Sklodowska Curie project, which I and other fourteen PhD students are involved in, is to explore general features of BCs and their roles in the neuronal network of the retina.

The coming optic light to the eye from the environment reaches the retina after passing from cornea, pupil, lens and vitreous body. The retina is considered to be a part of the brain where the vision processes start. It is so interesting for neuroscientist because interneurons in the brains are strongly connected, often more than thousands of connections for each neuron, but retina is less complicated. Retina is made of five layers, three neuronal and two synaptic layers. There are five kinds of neurons in the retina, photoreceptors, horizontal cells, bipolar cells, amacrine cells and ganglion cells. The coming light from the environment is absorbed by photoreceptors and after changing to electrical and chemical signals is transferred to the brain through ganglion cells as action potentials, after passing from horizontal, bipolar and amacrine cells [2].

RESULTS AND DISCUSSION

We used a reconstructed morphology of a retinal bipolar cell from real data and determined the exact places of compartments which contains sodium and calcium channels [3]. Figure 1 (left) shows different parts of the reconstructed cell, the big sphere represents the soma while small spheres show synaptic terminals contain calcium channels, thick lines show places of sodium channels, called initial segments, and regular lines shows compartments without ion channels. The neuron is modelled as electric circuit (Fig. 1, right) and by writing the current ohm's law for each compartment, we simulate the transmembrane voltages for every segment of the cell by solving a system of differential equations [3, 4]

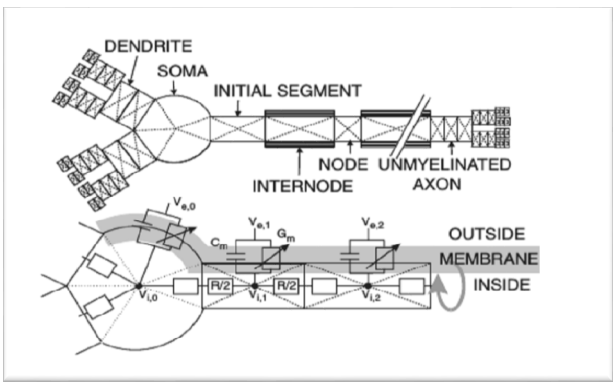

Figure 1: Left: Three dimensional reconstruction of the target cell. The upper part is the dendritic tree, followed by soma and axon with sections of high sodium channel density marked as thick lines. The axon has a branching part with synaptic endings that send signals to the ganglion cells. Right: A neuron is segmented in compartments differing in their functional role (top). Every compartment is modelled as a corresponding system of resistances and capacitance (bottom).

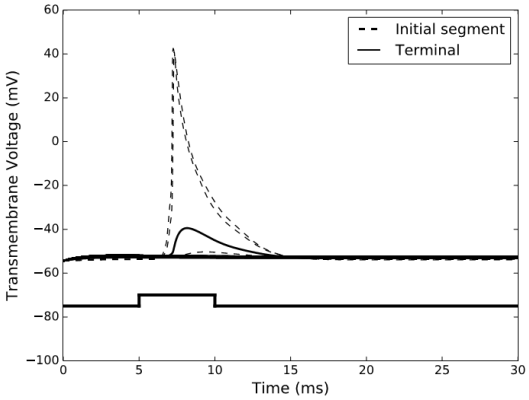

Figure 2: Transmembrane voltage versus time for selected compartments. The cell is stimulated intracellularly with a positive pulse of 0.2µA (bottom) while the electrode is in the soma. Compartments containing sodium channels extremely amplify the signal which supports depolarization of terminals which help vision perception.

We compared the needed intra- and extra- cellular amplitudes to elicit spikes in the terminals (calcium spike) as seen in [3, 6, 7, 8]. Intracellular stimulation has a large function in neurophysiology by making spikes in neurons artificially. We found that the least intracellular amplitude which is injected to the soma is around 0.2µA to make bipolar cell spike and it is around 5µA in the extracellular case where the electrode is 40µm far from the center of the soma near the dendrites.

CONCLUSION

Here we simulated the response of a specific bipolar cell which was stimulated with a microelectrode of spherical shape. For retinal implant simulations the electric field is generated via multichannel electrodes that should be modelled with finite element method. Other cell types can be simulated with the same technique in order to get more insight on strategies which should be used by the next generation of retinal implants.

Supported *by* the European Union's Horizon 2020 research and innovation programme under the Marie Sklodowska-Curie grant agreement No 674901 (switchboard) and the Austrian Science Fund (FWF), grant No. P 27335-B23.

REFERENCES

[1] Werginz, P, Rattay F. "**Past, present, future: a review on visual prostheses.** " Minerva medica 106 (1), 65-77, 2015.

[2] http://webvision.med.utah.edu

[3] Puthussery T et al. "Na_V1.1 channels in axon initial segments of bipolar cells augment input to magnocellular visual pathways in the primate retina" J Neurosci. 33:16045- 59, 2013.

[4] Rattay. F. "The basic mechanism for the electrical stimulation of the nervous system" Neuroscience 89 (2), 335-346, 1999.

[5] Werginz P et al. "Neural activation for different electrode designs in subretinal implants: a modeling study" Biomed. Tech 58, 4036, 2013.

[6] Saszik S and DeVries SH. "A mammalian retinal bipolar cell uses both graded changes in membrane voltage and all-or-nothing Na^+ spikes to encode light" .J Neurosci. 32:297–307, 2012.

[7] Cui, J. & Pan, Z. H. "Two types of cone bipolar cells express voltage-gated Na+ channels in the rat retina". Vis Neurosci. 25: 635–645, 2008.

[8] Baden T et al. "Spikes and ribbon synapses in early vision" Trends Neurosci 36:480–488, 2013.

Research Field *Sustainable Products and Solutions, Architecture and Urban Design*

Chairs and Reviewer:

Getzner, Michael
Univ.Prof. Mag.rer.soc.oec. Dr.rer.soc.oec.

E280 - Department of Spatial Planning
michael.getzner@tuwien.ac.at

Wimmer, Wolfgang
Ao.Univ.Prof. Dipl.-Ing. Dr.techn.

E307 - Institute for Engineering Design and Logistics Engineering
wolfgang.wimmer@tuwien.ac.at

Introduction

The recent international climate change treaties (e.g. Paris agreement, 2015) have again put a sustainable energy and resource consumption on the political agenda. Over 100 countries have committed themselves to s significant reduction of greenhouse gas emissions (GHG emissions) hopefully leading to an almost complete decarbonization of the economy.

These political goals will only be achieved if all areas of our day-to-day life (consumption, production, mobility, architecture and housing, urban design and structures) are transformed into a sustainable and decarbonized economy. In all these policy fields, the challenges in terms of new technologies, designs, social and political approaches, are enormous.

Sustainable products and solutions have a lower Product Carbon Footprint compared to a conventional solution use resources more efficiently and foster reuse of parts and components and recycle materials at all levels. Sustainable products and solutions refer to developments that contribute to a lower environmental impact through any of the following strategies:

- reduced resource consumption due to design considerations
- consuming less energy due to better energy efficiency
- durable and longer lifetime due to design and material aspects
- fit for a Circular Economy due to recylability and reusability

Papers in this track will deal with these issues in its broadest understanding, and while presentations will be based on a strong disciplinary pillar, they will also extend disciplinary boundaries in terms of inter- and transdisciplinarity.

SUMMERLY OVERHEATING OF BUILDINGS COMPARISON OF DIFFERENT CALCULATION METHODS AND DEVELOPMENT OF A TOOL FOR DESIGN AND PROOF

Joachim Nathanael Nackler[a], Klaus Kreč[b]

[a]E259 - Institute of Architectural Sciences
[b]E253 - Institute of Architecture and Design

INTRODUCTION

On one hand, regarding the energy efficiency of buildings and, in particular, the winter heat losses through the building envelope, it is state of the art to plan and build low-energy houses or even passive houses, that show significantly reduced heat energy consumption compared to older existing buildings. On the other hand not only in older buildings, but also in highly insulated new buildings, frequently uncomfortable, too warm indoor climate is occurring in summertime.

FUNDAMENTAL OF THE PROBLEM

Due to global warming and contemporary architecture, which uses a lot of glass and lightweight constructions, the problem of summerly overheating of rooms is ubiquitous. There is a simplified method acc. to the Standard B 8110-3, which is predominantly used for assessing the summerly heat protection in Austria. However, due to the simplified calculation approach, no good planning reliability can be assured and is thus far from the more realistic results and possibilities of thermal dynamic building simulation programs. Problem is, that building simulation programs are usually too complex and time-consuming to support architects in the design process. Many planning decisions, which are made in early planning phases, have significant influence on the summerly behaviour of the building and can hardly be changed afterwards or just with increased effort. Considerations regarding climate-friendly building should thus already take place in the design phase. Again, it is problematic that architects lack tools for evaluating the summerly heat protection that can be used easily.

Hence the goal is to develop a generally accessible, intuitive online tool that is not based on a simplified calculation methods, but generates realistic results. The architects will then be easily enabled to develop optimized designs regarding the summerly heat protection.

RESULTS

Important thermal steady state, as well as dynamic parameters are presented and discussed, especially the thermal storage capacity of building components and rooms is analysed in detail in order to eliminate often prevailing misunderstandings. In addition, various methods for assessing the summer suitability of rooms are compared, such as simplified (steady state) methods, more detailed 1D as well as 3D dynamic simulation methods. The advantages and disadvantages of these methods are analysed. A series of programs are presented that implement these methods. Furthermore, a major part of the dissertation is the validation of selected building simulation programs using the European Standard EN ISO 13791 and 13792.

All these steps were taken to achieve a sound foundation for the development of a tool for planners which is named Thesim3D: an intuitive online tool with a self-explaining interface that runs a detailed thermodynamic building simulation in the background.

The requirements for the tool have been set high: Simple and intuitive use, free accessibility to all target groups, no commercial programs, operating system independence, as well as independence of other programs, user based error minimization and the separation of user interface and simulation core. Thesim3D simulates the thermal behaviour of a room in the frequency domain using the so called periodically settled system (period length: 1 day). It is therefore in particular suitable for summer assessments acc. to the Standards. The periodic settled calculation approach as well as the description of the heat conduction and heat storage mechanisms by means of the component-matrix method (cf. [3]) have proven themselves as methods for the planning-accompanying computational simulation in such a good way that they were also incorporated into national and international standards (B 8110-3 [1], EN ISO 13791 [2], EN ISO 13786). Thanks to this method, results can be obtained in real time and different variants can be analysed very quickly. The dissolution of the heat balance equations using the periodic approach is described in the dissertation. The technology triad of the web, HTML, CSS and JavaScript was used to implement the user-interface Thesim3D. For the 3D-modeling of the room, Three.js, a 3D graphics API for the Web, based on WebGL, was used. On the server side, the simulation kernel is encapsulated by a Java web service, which enables communication with the client. The Java web service is the interface to the Geba V.10 simulation core, which is an extensive, thermal-dynamic building simulation program. Geba is validated according to the validation method of EN ISO 13792 to the best class 1.

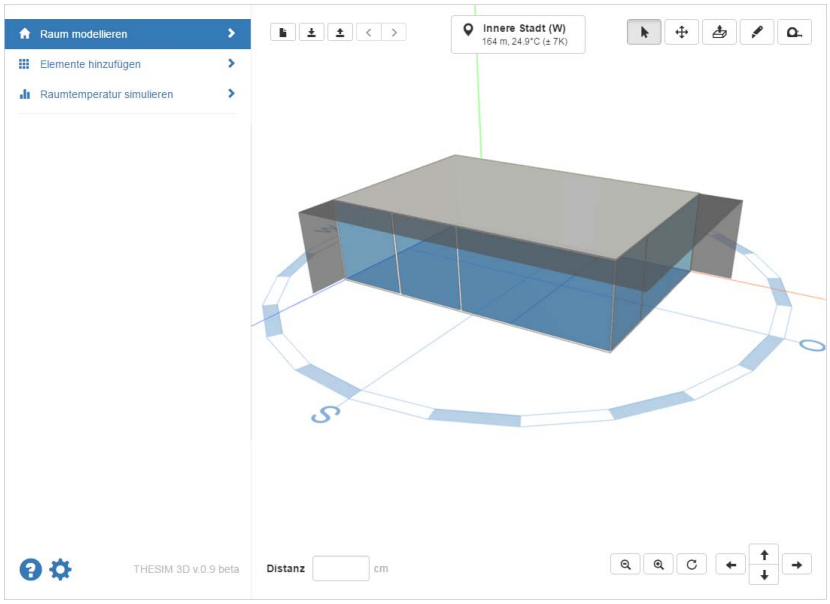

Figure 1: Thesim3D user-interface: easy modelling of 3D-room.

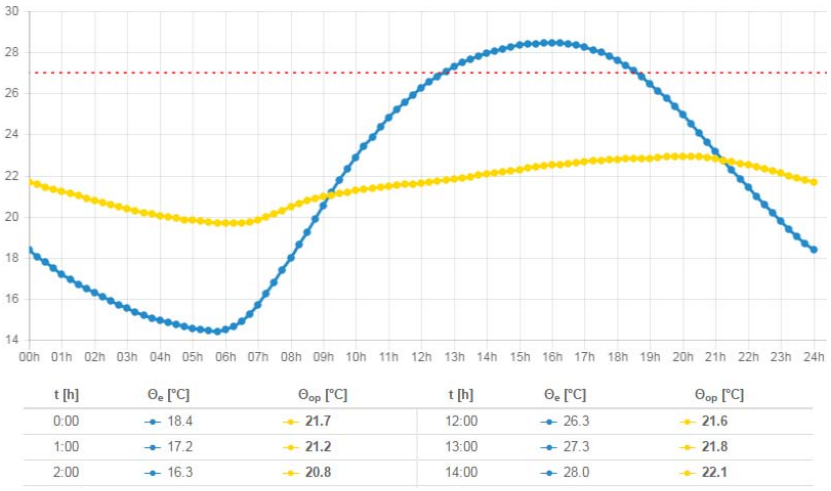

t [h]	Θ_e [°C]	Θ_{op} [°C]	t [h]	Θ_e [°C]	Θ_{op} [°C]
0:00	18.4	21.7	12:00	26.3	21.6
1:00	17.2	21.2	13:00	27.3	21.8
2:00	16.3	20.8	14:00	28.0	22.1

Figure 2: Small extract of extensive simulation results.

REFERENCES

[1] ÖNorm B 8110-3:2012, Wärmeschutz im Hochbau, Vermeidung sommerlicher Überwärmung

[2] ÖNorm EN ISO 13791:2012, Thermal performance of buildings, Calculation of internal temperatures of a room in summer without mechanical cooling – general criteria and validation procedures

[3] Haferland, F., W. Heindl und H. Fuchs: Ein Verfahren zur Ermittlung des wärmetechnischen Verhaltens ganzer Gebäude unter periodisch wechselnder Wärmeeinwirkung. Berichte aus der Bauforschung, 99, 1975.

LEARNING FROM TRADITIONAL VERNACULAR ARCHITECTURE

Taraneh Rouhi

E251 - Institute of History of Art, Building Archaeology and Restoration
Vienna University of Technology, Austria

INTRODUCTION

The peaked Kurdish black hair tent and the domed Turkish felt tent of Iran's frontierspeople are a symbol of a demanding lifestyle.[1] Every year, tribesmen with chattels and mobile architecture migrate along with their livestock from summer quarters to winter quarters, and vice versa. The present study aims to analyse the differences between two nomadic dwellings and attempts to examine the reasons of suitability of this type of architecture over the centuries.

COMPARING- DIFFERENCES BETWEEN KURDISH BLACK TENT AND TURKISH FELT TENT

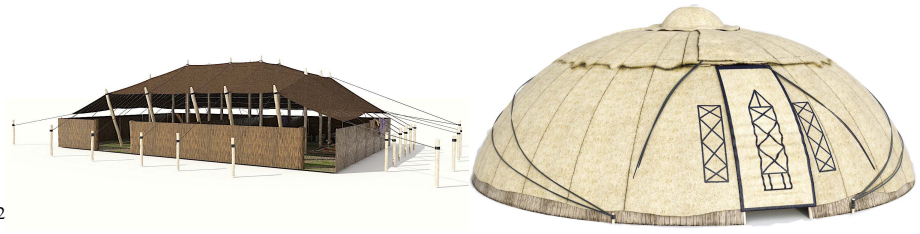

Picture 1: black tent & felt tent[2]

TYPE OF ARCHITECTURE	KURDISH BLACK TENT	TURKISH FELT TENT
1. Geometric shape or form	Black tent has a rectangular shaped	Felt tent has a dome shaped
2. Size and dimension of tent	-Length between 6 - 13 m -Width between 25 - 35 cm -Number of stripes Between 15 – 25	-24 poles: Floor diameters ~ 600-650 cm -26 poles: Floor diameters ~ 750 cm
3. Material	-Tent cloth: goat hair -Poles: poplar -Reed matting walls: apple tree branches are woven with goat hair -Ropes: goat hair - Equipment inside	Poles: firs tree -Covering structure: sheep wool -Short walls – reed mats are woven with goat hair, but nowadays industrial cotton string or industrial thin ropes is used -Cordage: sheep wool or industrial ropes
4. Structure	Tensile structure	Compression structure
5. Poles' forming	Straight or X	Curve
6. Connection between roof and wall	The roof (tent cloth) is separated from the wall (reed mats)	The wooden structure is covered with felts
7. Flexibility & changeable	Flexible structure	Rigid structure
8. Organisation inside the tent	Divided spaces	Single room
9. Connection between interior and outside	No clear separation of inside from outside	Clear separation of inside from outside
10. Setting up time	Black tent in less than 20 minutes	The felt tent in less than 40 min
11. Life expectancy	-Roof/tent cloth: six to ten years -Short walls: 6-8 years	-Structure – twenty years -Covering: five to ten years -Short walls: 8 years

SUSTAINBILITY

- Adaptation of features of West Azerbaijani nomads' black tents & East Azerbaijani/Ardabil nomads' felt tent in accordance with the nomadic lifestyle and related requirements:

DESIGN REQUIREMENT	KURDISH BLACK TENT	TURKISH FELT TENT
1. A shelter to provide the basic needs of nomads	Provides shade from the sun Protects from cold, wind, sand and dust Provides privacy for the occupants	

2. Lightness and portability/ potable architecture	Can be carried easily by pack animals (traditional method) or trucks (modern method)- felt tent traditional transportation with camel, black tent with donkey	
3. Simple to construct (easy assemble architecture)	Convenient setting up and packing up – nomad can set up their black tent in less than 20 minutes and felt tent in less than 40 min	
4. Accessible, local and inexpensive material	-Tent cloth: goat hair ✓ -Poles: poplar ✓ -Reed matting walls: apple tree branches are woven with goat hair ✓ -Ropes: goat hair or industrial ropes on the market ✓	Poles: firs tree- nomads bought the frame from the craftsmen ✗ -Covering structure: sheep wool ✓ -Short walls – reed mats are woven with goat hair, but nowadays industrial cotton string or industrial thin ropes is used ✓ -Cordage: sheep wool or industrial ropes on the market ✓
5. Simple to repair	The nomads have acquired appropriate skills in repairing their tents as necessary and do not require any specialist support to do so	
6. Practical (multifunctional architecture) □	Every tent is a complete living space, incorporating specific areas for sleeping, eating, entertaining guests and cooking. There is even a space for new-born livestock in black tent– very small in measurement and dimensions, but very efficient in use of space	
7. Flexible black tent and relatively flexible felt tent	-Can be extended or curtailed by adding or removing strips and poles -Interior tent spaces can be divided up and separated using reed mats	-Fix wooden structure– the main structure cannot be extended or curtailed -Felt tent is a single room and in the felt tent rarely has a physical partition
8. Life expectancy	-Roof/tent cloth: six to ten years -Short walls: 6-8 years	-Structure – twenty years □ -Covering: five to ten years -Short walls: 8 years
9. Cost effective architecture	The felt tent is more expensive than black tent, in my observation (summer 2015): ~ 4 milion. Toman= ~ 1000 euro: for 26 poles frame (usual size)	

- Adaptation of features of West Azerbaijani nomads' black tents & East Azerbaijani/Ardabil nomads' felt tent in accordance with settlements' climatic conditions:

1. Connection between interior and outside	No clear separation of inside from outside	Clear separation of inside from outside
2. Harmony with surrounding landscape	A Kurdish black tent, featuring peaks on its roof, creates wavy forms like a mountain in a mountain range	The hemisphere shape of felt tents in the mountains like a hilly landscape
3. Renewable and non-polluting energy	Natural ventilation Natural light	
4. Environmentally friendly material	-Tent cloth: goat hair -Poles: poplar -Reed matting walls: apple tree branches are woven with goat hair -Ropes: goat hair or industrial ropes on the market	Poles: firs tree- nomads bought the frame from the craftsmen -Covering structure: sheep wool -Short walls – reed mats are woven with goat hair, but nowadays industrial cotton string or industrial thin ropes is used -Cordage: sheep wool or industrial ropes on the market
5. Practical orientation	Depends on the climate, direction of wind and amount of sunlight needed in the summer	

CONCLUSION

The study conducted on the Kurdish black tent and Turkish felt leads to a set of comprehensive results regarding the reason of sustainability and survival. In fact, whatever kind of livelihood and environmental factors is imposed on them, it has made the reality of nomadic architecture continuous from the distant past to the present day. The results of the study indicate a complete harmony of nomadic housing within a movable lifestyle and regional climatic conditions that might be able to lead our architecture towards a reconciliation with nature.

NOTES AND REFERENCES

[1] The Peaked Kurdish black tent is nomadic architecture in the West Azerbaijan province and the domed Turkish felt tent is nomadic architecture in the East Azerbaijan and Ardabil provinces of Iran.

[2] Source of picture 1: modelling and rendering by author

INNOVATIVE GOVERNANCE FOR STRATEGIC UGI PLANNING: THE ROLE OF THE STAKEHOLDERS' NETWORKS ANALYSIS

Antonija Bogadi

E280 - Department of Spatial Development and Infrastructure & Environmental Planning

INTRODUCTION

Green infrastructure at a urban scale (UGI) is recognised for it's capacity to handle climate related threats[1], including support for biodiversity, improving human well-being, and it's potential to be more cost efficient than alternative adaptation approaches.

UGI and its mainstreaming into municipal planning is receiving increasing interest from academic and governmental bodies, but the strategies for it's systematic implementation and management in dynamic urban systems stand unclear [2].

The diversity of stakeholders and their different needs and perceptions about UGI complicate implementation processes, often resulting in conflicts about the objectives and spatial arrangement of UGI. Mapping and involving diverse stakeholders and creating the networks that outgrow formal organisational borders and hierarchies could strengthen collaboration and upgrade the governance to achieve desired goals.

RESEARCH SUMMARY

This research is investigating collaborative and multi-level governance settings which are designed based on the relevant stakeholder network analysis (SNA). SNA is considered a tool for predicting conflicts between the stakeholders and to set up most effective policies for UGI implementation [3].

Three case studies with existing SNA are chosen to examine that assumption, and their network structure is analysed through various actors' influence on the system, their position in the network and connections with the other actors. That analysis is further connected to the specific challenges that had occurred in UGI implementation, new policies brought to solve them and their outcomes.

EXPECTED RESULTS

Results demonstrate that SNA is useful for creating effective policies for UGI implementation because it gives an insight into the structure of the interactions between the actors, into the ways in which this structure affects the performance of the system and how it can be improved.

CONCLUSION

A network perspective could provide a valuable information to determine effective governance arrangements because it gives an insight into interactions types between the different actors and the ways in which ways existing structure can be influenced to increase the system performance. Another advantage of a network perspective is it's uniform language for describing complex systems in terms of nodes and links, which can have a wide application for helping creating a innovative governance arrangements for efficient UGI implementation.

REFERENCES

[1] Elmqvist, T., Fragkias, M., Goodness, J., Güneralp, B., Marcotullio, P. J., McDonald, R. I., ... & Wilkinson, C. (2013). Stewardship of the biosphere in the urban era. In *Urbanization, biodiversity and ecosystem services: Challenges and opportunities* (pp. 719-746). Springer Netherlands.

[2] Wamsler, C., & Pauleit, S. (2016). Making headway in climate policy mainstreaming and ecosystem-based adaptation: two pioneering countries, different pathways, one goal. *Climatic Change*, *137*(1-2), 71-87.

[3] Kenis, P., & Schneider, V. (1991). Policy networks and policy analysis: scrutinizing a new analytical toolbox. *Policy networks: Empirical evidence and theoretical considerations*, 25-59.

ARCHITECTURAL COMPETITIONS & SUSTAINABILITY: A CASE STUDY

Ulrich Pont, Ardeshir Mahdavi

E259.3 – Department of Building Physics and Building Ecology, TU Wien

INTRODUCTION

A number of recent initiatives address the thermal building performance of new and existing buildings. Moreover, in recent years architectural competitions demand the consideration of energy efficiency and environmental footprint aspects in their requirement documents. However, the question if and to which extent such aspects influence the jury decisions of competitions remains open. Toward this end, we present a case study on a competition of a large residential building in Austria. This competition specifically addressed the energy efficiency of the proposed designs. Buildings had to be designed in a way that "Passivhaus"-standard could be reached. Participants were required to add basic information such as proposed wall thickness, glazing orientation, and building compactness in their project deliverables. In a later stage, independent evaluators assessed and compared the sustainability of the proposed designs based on a simple point scheme. The energy performance of the designs was neither calculated by the participants nor by the external evaluators. In this contribution we evaluate the energy performance of the ranked designs via a normative energy certification method. Additionally we contrast, in case of one of the participating architectural firms, the designs with early stage work models and their calculated performance. The results might offer insights concerning the question if and to which extent the ranked energy performance of the proposed designs did influence the competition's ranking.

METHODOLOGY

Status Quo of consideration of sustainability criteria in architectural competitions: It is a widely accepted and well-known fact that buildings contribute to a major share of both energy consumption and emission of harmful substances. Moreover, domain specific laws and standard stipulate that the planning process of new buildings and retrofit efforts of existing structues have to result in highly-efficient buildings. However, a notable amount of building designs is generated via architectural competitions. Results of such competitions are regularly based on a ranking of a jury of architects and domain experts in the specific field of building. Whereas the consideration of sustainability can be found in many competition's tender document, it seems not clear, if the ecological performance of proposed building designs can be found in a decision ratings of competitions. In previous research activies [1,2] we captured the common practice of addressing sustainability in tender documents and required deliverables of competitions. In the present contribution we examine a case study competition and its results toward different sustainability criteria

The assessed architectural completion: The assessed competition was conducted in 2014/2015 and addressed the generation of highly-densified, highly-efficient social housing in a larger Austrian city. "Passivhaus"-Standard was a required aspect of the designs. Figure 1 illustrates a part of one of the awarded projects of the competition.

Three-fold-assessments: To assess the sustainability we compare the decision ranking of the competition's six awarded projects with three different other evaluations:

(i) The ranking based on a spread-sheet evaluation of the sustainability criteria, done by a consultancy agency that assessed the competition entries.

(ii) The results of calculations performed with a normative method suitable to assess the energy use of buildings, based on the information given in the competition entries. It has to be mentioned that the required level of detail for a comprehensive calculation of Key Performance Indicators (KPIs), or even a numeric energy performance simulation is regularly not available in the deliverables of competitions. This is the case in the present competition as well. Therefore, a number of assumptions had to be taken to be able to arrive at meaningful results.

(iii) A subjective evaluation of the six awarded projects by a large number of graduate students of Architecture and Building science. The students did rank the six buildings based on their subjective impression of model photographs of the proposed designs regarding energy efficiency, positioning of the building(s) on the corresponding building site, and on the their preference for residing in the corresponding project's residential units.

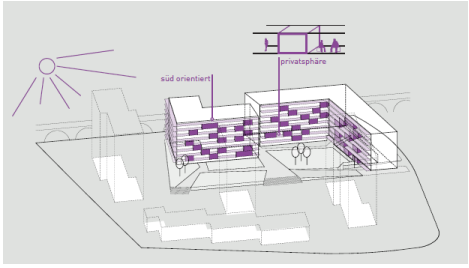

Figure 1: A part of one of the awarded contributions.

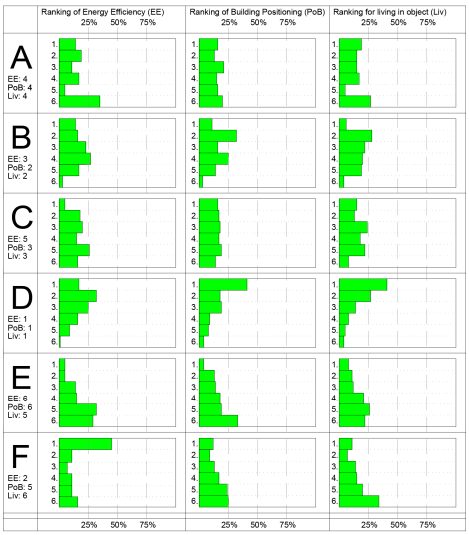

Figure 2: Subjective evaluation results

RESULTS AND DISCUSSION

In general, the comparison showed bid discrepancies between the different rankings. Figure 2 illustrates the results of the subjective evaluation by the graduate students. Interestingly, there is not only a difference between the subjective energy efficiency assessment and the calculated energy efficiency, but also differences in the subjective rankings between the energy efficiency, the building positioning, and the preferences regarding residing in one of the awarded projects.

CONCLUSION & FUTURE RESEARCH

In principle, the results of this study shows that there is a strong necessity to develop both objective and easy-to-use assessment criteria regarding sustainability for ranking of proposed architectural designs within competitions. Future research will extend the study to a number of competitions and suggest different evaluation criteria that can be used in assessment of proposed designs within such competitions.

REFERENCES

[1] U. Pont, K. Kiesel, M. Schuss, B. Sommer, K. Orehounig, A. Mahdavi: "A critical case study of decision criteria in architectural competitions" in: "Proceedings - First International Conference on Architecture and Urban Design - 1-ICAUD", EPOKA Univ.; Dep. of Arch. (Ed.); Epoka Univ. Press, 1 (2012), ISBN: 9789928-135-01-8; 9 S.

[2] K. Kiesel, U. Pont, A. Mahdavi: "Including sustainability criteria in architectural completion: A critical case study of current practices"; Advanced Materials Research - Web, 649 (2013), 4 S.

AN EMPERICAL APPROACH TO TIMBRE-BASED MODELS IN BROWNFIELD REDEVELOPMENT

Naghmeh Jafari[a], Astrid Bös[a], Matthias Ondra[a], Walter Schwaiger[a]

[a]E330 - Institute of Management Science - TU Wien

PROBLEM STATEMENT

Over the last several decades, extensive de-industrialization and land use changes of former military, industrial, and commercial sites across Europe have lead to a large number of derelict and underutilized lands with varying degrees of contamination also known as Brownfields [11]. Acute demands for land in and around cities, on the other hand, have made urban sprawl one of the major challenges facing Europe [10]. During the last decade, brownfield site remediation and revitalization has gained increasing attention as a sustainable land use strategy to combat urban sprawl [2] and additional infrastructure and mobility costs entailed in developing a free developable land. However, regeneration of contaminated fields is a complex and multidimensional problem that entails many risks and uncertainties, such as risk of liability claims, investment, usability, and marketability (stigma) risks [1]. The objective of this paper is to construct, calibrate and validate a risk assessment model in order to evaluate and predict the development potential of industrial brownfields that can assist investors and decision-makers.

METHODOLOGY

Several brownfield scoring schemes, prioritization tools, and identification approaches have been proposed in the literature that focus on various aspects of regeneration of brownfields, such as uncertainty assessment, environmental and health risk assessment, remediation cost assessment, etc. However, they are either developed case-by-case or lack a multidisciplinary approach [6]. One major project that merges most existing models into one is the Tailored Improvement of Brownfield Regeneration in Europe (TIMBRE), which assists the stakeholders to rank brownfields based on their redevelopment potential. The ranking is performed by using multi-criteria decision analysis methodology, which uses different components in a hierarchical structure, including dimensions, factors and indicators. On the highest level, dimensions account for specific aspects of redevelopment potential, such as local development potential, site attractiveness, marketability, and environmental risks. Each dimension is identified through factors, which lead to successful brownfield redevelopment. Indicators are used to simplify the factors to qualitative or quantitative measurable variables. After assigning weights to the indicators, they are aggregated by convex combination into factors, which are then weighted and aggregated into dimensions. Finally, dimensions are aggregated again to a final prioritization or ranking score [12].

Three model constructions are considered, which are separately calibrated and validated. Model 1, set as benchmark, follows the guidelines of TIMBRE. Four dimensions are chosen by experts, which have the most impact on the potential regeneration of a brownfield. Calibration of model 1 is performed by weighting the relevant factors produced from an expert-based questionnaire. The model is then validated by assessing its discriminatory power based on receiver operating characteristic (ROC) method. [13]

Model 2 uses statistical method of supervised learning to retrieve the most suitable variables and their weights such that the discriminatory power of the model is maximized. Linear discriminant analysis (LDA) aims to best discriminate between classes of a dependent categorical variable, depicted here by the fact that whether a brownfield is successfully regenerated or not with a linear combination of a set of continuous independent variables [8].

Model 3 focuses on the aspects of machine learning, dealing with the problem of big data. Here, a major part of all logistic regression models containing all possible combination of the variables available are calibrated and cross-validated. Based on the predictability of these models, the best one is chosen as a final model for each federal state.

REFERENCES

[1] Bartke, S. (2011). Valuation of market uncertainties for contaminated land. *International Journal of Strategic Property Management*, 15(4):356 - 378.

[2] BenDor, T. K., Metcalf, S. S., and Paich, M. (2011). The dynamics of brownfield redevelopment. *Sustainability*, 3(6):914 - 936.

[3] Bierens, H. J. (2004). Information criteria and model selection.*Manuscript, Penn State University.*

[4] Burnham, K. P. and Anderson, D. (2003). Model selection and multi-model inference.*A Pratical informatiotheoric approch. Sringer.*

[5] Claeskens, G. (2016). Statistical model choice.*Annual Review of Statistics and Its Application*, 3:233 - 256.

[6] Dasgupta, S., & Tam, E. K. (2009). ENVIRONMENTAL REVIEW: A Comprehensive Review of Existing Classification Systems of Brownfield Sites.*Annual Review of Statistics and Its Application*,11: 285 - 300.

[7] Fabozzi, F. J., Focardi, S. M., Rachev, S. T., and Arshanapalli, B. G. (2014). *The Basics of Financial Econometrics: Tools, Concepts, and Asset Management Applications*. John Wiley & Sons.

[8] Fisher, R. A. (1936). THE USE OF MULTIPLE MEASUREMENTS IN TAXONOMIC PROBLEMS. *Annals of Eugenics*, 7(2):179 - 188.

[9] Hosmer Jr, D. W. and Lemeshow, S. (2004). *Applied logistic regression*. John Wiley & Sons.

[10] Ludlow, D. (2006). Urban sprawl in europe: the ignored challenge.

[11] Nathanail, C. P. (2011). Sustainable brownfield regeneration.*In Dealing with Contaminated Sites*, pages 1079 - 1104. Springer.

[12] Pizzol, L., Zabeo, A., Klusacek, P., Giubilato, E., Critto, A., Frantal, B., Martinat, S., Kunc, J., Osman, R., and Bartke, S. (2016). Timbre brownfield prioritization tool to support effective brownfield regeneration.*Journal of environmental management*, 166:178 - 192.

[13] Zou, K. H., O'malley, A. J., Mauri, L. (2007). Receiver-Operating Characteristic Analysis for Evaluating Diagnostic Tests and Predictive Models. *Circulation*, 115(5): 654-657.

THE EMULATE PROJECT COURSE AS AN INSTANCE OF RESEARCH-GUIDED TEACHING

M. Vuckovic, S. Attila, R. Gallardo Gomez, N. Hodzic, V. Lisyana, R.P. Rissetto, M. Solman, T. Tezarek, N. Ghiassi, M. Taheri, F. Tahmasebi, U. Pont, A. Mahdavi

E259.3 – Department of Building Physics and Building Ecology, TU Wien

INTRODUCTION

University education aims at the advancement of the current state of knowledge. Toward this end, research-guided teaching provides a host of effective opportunities. Following this approach, the curricular development for the Master of Building Science programme on the TU Wien integrated a course into its current curriculum that offers a platform for research-inspired teaching. This course is named Project course, and during the Winter semester 2016/2017 students had the opportunity to deepen their knowledge via working on current trends and ideas within two research streams currently followed at the Department of Building Physics and Building Ecology. This contribution reports on the efforts and results of one of the two research streams, called the EMULATE project. The EMULATE project targets the conceptual development of innovative urban energy modelling environment. Currently, the interest in urban-scale energy modeling environments has been steadily increasing. This is in part due to the insight, that certain critical questions regarding the performance of the built environment cannot be sufficiently treated at the level of individual buildings. However, bound to achieve computational efficiency, past urban-scale modeling efforts frequently rely on various domain simplifications. For instance, heat transfer phenomena are captured using reduced order models. This could involve not only the simplification of the geometry and zonal complexity of modelled buildings, but also a significant reduction of the temporal resolution of the modelling results. As a consequence, certain important queries cannot be accommodated with appropriate levels of resolution. Specifically, the temporal dynamics of load patterns and their dependency on transient phenomena (e.g., weather conditions, inhabitants' presence and actions) cannot be realistically represented. To address these circumstances, the envisioned urban energy modelling environment combines various developments in the fields of urban building stock energy performance assessments, microclimate modelling, and occupancy modelling, towards the more realistic assessment of urban and neighborhood level energy assessments. Thereby, the students involved in the project course were given the task to explore the challenges and potentials of the essential features of the above-mentioned integrative environment, specifically, the simulation-supported assessment of urban building stock energy performance, microclimate modelling, occupancy modelling, and alternative urban development and densification schemes.

THE PROJECT COURSE OUTLINE

The project course was split into three different phases (see Fig. 1). The first phase was a research phase, which was used to report on existing research and current developmental activities in the field of urban-scale energy and environmental modeling. Thereby, four dedicated sub-groups were formed, each investigating a different modelling component. Two students investigated the possibilities of a simulation-supported assessment of urban building stock energy performance, two students investigated the methodology to infer local microclimatic boundary conditions from a number of location-dependent variables, two students investigated the representation of occupants'

presence and actions for building performance assessment purposes, and one student investigated the urban densification potentials. The research phase was concluded with a presentation of findings. The subsequent three-month period was dedicated to the investigation of the implementation potential of a number of modeling approaches, as identified in the research phase. This phase was complemented with frequent presentation and discussion sessions. In the final stage of the semester, the participants were asked to present their findings and critically reflect on both strengths and weaknesses of each modeling component. Finally, they were asked to write a comprehensive scientific summary report about the overall process.

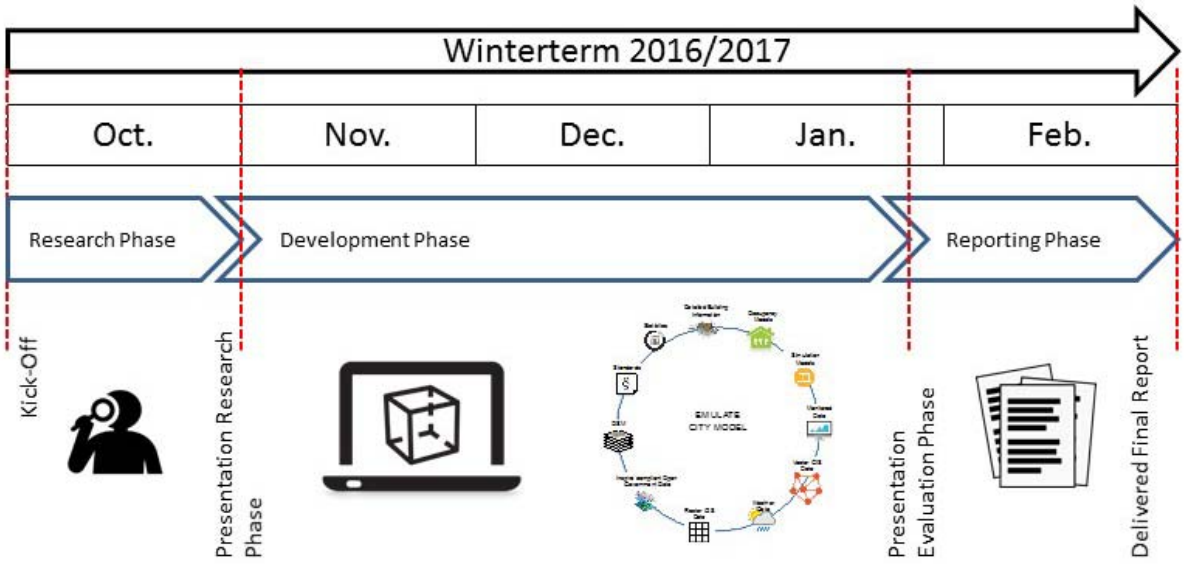

Figure 1: Flow chart illustrating the organizational character of the EMULATE project course

DISCUSSION AND CONCLUSION

The results of the project course encompassed interesting new ideas for integrative urban energy computing approach. Participants reported on the developmental efforts towards generation of a modular simulation-supported integrative urban decision support environment. As a research-guided teaching experience, the project course was perceived by all involved participants (students and instructors) as a satisfying and intellectually enriching experience. Hence, we shall further pursue this promising teaching approach and the corresponding structure in future semesters.

OASIS: FROM ILLIGAL DUMPING GROUND TO URBAN ASSET

Alma Demirović[a], Lejla Brulić[b]

[a]Sustainable Building Council, Sarajevo, Bosnia Herzegovina
[b]Association for help and development HAJDE, Sarajevo, Bosnia Herzegovina
alma@sbcouncil.eu

INTRODUCTION

The presented work deals with the urban transformation of a completely desolated land in Kakanj, one of the most polluted cities in Bosnia Herzegovina and home to roughly 39,000 residents. Immediately adjacent to the city centre, was a 5,500 m2 of land which within the last 30 years has been turned into an illegal dumping grounds. While this is in itself very adverse, in the past decade, with the expansion of the city, the location became active slums of Roma population. The city has been making efforts to urbanize and improve living conditions in the area by building social housing units for the settled population but this did little to remedy the overall situation.

To resolve the problem, a project was initiated explore the possibility of improving the area by transforming the neglected grounds into a functional urban form. The project faced several challenges. The location is a former mining waste dumping site that has been turned into an illegal dumping ground where communal and construction waste was redirected by those aiming to avoid fees of proper waste disposal. The goals for improvement were unclear and very limited funding was available for ecological and development initiatives including this project. Roma population that lives in improvised housing units have high unemployment and low education rates. Their main source of income is picking and gathering of secondary materials which also made relocation obsolete as it would not offer long term solutions. All these points were considered and in further text we describe the development of the project and show how communities could benefit from exploring urban design models that address human needs in parallel to building ecologically conscious spaces even in low-income communities where resources are scarce.

BEFORE: illegal dumping ground with active slums

SIGNIFICANCE AND APPROACH

The initial design land improvement parameters for the available space was simply defined as recreational space. This solution provided badly needed open space for local residents of all ages. The motivation to develop a design model was rooted in the central issue of environmental justice that everyone deserves to live in a community where they can reach their full potential. Research suggests that the place where one lives can be a major predictor of important life outcomes such as health, academic and career success due to direct relationship between the quality of a neighbourhood's built environment and access to the economic, political, and social resources needed to thrive [1][2]. Unfortunately, residents of this location live in a community that lacks the investments of these key resources.

During construction. Large amounts of debris has been removed.

However, our approach successfully improved the living conditions of the area. The design model had two main features: educational and ecological. *Educational aspect:* the goal was to stimulate children's natural curiosity by learning through play. This was achieved by intertwining a children's playground area with numerous low-cost high-impact educational activities and curiosities that include an Outdoor Classroom, a Weather Learning Station, a Human Sundial, numerous informational plaques, a Bee Garden and a Sun's Energy Station. These units allow for a higher degree of rapprochement with the environment, the elements and the interaction between them. Accounting the proximity of the town's soccer stadium, the remaining area was levelled and landscaped to offer conditions for various sports and recreational activities. In addition to increasing beautification of levels of the neighbourhood, the e*nvironmental aspect* focused on carefully selecting and combining the vegetation (trees, shrubs, perennials) based on their specific capabilities of absorbing large amounts of pollutants in short amounts of time with the ability to attract important pollinators (butterflies, bees, fireflies, insects etc.) by producing different types of foods (seeds, pollen, berries etc.) while blooming and/or producing fruit at specific times of the year thus ensuring availability of nourishment for these important providers of ecosystem services year round.

AFTER: Educational areas with playground with sports field under leveling works. Photograph taken from top floor of a newly constructed social housing unit.

RESULTS AND DISCUSSION

The result is a successfully completed urban transformation and design model that improved the living environment of the local residents who now spend time in uplifting and energizing surroundings. Both project and design model can be easily replicated to create similar environmentally conscious solutions in other communities that address human needs (social, psychological, educational, integration etc.) in parallel to building ecological components of to support biodiversity and increase the provisioning of vital ecosystem services. As this project demonstrates, it can be achieved with very limited resources. This project cost substantially less that it would have been to demolish and redevelop the area, and serves as a precedent for adaptive reuse.

CONCLUSION

Transforming abandoned and abused spaces in the urban fabric into enjoyable and useful urban forms area appears to be a key solution to converting city processes into more sustainable and circular urban environments. Instead of remaining as hindering areas in urban fabric, or being removed from existence, new unique uses can be found for these places which stimulate the community, city and economy. Furthermore, successful urban transformation projects rely on collaboration and input between government institutions, non-governmental and professional stakeholders. Though this type of collaboration often significantly complicates and lengthens the planning and design processes, it appears to be the formula for success for the redevelopment of abandoned inner-city structures.

REFERENCES

[1] Wilkinson, Richard G., and Michael Marmot. *Social determinants of health: the solid facts*. World Health Organization, 2003.

[2] Currie, Candace, et al. "Social determinants of health and well-being among young people." *Health Behaviour in School-aged Children (HBSC) study: international report from the* 2010 (2009): 271.

CAMILLO SITTE 2.0? A SEQUEL

Stefan J. Kubin

E260 - Institute of Urban Design and Landscape Architecture

INTRODUCTION

Camillo Sitte (1843–1903) is well known for his theoretical work “City Planning According to Artistic Principles” published in 1889. It is a milestone of urban design, which has not lost its validity even in the 21st century. Translated into several languages its influence has internationally spread over two centuries, although only giving an impression of the situation in late 19th century Vienna.

Given this, and ever since Sitte’s early death, scientists have discussed whether he has planned a sequel to his famous work. Unfortunately, there was no convincing evidence in the legacy of Camillo Sitte which is held in the University Archive of the TU Vienna.

“Camillo Sitte 2.0? A sequel” is the title and theme of my current PhD thesis. It examines the theory of a second volume to Sitte’s masterpiece, and how it may have influenced urban planning.

“CITY PLANNING ACCORDING TO ECONOMICAL AND SOCIAL PRINCIPLES”[1]

This title was introduced by Karl Henrici (1842–1927), for the second volume - a small hint given in his obituary on Camillo Sitte in 1904[2]. Henrici gave a short description of the operating principles of Sitte and suggested an almost finished book which may be published soon by Siegfried Sitte – the oldest son who followed the footsteps of his father and became architect and city planner himself.

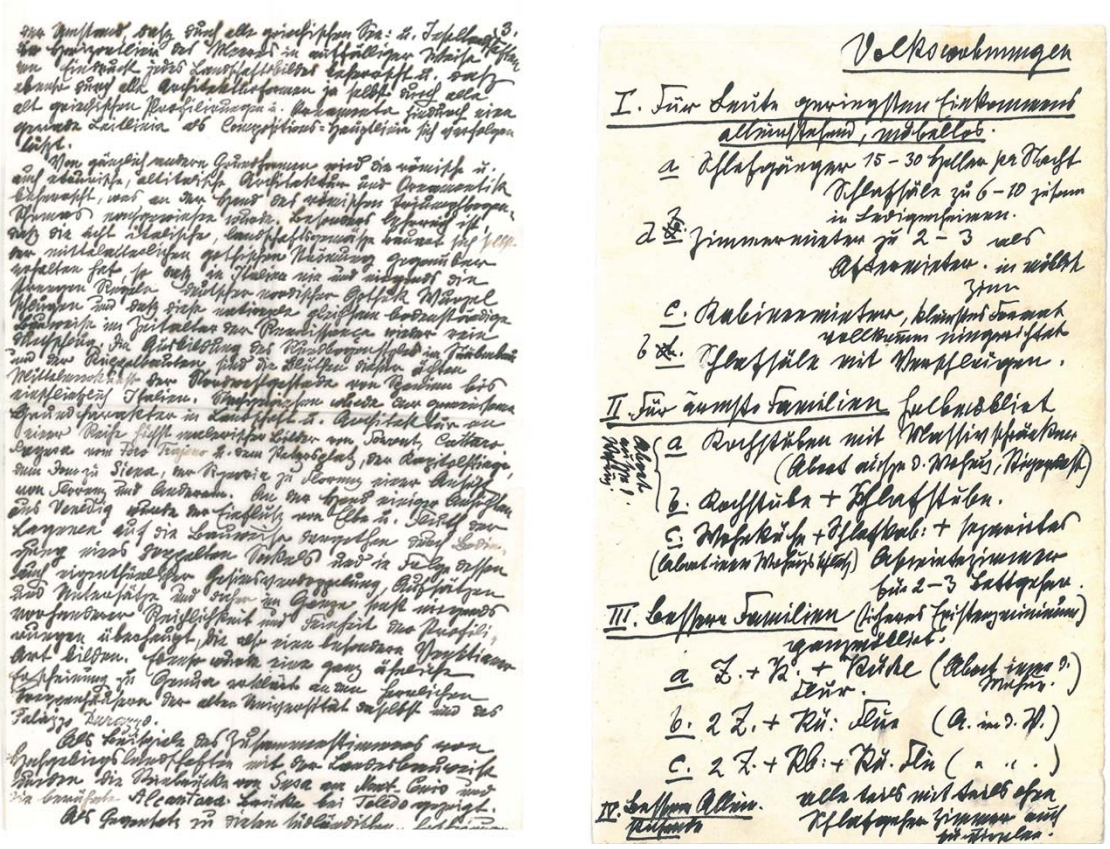

Figure 1: Two examples of autographs from Camillo Sitte

It is obvious that this sequel would have had a major impact on the scientific landscape and the discipline of urban design at all. But the sequel was never published and all traces to the book vanished.

The institute of Urban Design holds since the late 2000s a collection of two caskets which derives from the legacy of a former employee of the family Sitte[3]. It consists of different hand written materials, sketches and photographs from different scale. The material has never been published or examined. Preliminary research has proved so far, its connection to Camillo Sitte and his lost sequel. The major part are autographs of Sitte, written in old german script (see Figure 1).

The research on this collection puts up the main framework for my PhD thesis. Until now the given material has been sorted, archived and transliterated. It allows a deep insight on Sitte's sequel "City planning according to economical and social principles". It is to be clarified which theoretical questions occurred and what solutions Sitte would offer for the discipline.

Based on the ongoing research it will be possible to reconstruct the main structure of the planned second volume, thus giving an impression of the themes discussed by Camillo Sitte. The structure and themes of the sequel will be examined and critically commented within my thesis. It is obvious that Sitte's second volume would have influenced if not changed urban planning throughout Europe and the whole world. The thesis will link these two "City Planning" volumes and compare them due to its content, which of Sitte's ideas are repetitious, innovative or even revolutionary to the discipline.

The results of the PhD thesis shall lead to a publication adding to the "Camillo Sitte Edition"[4], comprising all materials according Sitte's theoretical and practical work.

REFERENCES

[1] The translated title was first introduced by Ralph Wurzer in his Master Thesis at University of Tennessee, see: Ralph Wurzer, Camillo Sitte and America: A Study of the Reception of Sitte's Ideas in American Planning Literature. University of Tennessee, Knoxville, Master Thesis 1988.

[2] „Zu einem zweiten Bande seines Buches, welcher den Titel: ‚Der Städtebau nach wissenschaftlichen und sozialen Grundsätzen' tragen, und von seinem Sohn, dem Architekten Siegfried Sitte, herausgegeben werden wird, ist das Material fast fertig zusammengetragen." Henrici, Karl: „Nachruf für Camillo Sitte" in: „Der Städtebau", Jahrg. 1, Heft 3, 1904. p. 34.

[3] Franz Stokreiter / Siegfried Sitte, Das Wirtschaftsbild (Beiträge zu Städtebau und Raumplanung, 24), Wien 1997, p. IX.

[4] The last volume of the Edition was published in 2014, see: Klaus Semsroth / Michael Mönninger / Christiane Crasemann Collins (Hrsg.), Camillo Sitte Gesamtausgabe. Schriften und Projekte, 6 Bde., Bd. 6, Entwürfe und städtebauliche Projekte, Wien-Köln-Weimar 2014.

Author Index

Q

R

S

T

U

V

W

Y

Z

SHIMADZU

Excellence in Science

TU WIEN VSS
VIENNA young SCIENTISTS SYMPOSIUM

JOIN THE ...

4th VIENNA young SCIENTISTS SYMPOSIUM (VSS)

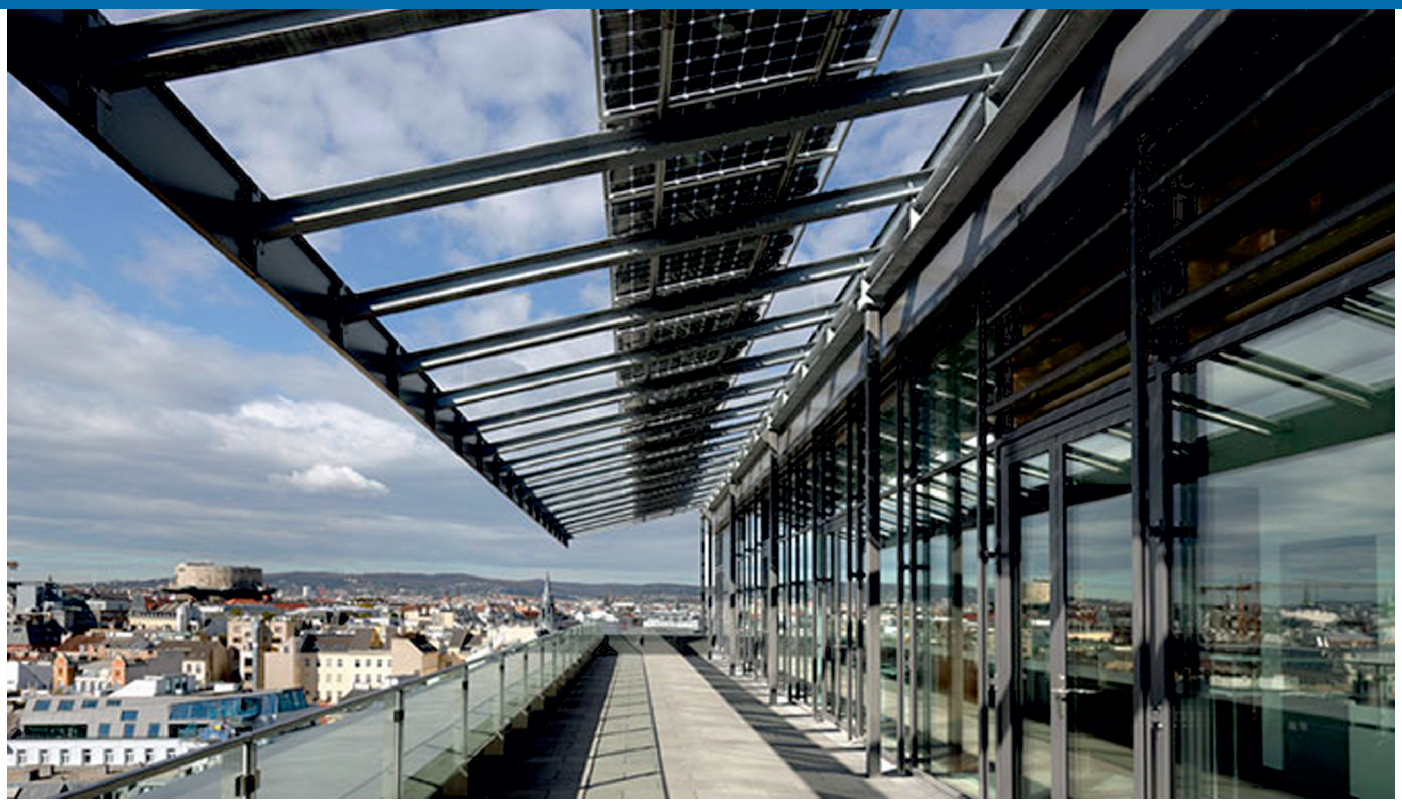

7-8 June 2018
TU WIEN,TUtheSky
Getreidemarkt 9, 1060 Vienna, Austria

Technische Universität Wien
vss@tuwien.ac.at
vss.tuwien.ac.at